
NORTH ATLANTIC TREATY
ORGANIZATION



AC/323(HFM-222)TP/731

SCIENCE AND TECHNOLOGY
ORGANIZATION



www.sto.nato.int

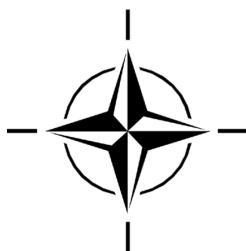
STO TECHNICAL REPORT

TR-HFM-222

Biological Effects of Ionising Radiation and Countermeasures

(Les effets biologiques des rayonnements
ionisants et leurs contre-mesures)

Final Report of Research Task Group HFM-222.



Published January 2018

Distribution and Availability on Back Cover



NORTH ATLANTIC TREATY
ORGANIZATION



AC/323(HFM-222)TP/731

SCIENCE AND TECHNOLOGY
ORGANIZATION



www.sto.nato.int

STO TECHNICAL REPORT

TR-HFM-222

Biological Effects of Ionising Radiation and Countermeasures

(Les effets biologiques des rayonnements
ionisants et leurs contre-mesures)

Final Report of Research Task Group HFM-222.

The NATO Science and Technology Organization

Science & Technology (S&T) in the NATO context is defined as the selective and rigorous generation and application of state-of-the-art, validated knowledge for defence and security purposes. S&T activities embrace scientific research, technology development, transition, application and field-testing, experimentation and a range of related scientific activities that include systems engineering, operational research and analysis, synthesis, integration and validation of knowledge derived through the scientific method.

In NATO, S&T is addressed using different business models, namely a collaborative business model where NATO provides a forum where NATO Nations and partner Nations elect to use their national resources to define, conduct and promote cooperative research and information exchange, and secondly an in-house delivery business model where S&T activities are conducted in a NATO dedicated executive body, having its own personnel, capabilities and infrastructure.

The mission of the NATO Science & Technology Organization (STO) is to help position the Nations' and NATO's S&T investments as a strategic enabler of the knowledge and technology advantage for the defence and security posture of NATO Nations and partner Nations, by conducting and promoting S&T activities that augment and leverage the capabilities and programmes of the Alliance, of the NATO Nations and the partner Nations, in support of NATO's objectives, and contributing to NATO's ability to enable and influence security and defence related capability development and threat mitigation in NATO Nations and partner Nations, in accordance with NATO policies.

The total spectrum of this collaborative effort is addressed by six Technical Panels who manage a wide range of scientific research activities, a Group specialising in modelling and simulation, plus a Committee dedicated to supporting the information management needs of the organization.

- AVT Applied Vehicle Technology Panel
- HFM Human Factors and Medicine Panel
- IST Information Systems Technology Panel
- NMSG NATO Modelling and Simulation Group
- SAS System Analysis and Studies Panel
- SCI Systems Concepts and Integration Panel
- SET Sensors and Electronics Technology Panel

These Panels and Group are the power-house of the collaborative model and are made up of national representatives as well as recognised world-class scientists, engineers and information specialists. In addition to providing critical technical oversight, they also provide a communication link to military users and other NATO bodies.

The scientific and technological work is carried out by Technical Teams, created under one or more of these eight bodies, for specific research activities which have a defined duration. These research activities can take a variety of forms, including Task Groups, Workshops, Symposia, Specialists' Meetings, Lecture Series and Technical Courses.

The content of this publication has been reproduced directly from material supplied by STO or the authors.

Published January 2018

Copyright © STO/NATO 2018
All Rights Reserved

ISBN 978-92-837-2055-3

Single copies of this publication or of a part of it may be made for individual use only by those organisations or individuals in NATO Nations defined by the limitation notice printed on the front cover. The approval of the STO Information Management Systems Branch is required for more than one copy to be made or an extract included in another publication. Requests to do so should be sent to the address on the back cover.

Table of Contents

	Page
List of Figures	viii
List of Tables	xi
List of Acronyms	xiv
Preface	xix
Foreword	xxii
Terms of Reference	xxiii
Acknowledgements	xxvi
HFM-222 Membership List	xxvii
Executive Summary and Synthèse	ES-1
Chapter 1 – High-Level Radiation Bioeffects	1-1
1.1 General Introduction	1-1
1.1.1 Biomarkers of Exposure and Effects	1-1
1.1.2 Medical Countermeasures (MedCM)	1-1
1.1.3 Modeling Guidance	1-1
1.2 Biomarkers of Exposure and Effects	1-2
1.2.1 Time-Dependent Relevance of Radiation Biomarkers to Distinguish Partial-Body from Total-Body Exposures	1-2
1.2.1.1 Introduction	1-2
1.2.1.2 Materials and Methods	1-3
1.2.1.3 Results	1-5
1.2.1.4 Discussion	1-5
1.2.1.5 Perspectives	1-6
1.2.2 PHE Cytogenetics Group Activities Related to Radiation Bioeffects and Countermeasures (2012 – 2015)	1-7
1.2.2.1 Rapid (Bio)Dosimetry Assays for Mass Casualty Triage	1-7
1.2.2.2 Development of Novel Statistical Data Analysis Methods for Biological Dosimetry	1-8
1.2.2.3 Biomarkers in Radiotherapy	1-8
1.2.2.4 Health Effects Following Exposure to Ionising Radiation and Other Genotoxins	1-8
1.2.2.5 Recent Improvements in Emergency Preparedness for Radiological Mass Casualty Scenarios	1-9
1.2.3 Establishment of Dicentric Chromosome Assay for Biological Dosimetry in Case of Suspect Radiation Exposure	1-10
1.2.3.1 Introduction	1-10
1.2.3.2 Results	1-11

1.2.3.3	Discussion	1-15
1.2.4	Cytokinesis-Block MicroNucleus Assay: Manual and Automated Scoring	1-16
1.2.4.1	Introduction	1-17
1.2.4.2	Aim	1-17
1.2.4.3	Study Design	1-17
1.2.4.4	Results	1-18
1.2.4.5	Discussion	1-19
1.2.4.6	Conclusion	1-19
1.3	Medical Countermeasures	1-20
1.3.1	Protection and Treatment with Nicotinic Acid and its Derivatives (A Mouse Model)	1-20
1.3.1.1	Introduction	1-20
1.3.1.2	Results	1-21
1.3.1.3	Conclusion	1-25
1.3.2	Cell / Transient Gene Therapy to Treat Acute Radiation Syndrome: Evaluation in Animal Models	1-26
1.3.2.1	Rationale of Cell Gene Therapy for Acute Radiation Treatment	1-26
1.3.2.2	Transient / Gene Therapy to Mitigate Radiation-Induced Hematopoietic Syndrome	1-27
1.3.2.3	Transient Gene Therapy to Mitigate Cutaneous Radiation Syndrome	1-27
1.3.2.4	Conclusion	1-28
1.3.3	AFRRI Program on Radiation Injury and Countermeasures: Moderate to High Radiation Doses	1-30
1.3.3.1	Mechanisms of Radiation Injury and Recovery	1-31
1.3.3.2	Mini-Pig Model of Acute Radiation Syndrome (ARS)	1-31
1.3.3.3	Medical Countermeasures (MedCM)	1-32
1.3.4	Attenuation of Radiation-Induced Gastrointestinal Damage by Epidermal Growth Factor and Bone Marrow Transplantation in Mice	1-33
1.3.4.1	Introduction	1-34
1.3.4.2	Material and Methods	1-34
1.3.4.3	Results	1-37
1.3.4.4	Discussion	1-48
1.3.4.5	Conclusion	1-51
1.3.5	EGF Attenuates Delayed Ionizing Radiation-Induced Tissue Damage in Bone Marrow Transplanted Mice	1-52
1.3.5.1	Introduction	1-52
1.3.5.2	Materials and Methods	1-53
1.3.5.3	Results	1-56
1.3.5.4	Discussion	1-64
1.3.5.5	Conclusion	1-66
1.4	Modelling	1-66
1.4.1	Scenarios and Urban Environment	1-67
1.4.2	Physiological Modeling of Health Effects	1-68
1.4.3	Physiological Models of Radiation	1-68

1.4.3.1	Radiation-Induced Performance Decrement (RIPD)	1-68
1.4.3.2	Physiological Models in RIPD	1-68
1.4.3.3	Example Application of RIPD	1-69
1.4.4	Health Effects from Nuclear and Radiological Environments (HENRE)	1-70
1.4.4.1	Combined Injury Model Development	1-71
1.4.4.2	Circulatory Shock	1-72
1.4.4.3	Hematopoietic Cell Kinetic Models	1-75
1.4.5	Treatment Models: Internalized Radionuclides	1-79
1.4.5.1	Prussian Blue Decorporation of Cs-137	1-79
1.4.5.2	DTPA Decorporation of Am-241 and Pu-238/239	1-80
1.4.5.3	Application of Decorporation Models	1-81
1.4.6	Summary	1-82
1.4.6.1	Additional Modelling Needs	1-82
1.4.6.2	Spectrum of Modelling and Analysis	1-83
1.4.6.3	Informing Operational Planning	1-83
1.5	References	1-83

Chapter 2 – Low-Level Radiation Bioeffects **2-1**

2.1	General Introduction	2-1
2.2	Biomarkers of Exposure and Effects	2-1
2.2.1	Gene Expression Changes Observed in Radiation Exposed Cohorts – Health Risk After Low-Level Radiation	2-1
2.2.1.1	Introduction	2-2
2.2.1.2	Materials and Methods	2-3
2.2.1.3	Results	2-6
2.2.1.4	Discussion	2-7
2.2.1.5	Acknowledgment	2-8
2.2.2	Retrospective Study by FISH Chromosome Painting Translocation in a Cohort of Italian Soldiers with Past Deployments in the Balkan Area: Preliminary Data	2-9
2.2.2.1	Introduction	2-9
2.2.2.2	Results	2-10
2.2.2.3	Discussion	2-14
2.2.3	Pilot Biomonitoring Study for Ionizing Radiation Exposure in Operational Theatres: Dog as Sentinel of Environmental Risk	2-16
2.2.3.1	Background	2-16
2.2.3.2	Study Design	2-17
2.2.3.3	Methods	2-17
2.2.3.4	Results	2-17
2.2.3.5	Conclusions	2-20
2.3	Early and Late Effects	2-20
2.3.1	Evaluation of the Effect of Low Doses of Low-LET Radiation on the Innate Anti-Tumor Reactions in Radio-Resistant and Radio-Sensitive Mice	2-20
2.3.1.1	Introduction	2-20
2.3.1.2	Results	2-22
2.3.1.3	Conclusions	2-31

2.3.2	Effect of Internal Contamination with Tritiated Water on the Innate Anti-Tumor and Inflammatory Reactions in Radio-Resistant and Radio-Sensitive Mice – A Preliminary Study	2-31
2.3.2.1	Introduction	2-31
2.3.2.2	Results	2-33
2.3.3	The Importance of Low-Dose Radiation Research: Models and Mechanisms to Develop Biomarkers, Countermeasures, and Improved Risk Assessment	2-38
2.3.3.1	Introduction	2-39
2.3.3.2	Long-Term Goals	2-40
2.3.3.3	Research Progress	2-40
2.3.3.4	Summary and Conclusions	2-45
2.4	References	2-46

Chapter 3 – Medical Radiation Preparedness 3-1

3.1	General Introduction	3-1
3.2	Diagnosing Acute Radiation Syndrome and Medical Management Based on Clinical Signs and Symptoms NATO HFM-222 Exercise 2015 – Preliminary Results	3-1
3.2.1	Introduction	3-1
3.2.1.1	Concept of the Exercise	3-2
3.2.1.2	Exercise Scenario	3-2
3.2.2	Material and Methods	3-3
3.2.2.1	The SEARCH Database and METREPOL	3-3
3.2.2.2	Exercise Cases	3-3
3.2.2.3	Input Data Format	3-3
3.2.2.4	Output Data Format	3-4
3.2.2.5	Participants	3-4
3.2.3	Results	3-4
3.2.3.1	Report Time	3-4
3.2.3.2	Recommendation for Hospitalization	3-4
3.2.3.3	Estimation of the Response Category (RC)	3-5
3.2.4	Discussion	3-6
3.3	Acknowledgements	3-7
3.4	References	3-7

Chapter 4 – NATO HFM-222 RTG Role 4 Biodosimetry Assays Survey and Biodosimetry Assays Technology Readiness Level Update 4-1

4.1	General Introduction	4-1
4.2	NATO Role 4 Biodosimetry Assays Survey	4-1
4.2.1	Introduction	4-1
4.2.2	Biodosimetry Survey Questionnaire Responses	4-2
4.2.2.1	Contact Information	4-2
4.2.2.2	General Information – Staffing of Laboratory	4-3
4.2.2.3	Biodosimetry Capability – From Blood Sample to Dose Estimation	4-5

4.2.2.4	Laboratory Equipment, Experience, and Network Participation	4-7
4.2.2.5	Experience with Collaboration and Networking	4-9
4.2.2.6	Prospects and Expectations from Participation in a NATO Biodosimetry Network (NBN)	4-9
4.2.2.7	The Value of the Establishment of a NATO Biodosimetry Network can be Useful for the Biodosimetry Laboratories	4-10
4.2.2.8	What are the Most Pressing Needs for your Laboratory?	4-10
4.2.2.9	Other Comments	4-11
4.2.3	Acknowledgments	4-11
4.3	NATO Role 4 Biodosimetry Assays Technology Readiness Level Update	4-11
4.3.1	Introduction	4-11
4.3.2	Diagnostic Criteria	4-12
4.3.3	NATO Technology Readiness Levels (TRLs)	4-13
4.3.4	Biodosimetry Assays TRL Scoring Responses	4-14
4.3.5	Discussion and Summary	4-16
4.4	Acknowledgements	4-17
4.5	References	4-17

Chapter 5 – References of Articles Published by HFM-222 Members Dealing with the RTG’s Activities (2012 – 2016) 5-1

5.1	Ionizing Radiation Bioeffects and Mechanisms	5-1
5.2	DNA Damage	5-1
5.3	Biodosimetry (Cytogenetics)	5-1
5.4	Biodosimetry (Proteomics)	5-2
5.5	Biodosimetry (Genomics)	5-3
5.6	Radiation Biomarkers	5-4
5.7	Radio-Protectants	5-5
5.8	Animal Models for the Study of G-ARS and RI-MODS	5-5
5.9	Post-Irradiation Treatments against Ionizing Radiation Injury (H-ARS and CRS)	5-6
5.10	Radiological Decontamination	5-7
5.11	Low-Level Radiation Bioeffects	5-7
5.12	Modeling and Medical Guidance	5-7

Annex A – Annual Meeting Agendas A-1

A.1	NATO HFM-222 RTG Meeting: Ionizing Radiation Bioeffects and Countermeasures, 14-15 May 2012, Neuilly-sur-Seine, France	A-1
A.2	NATO HFM-222 RTG Meeting: Ionizing Radiation Bioeffects and Countermeasures, 5-7 June 2013, Rome, Italy	A-3
A.3	NATO HFM-222 RTG Meeting: Ionizing Radiation Bioeffects and Countermeasures, 16-18 June 2014, Bethesda, MD, United States	A-5
A.4	NATO HFM-222 RTG Meeting: Ionizing Radiation Bioeffects and Countermeasures, 7-9 May 2015, Munich, Germany	A-8
A.5	NATO HFM-222 RTG Meeting: Ionizing Radiation Bioeffects and Countermeasures, 9-10 May 2016, Neuilly-sur-Seine, France	A-10

List of Figures

Figure		Page
Figure 1-1	Kinetic Relevance of Biochemical and Hematological Biomarkers to Distinguish TBI from PBI Animals	1-5
Figure 1-2	Dicentric and Acentric Dose-Effect Calibration Curves and Their Respective Coefficients of the Curve	1-12
Figure 1-3	DCA Automated Dose-Effect Calibration Curve and Previously Generate Manual Calibration Curve	1-13
Figure 1-4	Dose-Response Curves of MN Obtained by Manual Scoring, Automatic Scoring and with Semi-Automatic Scoring Mode	1-18
Figure 1-5	Chemical Structure of the Examined Compounds: NAc (Nicotinic Acid; Vitamin B ₃) and its Derivatives – MNA (1-Methylnicotinamide), 1.3-MAP (1-Methyl-3-Acetylpyridine), NA (Nicotinamide); 1.4-DMP (1.4-Dimethylpyridine)	1-21
Figure 1-6	Survival of the Lethally (7.5 Gy) Irradiated BALB/C Mice Fed NAc, NA, MNA, or 1.3-MAP (100 mg/kg b.m./day) in Drinking Water	1-22
Figure 1-7	Survival of the Lethally (7.5 Gy) Irradiated BALB/C Mice Fed 1.4-DMP (100 mg/kg b.m./day5) in Drinking Water	1-22
Figure 1-8	Adipocyte Stem Cells (ASC) Local Injection to Mitigate CRS in Mini-Pig Model	1-29
Figure 1-9	Colony Forming Efficiency in Percentage of Plated Skin Fibroblasts <i>In Vitro</i> Irradiated (25 Gy Gamma) and then Incubated 14 Days in Presence of Culture Media from Mock-ASC, Shh-ASC and Basic Culture Medium	1-30
Figure 1-10	Effect of Bone Marrow Transplantation (BMT) and Epidermal Growth Factor (EGF) on Animal Survival of C57BL/6 Mice After Whole Body Irradiation by 12 and 13 Gy	1-38
Figure 1-11	Effect of Bone Marrow Transplantation (BMT) and 3 Doses of Epidermal Growth Factor (EGF) on Animal Survival of C57BL/6 Mice After Whole Body Irradiation by 13 Gy	1-39
Figure 1-12	Effect of Bone Marrow Transplantation (BMT) and Epidermal Growth Factor (EGF) on Animal Survival of C57BL/6 Mice After Whole Body Irradiation by 11 Gy	1-57
Figure 1-13	Effect of Epidermal Growth Factor (EGF) on Animal Survival of C57BL/6 Mice After Whole Body Irradiation by 11 Gy	1-57
Figure 1-14	An Illustration of Radiation Shielding in the Urban Environment	1-67
Figure 1-15	Radiation-Induced Performance Decrement Software – RIPD 5.2	1-68
Figure 1-16	Structure of the Cell Kinetics Model, MarCell	1-69
Figure 1-17	Time Course Severity of Signs and Symptoms After a Complex Radiation Exposure Scenario	1-70
Figure 1-18	Structure of the Computational Engine for HENRE	1-70
Figure 1-19	HENRE 1.0 GUI with Prompt Injury Module	1-71

Figure 1-20	Pathophysiological Processes in Combined Radiation and Burn Injury	1-72
Figure 1-21	Model of Microvascular Exchange for Understanding the Circulatory Shock Mechanism	1-73
Figure 1-22	Plasma Volume Changes Over 48 Hours After 10, 20, and 30 %TBSA	1-73
Figure 1-23	Predicted Value of Minimum Plasma Volume as a Function of %TBSA Burn and Associated Probability of Mortality	1-74
Figure 1-24	Early Permeability Changes Observed After Radiation	1-74
Figure 1-25	Hematopoietic Cell Kinetic Model Structure	1-76
Figure 1-26	Simulated Thrombocyte Kinetics After 3 and 5 Gy Prompt Radiation	1-76
Figure 1-27	Radiation and Burn Combined Injury Hematopoietic Model	1-77
Figure 1-28	A Combined Radiation and Burn Injury Simulation Compared to Single Injury Predictions and Data	1-78
Figure 1-29	Platelet Concentration Following Combined Injury in Rats Compared with Murine Model Simulations	1-79
Figure 1-30	Decorporation Model for Cesium with Prussian Blue	1-80
Figure 1-31	DTPA Decorporation Model for Am and Pu	1-81
Figure 1-32	Development of Additional Models	1-82
Figure 1-33	Spectrum of Modeling to Inform Operational Planning	1-83
Figure 2-1	The Causal Pathway Depicts Genes Newly Adjusted After Radiation Exposure which Over a Latency of Decades are Involved in the Later Occurring Disease/Effect	2-3
Figure 2-2	Overview on the Study Design of the Chernobyl and the Mayak Worker Study	2-4
Figure 2-3	Phase I – Whole Genome Screening; Phase II – Validation	2-5
Figure 2-4	Examinations on the Chernobyl Radiation Victims and the Mayak Workers	2-6
Figure 2-5	Chromosome Aberrations Scored – Two-Way Translocation; One-Way Translocation; Deletion; Insertion; Loss and Gain of One Chromosome	2-12
Figure 2-6	Comparison Between Two-Way and One-Way Translocation Frequencies	2-13
Figure 2-7	Translocation Frequencies per 100 Cell Equivalents for the Different Age Intervals	2-13
Figure 2-8	Translocation Frequencies per 100 Cell Equivalents by Age and Geographic Region	2-14
Figure 2-9	Comparison Between the Frequencies of Translocations Observed in this Study and the Frequency of Translocations Reported by Sigurdson <i>et al.</i>	2-14
Figure 2-10	Proliferation Index (PI) Humans	2-18
Figure 2-11	Proliferation Index (PI) Dogs	2-18
Figure 2-12	MN Dose-Response Curve (MN/1000 BN Cells) Humans	2-18
Figure 2-13	MN Dose-Response Curve (MN/1000 BN Cells) Dogs	2-18
Figure 2-14	MN Frequency Pre- and Post-Deployment in Soldiers	2-19

Figure 2-15	MN Frequency Pre- and Post-Deployment in Army Dogs	2-19
Figure 2-16	DIC Frequency Pre- and Post-Deployment in Soldiers	2-20
Figure 2-17	Experimental Protocol for Studying of the Effect of Low Doses of Low-LET Radiation on the Innate Anti-Tumor Reactions in Radio-Resistant and Radio-Sensitive Mice	2-22
Figure 2-18	Development of Induced Metastases in the Lungs After Fractionated WBI of BALB/c and C57BL/6 Mice	2-23
Figure 2-19	Cytotoxic Activity of NK Cells After Fractionated WBI of BALB/c and C57BL/6 Mice	2-24
Figure 2-20	Inhibition of Cytotoxic Activity of NK Cells After Fractionated WBI of BALB/c Mice	2-25
Figure 2-21	Production of IFN- γ by NK Cell-Enriched Splenocytes and IL-2 by Splenocytes After Fractionated WBI of BALB/c Mice	2-26
Figure 2-22	Cytotoxic Activity of M ϕ After Fractionated WBI of BALB/c or C57BL/6 Mice	2-27
Figure 2-23	Production of NO by M ϕ After Fractionated WBI of BALB/c or C57BL/6 Mice	2-28
Figure 2-24	Production of IL-1 β , TNF- α and IL-12 by M ϕ After Fractionated WBI of BALB/c Mice	2-30
Figure 2-25	Experimental Protocol for Studying the Effect of Internal Contamination with Tritiated Water on the Innate Anti-Tumor and Inflammatory Reactions in Radio-Resistant and Radio-Sensitive Mice	2-33
Figure 2-26	Cytotoxic Activity of NK Cells After Contamination with HTO of BALB/c or C57BL/6 Mice	2-34
Figure 2-27	Production of NO by M ϕ Obtained from BALB/c or C57BL/6 Mice Contaminated with HTO	2-35
Figure 2-28	Blood Cell Counts in BALB/c or C57BL/6 Mice Contaminated with HTO	2-36
Figure 2-29	Spleen and Bone Marrow Cellularity in BALB/c or C57BL/6 Mice Contaminated with HTO	2-37
Figure 2-30	Global DNA Methylation: Early and Late Phase Transformed Clonal Cells	2-43
Figure 2-31	Neoplastic Transformation After Protracted Alpha Particle Exposure	2-44
Figure 2-32	Neoplastic Transformation After Protracted X-Ray Exposure	2-44
Figure 3-1	Analysis of the Results Regarding the Recommendation for Hospitalization of the Exercise Cases	3-5
Figure 3-2	Analysis of the Results Regarding the Diagnosed Response Category (RC)	3-6
Figure 4-1	NATO Technology Readiness Levels (TRLs)	4-13

List of Tables

Table		Page
Table 1-1	Analysis of Dicentric and Excess Acentrics, Distribution, u -Value and Dispersion Factor of Dicentric Chromosomes	1-12
Table 1-2	Results of Automated Scoring of DCA and Distribution, u -Value and Dispersion Factor of Dicentric Chromosomes	1-13
Table 1-3	Biological Dose Estimations Based on the Analysis of Dicentric Chromosomes in 500 Metaphases	1-14
Table 1-4	Dose Estimations Carried Out from Manual Scoring of Dicentric and Percentage of Inclusion Inside the Right Medical Class of Risk	1-14
Table 1-5	Dose Estimations Performed by Automated Scoring of Dicentric and Percentage of Inclusion Within the Appropriate Medical Class of Risk	1-15
Table 1-6	Biological Dose Estimations of Ten Blind Samples Based on the Analysis of Micronuclei by Manual and Semi-Automated Scoring	1-19
Table 1-7	Significant Changes in Spleen and Bone Marrow Cellularity, and Blood Cell Counts in BALB/C Mice Irradiated at 6.5 Gy and Fed MNA or 1.4-DMP in Drinking Water from Day -7, Day 0, or Day 7 of the Experiment	1-24
Table 1-8	Significant Changes in Spleen and Bone Marrow Cellularity, and Blood Cell Counts in BALB/C Mice Irradiated at 6.5 Gy and Fed NAc, NA or 1.3-MAP in Drinking Water from Day -7, Day 0, or Day 7 of the Experiment	1-25
Table 1-9	Hematopoietic Recovery in Highly Irradiated Monkeys (8 Gy Gamma Frontal TBI) Given Shh-ASC or Mock-ASCs	1-29
Table 1-10	Inflammatory Infiltration in Jejunum, Ileum and Colon Ascendens Expressed as the Median Value of Positive Findings (of Values ≥ 1) or 0 (No Positive Finding in the Group) and the Amount of Affected Animals in the Group	1-40
Table 1-11	Average Values for Microcolony Assay in Jejunum, Ileum and Colon Ascendens $\pm 2 \times$ Standard Error of Mean for N = 6 Animals Except for * N = 5 and ** N = 4 Animals	1-41
Table 1-12	Average Values for Length of Crypts and Height of Villi in Jejunum, Ileum and Colon Ascendens $\pm 2 \times$ Standard Error of Mean for N = 6 Animals Except for * N = 5 and ** N = 4 Animals	1-42
Table 1-13	Average Values for Cryptal Mitotic and Apoptotic Index and Villar Apoptotic Activity or Apoptotic Index at the Luminal Surface in Jejunum, Ileum and Colon Ascendens $\pm 2 \times$ Standard Error of Mean for N = 6 Animals Except for * N = 4 and ** N = 5 Animals	1-44
Table 1-14	Inflammatory Infiltration in Liver Expressed as the Median Value of Positive Findings (of Values ≥ 1) or 0 (No Positive Finding in the Group) and the Amount of Affected Animals in the Group	1-46
Table 1-15	Average Values for Blood Lymphocytes, Monocytes, Neutrophil Granulocytes and Thrombocytes $\pm 2 \times$ Standard Error of Mean for N = 6 Animals	1-46

Table 1-16	Average Values for Relative Representation of GFP ⁺ Cells in Blood, Bone Marrow, Peyers' Patches, and Lung $\pm 2 \times$ Standard Error of Mean for N = 6 Animals	1-47
Table 1-17	Average Values for GFP ⁺ Cells in Jejunum, Ileum, Colon Ascendens, and Liver $\pm 2 \times$ Standard Error of Mean for N = 6 Animals Except for * N = 5 and ** N = 4 Animals	1-48
Table 1-18	Histopathological Changes in Jejunum Expressed as the Median Value of Positive Findings (of Values ≥ 1) or 0 (No Positive Finding in the Group) and the Amount of Affected Animals in the Group	1-58
Table 1-19	Average Values of Morphometric Parameters, Apoptotic and Mitotic Activity in Jejunum $\pm 2 \times$ Standard Error of Mean	1-59
Table 1-20	Histopathological Changes in Ileum Expressed as the Median Value of Positive Findings (of Values ≥ 1) or 0 (No Positive Finding in the Group) and the Amount of Affected Animals in the Group	1-59
Table 1-21	Average Values of Morphometric Parameters, Apoptotic and Mitotic Activity in Ileum $\pm 2 \times$ Standard Error of Mean	1-60
Table 1-22	Histopathological Changes in Colon Transversum Expressed as the Median Value of Positive Findings (of Values ≥ 1) or 0 (No Positive Finding in the Group) and the Amount of Affected Animals in the Group	1-60
Table 1-23	Average Values of Morphometric Parameters, Apoptotic and Mitotic Activity in Colon Transversum $\pm 2 \times$ Standard Error of Mean	1-61
Table 1-24	Histopathological Changes in Liver Expressed as the Median Value of Positive Findings (of Values ≥ 1) or 0 (No Positive Finding in the Group) and the Amount of Affected Animals in the Group	1-61
Table 1-25	Average Values of Plasma Cytokine Levels (pg/ml) $\pm 2 \times$ Standard Error of Mean	1-62
Table 1-26	Average Values of Bone Marrow Quantitative and Qualitative Parameters $\pm 2 \times$ Standard Error of Mean	1-62
Table 1-27	Peripheral Blood Cell Counts and Weight of Spleen $\pm 2 \times$ Standard Error of Mean Evaluated 63 Days after Irradiation	1-63
Table 1-28	Relative Representation (%) of GFP ⁺ Cells in Different Tissues $\pm 2 \times$ Standard Error of Mean	1-64
Table 1-29	Relationship between Circulating Blood Volume Loss and Risk of Circulatory Shock from Hypovolemia	1-75
Table 1-30	48-hr Mortality CI Predictions (in %) Based on Simulated Plasma Volume Minimums	1-75
Table 1-31	Efficacy of Different Treatment Regimens of Cs-137 with Prussian Blue	1-81
Table 2-1	Chromosomes Aberrations and Relative Frequencies Observed in the Control Population Analysed	2-11
Table 2-2	Effect of Alpha Particles and X-rays on Non-Targeted Radiation Population	2-41
Table 4-1	Radiation Dose and Injury Assessment Modalities	4-1
Table 4-2	Contact Information	4-2

Table 4-3	Information about the Staffing Relative to the Various Assays of the Biodosimetry Laboratories	4-4
Table 4-4	Laboratory Capabilities	4-5
Table 4-5	Laboratory's Equipment, Biodosimetry Experience, and Participation in Networks and Exercises	4-8
Table 4-6	Radiation Dose and Injury Assessment Modalities	4-11
Table 4-7	Various Parameters for Diagnostic Criteria in Role 4 Biodosimetry Assays	4-12
Table 4-8	TRL Assessment for Cytogenetic Assays	4-14
Table 4-9	TRL Assessment for Gene Expression and Biochemistry Assays	4-15
Table 4-10	TRL Assessment for Physical Dosimetry and Radionuclide Counting Assays	4-16

List of Acronyms

1.3-MAP	1-Methyl-3-Acetylpyridine
1.4-DMP	1.4-Dimethylpyridine
A&E	Accident and Emergency
ACE	Allied Command Europe
AFFRI	Armed Forces Radiobiology Research Institute (United States)
AGRS	Acute Gastrointestinal Radiation Syndrome
AJP	Allied Joint Publication
ALC	Absolute Lymphocyte Count
ALP	Alkaline Phosphatase
ALT	Alanine AminoTransferase
Am	Americium
AML	Acute Myeloid Leukemia
ANC	Absolute Neutrophil Count
ANG2	Angiopoietin 2
AP	Allied Publication
ARA	Applied Research Associates
ARS	Acute Radiation Syndrome
ASC	Adipocyte Stem Cell
AST	Aspartate AminoTransferase
BARDA	Biomedical Advanced Research and Development Authority
BAT	Biodosimetry Assessment Tool
BM	Bone Marrow
BMT	Bone Marrow Transplantation
BN	Binucleated cells
BW	Biological Weapon
C	Cutaneous
CAN	Canada
CBLB613	naturally occurring Mycoplasma-derived lipopeptide ligand for the Toll-like receptor 2/6
CBMN	Cytokinesis Block Micronucleus
CBRN	Chemical, Biological, Radiological, Nuclear
CBRNMedWG	Chemical, Biological, Radiological, Nuclear Medical Working Group
CDG	Clinical Decision Guidance
CDX	Celldex
CE	Cell Equivalent
CFU-GM	Colony-Forming Unit – Granulocyte/Macrophage
CI	Combined Injury
CIPRO	Ciprofloxacin
CK	Creatine Kinase
CM	Countermeasure
CMA	Concamamycin A
COMEDS	Committee of the Chiefs of Military Medical Services in NATO
CONCERT	European Joint Programme for the Integration of Radiation Protection Research
CREAL	Centre for Research in Environmental Epidemiology
cRNA	coding RNA
CRP	C-Reactive Protein
CRS	Cutaneous Radiation Syndrome
CRSSA	Centre de Recherches du Service de Santé des Armées

Cs	Cesium
CW	Chemical Weapon
CZE	Czech Republic
DCA	Dicentric Chromosome Assay
DEBR	Département des Effets Biologiques des Rayonnements (France)
DEU	Germany
dF	degrees of Freedom
DIC	Dicentric
DNA	Deoxyribonucleic Acid
DoD	Department of Defense (United States)
DoREMi	Low-Dose Research towards Multi-disciplinary Integration network of excellence
DRF	Dose-Reduction Factor
DT3	Delta-Tocotrienol
DTPA	Diethylene Triamine Pentaacetic Acid
DTRA	Defence Threat Reduction Agency
DU	Depleted Uranium
EACK	Emergency Antiapoptotic Cytokine therapy
EGF	Epidermal Growth Factor
EPD	Equivalent Prompt Dose
EPO	Erythropoietin
EPR	Electron Paramagnetic Resonance
Erk	Extracellular Signal-regulated Kinase
EU	European Union
EURADOS	The European Radiation Dosimetry Group
FDA	Food and Drug Administration (United States)
FDC-P1	Factor Dependent Continuous – Paterson 1
FGF	Fibroblast Growth Factor
FISH	Fluorescence <i>In Situ</i> Hybridation
Flt3L	FMS-like tyrosine kinase-3 Ligand
FRA	France
FRAT	First-responders Radiological Assessment Triage
G/GI	Gastrointestinal
G-ARS	Gastrointestinal ARS
GBR	Great Britain
G-CSF	Granulocyte Colony-Stimulating Factor
GFP	Green Fluorescent Protein
GT3	Gamma Tocotrienol
GUI	Graphical User Interface
Gy	radiation dose
H	Hematopoietic
H-ARS/HARS	Hematological Acute Radiation Syndrome
Hb	Hemoglobin Level
HENRE	Health Effects from Nuclear and Radiological Environments
HFM	Human Factors and Medicine (Panel)
HNCG	Hematological, Nervous, Cutaneous, Gastrointestinal
HPA	Health Public Agency
HRS	Hematopoetic Radiation Syndrome
HSC	Hematopoietic Stem Cell
HSPC	Hematopoietic Stem and Progenitor Cell
HTO	Tritiated water

HUMN	Human Micronucleus project
HUN	Hungary
HUVEC	Human Umbilical Vein Endothelial Cell
IAEA	International Atomic Energy Agency
IAEA-CRP	International Atomic Energy Agency – Coordinated Research Project
ICAM	Intercellular Adhesion Molecule
ICRP	International Commission on Radiological Protection
IFN	Interferon
IL	Interleukin
IND	Improvised Nuclear Device
IOS	Apple Operating System
IR	Irradiation
IRBA	Institut de Recherche Biomédicale des Armées (France)
ISO	International Organization for Standardization
ITA	Italy
i.v.	intravenous
LABGenMil	Laboratorio Avanzato di Biodosimetria Genetica Militare
LCL	Lower Confidence Limit
LD	Lethal Dose
LDH	Lactico DeHydrogenase
LDR	Low-Dose Radiation
LET	Linear Energy Transfer
LF UK / LFUK	Lékařská Fakulta Univerzita Karlova
LLC	Louis Lang Carcinoma
MAD	Mean of the Absolute Differences
MAPK	Mitogen-Activated Protein Kinase
MCV	Mean Corpusclar Volume
MedCM	Medical Countermeasure
MELODI	Multi-disciplinary European Low-Dose Initiative
METREPOL	Medical treatment protocols for radiation accident victims
MHC	Major Histocompatibility antigen
miRNA	micro Ribonucleic Acid
MMO	Military Medical Operation
MN	Micronucleus
MNA	1-Methylnicotinamide
MODS	Multi-Organ Dysfunction Syndrome
MOF	Multi-Organ dysfunction Failure
MONO	Monocyte count
mRNA	messenger RNA
MS	Median Survival
MSC	Mesenchymal Stem Cell
MS-PCR	Methylation-Sensitive PCR
mTOR	mechanistic Target Of Rapamycin
Multibiodose	Multi-disciplinary biodosimetric tools to manage high scale radiological casualties
MURAD	Moscow-Ulm Radiation Accident Database
N	Neurovascular
NA	Nicotinamide
NAc	Nicotinic Acid
NATO	North Atlantic Treaty Organization
NBN	NATO Biodosimetry Network
NCI	National Cancer Institute

NGDS	Next-Generation Diagnostic System
NHP	Non-Human Primate
NIHR	National Institute for Health Research
NK	Natural Killer (Cell)
NLD	Netherlands
NLR	Neutrophil-to-Lymphocyte Ratio
NO	Nitric Oxide
NOR	Norway
NR	Nuclear, Radiological
NRPB	National Radiological Protection Board
NTE	Non-Targeted radiation Effect
OPERRA	Open Project for European Radiation Research Area
OSL	Optically Stimulated Luminescence
PAC	Program Area Committee
PAF	Platelet-Activating Factor
PB	Phenylbutyrate
PB	Prussian Blue
PBI	Partial-Body Irradiation
PBS	Phosphate-Buffered Saline
PCC	Premature Chromosome Condensation
PCR	Polymerase Chain Reaction
PDGF	Platelet-Derived Growth Factor
PfP	Partnership for Peace
PGL ₂	Prostacyclin
PHE CRCE	Public Health England Centre for Radiation, Chemical and Environmental hazards (Great Britain)
PHE	Public Health England
PI	Proliferation Index
p-IRES2	plasmid – Internal Ribosome Entry Site
PLSDA	Partial Least Square Discriminant Analysis
PLT	Platelets
POL	Poland
PRT	Portugal
Pu	Plutonium
QA/QC	Quality Assurance / Quality Control
qRT-PCR	quantitative Reverse Transcription – Polymerase Chain Reaction
R/N / RN	Radiological and Nuclear
RANET	Radiation Assistance Network
RARAF	Radiological Research Accelerator Facility
RBC	Red Blood Cells
RBE	Relative Biological Effectiveness
RC	Response Category
RCI	Radiation Combined Injury
RDD	Radiation Dispersal Device
RDT&E	Research, Development, Test, and Evaluation
REAC/TS	Radiation Emergency Assistance Center / Training Site (United States)
RED	Radiation Exposure Device
REDD	Regulated in Development and DNA damage responses
REMPAN	Radiation Emergency Medical Preparedness and Assistance Network
RENEB	Realizing European Network in Biodosimetry
RES	Radiation Exposure Status

rh	recombinant human
RIBE	Radiation-Induced Bystander Effect
RI-MODS/MOF	Radiation-Induced Multi-Organ Dysfunction Syndrome / Multi-Organ dysfunction Failure
RIPD	Radiation-Induced Performance Decrement
RNA	Ribonucleic Acid
RPD	Radiation Products Design
RTA	Research Technology Agency (NATO)
RTB	Research and Technology Board
RTD	Radiation Threshold Dose
RTG	Research Task Group
SAA	Serum Amyloid Protein
SE	Standard Error
SEARCH	System for Evaluation and Archiving of Radiation accidents based on Case Histories
SEM	Standard Error of the Mean
SFT3	Stem Cell factor, FLT-3 ligand and interleukin-3 combination
Shh	Sonic hedgehog
siRNA	small interfering RNA
SIRS	Systemic Inflammatory Response Syndrome
SME	Subject-Matter Expert
SOLO	Epidemiological studies of exposed populations in the Southern Urals
SOM23	Somatostatin analog
SPRA	French Defence Radiation Protection Service (France)
STANAG	Standardisation Agreement
STO	Science and Technology Organization
SUBI	Southern Urals Biophysics Institute (Russia)
TBD	To Be Determined
TBI	Total Body Irradiation
TBSA	Total Body Surface Area
TENEB	Towards a European Network of Excellence in Biological dosimetry
TF	Tissue Factor
Th/M	Thlymphocyte/Macrophage
TLD	Technical Laboratory Director
TNF	Tumor Necrosis Factor
TPP	Techno Plastic Product
TRL	Technology Readiness Level
U.S./USA	United States of America
UCL	Upper Confidence Limit
UK	United Kingdom
UN	United Nations
USUHS	University of the Health Sciences (United States)
VC	Vitamin C
vWF	von Willebrand Factor
WBC	White Blood Cells
WBI	Whole Body Irradiation
WHO	World Health Organisation
WMD	Weapons of Mass Destruction
XA	Annonaceae
ZUB	Zentrale Unterstützungsstelle des Bundes (Germany)

Preface

Thirty years ago when the proceedings of the 1985 workshop of the NATO Research Study Group (RSG-5) on the Assessment of Ionizing Radiation Injury in Nuclear Warfare [Ottawa, Canada, DS/A/DR (86) 191] were published, the main concern of both the NATO Military Command and the Medical Advisor was to predict the performance decrement and medical outcome of irradiated troops following a nuclear detonation. Since the end of the Cold War, the Radiological/Nuclear (RN) threat has changed but is still present and unexpected. Nuclear weapons remain Weapons of Mass Destruction (WMD) whereas the emergence of technologically skilled terrorist groups and rogue states has made multi-form the scenarios of malevolent ionizing radiation exposure. Regarding the number of victims involved in such RN situations, small size to mass casualty events may happen. Radiation Dispersal Devices (RDD), Radiation Exposure Devices (RED) and Improvised Nuclear Devices (IND) are plausible detrimental tools. This threat has recently been emphasized by the European Parliament [1] and dedicated training courses are organized under the European Commission's umbrella [2].

The rationale of the HFM-222 RTG activities is based on the Allied Joint doctrine for comprehensive chemical, biological, radiological, and nuclear defence (AJP-3.8). The CBRN threat environment has broadened the battlefield to the globe. This includes the Alliance's populations, territory and forces without any restriction concerning temporal, geographical, social or political limits. Forces must be prepared to execute and support prevention, protection, and recovery measures and operations during a CBRN incident that affects both civilian populations and military forces. The RN threat remains a critical concern for all NATO military commanders and medical advisors. Medical radiation preparedness requires a full-spectrum understanding of the mechanisms of action of ionizing radiation, rapid diagnosis of exposure, and how to most effectively counter their effects – either pre- or post-exposure. In the context of defence operations in a RN environment, whatever the mission to be fulfilled, any efforts should contribute to prevent fatalities, better take care of radiation casualties and optimize return to duty. The HFM-222 RTG has therefore aimed at optimizing available countermeasures and bridging medical gaps.

The main challenge of this RTG was to take into account updated scenarios of the RN threat in order to develop appropriate MedCM. Two exercises based on RED scenarios were performed and exploited by the RTG (2011 – 2012 and 2015 – 2016). The first one resulted in five 2013 publications in radiation research with a front cover in the Journal *Radiation Research*, and another international publication to come for the second exercise. Other exercises dedicated to RDD and IND scenarios, and radiation accidents should be carried out in a near future. The difficulty resides in the fact that so far NR events have been accounted for almost only by accidents. Consequently research in radiation biology has been dealing with models simulating more often accidents than RDD or IND. In a consistent manner, NATO's dual activities lead this organization to promote actions to build a bridge between civilian and defence CBRN CM.

Modelling is very helpful to unravel complex threats and consequent injuries. This RTG has been involved in RN environments modelling, physiological modelling and injury criteria modelling. Indeed it is necessary to model the number and the diversity of casualties caused by terrorist devices or warfare operations because of the complexity of combined injuries (blast, trauma, thermal burns, external and internal irradiation, external and internal contamination, any combination of the above) and to include demographics that can influence individual response to irradiation. Here an additional layer of research should include a better knowledge of individual radio-sensitivity. Furthermore, an inflammation model being developed for combined injury may provide a resource for estimating latent multi-organ failure. A model for partial-body exposures is also being developed. The RTG produced different mature and deployable software tools dealing with the assessment triage (i.e., Mobile-FRAT an Android and IOS-based application) or the evaluation of Radiation-Induced Performance Decrement (RIPD) and Health Effects from Nuclear and Radiological Environments (HENRE) which integrate complex exposure scenarios.

In a comprehensive way, to ensure Forces health protection, pre-incident, during incident and post-incident medical care, and then rehabilitation, appropriate medical countermeasures have to be designed, developed, validated and made available to the Forces. Regarding defence operations in an identified RN environment, use of radio-protectants may be a good option warranting dedicated research and development studies. Candidate molecules

have been evaluated by this RTG. Unfortunately, when considering terrorists attacks that are unexpected in nature, the prophylactic approach is of low utility and all biomedical research efforts should be focused on diagnosis, mitigation and treatment of RN damage. Significant efforts were made to mitigate external irradiation toxicity using hematopoietic growth factors (e.g., G-CSF), cytokines and cell/gene therapy. Several studies are included in the Technical Report. Future research should be focused on deployable, well tolerated and effective mitigators and therapeutics. Moreover, always regarding high-level radiation exposure, new combined injury models and a better knowledge of the development of RI-MODS/MOF are needed.

Another new challenge had to be faced with respect to the societal evolution and peoples' concerns about low-level radiation issues. On one hand, anti-nuclear lobbies challenge the civil nuclear energy and the nuclear deterrent, on the other, low-level radiation issues have become an increasing matter of concern after the Fukushima catastrophe. The understanding of RN health challenges embraces not only acute and delayed toxicity of high-level radiation, but also low-level radiation toxicity, in particular carcinogenesis. The matter for this RTG was not to define what a low dose is, but to identify late deterministic or stochastic bioeffects of radiation doses below the ARS threshold for soldiers and populations exposed to an accidental or malevolent RN environment.

Interestingly, an initiative was launched by this RTG to get a better knowledge of NATO RN medical technical capabilities. A survey on current biodosimetry capabilities has been performed and NATO Role 4 biodosimetry assays TRL has been updated. This kind of survey should now be extended to other capabilities such as operational radiological triage, radiological decontamination and ARS therapeutics.

Also of interest for the NATO NR medical community are studies carried out by radiation physicists. As an example, a special issue of *Health Physics* [3] presents a body of experimental work characterizing the outdoor atmospheric release of short-lived radioisotopes, used as tracers, in order to simulate real-world threat or accident scenarios involving the dispersion of radioactive material. The use of short-lived radioactive tracers made it possible to perform experiments that are impossible to perform using long-lived isotopes and high activities. To complement this work and identify appropriate MedCM, it would be valuable to develop animal models of RDD.

Regarding the medical management of long-term effects of ionizing radiation, it is fortunate that radiotherapy patients can benefit from a better and longer quality of life thanks to optimized care. Moreover, A-bomb survivors could have been followed in the long-term allowing important clinical observations. As a counterpart, significant morbidity related to radiation-induced (high radiation levels to fractionated intermediate radiation levels with high dose rates) multi-organ toxicity remains to be mitigated.

As mentioned in AJP-3.8 doctrinal document, casualty management in a CBRN environment refers to post-incident medical capabilities that are used to preserve the health of the force, to deliver optimal care to casualties and to maximize the rate at which casualties return to duty. In the aftermath of a RN incident, the number of casualties may far exceed the capacity of the medical treatment system. The medical planning staff must develop a plan for managing a substantial increase in casualty flow and the demand for treatment. The plan must address decontamination handling and movement of radiation casualties, and treating the wide range of RN injuries and illnesses. Optimized medical plans are required.

A future objective of the current members of this RTG is to mount training courses for medical first responders to disseminate knowledge and expertise, identify best practices, capacity building, create synergies among NATO Member Nations, and contribute to radiation preparedness and resilience to mass casualties resulting from acts of terror using ionizing radiation.

To conclude, it was not possible to address all the issues raised in the Terms of Reference. However, significant work has been made by the HFM-222 RTG and useful deliverables have been produced. Moreover, we advise the reader to consult the 80 scientific publications (and more to come) produced by the members of the RTG during the 2012 – 2016 period, which are listed in Chapter 5.

Exchanges with NATO non-medical RN experts as well as non-NATO medical experts is welcome in order to better take into account all aspects of the RN threat that may affect the Forces and civilians populations. The joint efforts of

the HFM-222 RTG must certainly be pursued in a follow-on RTG that would include more Nations to fill remaining gaps.

- [1] [http://www.europarl.europa.eu/RegData/etudes/BRIE/2015/572806/EPRS_BRI\(2015\)572806_EN.pdf](http://www.europarl.europa.eu/RegData/etudes/BRIE/2015/572806/EPRS_BRI(2015)572806_EN.pdf), (The European Parliament. briefing December 2015).
- [2] European Commission, Directorate General Migration and Home Affairs. A training course on the triage, monitoring and treatment of Mass Casualties resulting from a Terrorist Attack involving Ionising Radiation. Campus Vesta, Belgium September 25-29, 2016.
- [3] Health Physics (Special Issue) 2016:110;399- 547.

Foreword

The Human Factors and Medicine Panel of the NATO's Science and Technology Organization (STO/HFM) has long been recognizing the risks of radiation threats to military forces. Indeed, significant gaps still exist in our understanding of mechanisms of radiation-induced biomedical effects, threat assessment capabilities, and medical countermeasures to protect, mitigate, treat, and manage acute as well as late radiation effects relevant to the military personnel and operations. The STO/HFM Research Task Group 222 (HFM-222/RTG) entitled "Ionizing Radiation Bioeffects and Countermeasures: Current Status and Future Perspectives" started its activity in the spring of 2012 as a follow-on from the previous HFM-099/RTG-033 "Radiation Bioeffects and Countermeasures"; in 2015 the activity of the HFM-222/RTG was extended till June 2016. The Group, composed of representatives of eight NATO Nations (CZE, DEU, FRA, GBR, ITA, NLD, POL, USA) and Armenia was very active through its lifespan holding one meeting every year from 2012 to 2016. The functioning of the HFM-222/RTG was skillfully arranged and led by its chairman, Dr. Francis J. Hérodin (FRA), Head of the Radiobiology Department of the French Armed Forces Biomedical Research Institute (Institut de Recherche Biomédicale des Armées). Under his leadership, the RTG has provided a venue to convene nineteen radiobiology experts from a broad spectrum to share pertinent knowledge.

I commend the HFM-222/RTG for its efforts and the valuable content of the Final Report which reflects considerable progress in research on health effects of both high and low levels of ionizing radiation focusing on biological dosimetry (diagnostic and predictive indicators), radio-protectors, mitigators, treatment of Acute Radiation Syndrome (ARS), and prevention of late effects. Especially commendable are the tangible deliverables of the Task Group such as improving triage of casualties in a large-scale radiation incident, development of deployable medical planning tools, contribution to the FDA approval of granulocyte colony-stimulating factor (filgrastim) to mitigate radiation-induced neutropenia, and last but not least, eighty peer-reviewed publications.

Certainly, not all radiobiology gaps applicable to operations of NATO forces have been addressed and filled by the HFM-222/RTG. Indeed, additional work is needed to translate the results of the state-of-the-art radiobiological research into workable standard procedures of, for example, rapid and reliable diagnostics, allocation of scarce medical resources, treatment following medical evacuation, handling of combined injuries, detection and exploitation of plausible beneficial effects of low-level exposures, etc. These and other relevant challenges underscore the importance to continue the activities of the HFM-222/RTG in a future edition of the Radiation Bioeffects and Countermeasures Task Group.

*Col (ret) Prof Marek K. Janiak, MD, PhD
HFM-222 RTG mentor*

Terms of Reference

I. ORIGIN

A. Background

Proliferation of radioactive material, nuclear weapons and nuclear power facilities has increased the likelihood that multinational military forces will encounter a local or widespread radiological hazard. Such nuclear/radiological hazards can result from hostile acts short of nuclear war to the deliberate spread of radioactive material from industrial or medical sources, accidental or intentional destruction of nuclear facilities during a conflict, accidents involving radiation sources, or the detonation of improvised nuclear devices by terrorists, failing countries or hostile forces. These radiation hazards have the potential of disrupting and compromising NATO military operations, and therefore represent a current and creditable threat issue.

Recommended countermeasures must take into account operational as well as medical implications of exposure to ionizing radiation over a sizable range of exposure intensities, qualities, and durations. Consideration of this potential variation in radiation exposure intensities is in part captured by the NATO STANAG 2083 and its listing of Radiation Exposure Status (RES) categories ranging 1 through 3.

Of additional concern, is that the nuclear/radiological hazard is amplified by the proliferation of the weapons of mass destruction, biological and chemical threat agents, and other environmental stressors, that may present during a mission.

Previous research study groups (e.g., NATO HFM-099/RTG-033) on ionizing radiation injury have concentrated almost exclusively on the dosimetry and biological effects of the high doses associated with general nuclear war. The management of early acute effects of such radiation exposures and their impact on continued operational availability of exposed personnel and ultimately survival predominated. The changing world order and consequent defence planning assumptions do not exclude high-dose exposure (though in different circumstances), but predicate a new emphasis on the lower doses that may be encountered in future operations whether through accident or hostile intent. These exposures may produce some acute effects that may impact on operational performance, but the principal risk will be in long-term effects and in the outbreak of a mass panic amongst the potentially exposed public, fuelled by a general fear of radiation and the uncertainty about the individual exposure level.

Thorough evaluation of major late-arising pathologies (e.g., cancer, fibrosis, chronic recurrent infections) in terms of pathogenesis and the identification, development, and testing of safe and effective medical countermeasures require considerably more time than the three-year study cycle allotted by the NATO RTO.

Despite the successes of previous Research Task Groups in developing essential procedures and equipment requirements to manage the extreme radiological hazards associated with nuclear weapons in the context of general war, the reduced risk of general nuclear war has made past assumptions about acceptable levels of radiological contamination and acceptable doses of radiation to soldiers inadequate. Although these exposure levels and associated health hazards have been revisited, justified, and considered relative to currently acceptable peacetime limits for occupational/non-occupational workers (by virtue of the NATO ACE Directive 80-63), still additional re-evaluation and refinement of these radiation exposure guidelines are needed, particularly in light of the fact that current exposure guidelines do not take into account the effects of exposure rate, radiation quality and committed dose.

The need to research and develop new and improved methods to counter these nuclear/radiological threats is clear and unambiguous. The current biotechnology/bioengineering revolution is presenting unprecedented opportunities to significantly extend our understanding of the molecular and cellular details of radiation toxicity (early and late effects), thus enhancing our capacity for strategic design and development of safe and effective pharmacologic/biologic countermeasures, as well as tissue regeneration approaches.

The Research Task Group HFM-099/RTG-033 made significant progress toward developing essential scientific bases upon which to build new bioassessment tools and to develop new and better methods for preventing and treating injuries associated with ionizing radiation exposure. This work warrants a continuation of effort, thus a new three-year study cycle is proposed.

B. Justification

Medical and armament planners require scientifically founded data to develop guidance and recommendations in order to deal with the new situation described above. Recommendations must take into account operational as well as medical implications of exposure to ionizing radiation at a range from RES Category 1 through 3 (STANAG 2083). Similarly, planners need to consider the radiological guidelines set forward in the ACE Directive 80-63. Further, due to the proliferation of weapons of mass destruction, interactions with BW/CW agents and other stressors as well as medical prophylaxis may also be addressed.

It is, therefore, clear that currently available physical and biomedical scientific data are not sufficient to develop the necessary advice for commanders in emergency situations, nor are doctrine, training, and equipment. The findings and recommendations will be passed on to the appropriate groups responsible for preparing guidelines for operations in low-level radiation environments.

The proposed new Research Task Group is required because no Member Nation has the expertise and resources in all these areas of interest; therefore, a cooperative effort is necessary and should address the topics as listed below.

II. OBJECTIVES

A. Research Area and Scope

In a preliminary phase, currently available medical countermeasures and biodosimetric methods, and the state-of-the-art in Research, Development, Test, and Evaluation (RDT&E) on ionizing radiation bioeffects and medical countermeasures being conducted by the various Nations' respective programs will be reviewed.

The research area and scope of the proposed RTG will be “to develop the scientific basis for new and improved methods to prevent, assess, treat, and manage casualties and long-term health effects (stochastic and non-stochastic) associated with ionizing radiation exposure from evolving threats in military operations. To focus mainly on early events related to Radiological Dispersal Device (RDD) and Radiological Exposure Device (RED) scenarios to improve medical responses for mass casualty management.”

B. Specific Goals

The specific goals of the RTG and topics to be covered will include the state-of-the-art in:

- Research into mechanisms of action of ionizing radiation injury:
 - Establishment of origins and mechanisms of acute radiation-induced pathology
 - Establishment of origins and mechanisms of delayed Multi-Organ Dysfunction Syndrome and Failure (MODS/MOF)
 - Development and characterization of suitable animal models for the study of acute radiation syndrome and Multi-Organ Dysfunction Syndrome and Failure (MODS/MOF)
 - Identification of biomarkers of ionizing radiation exposure that correlates between animals and human.
- RDT&E into radio-protectants (administered before irradiation):
 - Mechanism of protection to include correlate / surrogate markers of protection
 - Relative efficacy and limitations of promising classes of radio-protectants.
- RDT&E into post-irradiation treatments against ionizing radiation injury:
 - Mechanisms of disease mitigation or treatment

- Relative efficacy and limitations of promising classes of radiation mitigators and treatments.
- Research and development on biodosimetric methods to estimate the level of radiation exposure and severity of radiation injury:
 - Standardized rapid dose assessment for triage of potentially exposed personnel and mass-casualty management
 - Development of broad-spectrum bioassessment tools for sensitive, accurate, and reliable detection of radiation-associated injuries. Consider a multi-parameter approach to assist in the prediction of clinical outcome
 - Considerations: cost per test, complexity, interference effects, sample collection and preparation, storage, shelf life.
- Identification of predictors, indicators and prophylactic or therapeutic treatments for radiation-induced late effects such as cancer, cardiovascular disease, cataractogenesis or fibrosis.
- Integration of medical expertise and RDT&E to provide specific recommendations to NATO COMEDS. Guidance to inform field commanders and deployed forces.

C. Deliverables

These activities will culminate in the publication of a Technical Report and may serve as the basis for a Research Symposium on the subject.

D. Duration of Technical Team

This Technical Team will be chartered for three years upon RTB approval: 2012 – 2015.

III. RESOURCES

A. Membership

Nations participating (tentative): CAN, CZE, DEU, FRA (Leader), GBR, HUN, NLD, NOR, PRT, and USA. An updated list of participating Nations in the RTG will be made by the HFM via liaison reports. Nominations are encouraged from NATO.

B. National/NATO Resources Required

Sufficient resources in terms of personnel, equipment, and supplies are currently available within the research facilities of each of the participating Member Nations.

General administrative guidance and support from NATO/RTA is requested, along with technical and financial assistance in publishing and distributing technical reports. Financial support for RTG-associated travel, including PFP delegates and RTG consultants is requested as well.

IV. SECURITY CLASSIFICATION LEVEL

Unclassified/Unlimited.

V. PARTICIPATION BY PARTNER NATIONS

Membership of the RTG is open; participation by Partner Nations is available.

VI. LIAISON

Liaison and coordination with COMEDS, in particular the NATO CBRN Medical Working Group.

Acknowledgements

Pr. Dr. Marek K. Janiak (POL) served as the Referee for the Ionizing Radiation Bioeffects and Countermeasures HFM-222 RTG. He provided helpful guidance to this RTG. The HFM-222 RTG Chair also extends thanks to all members who contributed to the success of the RTG tasks. There were five annual HFM-222 RTG meetings that were key events in the conduct of the RTG activities. The Chair is grateful to the respective host Nations, Institutes' leadership, and gives credit to the local hosts who organized the meetings and provided excellent social activities. In addition, the excellent editorial, publishing, and graphic support services by the NATO STO Publication Office / Editor are gratefully acknowledged.

Francis Hérodin (FRA)
HFM-222 RTG Chair

HFM-222 Membership List

Col. Pr. Dr. Michael ABEND
Bundeswehr Institute of Radiobiology
Deputy Director
Neuherbergstrasse 11
D-80937 München
GERMANY
Email: michaelabend@bundeswehr.org

Dr. Artak BARSEGHYAN
Engineering Academy of Armenia
Teryan 105, bld. 17
Yeravan 0009
ARMENIA
Email: artakbarseghyan@yahoo.com

Dr. William BLAKELY
Armed Forces Radiobiology Research Institute
Uniformed Services University of Health
Sciences
8901 Wisconsin Avenue
Bethesda, MD 20889-5603
UNITED STATES
Email: William.blakely@usuhs.edu

Dr. Andrea DE AMICIS
Ministero della Difesa
Histology & Molecular Biology Section
Italian Army Medical & Veterinary Research
Centre
Via di Santo Stefano Rotondo 4
00184 Roma
ITALY
Email: andre.deamicis@gmail.com

Dr. Stefania DE SANCTIS
Ministero della Difesa
Histology & Molecular Biology Section
Italian Army Medical & Veterinary Research
Centre
Via di Santo Stefano Rotondo 4
00184 Roma
ITALY
Email: stefania.desanctis@gmail.com

LtCol. Dr. Harald DOERR
Bundeswehr Institute of Radiobiology
Neuherbergstrasse 11
D-80937 München
GERMANY
Email: haralddoerr@bundeswehr.org

Col. Dr. Michel DROUET
Institut de Recherche Biomédicale des Armées
BP 73, F-91223 Brétigny-sur-Orge
FRANCE
Email: michel.drouet@irba.fr

Dr. Francis Jean HÉRODIN (Chair)
Institut de Recherche Biomédicale des Armées
Head of Radiobiology Department
BP 73, F-91223 Brétigny-sur-Orge
FRANCE
Email: francis.herodin@irba.fr

LTC Matthew HOEFER
Armed Forces Radiobiology Research Institute
Uniformed Services University of Health Sciences
Building 42
8901 Wisconsin Avenue
Bethesda, MD 20889-5603
UNITED STATES
Email: matthew.hoefer@usuhs.edu

Col. Lester A. HUFF
Armed Forces Radiobiology Research Institute
Uniformed Services University of Health Sciences
Building 42, Room 3432-H
8901 Wisconsin Avenue
Bethesda, MD 20889-5603
UNITED STATES
Email: lester.huff@us.af.mil

Pr. Marek JANIĄK
Military Institute of Hygiene & Epidemiology
Head, Dept. of Radiobiology & Radiation Protection
128 Szaserów Street
04-141 Warsaw
POLAND
Email: mjaniak@wihe.waw.pl

Mr. Tjerk KUIPERS
Health Physics, Military Healthcare & Occupational
Health Expertise Co-ordination Centre
Support Command, Ministry of Defence
Korte Molenweg 3
Doorn Villa Aardenburg, Room 206
P.O. Box 185
3940 AD Doorn
NETHERLANDS
Email: tp.kuipers.01@mindef.nl

Col. Dr. Florigio LISTA
Ministero della Difesa
Head Histology & Molecular Biology Section
Italian Army Medical & Veterinary Research
Centre
Via di Santo Stefano Rotondo 4
00184 Roma
ITALY
Email: romano.lista@gmail.com

Dr. Mark H. WHITNALL
Armed Forces Radiobiology Research Institute
Uniformed Services University of Health
Sciences
8901 Wisconsin Avenue
Bethesda, MD 20889-5603
UNITED STATES
Email: mark.whitnall@usuhs.edu

Dr. Alexandra MILLER
Armed Forces Radiobiology Research Institute
Uniformed Services University of Health
Sciences
8901 Wisconsin Avenue
Bethesda, MD 20889-5603
UNITED STATES
Email: alexandra.miller@usuhs.edu

Dr. Ewa NOWOSIELSKA
Adjunct/Dept of Radiobiology and Radiation
Protection
4 Kozielska St.
01-163 Warsaw
POLAND
Email: enowosielska@wihe.waw.pl

Maj. Dr. Jaroslav PEJCHAL
University of Defence
Faculty of Health Sciences
Head of Radionuclear Group Centre of Advances
Studies
Trebeska 1575
500 01 Hradec Kralove
CZECH REPUBLIC
Email: jaroslav.pejchal@seznam.cz

Col. Dr. Matthias PORT
Bundeswehr Institute of Radiobiology
Director
Neuherbergstrasse 11
D-80937 München
GERMANY
Email: matthias.port@gmail.com

Dr. Daniela STRICKLIN
Applied Research Associates Inc.
801 N. Quincy Street, Suite 700
Arlington, VA 22203
UNITED STATES
Email: dstricklin@ara.com

Biological Effects of Ionising Radiation and Countermeasures

(STO-TR-HFM-222)

Executive Summary

Task Group 222 of the Human Factors and Medicine (HFM) Panel of NATO/STO (HFM-222 RTG) was created in order to better deal with the medical aspects of the current Nuclear and Radiation (NR) threat that could affect NATO forces during defence operations. The overall objective of the group was to develop and propose medical countermeasures optimised with respect to this threat. The work plan was based on policy document AJP-3.8 whose principal aim is to improve the diagnosis, prevention and treatment of the health effects of exposure to low and high doses of ionising radiation. The NR threat is in fact still probable, diverse and unpredictable. It must be dealt with medical effectiveness by acquiring more detailed understanding of the toxicity of radiations and of the mechanisms of action involved in order to determine suitable countermeasures. This threat must also be anticipated by table-top or application exercises based on scenarios of the use of NR agents on military and civilian targets. These exercises help raise the level of radiobiological preparation of NATO's medical staff by additional training of players involved.

The eight Nations participating in HFM-222 have not claimed to have resolved all shortfalls in the medical management of irradiated and radio-contaminated victims. The group examined primarily questions of external irradiation, in particular the diagnosis and treatment of the acute radiation syndrome, including the early and late biological effects of high doses. In addition, the group pointed out the importance of determining the effects of low doses in order to cope with the public health challenges arising from Fukushima-type accidents or malevolent dispersion of radioactive materials, e.g., "dirty bombs".

In practice, the group optimised diagnostic tools using multi-parametric biological dosimetry (cytogenetics, haematology, proteomics and genomics). Aiming at augmented efficiency, the group progressed from the traditional concept of dose biomarkers (biological estimation of total irradiation dose received) to that of biomarkers of effects and damage with an eye towards both the victims' diagnosis and prognosis. It improved the treatment of the radio-induced haematology syndrome (high total doses) and contributed to the Food and Drug Administration's approval of the use of a haematopoietic growth factor, filgrastim, to rapidly treat victims exhibiting haematological failure. Cell and gene therapy tools have been developed, in particular using mesenchymal stem cells from adipose tissue, to treat the cutaneous radiological syndrome (very high localised doses); relevant study models of the effects of low doses were also developed. All the scientific results obtained by HFM-222 have not reached the same level of technological maturity; these results involve almost 70 international publications. Several modelling tools applied to various aspects of radiological damage are very useful – biodosimetry and triage software applications are operational and deployable, including Mobile-FRAT (First-responders Radiological Assessment Triage). A survey of the capacities of HFM-222 members' biodosimetry laboratories and of their technological competence was conducted. Finally, a table-top exercise has enabled the group to arrive at a rapid and reliable diagnosis and prognosis involving 200 medical cases of externally irradiated victims based on clinical signs and symptoms, and on haematology parameters.

The ongoing development of powerful cell and molecular biology techniques, as well as sophisticated biomathematical models, explain the extension of the work of HFM-222 in the context of a new RTG to last for three years in order to continue to anticipate the triage of irradiated and contaminated victims and to make their medical management more effective.

Les effets biologiques des rayonnements ionisants et leurs contre-mesures

(STO-TR-HFM-222)

Synthèse

Le groupe de travail 222 du panel HFM de l'OTAN/STO (HFM-222 RTG) a été créé pour mieux prendre en compte les aspects médicaux de la menace nucléaire et radiologique (NR) actuelle pouvant affecter les forces de l'OTAN dans le cadre d'opérations de défense. L'objectif global du groupe a été de développer et de proposer des contre-mesures médicales optimisées vis-à-vis de cette menace. Le plan de travail s'est fondé sur le document de doctrine AJP-3.8 et a visé principalement à améliorer le diagnostic, la prévention et le traitement des effets sanitaires dus à l'exposition à des fortes doses et à des faibles doses de rayonnements ionisants. En effet, la menace NR est toujours probable, diverse et inattendue. Elle doit être combattue avec efficacité sur le plan médical en approfondissant la connaissance de la toxicité des radiations et celle des mécanismes d'actions impliqués afin d'identifier des contre-mesures adéquates. Cette menace doit aussi être anticipée par des exercices de table ou d'application basés sur des scénarios d'utilisation malveillante des agents NR vis-à-vis des forces armées et des populations civiles. En renforçant la formation des acteurs, ces exercices contribuent à augmenter le niveau de préparation radiobiologique des personnels médicaux de l'OTAN.

Les huit nations participant au HFM-222 ne prétendent pas avoir comblé toutes les lacunes dans le domaine de la prise en charge médicale des blessés irradiés et radiocontaminés. Le groupe a étudié essentiellement les questions d'irradiation externe et, en particulier, le diagnostic et le traitement du syndrome aigu d'irradiation. Les effets biologiques précoces et tardifs des fortes doses ont été étudiés. De plus, le groupe a relevé l'importance d'étudier les effets des faibles doses pour répondre aux défis sanitaires liés à des accidents type Fukushima ou à la dispersion malveillante de matières radioactives.

En pratique, le groupe a optimisé les outils diagnostiques utilisant la dosimétrie biologique multiparamétrique (cytogénétique, hématologie, protéomique et génomique). Visant une plus grande efficacité, le groupe est passé de la conception traditionnelle des biomarqueurs de dose (estimation biologique de la dose d'irradiation globale reçue) à celle de biomarqueurs d'effet et de dommage visant à la fois le diagnostic et le pronostic des victimes. Il a amélioré le traitement du syndrome hématologique radio-induit (doses fortes globales) et contribué à l'approbation par la *Food and Drug Administration* de l'utilisation d'un facteur de croissance hématopoïétique, le filgrastim, pour traiter rapidement les victimes développant une détresse hématologique. Des outils de thérapie cellulaire et génique utilisant notamment des cellules souches mésenchymateuses du tissu adipeux ont été développés pour traiter le syndrome cutané radiologique (doses très élevées localisées). En outre, des modèles pertinents d'étude des effets des faibles doses ont été développés. Les résultats scientifiques obtenus par le HFM-222 n'ont pas tous la même maturité technologique. Près de 70 publications internationales ont été réalisées. Plusieurs outils de modélisation des différents aspects du dommage radiologique sont très utiles, des logiciels de biodosimétrie et de triage sont opérationnels et déployables, parmi lesquels l'application Mobile-FRAT (*First-responders Radiological Assessment Triage*). Un inventaire capacitaire des laboratoires de biodosimétrie des membres du HFM-222 et de leur maîtrise technologique a été conduit. Enfin, un exercice de table a permis au groupe de poser un diagnostic et un pronostic rapides et fiables sur 200 cas médicaux d'irradiés externes à partir des signes et symptômes cliniques et des paramètres hématologiques.

Le développement continu de techniques puissantes de biologie cellulaire et moléculaire ainsi que de modèles biomathématiques sophistiqués justifie la poursuite des travaux du HFM-222 dans le cadre d'un nouveau RTG pour un mandat de trois ans afin d'anticiper encore le triage des blessés irradiés et contaminés et de rendre plus efficace leur prise en charge médicale.



Chapter 1 – HIGH-LEVEL RADIATION BIOEFFECTS

1.1 GENERAL INTRODUCTION

1.1.1 Biomarkers of Exposure and Effects

Evaluating the damage remains the first priority following high-dose exposure to discard the flow of worried wells and ensure the optimal use of the limited amounts of available treatments. Time constraints are a big challenge, which justifies the current research effort from numerous teams to identify new tools more flexible than the dicentric assay gold standard (DIC). Establishment of automated scoring is underway applied to different approaches (DIC, PCC, cytokinesis-block micronucleus assay – A. De Amicis). Identifying biomarkers to discriminate/separate total-body irradiation from partial-body irradiation is another challenge. Thus, in an elegant baboon study this was achieved during the prodromal and the manifest phase of Acute Radiation Syndrome (ARS) using biochemical markers and hematological parameters (aspartate aminotransferase, creatine kinase, lactate dehydrogenase, urea, Flt3-ligand, iron, C-reactive protein, absolute neutrophil count and neutrophil-to-lymphocyte ratio for the early period, and Flt3-ligand, iron, platelet count, hemoglobin, monocyte count, absolute neutrophil count and neutrophil-to lymphocyte ratio for the ARS phase; M. Valente, F. Hérodin). Improvements in emergency preparedness for radiological mass casualty scenarios performed by non-NATO networks were also updated (K. Rothkamm).

1.1.2 Medical Countermeasures (MedCM)

MedCM include protection, mitigation and repair of radiation-induced damage including cell therapy approaches. Target tissues are represented by the METREPOL Hematopoietic-Neurovascular-Cutaneous-Gastro-intestinal categorization and different strategies have been developed for some years to especially mitigate (stem) cell death and inflammatory/thrombotic processes. Indeed, regarding radio-protectors/mitigators, anti-thrombotic and anti-inflammatory agents may represent useful tools. From numerous drugs, derivatives of nicotinic acid (NAc, NA, MNA, 1.4-DMP and 1.3-MAP) were tested and depending on the time of application showed some efficacy not related with mitigation of the hematopoietic syndrome (M. Janiak, E. Nowosielska). AFFRI remains strongly involved in this topic identifying numerous promising candidates against pure radiation (gamma rays, mixed neutron/gamma rays) and radiation combined with other injury (combined injury) with clear path to licensure whose advanced development is still hampered by the limitation of funding (M. Whitnall). IRBA/CRSSA has also emphasized for some years the benefit of early cytokine injection to mitigate hematological toxicity. Therefore, following the 2015 FDA announcement of Granulocyte-Colony Stimulating Factor indication to stimulate residual hematopoiesis in accidental settings, this strategy will now be endorsed by NATO members in addition to supportive care recommendations (AMedP-7.1, CBRNMedWG). With respect to animal rules, mini-pig was validated by AFFRI as a valuable model in this area. Regarding cytokines and extra-hematological toxicity, mitigation of gastro-intestinal sub-syndrome by Epidermal Growth Factor was also confirmed in a bone-marrow transplantation mouse model (J. Pejchal). Finally, cell/transient gene therapy was evaluated at IRBA. Reduction of damages at the hematopoietic niche level with multi-lineage recovery was demonstrated in highly irradiated monkeys (sonic hedgehog morphogene construct) in addition to the therapeutic potential of local injection of Adipose derived stem cell towards Cutaneous Radiation Syndrome (M. Drouet). Apart from Mesenchymal Stromal Cells, these strategies may appear still in their infancy but are promising for the future.

1.1.3 Modelling Guidance

Physiologically-based mathematical models have been developed to predict morbidity and lethality of acute radiation syndrome and to evaluate the efficacy of mitigating treatments with a specific effort to explore complex associated pathologies (burn, trauma, radiation combined injury) and mimic scenario allowing the prediction of practical needs (D. Stricklin).

1.2 BIOMARKERS OF EXPOSURE AND EFFECTS

1.2.1 Time-Dependent Relevance of Radiation Biomarkers to Distinguish Partial-Body from Total-Body Exposures

Abstract

In a large-scale radiation event the ability to discriminate Partial-Body Irradiation (PBI) from Total-Body Irradiation (TBI) will be essential to optimise medical care, as the later will be more likely to lead to an Acute Radiation Syndrome (ARS) and therefore a need of hematologic support.

To identify the usefulness of several biomarkers in this TBI vs PBI distinction, pairs of baboons (n=18) were subjected to dose-equivalent ⁶⁰Co gamma radiation with varying percentages of Bone Marrow (BM) exposed: 5 Gy TBI; 7.5 Gy left hemibody/2.5 right hemibody TBI; 5.55 Gy 90% PBI; 6.25 Gy 80% PBI; 10 Gy 50% PBI, 15 Gy 30% PBI) or 2.5 Gy (2.5 Gy TBI; 5 Gy 50% PBI.

Over fifty markers were studied from before to up to 200 days after irradiation. A partial least square discriminant analysis was used to validate this model for the distinction between TBI and PBI. Then, all the individuals were combined in two groups, TBI (n=6) and PBI (n=12), for comparison using a logistic regression and a non-parametric statistical test. Nine plasmatic biochemical and most of hematological parameters allowed a distinction of the two groups during the prodromal phase and the manifest illness phase. The most discriminating biomarkers were aspartate aminotransferase, creatine kinase, lactico dehydrogenase, urea, Flt3-ligand, iron, C-reactive protein, absolute neutrophil count and neutrophil-to-lymphocyte ratio for the early period, and Flt3-ligand, iron, platelet count, hemoglobin, monocyte count, absolute neutrophil count and neutrophil-to-lymphocyte ratio for the ARS phase. These results suggest that total exposures can be distinguished from partial irradiations within a range of 2.5 to 5 Gy TBI.

1.2.1.1 Introduction

It is very likely that a Radiological or Nuclear (RN) event will lead to a heterogeneous population, with diverse degrees of shielding and radiation doses. In case of a large-scale event, the ability to quickly reassure the “worried well” will be essential to concentrate the limited medical aid to the exposed victims. Then, determining the extent of exposure to their body will be vital to ensure an effective medical care, as TBI and PBI patients have different clinical prognosis.

There is an ongoing search for biomarkers capable of easily supplying this exposure information at the different phases of clinical evolution to improve medical management.

The Dicentric Chromosome Assay (DCA) has been the biodosimetry gold standard for decades as it can be used in peripheral blood lymphocytes to estimate ionizing radiation dose and to identify heterogeneous exposures [183]. However, this technique has a few important drawbacks – results are only available 3 days following blood sampling and the heterogeneity information provided does not express organ-specific damages [183], [238].

In this work, over fifty biomarkers (in addition to the DCA assay) were tested to determine their usefulness over time in the distinction between total and partial exposures to ionizing radiation. A non-human primate animal model was chosen for its proximity to humans in genetics, physiology and corpulence (and, therefore, dose distribution) [98]. TBI and dose-equivalent PBI exposures of 2.5 Gy and 5 Gy were used. At this dose range, the species used develops ARS for mainly global exposures [95], making the partiality of the exposure particularly relevant for medical care.

The evaluation lasted until 200 days after exposure to cover both the initial period of diagnosis and also that of manifest illness, when this biomarker information can still impact the physicians' decision on patients' treatment.

1.2.1.2 Materials and Methods

1.2.1.2.1 Irradiations

The exposures were carried out as described in Ref. [241]. Briefly, eighteen adult male *Papio anubis* baboons were exposed to a horizontal and homogeneous field of gamma rays delivered by a ⁶⁰Co source to perform either global or partial irradiations:

- 2.5 Gy TBI (n = 2) and their corresponding PBI of 5 Gy 50% (hemibody, n = 2).
- 5 Gy TBI (n = 2), TBI hemi-body heterogeneous equivalents 7.5 Gy / 2.5 Gy (n = 2) and their corresponding PBI of 10 Gy 50% (hemibody, n = 2), 5.55 Gy 90% (n = 2), 6.25 Gy 80% (n = 3 where the legs were shielded and n=1 where the head was shielded), 15 Gy 30% (n = 2).

Shielding for partial exposures was done using a 20 cm thick lead screen.

1.2.1.2.2 Parameters Measured

Fifty-one parameters were recorded in this work, at different time-points, from before exposure up to 200 days after irradiation. For clinical dosimetry the intensity of 7 symptoms was scored (i.e., score 0, 1, 2 or 3):

- Vomiting;
- Erythema;
- Diarrhea;
- Petechiae;
- Hair loss;
- Fever; and
- Body weight loss.

Nine hematological parameters were observed:

- Absolute Neutrophil Count (ANC);
- Absolute Lymphocyte Count (ALC);
- Neutrophil-to-Lymphocyte Ratio (NLR);
- Red Blood Cells (RBC);
- Monocyte Count (MONO);
- Platelet Count (PLT);
- Hemoglobin Level (Hb);
- Hematocrite; and
- Mean Corpuscular Volume (MCV).

Seven coagulation and fibrinolysis factors were evaluated:

- Activated partial thromboplastin time;

- Prothrombin time;
- Thrombin time;
- Fibrinogen level;
- Factor V;
- Fibrin d-dimer; and
- Monomer.

The following 26 plasmatic biomarkers were measured:

- Albumin;
- Total protein;
- Chloride;
- Sodium;
- Potassium;
- Lactate;
- Alanine Aminotransferase (ALT);
- Aspartate Aminotransferase (AST);
- Amylase;
- Creatine Kinase (CK);
- Lactico Dehydrogenase (LDH);
- Alkaline Phosphatase (ALP);
- Cholesterol;
- Triglycerides;
- Urea;
- Creatinine;
- Glucose;
- Citrullin;
- Erythropoietin (EPO);
- Flt-3 Ligand;
- Iron;
- C3c;
- C-reactive protein;
- Haptoglobin;
- Orosomucoid; and
- Transferrine.

Dicentrics frequency and cell distribution were assessed (2 parameters) by scoring at least 250 lymphocytes (or 100 dicentrics) per sample.

1.2.1.2.3 Statistical Analysis

The first step of the statistical analysis was the validation of the model using a soft independent modelling of class analogy using a non-linear iterative Partial Least Square Discriminant Analysis (PLSDA) on the individual biomarker values from fourteen 5 Gy exposures (TBI and their PBI equivalents). As a second approach, the baboons were separated in two groups, TBI (n = 6) and PBI (n = 12), to be compared using univariate logistic regression analysis.

Finally, the Mann and Whitney non parametric rank test was used on all data (18 animals) to determine the potential of each biomarker to distinguish TBI from PBI for a given time independently of what the values were before exposure.

These experiments were approved by the French Army Animal Ethics Committee (No 2010/12.0) and all animals were treated in compliance with the European legislation.

1.2.1.3 Results

1.2.1.3.1 Clinical and Biological Dosimetry

With respect to clinical parameters, both TBI and PBI animals with cutaneous areas exposed to 7.5 Gy or higher developed erythemas from d2 to d6 and hair loss from d21. However, petechiae only occurred in TBI animals (at around d15).

The dicentric assay was mostly effective at classifying PBI 1 day after exposure – 92%. At later times (28 and 200 days), TBI incorrectly classified as PBI begin to appear.

The PLSDA of the exposures equivalent to 5 Gy showed a significant discrimination between TBI and PBI animals. An univariate logistic regression on the data of all animals (6 TBI baboons versus 12 PBI baboons), showed that 23 variables were either significantly associated with the exposure or represented a complete separation of the TBI from the PBI data set at certain time points post exposure. AST, CK, iron, Flt-3 Ligand, red blood cells, Hb, PLT and DIC were among the biomarkers identified. The Mann and Whitney test identified the same parameters for larger time windows (Figure 1-1).

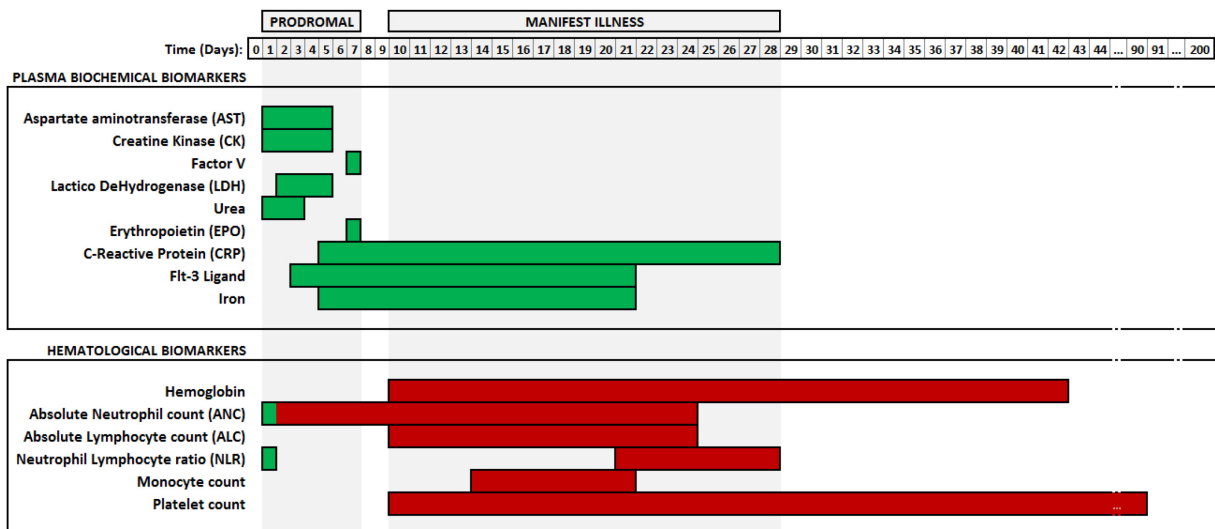


Figure 1-1: Kinetic Relevance of Biochemical and Hematological Biomarkers to Distinguish TBI from PBI Animals. Coloured bars indicate the period when the biomarker is able to distinguish partial from total exposures (i.e., the days for which the mean value of the marker was statistically different between the TBI and PBI groups using the Mann and Whitney test. Results are therefore independent of pre-irradiation values). Green means the biomarker values increased with exposure, and Red means the biomarker values decreased with exposure.

1.2.1.4 Discussion

In case of a mass casualty RN event, medical responders will need to reassure the “worried well”, but also distinguish PBI from TBI irradiated victims to provide an adapted hematologic support as soon as needed. The main objective of this work was the identification of deployable exposure biomarkers that could be used in the diagnosis and prognosis of ionizing radiation exposure victims.

As a relevant radiation model for humans, adult baboons were exposed to different situations of TBI and their PBI equivalents in a range of doses which accounts for documented radiation accidents. PLSDA

applied to the exposures equivalent to 5 Gy validated the model as it showed a clear discrimination between TBI and PBI animals. This first method of analysis allows the classification of individuals based on a great number of samples, despite the small groups of animals and was used to validate the experimental radiation model based on pairs of baboons.

The slope of peripheral blood lymphocyte count and the levels of plasmatic parameters such as C-Reactive Protein (CRP), Interleukin 6 (IL-6), Serum Amyloid Protein (SAA) and amylase are relevant early bio-indicators of exposure for TBI [32], [168], [169]. Nevertheless, the reliability of these markers to discriminate between TBI and PBI has not yet been established.

CRP is an inflammatory marker previously identified as a relevant early bio-indicator of global exposure [32], [168], [169] although not specific to ionizing radiation exposures. In these experimental conditions, CRP values could be used to discriminate PBI from TBI, but only 5 days after exposure [100]. Our results confirm Flt3-ligand as an early indicator of BM aplasia [29]. Previous studies on radiotherapy patients and mice had shown a correlation of plasma Flt3-ligand and the proportion of irradiated bone marrow [33], [106]. Indeed, the Flt3-ligand values obtained in this study were sufficiently robust to separate even the similar exposures of TBI and 90% PBI. As BM aplasia sets in, the hematologic parameters ANC, ALC, Hb, MONO and PLT decrease. This has been observed before. Blakely et al. [33], for example, showed in mice that increases in the body fraction exposed induced progressive decreases in lymphocyte counts and increases in the NLR with no significant differences in the neutrophil and platelet counts [33]. The values of these hematological biomarkers and Flt3-ligand were statistically different between TBI and PBI groups and could therefore help decide the hematologic support the patient requires. Other early changes related to hematopoiesis occurred such as iron level increase and decrease of Hb and EPO levels.

Different markers of tissue injury such as AST, LDH and CK rose greatly early after exposure with higher levels following TBI. Urea increased in all irradiation situations, but greater after TBI likely to reflect a transient kidney dysfunction. Additional deployable parameters such as the blood reticulocyte count could be added to the list. Regarding citrulline considered as a relevant gastro-intestinal damage bioindicator, its levels did not appear relevant for distinguishing TBI vs PBI. This study strongly suggests that among the numerous parameters investigated in baboons irradiated within the range of 2.5 to 5 Gy, several biomarkers are capable of distinguishing the type of exposure at least within the dose range studied.

In accidental or malevolent situations, clinical signs and symptoms will be the main tools for early triage [97]. A recent NATO exercise performed by the HFM-222 RTG showed that it would be possible to properly triage a high number of casualties using the METREPOL severity grading scale, based on d1-d3 clinical signs and symptoms. Furthermore, this clinical data time window allows the prediction of severity (RC0-4), the late occurrence of a hematologic ARS and the requirement for hospitalization. In this context, validated biomarkers could then be included to optimize diagnosis and prognosis in order to provide irradiated casualties with better medical care.

1.2.1.5 Perspectives

As suggested in the discussion and already reported by Refs. [32] and [186], the use of a single bioindicator cannot recapitulate the complexity of radiation exposures caused by accidental or malevolent events. Only the association of clinical and biological dosimetry (multi-parameter approach) would be appropriate for casualty triage and further re-evaluation. Moreover, preliminary data suggest that other plasmatic parameters could be useful radiation biomarkers such as thrombopoietin and CD117. A study involving radiotherapy patients will be the next logical step to validate the results of these experiments.

1.2.2 PHE Cytogenetics Group Activities Related to Radiation Bioeffects and Countermeasures (2012 – 2015)

Abstract

Public Health England's Cytogenetics Group at the Centre for Radiation, Chemical and Environmental Hazards aims to develop, validate and apply quantitative biomarkers for exposure to and health effects of environmental hazards, mainly ionising radiation. DNA-damaging effects and statistical data analysis have been the main focus of interest for a number of years now. Recent work can be roughly divided into four areas:

- 1) *Rapid (bio)dosimetry assays for mass casualty triage;*
- 2) *The development of statistical data analysis methods for biological dosimetry;*
- 3) *Biomarkers in radiotherapy; and*
- 4) *Health effects following exposure to ionising radiation and other genotoxins.*

This manuscript summarises recent activities of the Task Group in these areas and outlines briefly how recent initiatives have improved our preparedness for radiological mass casualty scenarios.

1.2.2.1 Rapid (Bio)Dosimetry Assays for Mass Casualty Triage

We published general reviews on radiation biomarkers [175], biological dosimetry [201] and DNA damage foci [196]. We also completed a UK Home Office-funded project on development of protein biomarker assays for rapid triage of radiation casualties [199] and the EU Multibiodose project (www.multibiodose.eu). In the latter project we contributed to work packages on the dicentric [188], [191] and micronucleus assays [233] and led the gamma-H2AX [195] and software work packages [5]. All efforts culminated in a recent inter-assay inter-laboratory intercomparison exercise [4]. See Ref. [191] for a summary of the EU Multibiodose project and Ref. [116] for an operational guidance document that has been prepared and is available from the Multibiodose website. We contributed to two 'telescoring' exercises for the dicentric assay [187], [225] established and validated a Co-60 calibration curve for the semi-automated dicentric assay using Metasystems' 'DCScore' dicentric detection system [189], [190] and for the (semi-)automated micronucleus assay using the MNScore module [233]. We published a rapid 96 well lyse/fix sample processing method for the gamma-H2AX assay which requires only finger-prick-sized blood volumes [152] and investigated the potential of combining the gamma-H2AX assay with an apoptosis assay for more reliable dose estimation in situations where the exact time since exposure is not known [104]. Preliminary [1] and full results from the recent NATO biodosimetry exercise were published [17], [25], [193], [197], [200]. The EU RENEb project (2012 – 2015; www.reneb.eu) aims to establish a European biodosimetry assistance network [126], [127], [248] and we recently contributed to the first and second intercomparison exercises for the dicentric, micronucleus, FISH and gamma-H2AX assays [18]. We also contributed to a capacity survey [146] and helped organise and evaluate a mainly Eastern European dicentric intercomparison exercise for WHO BioDoseNet (www.biodosenet.org).

In addition, we have been involved in two Optically Stimulated Luminescence (OSL) dosimetry projects (collaboration with R Tanner, PHE and I Bailiff, Durham) which aim to complement our biodosimetry capabilities and capacities using resistors from personal electronic devices such as mobile phones [123], [124], [213]. Results from the first European intercomparison (in collaboration with EURADOS WG10) are encouraging [20].

Finally, we have been contributing to a EURADOS WG10 task group on scoping the usefulness, limitations and knowledge gaps of biodosimetry in internal or mixed internal/external exposure scenarios. Initial results were presented at the MELODI Workshop 2013 in Brussels, Belgium. Draft reports have been prepared for different scenarios and will be published in due course.

1.2.2.2 Development of Novel Statistical Data Analysis Methods for Biological Dosimetry

We recently completed a collaborative (with N. Maznyk, V. Vinnikov and I.M.R. Kharkov), Royal Society-funded ‘statistics in radiation cytogenetics’ project which allowed us to take first steps towards more advanced cytogenetic data distribution analysis [9] and Bayesian methods to improve the accuracy of dose estimations and associated uncertainties. We published a review of Bayesian methods that can be used to improve the accuracy of dose estimations and associated uncertainties [10]. A related PhD project started in October 2012 and was completed in October 2015, in collaboration with P. Puig (Barcelona). Major outputs include a new inverse regression model for radiation biodosimetry [101] and a new Bayesian model for partial body irradiation estimation [102]. A separate NIHR-funded collaborative project with J. Einbeck at Durham University investigated the scope for random effects modelling in biological dosimetry [166].

The existing DoseEstimate software package has been improved and a software package for advanced statistical analysis of cytogenetic calibration and dosimetry data, CytoBayesJ, has been developed as a software tool to support Bayesian and Bayesian-like data analysis procedures for cytogenetic data [11]. An implementation in “R” was also produced in a collaborative project with CREAL in Barcelona [154]. A free software package, Multibiodose, has been developed in order to facilitate triage categorisation based on dosimetry results from a range of assays [5]. It can be downloaded from <http://www.multibiodose.eu/software.html>.

A EURADOS WG10 task on uncertainties, chaired by L. Ainsbury and F. Trompier, aims to harmonise data analysis among laboratories. The Task Group has drafted a manuscript that summarises data analysis methodologies used in retrospective dosimetry.

1.2.2.3 Biomarkers in Radiotherapy

Following very promising results (obtained in a recently completed PhD project) suggesting a modest to strong association of residual 53BP1 foci and chromosome aberrations in *ex vivo*-irradiated blood lymphocytes with late normal tissue toxicity in breast radiotherapy patients [50] we started a larger study (collaboration with J. Yarnold, I.C.R. Sutton and D. Azria, Montpellier) to confirm these associations and any links to radiation-induced apoptosis in 400 prostate and breast cancer radiotherapy patients, to be completed in 2014. We demonstrated the usefulness of gamma-H2AX immunohistochemistry for *in situ* dose mapping in microbeam radiotherapy [198] and are involved in the EU COST project *Syra3* on radiotherapy using synchrotron radiation (www.cost.eu/domains_actions/bmbs/Actions/TD1205; project website www.syra3.eu). Two original papers were published on mechanisms underlying radiotherapy fraction size sensitivity [215], [216] based on a recently completed PhD project. A review on this topic has now also been published [214]. Two other reviews on biomarkers in radiotherapy and radiology were also published [51], [142].

Pilot data investigating a potential association between DNA double-strand break repair, apoptosis induction and late normal tissue damage following radiotherapy are now published [49] and we have completed the scoring for the 400-patient-study of possible associations between clinical radio-sensitivity and cytogenetic, gamma-H2AX and apoptosis markers in lymphocytes. Data are currently being re-analysed and being written up for publication.

1.2.2.4 Health Effects Following Exposure to Ionising Radiation and Other Genotoxins

Our current work includes APC (Min/+) mouse radiation carcinogenesis studies involving split-dose X-rays [86] and tritium intake vs. chronic gamma-exposure, in order to determine the RBE of tritium for this endpoint. We won an EU DOREMI grant to fund the chronic gamma-exposure arm of our APC (Min/+) mouse radiation carcinogenesis studies which are being performed in collaboration with the Norwegian FIGARRO irradiation facility.

Following the recent discussions about radiation-induced cataract risk [37] a small collaborative project (with R. Quinlan, Durham) on radiation-induced cataracts was initiated in 2012 which focuses on low-dose responses in the murine eye lens. Results on low-dose responses in the murine eye lens were written up and recently published [144]. A cataract-related summary of recent UK research [38], a commentary [84] and a survey of eye lens doses in the UK medical sector were published [6].

Experimental work has been completed in the EU SOLO project (<http://solo-fp7.eu/>) on FISH-based lifetime exposure assessments of former Mayak workers and Techa river residents in order to study the association between cumulative dose and health risks. Several FISH data sets have been written up and published [55], [218], [250], [251]. A paper has been published on the question what FISH actually measures in cases of incorporated radionuclides for the Southern Urals populations [8].

Tissue and blood samples have been collected, processed and analysed for a pilot study of biological effects of nanomaterials intratracheally instilled into rats. A cytogenetic study of combined exposure to radiation and selected genotoxic chemicals has been completed. Results for combined exposure to radiation and sodium arsenite have been published [164], whilst those for other genotoxins are being written up. Work has started on updating quantitative health effects modelling for radiation emergency scenario planning [56].

1.2.2.5 Recent Improvements in Emergency Preparedness for Radiological Mass Casualty Scenarios

Over the past 5 – 10 years, emergency preparedness systems and policies for radiological mass casualty scenarios have been considerably improved. A number of recent initiatives have enhanced the UK national, European and global capabilities and capacities for investigating, managing and responding to radiological incidents:

- In 2010, the HPA published an updated guidance document on outbreaks and incidents of unusual illnesses, as an aid to decision-making for health professionals and other health protection personnel. It also aims to assist in making a judgement about whether an outbreak or incident is due to natural or accidental cause or deliberate release [153].

Through a European scoping exercise called TENEB [265], the original tripartite assistance network for biodosimetry – which was based on a memorandum of understanding between France, Germany and the UK – has led to the creation of a pan-European network for biological and retrospective dosimetry (RENEB). At a global level, the World Health Organization's BioDoseNet biodosimetry assistance network fulfils a similar role. Recent activities of these networks have been described in the first section of this report. Furthermore, the International Atomic Energy Agency (IAEA) has set up a global Response and Assistance Network (RANET) for providing international assistance following a nuclear or radiological incident or emergency (<http://www-ns.iaea.org/tech-areas/emergency/ranet.asp>).

- Considerable effort has gone into research and development of rapid assays for radiation exposure assessment to assist triage in a large-scale radiological event. Thanks to these efforts, initial estimates are now available within a few hours (instead of 2 – 3 days) and a much larger throughput can now be achieved. The main outputs have been summarised in the first section of this report.
- Novel data analytical approaches and tools have been devised for enhanced assessment of the uncertainties associated with any dose estimation. This is of crucial importance especially in a mass casualty situation where 'triage mode' operation necessitates larger uncertainties. More details and references are provided in the section on Area 2.

Together, these activities have strengthened the radiological emergency response system by:

- i) Providing better guidance on early detection;

- ii) Improving capacity, expertise and resilience through international networks; and
- iii) Supporting triage through the development of rapid exposure assessment tools and algorithms guiding their deployment and data interpretation, depending on the specific exposure scenario.

1.2.3 Establishment of Dicentric Chromosome Assay for Biological Dosimetry in Case of Suspect Radiation Exposure

Abstract

The risk of accidental human exposure is linked to the use of ionizing radiation sources in medical, research and industrial areas. Furthermore, the possibility of terrorist attack using radiological or nuclear devices must be considered. Dose estimation is the first important step for medical treatment of subjects exposed to ionizing radiation. For this purpose, clinical signs/symptoms and biological dosimetry are the two main approaches to assess radiation exposure. Biodosimetry is a method to measure the ionizing radiation dose absorbed by an individual using biological markers. This type of approach is useful when an individual is accidentally exposed and physical dosimetry is not available or uncertain. The most validated assay for biodosimetry and radiation injury assessment is the gold standard Dicentric Chromosome Assay (DCA). Prerequisite for dose assessment is the establishment of a dose-effect calibration curve.

1.2.3.1 Introduction

Due to an increasing concern about the threat of radiological or nuclear terrorism, the preparedness for medical management of radiation events is of great importance [182], [234]. Appropriate medical management of a radiation accident encompasses various factors such as the number of victims and the level of radiation exposure [57]. Particularly in mass-casualty events, a rapid classification of victims in medical treatment groups has to be done. For this purpose, clinical signs /symptoms and biological dosimetry are the two main approaches to assess radiation exposure. The first method used to correlate human biological parameters with absorbed dose is based on the observation of intensity, frequency and duration of some symptoms displayed after radiation overexposure [110].

Individuals with little or no exposure, not facing acute health impairments, have to be distinguished from those with mild, moderate or severe doses in order to allocate the best medical resources [253].

The applicability of the available assays of biological dosimetry is based on the analysis of the chromosome damage present in peripheral blood lymphocytes, which is convenient because its collection is non-invasive and it is easy to obtain. The occurrence frequency of unstable aberration, namely dicentric [26], is most often used to estimate absorbed doses.

The Dicentric Chromosome Assay (DCA) provides dose estimates in acutely irradiated individuals based on the frequency of radiation-specific dicentric chromosomes in irradiated subject's peripheral blood lymphocytes. DCA is very sensitive due to a low and stable background dicentrics frequency (1 – 2 per 1000 metaphase spreads). Laboratory protocols have been standardized by the International Organization for Standardization [21], [112] and dose levels as low as 0.1 – 0.2 Gy can be detected, when 500 – 1000 metaphase spreads are analysed [108]. Analysis of 500 – 1,000 metaphase spreads per irradiated subject, however, is neither practical as it is labour-intensive, nor essential in a radiation mass casualty event, where acute risk of ARS development needs to be assessed for potentially a large number of individuals to making treatment decisions. Therefore, in these situations, the precision of estimated doses may be decreased to improve throughput by reducing the number of metaphases analysed. Analysing only 50 metaphase spreads, contrary to the routine analysis of 500 – 1,000 metaphases, increases the threshold level of detection to 1 – 2 Gy, which is still adequate to guide treatment of ARS [140], [141], [249], while vastly increasing the speed of analysis and hence dose estimations [141]. A recently published International Organization for

Standardization (ISO) standard specifically addresses the use of the DCA for triage dose estimation applications for radiological mass casualties [113]. For cytogenetic triage, only 20 – 50 metaphases spreads per subject are scored instead of the 500 – 1,000 scored for routine analysis [249]. Provided results allow a stratification of exposed individuals into broad 1.0 Gy categories, which is considered to be sufficient for preliminary medical triage [141], [249]. Due to the necessity of a rapid individual dose assessment allowing categorization of victims as soon as possible after a radiation accident, a high-throughput chromosome analysis is required, especially after a mass-casualty event.

The second strategy is the automation of dicentric scoring using image analysis software. In automated dicentric scoring, 1000 metaphases can be analysed for triage in 1 hour and 3000 for individual dosimetry in 3 hours, with a 3-fold reduction in analysis time. For triage the automatic detection of dicentrics has been validated [245].

In this study, we have established manual and automated calibration curves for DCA. After, calibration curves were validated evaluating the dose prediction accuracy through the analysis of blind samples irradiated with single different doses of X-rays.

1.2.3.2 Results

1.2.3.2.1 Manual Calibration Curve

In Table 1-1A, the results of analysis of dicentrics and excess acentrics fragments are reported. The background aberration frequency was 0.3 dicentrics per 1,000 cells. After irradiation exposure, ranging from 0.25 to 4 Gy, a total of 8,855 metaphases analysed revealed 3,166 dicentric chromosomes (including 38 tricentric chromosomes that were counted as two dicentrics) and 223 centric rings. Table 1-1B, reports the distribution, the u-value and the dispersion factor of dicentric chromosomes. The cells containing dicentrics increase with absorbed dose and the distribution follows the Poisson distribution with u-values between ± 1.96 . Figure 1-2 shows the dicentrics and acentrics dose-effect calibration curves established by the data derived from all scorers. For dicentrics dose-effect calibration curve a weighted chi squared of 5.91 was observed with 5 degrees of freedom that resulted in a p value of 0.32. The z-test for alpha and beta coefficient of dose-effect curve returned a $p < 0.001$. For acentrics data a weighted chi squared of 12.1 was observed with 5 degree of freedom that resulted in a p value of 0.03. The z-test for alpha coefficient resulted in $p < 0.01$ and for beta coefficient in $p < 0.001$.

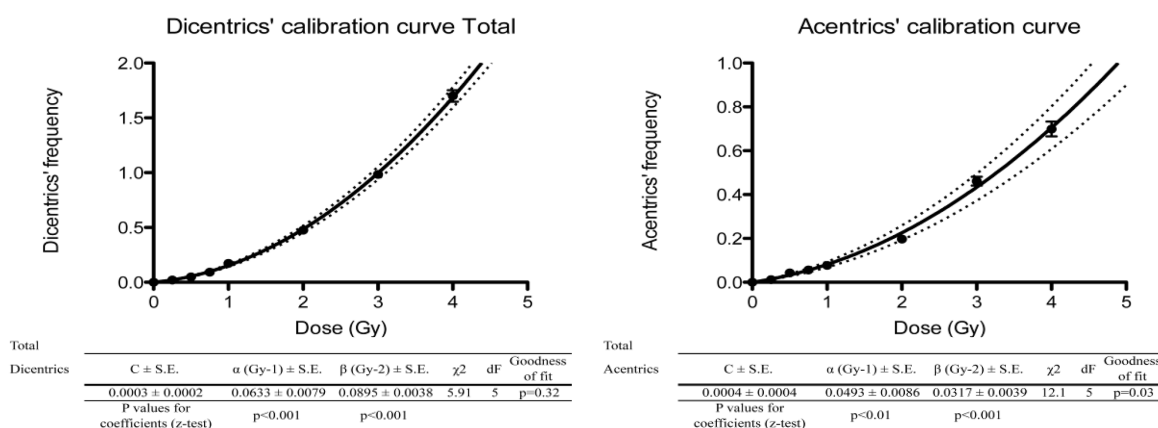
Table 1-1: Analysis of Dicentrics and Excess Acentrics (A), Distribution, μ -Value and Dispersion Factor of Dicentric Chromosomes (SEM = Standard Error of the Mean).

A

Total	Dose (Gy)	Cells	Dicentrics	Centric Rings	Acentrics	Dicentrics frequency \pm SEM	Acentrics frequency \pm SEM
	0	7062	2	0	5	0.0003 \pm 0.0002	0.0004 \pm 0.0002
	0.25	1500	32	1	51	0.021 \pm 0.004	0.012 \pm 0.003
	0.5	1500	73	3	141	0.049 \pm 0.006	0.043 \pm 0.005
	0.75	1500	140	15	239	0.093 \pm 0.008	0.056 \pm 0.006
	1	1500	260	27	403	0.173 \pm 0.011	0.077 \pm 0.007
	2	1139	542	33	799	0.476 \pm 0.020	0.196 \pm 0.013
	3	1114	1096	85	1694	0.984 \pm 0.030	0.461 \pm 0.020
	4	602	1023	59	1503	1.700 \pm 0.053	0.699 \pm 0.034

B

Total	Dose (Gy)	Cells	Dicentrics	Dicentrics' distribution							Tricentrics	μ value	Dispersion factor $S^2 Y^{-1}$
				D0	D1	D2	D3	D4	D5	D6			
	0	7062	2	7060	2	0	0	0	0	0	0	-0.012	1
	0.25	1500	32	1468	32	0	0	0	0	0	0	-0.575	0.979
	0.5	1500	73	1427	73	0	0	0	0	0	0	-1.32	0.952
	0.75	1500	140	1366	128	6	0	0	0	0	0	-0.191	0.993
	1	1500	260	1257	226	17	0	0	0	0	0	-1.15	0.958
	2	1139	542	699	348	82	10	0	0	4	4	-1.47	0.938
	3	1114	1096	436	374	209	79	14	1	11	11	0.705	1.03
	4	602	1023	115	172	161	103	38	10	3	23	-0.861	0.95



Automated Calibration Curve

Figure 1-2: (Left) Dicentric and Acentric Dose-Effect Calibration Curves and (Right) Their Respective Coefficients of the Curve (SE = Standard Error; dF = degrees of Freedom).

In Table 1-2A, the results of automated scoring of DCA are reported. At background level were observed 2 dicentrics in 5136 metaphases analysed that correspond to a frequency of about 0.4 dicentrics per 1,000 metaphases. After radiation exposure, ranging from 0.25 to 4 Gy, a total of 539 dicentrics were observed in 11,564 metaphases scored. The trend of dicentrics frequency increased with dose ranging from 0.008 at 0.25 Gy to 0.271 at 4 Gy exposure of X-rays. Table 1-2B reports the distribution, the μ -value and the dispersion factor of dicentric chromosome. The cell containing dicentrics increase with absorbed dose and the distribution follows the Poisson distribution with μ -values between ± 1.96 . Figure 1-3 shows the new

DCA automated dose-effect calibration curve compared to the manual calibration curve. The automated dose-effect curve was analysed for goodness of fit with linear-quadratic model $y = C + \alpha D + \beta D^2$ and the p value for coefficient α and β was also calculated. A weighted chi squared of 3.79 was observed with 5 degrees of freedom that resulted in a p value of 0.58. The z-test for alpha and beta coefficient of dose-effect curve returned a $p < 0.01$. The following equation derived: $Y = 0.0004(\pm 0.0003) + 0.0186(\pm 0.0030)D + 0.0131(\pm 0.0016)D^2$.

Table 1-2: (A) Results of Automated Scoring of DCA and (B) Distribution, μ -Value and Dispersion Factor of Dicentric Chromosomes (SEM = Standard Error of the Mean).

A	Dose (Gy)	Cells	Dicentrics	Dicentrics frequency \pm SEM	Dose (Gy)	Cells	Dicentrics	Dicentrics' distribution					μ value	Dispersion factor $S^2 Y^{-1}$	B
								D0	D1	D2	D3	D4			
	0	5136	2	0.0004 \pm 0.0003	0	5136	2	5134	2	0	0	0	-0.014	1	
	0.25	2461	19	0.008 \pm 0.002	0.25	2461	19	2442	19	0	0	0	-0.264	0.993	
	0.5	2360	24	0.010 \pm 0.002	0.5	2360	24	2336	24	0	0	0	-0.342	0.99	
	0.75	2819	63	0.022 \pm 0.003	0.75	2819	63	2757	61	1	0	0	0.369	1.01	
	1	1576	48	0.030 \pm 0.004	1	1576	48	1529	46	1	0	0	0.336	1.01	
	2	939	88	0.094 \pm 0.010	2	939	88	854	82	3	0	0	-0.534	0.976	
	3	947	172	0.182 \pm 0.014	3	947	172	792	140	14	0	1	1.14	1.05	
	4	462	125	0.271 \pm 0.024	4	462	125	354	95	9	4	0	1.03	1.07	

DCA Manual vs Automated Calibration Curve

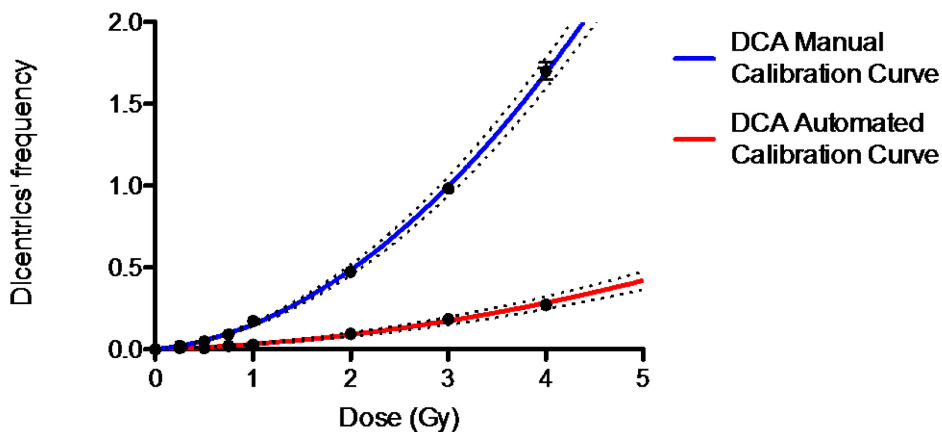


Figure 1-3: DCA Automated Dose-Effect Calibration Curve and Previously Generate Manual Calibration Curve.

1.2.3.2.2 Dose Estimations in Standard Mode

To test the new established calibration curve for dose prediction accuracy, we have analysed 5 irradiated blood aliquots in a blind mode. Table 1-3 reports the results of biological dose estimations based on the analysis of dicentric chromosomes in 500 metaphases and their 95% upper and lower confidence limit estimated by comparing the observed dicentrics frequencies with the fitted dose-effect calibration curve. All physical doses used were included within the 95% upper and lower confidence intervals and the percentage errors of prediction ranged from -7.1 to 14.3 indicating under and over estimation of the physical absorbed dose.

Table 1-3: Biological Dose Estimations Based on the Analysis of Dicentrics Chromosomes in 500 Metaphases. LCL: 95% Lower Confidence Limit; UCL: 95% Upper Confidence Limit.

Dose (Gy)	Cells	No. of slides	No. of dicentrics	Dicentrics per cell	Estimated Dose (Gy) (LCL/UCL)	Error (%)
0.1	500	2	2	0.004	0.1 (-0.03/0.13)	0
0.7	500	2	58	0.116	0.8 (0.70/0.97)	14.3
1.4	500	2	123	0.246	1.3 (1.21/1.48)	-7.1
2	500	2	253	0.506	2.1 (1.93/2.17)	5.0
2.6	500	2	356	0.712	2.5 (2.38/2.60)	-3.8

1.2.3.2.3 Dose Estimations in Manual Triage Mode

The dose estimates were performed in triage manual mode for DCA ranging from 20 to 50 cells in blind samples irradiated with unknown doses. In Table 1-4A, the DCA dose estimations are reported. For each physical dose 10 estimations were performed for each sub-set of cells scored. The variance decreased with the increase of the number of cell analysed at each dose. Using the uncertainty interval of ± 0.5 Gy all estimations at 50 cells were considered accepted. Excluding the 1.4 Gy exposure sample all estimations were acceptable just after 30 cells analysed. Splitting the physical doses into different classes of medical risk we have observed a 75 – 95 % of discrimination for the two < 1 Gy doses, an 80% for dose between 1 – 2 Gy and an 80 – 90 % of discrimination for doses ≥ 2 Gy (Table 1-4B).

Table 1-4: Dose Estimations Carried Out from Manual Scoring of Dicentrics (A) and Percentage of Inclusion Inside the Right Medical Class of Risk (B).

A

											Based on ± 0.5 Gy uncertainty interval		
Physical Dose 0.1 Gy											Variance	Accepted	Not accepted
20 cells	0.0	0.0	0.0	0.0	0.0	0.0	0.0	0.0	0.0	0.0	0.00	10	0
30 cells	0.0	0.0	0.0	0.0	0.0	0.0	0.0	0.0	0.3	0.0	0.01	10	0
40 cells	0.0	0.0	0.0	0.0	0.0	0.3	0.0	0.0	0.3	0.0	0.01	10	0
50 cells	0.0	0.0	0.0	0.0	0.0	0.2	0.0	0.0	0.2	0.0	0.01	10	0
Physical Dose 0.7Gy											Variance	Accepted	Not accepted
20 cells	0.8	0.5	1.4	0.0	1.0	0.0	0.8	1.0	1.0	1.5	0.23	6	4
30 cells	0.9	0.3	1.2	0.3	0.9	0.3	0.6	0.8	0.9	1.2	0.10	10	0
40 cells	0.8	0.3	1.0	0.8	0.9	0.5	0.5	0.9	0.8	1.2	0.07	10	0
50 cells	0.9	0.2	1.2	0.7	0.9	0.8	0.5	0.9	0.9	1.2	0.07	10	0
Physical Dose 1.4 Gy											Variance	Accepted	Not accepted
20 cells	0.8	1.2	1.9	0.8	1.4	1.4	1.2	1.4	1.4	1.8	0.12	8	2
30 cells	1.2	0.9	1.7	0.8	1.3	1.2	1.4	1.4	1.6	2.0	0.12	8	2
40 cells	1.4	0.9	1.6	0.6	1.3	1.3	1.5	1.4	1.5	1.7	0.10	9	1
50 cells	1.3	0.9	1.5	0.9	1.3	1.4	1.4	1.3	1.5	1.8	0.06	10	0
Physical Dose 2 Gy											Variance	Accepted	Not accepted
20 cells	2.0	2.0	2.2	2.0	2.2	1.5	2.0	2.2	2.2	2.2	0.03	10	0
30 cells	2.0	2.2	2.0	1.8	2.3	1.6	2.0	2.3	2.3	2.2	0.05	10	0
40 cells	1.9	2.2	2.1	1.7	2.2	1.7	2.0	2.3	2.2	2.4	0.05	10	0
50 cells	1.9	2.0	2.0	1.9	2.2	1.9	1.9	2.2	2.0	2.3	0.02	10	0
Physical Dose 2.6 Gy											Variance	Accepted	Not accepted
20 cells	2.9	1.8	2.6	2.0	2.5	2.7	3.2	2.5	2.1	2.9	0.17	7	3
30 cells	2.7	2.1	2.5	2.3	2.6	2.6	2.8	2.3	2.5	2.8	0.05	10	0
40 cells	2.8	2.2	2.3	2.3	2.5	2.6	2.7	2.3	2.6	3.0	0.06	10	0
50 cells	2.9	2.2	2.1	2.5	2.3	2.5	2.6	2.1	2.6	2.9	0.08	10	0

B

Class of risk	Dose range	Estimations	% of inclusion in the adequate medical class of risk			
			20 cells	30 cells	40 cells	50 cells
1	<1Gy	20	75	90	95	90
2	1-2Gy	10	80	80	80	80
3	2-4Gy	20	80	90	85	80

1.2.3.2.4 Dose Estimations in Automated Triage Mode

The dose estimates were performed in triage automated mode for DCA ranging from 20 to 500 cells in blind samples irradiated with unknown doses. Table 1-5A reports the estimates performed with DCA automated mode. The variance decreased increasing the number of cells scored and using the uncertainty interval of ± 0.5 Gy accepted for triage dicentric assay all estimations from 200 cells were considered accepted. Analysing physical doses into different classes of medical risk we observed that beyond 200 scored cells all estimations were included into the appropriate class (Table 1-5B).

Table 1-5: Dose Estimations Performed by Automated Scoring of Dicentrics (A) and Percentage of Inclusion Within the Appropriate Medical Class of Risk (B).

A

	Physical Dose (Gy)					Variance	Based on ± 0.5 Gy uncertainty interval	
	0.1	0.7	1.4	2	2.6		Accepted	Not accepted
20 cells	0.0	0.0	0.0	2.7	4.9	1.62	1	4
30 cells	0.0	0.0	1.6	2.1	4.4	0.68	3	2
40 cells	0.0	0.8	2.1	2.5	3.9	0.25	3	2
50 cells	0.0	0.7	1.9	2.1	4.0	0.50	4	1
100 cells	0.0	1.0	1.5	1.9	3.3	0.15	4	1
200 cells	0.0	0.6	1.5	2.3	3.1	0.11	5	0
300 cells	0.0	0.8	1.5	2.2	3.0	0.07	5	0
400 cells	0.0	0.8	1.4	2.0	2.9	0.04	5	0
500 cells	0.0	0.8	1.6	2.0	2.8	0.04	5	0

B

Class of risk	Dose range	Estimations	% of inclusion in the adequate medical class of risk								
			20 cells	30 cells	40 cells	50 cells	100 cells	200 cells	300 cells	400 cells	500 cells
1	<1Gy	2	100	100	100	100	50	100	100	100	100
2	1-2Gy	1	0	100	0	50	100	100	100	100	100
3	2-4Gy	2	50	50	100	100	50	100	100	100	100

1.2.3.3 Discussion

The Dicentric Chromosome Assay (DCA) is the “gold standard” biodosimetry method for radiation dose assessment. DCA can be used for rapid dose assessment of individuals in the early period followed by radiological or nuclear incident for optimum medical aid. DCA application in radiation mass casualties needs great sample processing and chromosome aberration analysis capability. The usefulness of DCA to assess health risks and to guide medical treatment decisions has been demonstrated in several radiation accidents involving mass casualties [93], [183], [184], [204], [208].

In this work we produced a manual and automated dicentric chromosomes dose-effect calibration curves as a fundamental prerequisite for dose estimation purpose in case of radiological/nuclear adverse events. The curves was elaborated from blood samples derived from 11 healthy donors for background level of dicentrics and one sample exposed to 7 different dose of X-rays.

The evaluations of 500 metaphases in 5 blind X-rays exposure blood samples to simulate whole body exposure have showed the consistency of derived dose estimation data. All physical doses were within the 95% estimated confidence limits demonstrating the usefulness of the new established dicentric dose-effect curve, the technical competence and the good practice performance in metaphases scoring.

Furthermore, the aim of this study was to evaluate the triage mode scoring for DCA as possible high-throughput screening tools for radiation biological dosimetry. Rapid triage scoring can be applied to several cytogenetic assays employed in biological dosimetry. It has been determined that DCA dose estimates by scoring 50 cells (or 30 dicentrics) can ensure sufficient accuracy to be useful for the medical community. It has been shown that this method of scoring will deliver dose estimates within 1 Gy with a ± 0.5 Gy uncertainty interval of the physical dose [112], [234]. Compared to standard dicentric scoring of 500 or 1,000 cells, this triage method increases the overall throughput up to 20 times. Based on our estimations, the data were in agreement with previous reports on DCA triage dose assessment. All estimations were considered valuable in the uncertainty interval of ± 0.5 Gy after scoring 50 metaphases. The same results were obtained scoring 30 cells but the 1.4 Gy dose. For this dose, after scoring of 30 metaphases we found two not accepted values, respectively one underestimated and one overestimated by 0.1 Gy, and after scoring of 40 metaphases there was one not accepted underestimated value by 0.3 Gy. However, considering 150 dose estimations ranging from 30 to 50 metaphases, the not accepted ones were only three (2%). Regarding medical class of risk, after scoring of 50 cells the dose estimates didn't fit in the right classes for an overestimation of 0.2 Gy (two 1.2 Gy estimations in 0.7 Gy physical dose) and an underestimation of 0.1 Gy (two 0.9 Gy estimations in 1.4 Gy physical dose and four 1.9 estimations in 2 Gy physical dose). This didn't allow a complete separation between the < 2 Gy exposure (individuals with long-term surveillance) and > 2 Gy (treatment urgently needed, low mortality with suitable treatment) that are the crucial classes for triage discrimination. The complete separation didn't occur for 4 estimations into 2 Gy exposure that were estimated as 1.9 Gy leading to grading four hypothetical individuals in the < 2.0 Gy interval, although they needed urgent medical treatments.

Automated scoring is considered a useful tool for a rapid triage of individuals accidental exposed to radiological/nuclear sources. In this study we compared the dose estimation carried out with automated detection system of DCA and CBMN. The automated scoring of DCA was performed from 20 to 500 cells. Based on the ± 0.5 Gy interval of uncertainty of dose estimation after scoring of 200 cells all estimates were accepted. Considering the adequate insertion into medical class of risk after 200 cells scored all estimates fell into appropriate classes and this trend was maintained up to 500 cells scored.

In conclusion, all estimations performed showed a good agreement with the physical dose considering the ± 0.5 Gy uncertainty interval. Based on our data the scoring of 30 metaphases or 100 binucleated cells can be useful for medical response in case of a large-scale nuclear accident. Furthermore, the good results obtained with automated scoring support the idea that automation could be a good alternative to manual scoring to improve the laboratory capabilities reducing the time necessary for analysis. Considering the aim of classifying into clinically relevant classes, our data demonstrated that the triage mode was not always able to discriminate each class. Rapid triage assays are approximate, but can still help medical personnel to make decisions for the first aid of the victims, especially very high exposed, considering also clinical signs and symptoms. Medical personnel would still communicate discrepancies between clinical symptoms and triage dose estimations to improve accuracy by scoring more cells.

1.2.4 Cytokinesis-Block MicroNucleus Assay: Manual and Automated Scoring

Abstract

The Cytokinesis-Block Micronucleus (CBMN) assay is a standardized and validated cytogenetic method for radiation dose assessment, proposed as an alternative to the Dicentric Chromosome Assay (DCA), the "gold standard" in biological dosimetry, because it requires less time and cytogenetic skill. Nevertheless,

for a reliable use of CBMN assay in large-scale radiological/nuclear accidents, this analysis needs further strategies to be faster, e.g., the automated micronucleus scoring. The aim of our study is to validate the automated MN scoring. As essential prerequisite, manual and automated dose-effect curves were established and the quality of both the calibration curves was assessed by evaluation of the dose prediction accuracy of 10 blood blind samples. Then, the accuracy of the dose assessment based on manual and automatic scoring mode was compared.

1.2.4.1 Introduction

The Cytokinesis-Block Micronucleus (CBMN) assay in peripheral blood lymphocytes, based on the number of Micronuclei (MN) in Binucleated cells (BNcells), is one of the best established method for radiation dose assessment [232], [252]. Although less specific, it has been indicated as an alternative to the Dicentric Chromosome Assay (DCA), the “gold standard” for biodosimetry [111], because MN scoring is much faster and requires fewer skills. A detailed description of the scoring criteria for MN was reported in the HUMAN MicroNucleus (HUMN) project [66].

The number of radiation-induced MN is strongly correlated with radiation dose and the frequency of MN observed can be converted into an absorbed dose by reference to an “*in vitro*” generated calibration curve that was described by linear-quadratic dose-response functions for low LET radiation [252].

Although the CBMN assay is easier and faster than dicentric analysis, the application of this assay as biodosimetry tool in large-scale radiation events requires the development of new scoring approaches for a reliable and fast dose assessment. Two main scoring strategies were proposed to speed up cytogenetic analysis for population triage in radiation mass casualties. One is the triage mode of scoring that provides a lower number of analysed metaphases and cells [141]. For CBMN assay only 200 binucleated cells/subject were suggested to be scored to detect radiation doses > 1 Gy [148].

The other promising strategy is the automated scoring by sophisticated image analysis systems. A quite recent automated system is Metafer4 (MetaSystems) with the software module for Cytokinesis Block MicroNucleus analysis (MNScore) that allows to identify binucleated cells and to detect and count MN close to the main nuclei in BNcells.

However, this system is not fully automated and still requires visual validation by a scorer [194], [244]. This validated automated scoring is common called semi-automated scoring.

1.2.4.2 Aim

The aim of this study is the comparison between manual and automated MN scoring in order to contribute to the development and validation of an automated CBMN assay for population triage in large-scale radiation accidents.

1.2.4.3 Study Design

This study is part of the NATO exercise 2011 organized under the umbrella of NATO Research Task Group RTG-033 “Radiation Bioeffects and Countermeasures” [192], [197].

The study was divided in two phases:

- 1) Establishment of MN calibration curves by manual and automated scoring of slides prepared from blood samples of a healthy male donor irradiated with seven X-ray increasing doses (0.25-0.5-0.75-1-2-3-4 Gy).
- 2) Evaluation of dose prediction accuracy for manual and automated MN scoring, by estimating biological dose of ten blind samples (irradiated with unknown X-ray doses) of the same donor.

1.2.4.4 Results

1.2.4.4.1 Dose-Response Calibration Curves

To generate the manual calibration curve 4,000 binucleated cells were analysed for each dose point in manual mode in transmitted light.

To establish automated calibration curve we used Metafer4 MNScore system which scored in fluorescence a variable number of cells for each dose point (the number of cells decrease with increasing radiation dose) that were then validated by a scorer. After visual validation from 1.5 to 6 % of these cells were rejected because they didn't comply the standardized scoring criteria, and a range from about 600 to 5,000 BNcells/dose were analysed. A dose-related increase in number of discarded cells was observed.

Figure 1-4 shows the calibration curves at 7, increasing doses of X-rays from 0.25 to 4 Gy obtained respectively by manual, automated and semi-automated scoring. Dose-response curves of micronuclei described in Figure 1-4, were fitted by a linear quadratic equation (95% confidence limits), using the Dose Estimate software [7]. A dose-related increase in the MN frequency was observed for all the three scoring modes, but a lower MN frequency of fully automated scoring was clear.

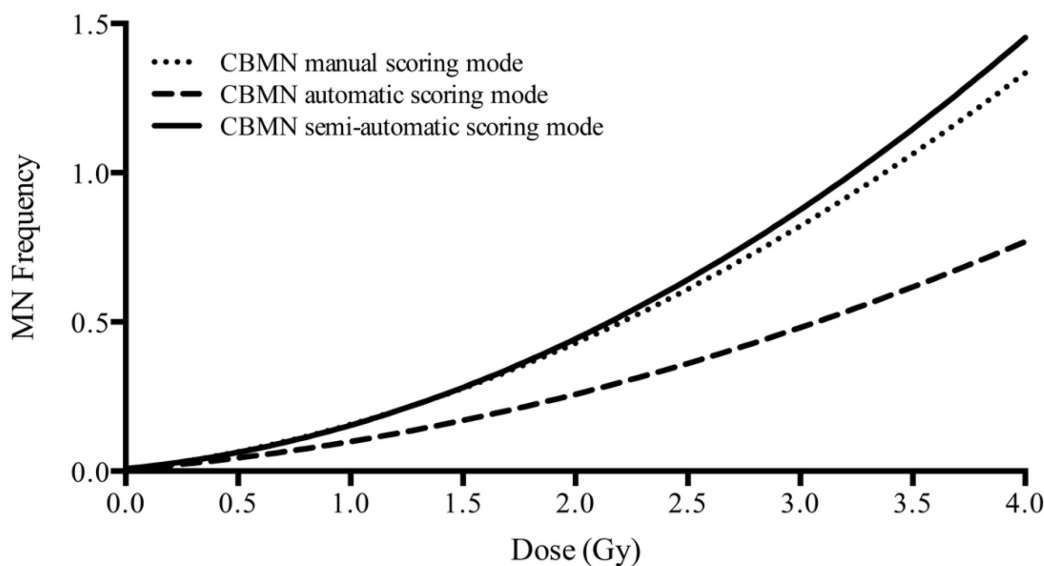


Figure 1-4: Dose-Response Curves of MN Obtained by Manual Scoring (black, dotted line), Automatic Scoring (black, dashed line) and with Semi-Automated Scoring Mode (black, full line). On the y-scale the MN Frequency defined as number of micronuclei on number of binucleated cells scored.

The comparison of the results obtained by manual, automated and semi-automated scoring at each dose was performed by Paired *t*-test that indicated a good agreement between the manual and the semi-automated curves. This test has shown instead a low agreement between the manual curve and the automatic curve.

The dose prediction accuracy was evaluated assessing the radiation dose of 10 blind samples from the same subject irradiated at different X-ray doses from 0 to 6.4 Gy. 2,000 BN cells per sample were scored in manual mode. The number of BN cells detected by the automatic system was highly variable for each sample after visual validation. To estimated doses, the MN frequencies observed with manual and semi-automated modes were referred to the respective dose -effect curves. The number of BNcells detected by the automatic system, after validation, ranges from 155 to 3314 BNcells per sample and after visual validation the percentage of rejected cells was quite low (from about 1.5 to 9 %), except for the highest dose of 6.4 Gy

(about 40%). The dose prediction accuracy was evaluated for manual and semi-automated scoring approaches by the Mean of the Absolute Differences (MAD) between physical and estimated doses [192], [197]. The results of this prediction dose exercise are reported in Table 1-6. It was observed that estimated doses by both scoring modes are very close to the physical doses and also estimated doses of blind samples at higher doses stay within the real dose plus minus 20%. Only the blind sample at the highest dose of 6.4 Gy shows a clear underestimation for both scoring approaches. Excluding this dose the differences in MAD and incorrect dose estimation are much improved (MAD value decreases from 0.37 Gy to 0.22 Gy in manual mode and from 0.40 Gy to 0.15 Gy in semi-automated mode). The elimination of the 6.4 Gy dose can be justified since in the calibration curve the highest dose is 4 Gy, then dose > 4 Gy may be underestimated. Furthermore, comparison between actual doses and estimated doses was performed using Spearman's correlation test (value of correlation coefficient r_s from -1 to +1). Correlation coefficients for manual scoring ($r_s = 0.997$) and for semi-automated scoring ($r_s = 0.976$) indicate a high correlation between physical doses and estimated doses in both modes.

Table 1-6: Biological Dose Estimations of Ten Blind Samples Based on the Analysis of Micronuclei by Manual and Semi-Automated Scoring.

Estimated dose	Physical dose (Gy)										MAD (Gy)	MAD w/o 6.4 Gy	r Spearman	P
	0	0.1	0.7	1.4	2	2.2	2.6	3	4.2	6.4				
Manual MN/2000 BN	0.0	0.0	0.6	1.2	1.9	2.0	2.2	2.7	3.6	4.7	0.37	0.22	0.997	<0.0001
Semi-automated MN/variable BN ^a	0.1	0.0	0.6	1.4	2.0	2.1	2.5	2.6	3.8	3.7	0.40	0.15	0.976	<0.0001

1.2.4.5 Discussion

In this study on CBMN assay, a comparison between manual and automated scoring was performed using the automated system Metafer4 MNScore (MetaSystem) which however requires visual validation by a scorer. A considerable decrease of BNcells number detected by MNScore was observed at the higher doses due to the presence of apoptotic nuclei. As reported in previous studies [35], [263], the results obtained by manual and automated scoring showed lower MN frequencies at higher doses in fully automated analysis than in manual mode probably because the system doesn't detect MN which are in contact with the main nuclei and more MN close to each other [194]. Micronucleus frequencies of manual and semi-automated scoring are similar and the respective calibration curves showed a good agreement. Also the results obtained in dose prediction exercise by manual scoring and semi-automated scoring are similar. In fact, a good correlation between physical and estimated dose was observed for both approaches. The lower accuracy in the estimation for dose at 6.4 Gy could be explained since this dose is out of the dose range considered in the calibration curves.

1.2.4.6 Conclusion

Our study confirms that the automated CBMN assay is a promising strategy to achieve a rapid and reliable dose assessment for population triage in large-scale radiological/nuclear accidents, although it still requires the visual validation by a scorer. The good agreement of the results between manual and semi-automated scoring obtained in this study encourages research to implement automated MN analysis by improvement of CBMN protocols for the automated scoring and optimization of classifier setting for a better BNcells and MN detection, in order to improve the automatic performance and to reduce the involvement of a scorer. The HUMN project is focused on the establishment of standardized criteria for automated scoring and on the organization of intercomparison exercises on automated analysis, in order to evaluate the performance of this approach compared to manual mode. These exercises are useful to assess the interlaboratory variability using the same or different automated systems and/or classifiers.

1.3 MEDICAL COUNTERMEASURES

1.3.1 Protection and Treatment with Nicotinic Acid and its Derivatives (A Mouse Model)

1.3.1.1 Introduction

In today's world, people can be inadvertently exposed to ionizing radiation during accidents in nuclear power plants, a nuclear war, or nuclear/radiological terrorist incidents. In these instances some of the casualties may sustain high (i.e., > 1 Gy) doses of radiation. Likewise, high doses may be absorbed by normal tissues of oncological patients treated with local radiotherapy. Short-term exposures to radiation at doses in excess of 1 – 2 Gy may result in acute radiation syndrome, skin 'burns', and/or other injuries commonly associated with the development of both primary and secondary thrombosis and inflammation.

Ever since the harmful effects of ionizing radiation were recognized, a quest has been pursued for effective radio-protectors, i.e., compounds designed to reduce radiation-induced damage in normal tissues. For many decades, a 'radio-protector' referred to a free radical scavenger that prevents fixation of the initial radiochemical events after radiation exposure. It is now clear, however, that potentially useful agents may also act through a variety of other mechanisms, such as hydrogen donation to targeted molecules, formation of mixed disulfides, delay of cellular division, and induction of hypoxia in tissues [160]. According to the time of their application versus the time of radiation exposure, radio-protectors can be divided into three groups [221]:

- Prophylactic agents (protectors), which are given before the exposure;
- Mitigators – given during or shortly after the exposure but still before the manifestation of an overt injury; and
- Therapeutic (remedial) agents – active after application post-exposure when overt symptoms may have already developed.

All of these should be selective in protecting normal, but not neoplastic, tissues from ionizing radiation, should be delivered with relative ease, and should exhibit minimal toxicity [52].

Thus far, the only registered radio-protective compound is amifostine (Ethyol®), which is almost exclusively used to reduce side effects of radiotherapy of the head and neck cancers. However, administration of amifostine is associated with numerous side effects (e.g., nausea, vomiting, hypotension, salivation, dizziness, somnolence, fever, hypocalcemia) and it is effective only when used 15 – 30 minutes before the irradiation. Currently, intensive investigations are carried out on other types of substances (e.g., cytokines, vitamins, plant extracts, pharmacological agents, hormones) as potential radio-protectors.

Development and evolution of disorders caused by absorption of high (> 1 Gy) doses of ionizing radiation primarily hinges on the loss of bone marrow and peripheral blood cells as well as on the damage and dysfunction of vascular endothelium. Despite a significant reduction in the number of circulating thrombocytes, intravascular clotting increases after irradiation owing to the enhanced adhesion and aggregation of platelets on the surface of the endothelium [254]. This phenomenon is associated with the elevated expression of tissue factor (TF, a.k.a. factor III, thrombokinase, or CD142) [255], von Willebrand Factor (vWF) [34], and Platelet-Activating Factor (PAF) [147], as well as with the decreased vascular fibrinolytic activity [94] and reduced expression of Thrombomodulin (TM) [256], Prostacyclin (PGL₂) and the prostacyclin receptor [105] in endothelial cells. It is therefore plausible that anti-thrombotic and anti-inflammatory agents may protect against and/or mitigate the development/progression of radiation-induced pathologies.

Some derivatives of nicotinic acid (a.k.a. vitamin PP, vitamin B₃, or niacin), such as MNA, exert both anti-thrombotic and anti-inflammatory properties owing to their capacity to stimulate secretion of prostacyclin

(PGI₂) by the vascular endothelial cells and down-regulate the levels of pro-inflammatory cytokines (IL-1 β , IL-6, IL-8, and TNF- α) in peripheral blood [2], [19], [40], [41], [48], [81], [266]. Moreover, as substances originating from a vitamin, nicotinic acid derivatives should be non-toxic in small quantities and thus unlikely to evoke any serious side effects. Indeed, as a non-toxic ingredient MNA is included in a number of cosmeceuticals produced by a healthcare company Pharmena SA. In view of the above, the aim of the present study was to assess potential radio-protective and radio-remedial effects of the selected pyridinium salts.

In the present study, the 30-day survival of BALB/c mice was assessed after Whole Body Irradiation (WBI) with 7.5 Gy γ -rays. NAc, NA, MNA, 1,4-DMP, and 1,3-MAP were given to the animals in drinking water at 100 mg/kg b.m. daily, starting 7 days before, on the day of, or 7 days after the exposure to ionizing radiation and continued until the mice's death or the end of observation. Another group of mice was exposed (WBI) to 6.5 Gy γ -rays and on the selected days after the irradiation spleen and bone marrow cellularities as well as the leukocyte and thrombocyte counts in peripheral blood were assessed.

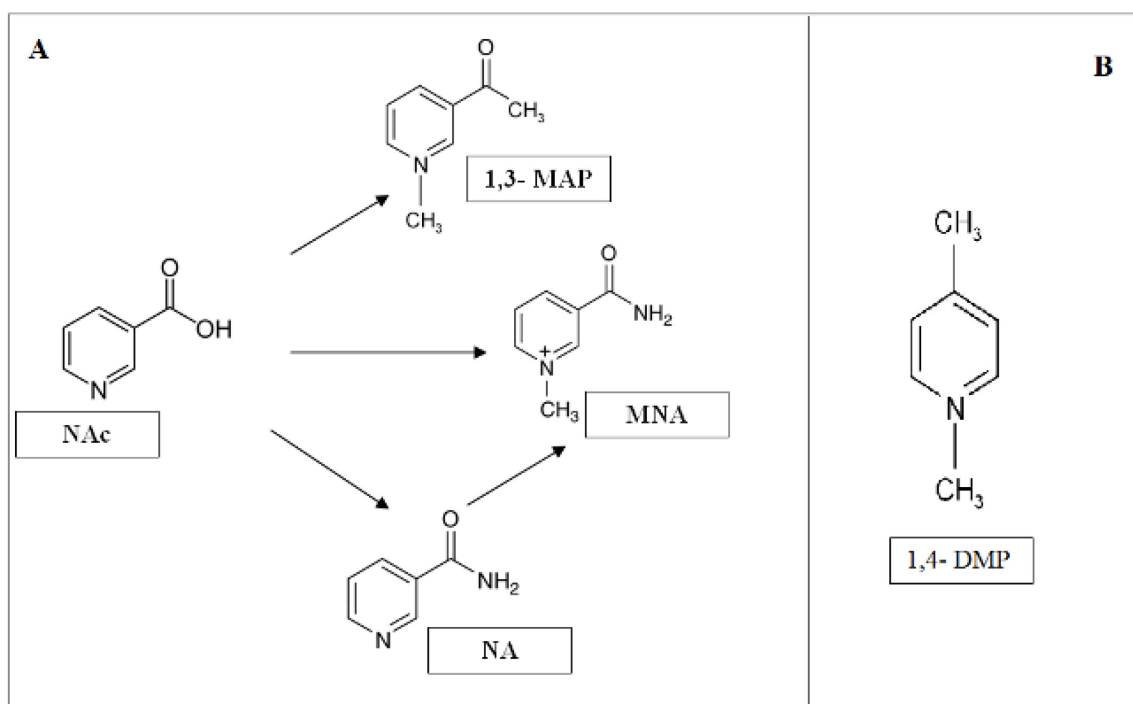


Figure 1-5: Chemical Structure of the Examined Compounds: (A) NAc (Nicotinic Acid; Vitamin B₃) and its Derivatives – MNA (1-Methylnicotinamide), 1,3-MAP (1-Methyl-3-Acetylpyridine), NA (Nicotinamide); (B) 1,4-DMP (1,4-Dimethylpyridine).

1.3.1.2 Results

The examined derivatives of nicotinic acid have been previously shown to exert both anti-inflammatory and anti-thrombotic properties [2], [19], [40], [41], [48], [81], [266]. In the present study, we demonstrated that NAc significantly improved survival of mice from groups in which its administration started 7 days before and 7 days after WBI of BALB/c mice at 7.5 Gy γ -rays; no such effects were observed in mice given NA (Figure 1-6 – NAc and 2-NA). Administration of MNA when started 7 days before or 7 days after the irradiation significantly enhanced survival of the lethally irradiated mice; the effect was more pronounced when application of MNA began after the irradiation (Figure 1-6 – MNA). In turn, application of 1,3-MAP significantly prolonged the survival only when the administration started 7 days after the irradiation (Figure 1-6 – 1,3-MAP).

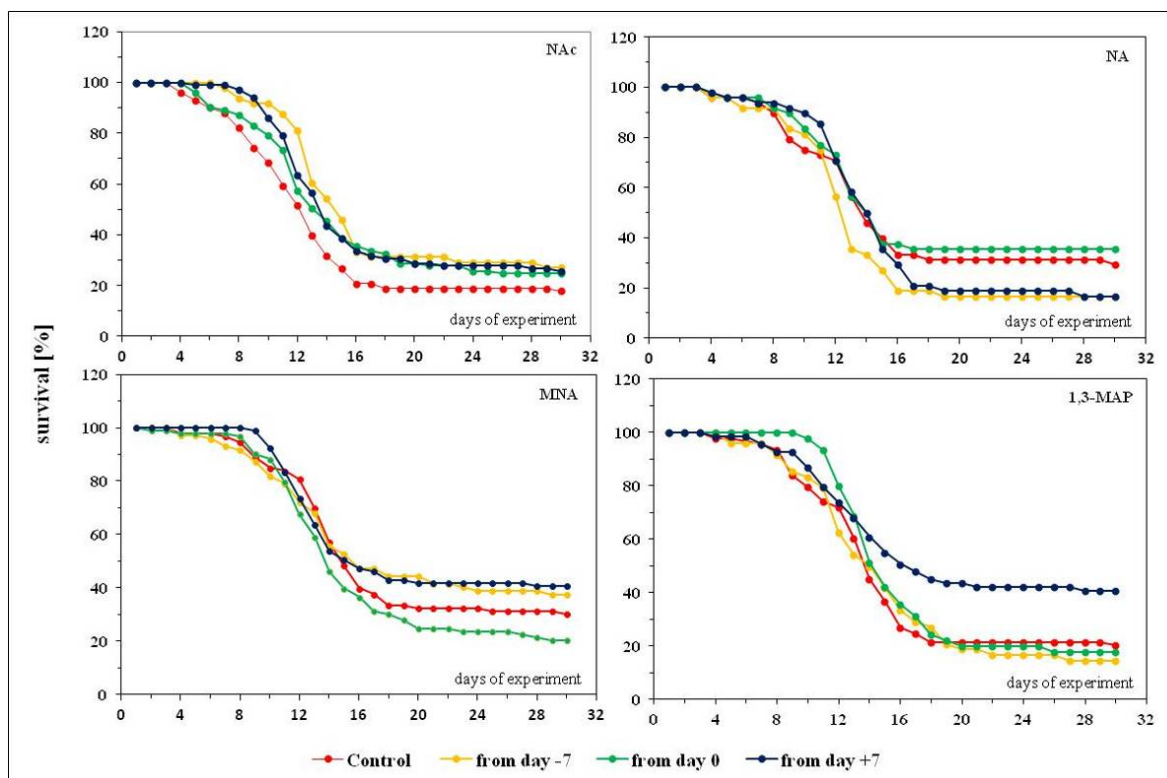


Figure 1-6: Survival of the Lethally (7.5 Gy) Irradiated BALB/C Mice Fed NAc, NA, MNA, or 1,3-MAP (100 mg/kg b.m./day) in Drinking Water. Application of the NAc derivatives began on Days -7, 0, or +7 of the experiment. Each experimental group consisted of at least 48 animals.

As shown in Figure 1-7, administration of 1,4-DMP, regardless of the starting day relative to WBI, also significantly increased the survival of mice, the effect being most pronounced when the administration began on the day of the irradiation.

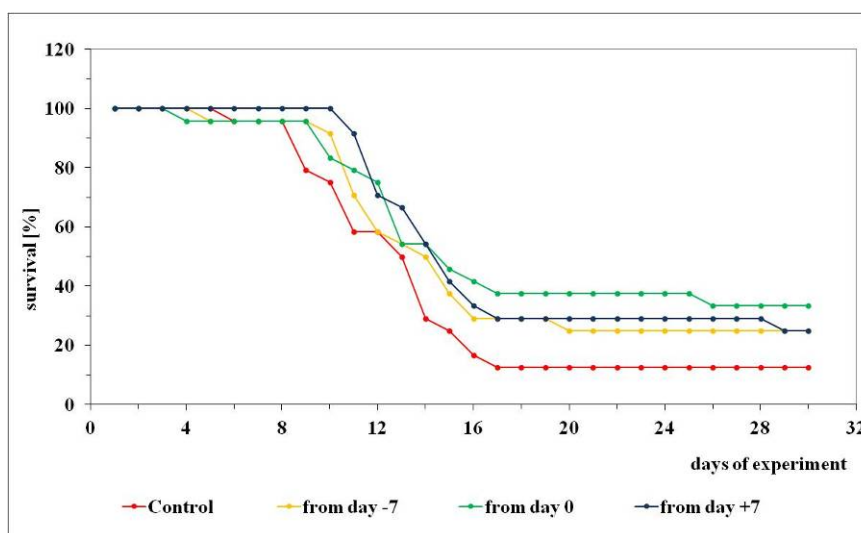


Figure 1-7: Survival of the Lethally (7.5 Gy) Irradiated BALB/C Mice Fed 1,4-DMP (100 mg/kg b.m./day5) in Drinking Water. Application of 1,4-DMP started on Day -7, Day 0, or Day +7 of the experiment. Each experimental group consisted of at least 24 animals.

To our knowledge, this is the first study to demonstrate that application of the NAc derivatives and 1.4-DMP, which started 7 days before (radio-protective activity) or, most notably, as late as 7 days after (radio-remedial activity) the exposure of mice to a lethal dose of γ -rays, increased the survival of the animals. Indeed, although no directly comparable data are available, radio-protective capacities have so far been demonstrated only when other compounds examined in various experimental models were administered either before or shortly after lethal irradiations of the animals. These include [3], [16], [27], [76], [83], [87], [137], [203], [210], [211]:

- Somatostatin analog (SOM23);
- γ -, δ - and α -tocotrienols;
- Naturally occurring Mycoplasma-derived lipopeptide ligand for the Toll-like receptor 2/6 (CBLB613);
- Ex-Rad (a small molecule kinase inhibitor developed for modifying cell cycle distribution patterns in cancer cells subjected to radiation therapy and identified as a potential candidate for radiation protection studies);
- *Saccharomyces cerevisiae*-derived powder containing Zn, Mn, Cu, or Se;
- *Mentha* extract;
- Recombinant IL-1 β ;
- Annonaceae (XA); and
- Vitamin C (VC).

However, none of these substances has evidenced a radio-remedial activity of the tested compound when it was given later than several hours post irradiation. Hence, such an activity demonstrated by us for the selected derivatives of NAc and 1.4-DMP applied to the lethally irradiated mice from day 7 after exposure to a lethal dose of gamma-rays warrants further exploration, even though the increase in the survival rate did not exceed 20%.

A whole- or partial-body irradiation at doses greater than 1 Gy result in the acute radiation syndrome the earliest manifestation of which is the hematopoietic syndrome [89] characterized by a massive loss of Hematopoietic Stem Cells (HSC) in the bone marrow followed by cytopenia in the blood. Pluripotent HSC, which provide all of the downstream components of the blood [90], are non-lineage committed and capable of self-renewal. Since a cell's radio-sensitivity is inversely related to its maturational state HSC are moderately radio-resistant and with their transition to progenitor cells they become more sensitive to radiation [149], [178]. Indeed, our present studies demonstrated that WBI of mice at 6.5 Gy γ -rays dramatically reduced the numbers of circulating leukocytes and platelets as well as the total numbers of bone marrow and spleen cells (Table 1-7). However, when such irradiated mice were fed one of the tested NAc derivatives or 1.4-DMP inconsistent changes in the numbers of these cells were obtained compared to the irradiated mice which drank water without any additives – in some cases the numbers were down, while in other cases up-regulated (Table 1-7 and Table 1-8). It is therefore unlikely that stimulation of haematopoiesis by the NAc derivatives or 1.4-DMP is the underlying mechanism of the survival-enhancing activities of these compounds demonstrated in the lethally (7.5 Gy) irradiated mice.

Table 1-7: Significant Changes in Spleen and Bone Marrow Cellularity, and Blood Cell Counts in BALB/C Mice Irradiated at 6.5 Gy and Fed MNA or 1.4-DMP in Drinking Water from Day -7, Day 0, or Day 7 of the Experiment. Each experimental group consisted of ten animals.

Examined Parameters		Day	Non-Irradiated Control	Irradiated Control	MNA			1.4-DMP		
					-7	0	+7	-7	0	+7
Spleen	Number of cells x 10 ⁶	7	200	5.1	5.0	1.7	3.6	4.7	10.6	8.1
		10		5.2	3.0	5.3	3.3	22.0	13.8	22.0
		14		8.3	3.6	6.4	3.3	15.2	28.8	30.0
		30		118.6	119.1	111.2	86.2	144.6	83.8	81.8
	Viability [%]	7	98.2	74.4	69.3	66.7	64.0	85.0	93.0	86.7
		10		89.0	80.5	84.4	77.2	93.7	91.2	91.0
		14		88.9	87.2	87.8	81.5	91.7	93.2	91.3
		30		81.9	86.7	90.4	89.8	86.0	86.5	79.4
Bone Marrow	Number of cells x 10 ⁴	7	625	7.5	7.8	13.2	6.1	14.8	10.8	9.0
		10		24.2	9.7	19.1	6.3	38.5	47.8	27.0
		14		38.3	26.8	38.8	9.7	46.3	101.6	44.9
		30		430.0	691.9	568.1	646.3	597.5	729.6	617.0
	Viability [%]	7	95.6	89.5	89.9	89.4	89.6	89.0	88.9	89.2
		10		90.6	88.5	88.0	84.8	89.3	84.8	82.8
		14		87.6	86.6	85.7	91.2	85.7	89.9	84.5
		30		96.6	98.1	98.7	98.8	97.7	98.2	98.0
WBC [10 ³ /μl]	7	9.1	0.9	0.6	1.0	0.9	0.7	1.0	0.9	
	10		0.2	0.3	0.2	0.4	0.5	0.3	0.2	
	14		0.7	0.3	0.3	0.2	0.4	0.5	0.4	
	30		9.2	7.6	11.9	8.9	7.1	6.0	5.6	
RBC [10 ⁶ /μl]	7	8.8	7.8	8.7	8.8	9.3	7.0	7.2	6.7	
	10		7.5	7.2	7.6	8.1	6.6	5.8	6.4	
	14		5.8	5.7	6.4	6.2	6.3	4.5	5.5	
	30		8.2	8.1	7.8	7.8	8.1	8.5	8.4	
PLT [10 ³ /μl]	7	637.5	67.0	74.5	84.0	70.0	39.5	51.0	55.5	
	10		40.5	67.0	33.0	27.0	50.5	61.0	42.5	
	14		114.0	74.0	60.5	61.0	90.0	124.0	52.0	
	30		545.5	536.0	677.0	506.0	551.5	385.0	489.5	

Table 1-8: Significant Changes in Spleen and Bone Marrow Cellularity, and Blood Cell Counts in BALB/C Mice Irradiated at 6.5 Gy and Fed NAc, NA or 1.3-MAP in Drinking Water from Day -7, Day 0, or Day 7 of the Experiment. Each experimental group consisted of ten animals.

Examined Parameters		Day	Irradiated Control	NAc			NA			1.3-MAP		
				-7	0	+7	-7	0	+7	-7	0	+7
Spleen	Number of cells $\times 10^6$	7	5.1	1.2	2.0	1.9	6.6	5.8	7.0	4.7	4.5	5.4
		10	5.2	5.8	4.0	5.0	11.4	13.6	18.6	3.3	3.6	3.4
		14	8.3	5.2	3.6	3.4	28.0	19.2	34.2	3.4	3.8	4.0
	Viability [%]	7	74.4	37.0	31.0	35.3	80.8	74.1	78.6	63.1	59.1	86.5
		10	89.0	91.9	89.9	89.0	87.2	91.2	91.1	77.3	80.3	84.4
		14	88.9	81.2	67.6	69.4	89.3	92.6	93.8	85.4	84.2	86.8
Bone Marrow	Number of cells $\times 10^4$	7	7.5	4.3	3.0	8.3	7.5	9.5	12.9	4.8	7.1	6.8
		10	24.2	1.3	13.8	11.2	23.5	51.5	32.0	13.2	20.7	22.6
		14	38.3	17.6	2.7	7.0	11.4	137.5	63.6	48.0	13.7	12.5
	Viability [%]	7	89.5	88.5	94.3	93.3	89.5	90.5	89.6	91.4	89.5	89.5
		10	90.6	91.5	89.0	88.9	88.9	90.7	88.6	88.3	88.2	87.6
		14	87.6	87.2	86.8	77.0	89.7	91.3	84.8	89.9	74.2	88.5
WBC [$10^3/\mu\text{l}$]	7	0.9	0.8	0.4	0.3	0.9	0.5	0.8	0.8	1.3	1.2	
	10	0.2	0.3	0.2	0.3	0.3	0.3	0.3	0.3	0.2	0.3	
	14	0.7	0.5	N/A	0.4	0.5	0.4	0.9	0.6	0.3	0.6	
RBC [$10^6/\mu\text{l}$]	7	7.8	8.3	8.1	8.5	7.7	7.3	7.2	8.5	8.8	9.0	
	10	7.5	7.3	6.0	7.5	7.5	7.0	6.9	8.0	8.5	8.1	
	14	5.8	6.2	N/A	6.4	5.5	4.5	6.0	6.7	6.0	6.1	
PLT [$10^3/\mu\text{l}$]	7	67.0	82.0	65.0	71.0	51.0	44.5	64.0	126.0	84.0	140.0	
	10	40.5	65.0	41.0	36.0	36.0	33.5	35.0	42.0	38.0	54.0	
	14	114.0	76.0	N/A	45.0	55.0	103.0	77.0	60.0	53.0	64.5	

N/A = Not Available.

Only few reports provide results of studies in which the authors assessed similar parameters. In contrast to our present investigation, however, most of the available data indicate a clear protective effect of the examined compounds reflected by stimulation rather than suppression of haematopoiesis. Such effects were demonstrated for SOM230, γ - and δ -tocotrienol; *Mycoplasma*-derived CBLB613; recombinant interleukin-1 β ; the *Mentha piperita* extract [27], [76], [87], [137], [202], [203], [211].

1.3.1.3 Conclusion

- 1) Depending on the time of application of the examined compounds significantly increased survival of the lethally irradiated BALB/c mice:
 - 1.4-DMP – when administered before, on the day of, or after the irradiation;

- NAc and MNA – when administered before or after the irradiation; and
 - 1.3-MAP – only when administration started after the irradiation.
- 2) Results obtained in mice exposed at 6.5 Gy suggest that stimulation of haematopoiesis is not the likely explanation of the enhanced survival and that other mechanisms (e.g., mitigation of radiation-induced inflammation, thrombosis, and/or depressed endothelial function) need to be considered.
 - 3) Hopefully, the obtained results will contribute to verification of the prevailing belief that all the currently known ‘radio-protectors’ are either totally ineffective or practically useless owing to the associated toxicity. Most importantly, the results should provide grounds for the development of novel radio-remedial agents which, when applied several hours or days post-exposure, can effectively ameliorate the severity and/or progression of radiation injuries induced in normal tissues of patients undergoing radiotherapy as well as in victims of radiation accidents and terrorist events in which radiological and/or nuclear weapons have been used.

1.3.2 Cell / Transient Gene Therapy to Treat Acute Radiation Syndrome: Evaluation in Animal Models

Abstract

Acute Radiation Syndrome represents the clinical response of radiation-sensitive key tissues (i.e., hematopoietic, gastro-intestinal, neuro-vascular and cutaneous) following exposure to high doses of ionizing radiation. In this context, cell/gene therapy approaches have been developed by our group and others to repair damaged tissues or replace eradicated cells. Today mesenchymal stem injection is one of the most promising strategies whereas gene therapy is still in its infancy but could represent a valuable approach in the future.

1.3.2.1 Rationale of Cell Gene Therapy for Acute Radiation Treatment

Following Total-Body Irradiation (TBI) or significant partial-body irradiation, Acute Radiation Syndrome (ARS) represents the clinic consequence of the complex interplay between irradiated tissues including cross talks between:

- Distant organs;
- Vascular damages;
- Inflammatory response; and
- Stem cell niche disorders.

Major radiosensitive tissues are:

- Hematopoietic/H (> 2 Gy TBI);
- Gastrointestinal/G (> 10 Gy);
- Neurovascular/N (> 30 Gy); and
- Cutaneous (> 25 Gy) (METREPOL scoring HNCG).

In severe cases ARS is likely to evolve towards Radiation-Induced (RI) Multiple Organ Dysfunction then Failure syndrome (RI-MODS/MOF) [59] mainly linked to the Systemic Inflammatory Response Syndrome (SIRS). Pathophysiology of ARS strongly involves stem cell death leading to hypoplasia and barrier disruptions. In this context cell/gene therapy has been proposed for many years to replace eradicated tissues and more recently to mitigate radiation-induced damage via trophic factor production.

1.3.2.2 Transient / Gene Therapy to Mitigate Radiation-Induced Hematopoietic Syndrome

The hematopoietic syndrome associates immunosuppression, coagulation disorders, SIRS and pancytopenia which mainly results from the death of Hematopoietic Stem and Progenitor Cells (HSPCs). Granulocyte colony stimulating factor is the gold standard for heterogeneous irradiations at a dose about Lethal Dose 50% (LD50%) and medical management would consist of allogeneic hematopoietic stem cell transplantation in case of bone marrow eradication above the cytokine efficacy threshold (>7 Gy) [60] despite unsolved morbidity/mortality complications. Thus identifying new drugs and developing new strategies remain a priority especially in order to manage a mass casualty scenario with two major goals:

- Raising up the HSPC transplantation threshold; and
- Prevention/cure of RI-MOF.

This was the rationale of the “Emergency Antiapoptotic Cytokine (EACK) therapy” which aimed at counteracting the spreading HSPC’s RI apoptosis during the first 48 hours. Thus our group tested *in vitro* and *in vivo* the thrombopoietin, Stem Cell factor, FLT-3 ligand and interleukin-3 combination (SFT3) which in our hand was the most effective. We showed that short-term injection of the SFT3 combination to mice soon after lethal Total Body gamma-Irradiation (TBI) promoted survival [96]. We also showed a complete, long-lasting protection of hematopoiesis (i.e., an absence of cytopenia) in monkeys treated with SFT3 (each factor given intravenously at 50 µg/kg) 2 hours after 5 Gy gamma TBI [60]. In 7 Gy gamma irradiated monkeys (i.e., a dose higher than LD 50% at 60 days) [99], the single SFT3 injection (2 hours delay) was still capable of reducing the period of thrombocytopenia but not that of neutropenia.

In an effort to overcome the limits of EACK we hypothesized the feasibility of a global niche treatment. The goal was to achieve an effective stimulation of both hematopoietic and supportive cells. Local injection of mesenchymal cells manipulated *ex vivo* was performed to locally produce the trophic factor(s) during a short but significant period (i.e., transient gene therapy strategy). Viral tools were discarded to achieve clinical use. This strategy was evaluated in highly irradiated monkeys. Transduced cells were injected via an intra-osseous way in order to act locally. This approach especially aims at targeting the bone marrow vascular niche and at stimulating residual HSPCs. Sonic hedgehog (Shh) morphogene was tested as a first candidate based on its proangiogenic activity and its capacity to stimulate HSPCs [30], [179]. Adipocyte Stem Cells (ASCs) were used as vector cells following nucleofection with mock or Shh-pIRES2 plasmids according to Amaxa technology. Eight (8)-Gy gamma irradiated monkeys were injected 48 hours following TBI to mimic logistic constraints. In this study, injected monkeys ($> 2 \times 10^6$ Shh-ASC/kg) exhibited an accelerated multi-lineage recovery when compared with mock-ASCs treated monkeys [58].

1.3.2.3 Transient Gene Therapy to Mitigate Cutaneous Radiation Syndrome

The biological responses of the skin to high-dose ionizing radiation occur in a characteristic temporal pattern mainly depending on radiation quality, dose rate, total dose, and cellular conditions. Immediately after irradiation, synthesis and action of cytokines by skin cells (epidermal keratinocytes, dermal fibroblasts, and resident immunocompetent cells including dermal dendritic cells, neutrophils, eosinophils, and lymphocytes) is initiated and continues as a cascade during all stages of Cutaneous Radiation Syndrome (CRS). This result in the classical clinical evolution of CRS characterized by the delayed onset of the manifestation stages:

- Transient early erythema;
- Dry and then wet desquamation;
- Derma ischemia or necrosis for doses above 20 Gy [131]; and
- Late fibrosis.

Regarding cellular tools, Friedenstien and co-workers were the first to describe spindle-shaped cells, i.e., fibroblasts-like cells derived from Bone Marrow (BM) that attached to tissue culture plastic and formed

colonies termed colony-forming unit-fibroblast [75]. In fact, such cells are also resident in parenchymal non-hematopoietic tissues such as muscle, fat (Adipocyte Stem Cells (ASCs)) or liver as well as from peripheral blood and umbilical cord blood or gingival tissue. These cells represent a heterogeneous population only a fraction of which should be named stem cells [47], [236]. Regarding functional characterization Mesenchymal Stem Cells (MSCs) retain the capacity to differentiate *in vitro* into bone, cartilage and adipose following *specific* stimulation. Attempts to define their phenotype were made in different global consensus. Classically MSCs lack the expression of hematopoietic cell markers such as:

- CD45 (common leucocyte antigen);
- CD14 (monocyte surface protein); and
- CD34 (mucosialin).

In contrast they express typical surface antigens such as:

- CD44 (hyaluronate receptor);
- CD106 (vascular cell adhesion molecule-1);
- CD90 (Thy-1);
- CD29 (integrin beta 1); and
- CD73 (SH-3/SH-4).

They may represent specialized vascular pericytes [47], [177]. They are described as mobile cells and circulation processes have been modeled from leucocyte transmigration sequence. MSCs respond to stress signals – among which irradiation – in animal models exhibiting a specific homing towards damaged tissues following systemic or local injection [47], [73].

MSCs represent promising tools in regenerative medicine to favour wound healing especially following exposure to high dose of ionizing radiation. Their mechanisms of action remain unclear. Local paracrine effects are likely to be predominant but some level of transdifferentiation/plasticity may occur albeit only a marginal level of engraftment has been reported in transplantation studies. MSCs are low immunogenic cells (MHC I⁺ / MHC II^{neg} / costimulatory molecules^{neg}) with immunomodulatory properties which can be transplanted in an allogeneic context the efficacy of which is not fully validated. From encouraging results in animal models autologous BM-MSC were used in clinic and today a few patients (up to 70 Gy of local exposure associated with a heterogeneous irradiation and hematopoietic syndrome) have received a compassionate protocol using autologous BM-MSC.

Modifying MSC's secretome may enhance their repair capacity. Genetically-manipulated stem cells would represent therapeutic agents per se and via specific additive trophic factor(s) delivery. Feasibility of transient gene therapy for CRS has been recently evaluated *in vivo* in the mini-pig model by our group [185]. ASCs were nucleofected with a pIRES2 plasmid coding for Shh. In this preliminary study the injection of *ex vivo* manipulated ASCs was well tolerated.

1.3.2.4 Conclusion

Today mesenchymal stem cells represent the most promising cellular tool to favour the repair of highly irradiated extrahematologic tissues albeit only limited cohorts of treated victims have been injected with autologous cells. Gene therapy is still in its infancy but work is going on to determine whether it could represent a valuable approach in the future.

Table 1-9: Hematopoietic Recovery in Highly Irradiated Monkeys (8 Gy Gamma Frontal TBI) Given Shh-ASC or Mock-ASCs.

Parameters	Mock-ASC Injected Group, Mean +/- SD (n = 4)	Shh-ASC Injected Group, Mean +/- SD (n = 4)
Duration of neutropenia, ANC < $0.5 \times 10^9/L$	17.7 +/- 2.6	14.2 +/- 1
Duration of thrombocytopenia, PLT < $20 \times 10^9/L$	10 +/- 2.2	4.75 +/- 1.8
Duration of lymphopenia, ALC < $1 \times 10^9/L$	29.7 +/- 3	27.75 +/- 4.2
Duration of anemia, hemoglobin level < 10 g/dL	50.7 +/- 31	15.5 +/- 3.6

ANC: Absolute Neutrophil Count; ALC: Absolute Lymphocyte Count; PLT: Platelet. Two mock-ASC monkeys died on days 19 and 196.

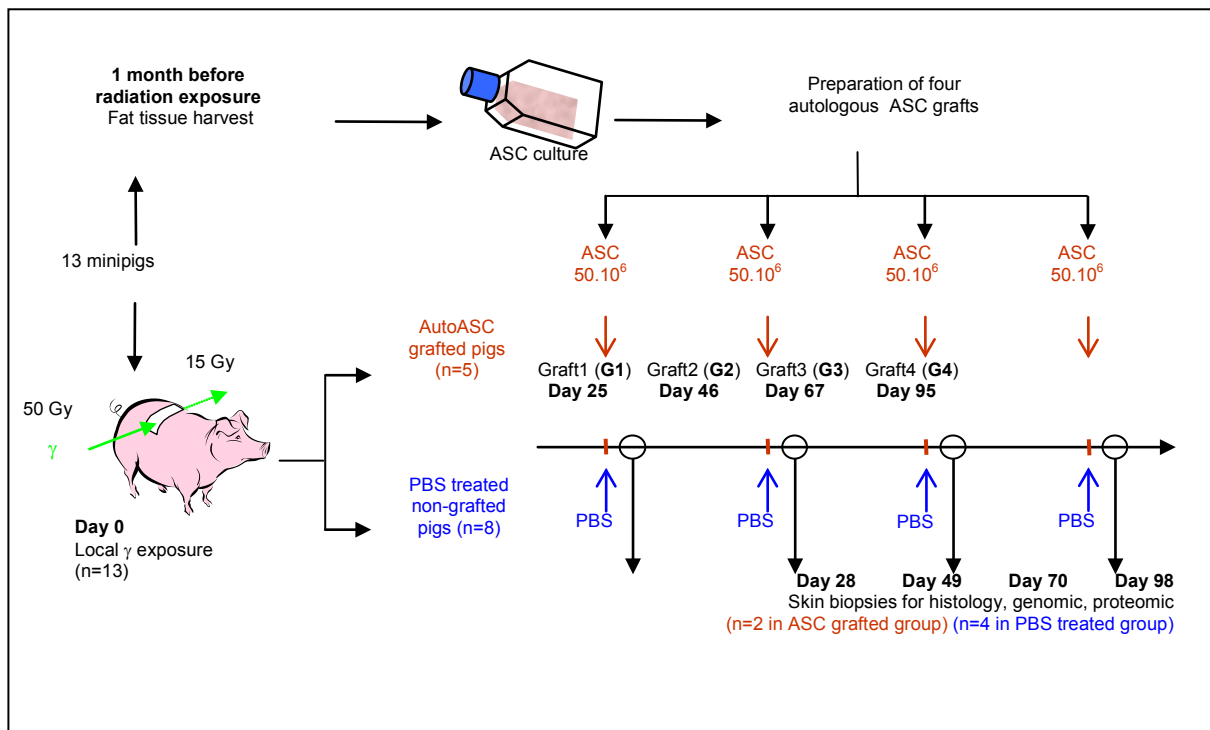


Figure 1-8: Adipocyte Stem Cells (ASC) Local Injection to Mitigate CRS in Mini-Pig Model. Experimental schedule; clinical evolution in PBS and ASC treated mini-pigs. Adapted from PloS one [72].

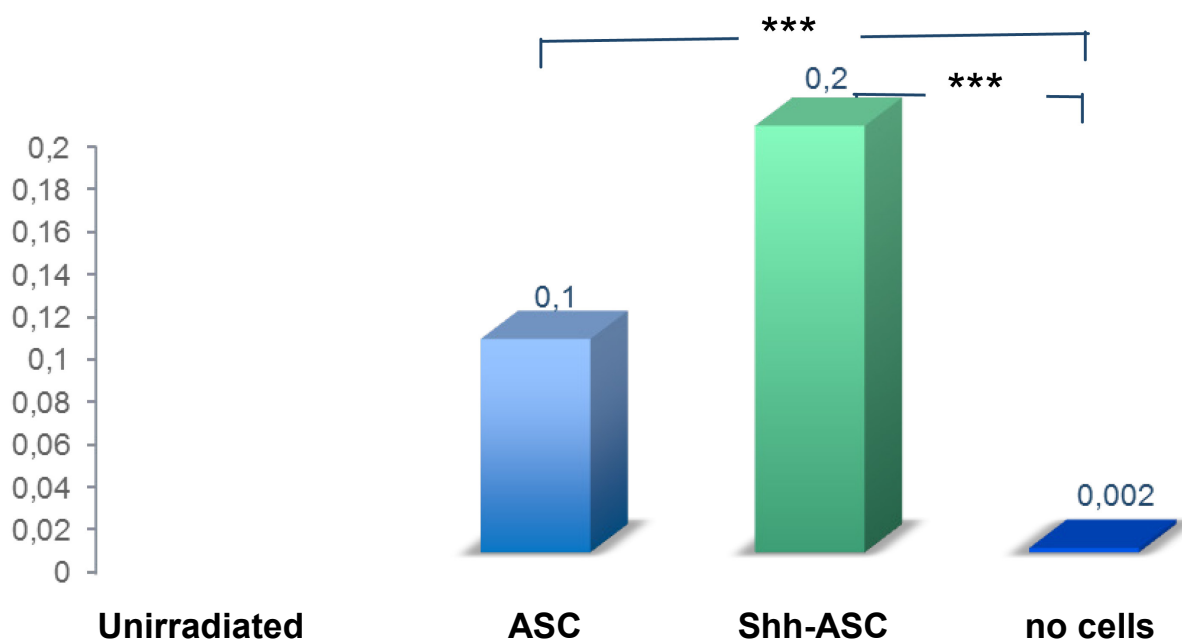


Figure 1-9: Colony Forming Efficiency in Percentage of Plated Skin Fibroblasts *In Vitro* Irradiated (25 Gy Gamma) and then Incubated 14 Days in Presence of Culture Media from Mock-ASC, Shh-ASC and Basic Culture Medium.

1.3.3 AFRRRI Program on Radiation Injury and Countermeasures: Moderate to High Radiation Doses

Abstract

Recent events in the Middle East and Europe highlight the need to prepare responses to weapons of mass destruction, including radiological/nuclear attacks. An important component of defence against such weapons is safe and effective Medical Countermeasures (MedCM) to be administered before and/or after radiation exposure. Current countermeasure candidates possess efficacies in preclinical studies indicating tens of thousands of people could be saved in mass casualty scenarios. Rescue or clean-up personnel entering radioactively contaminated sites could extend their time of operation 20 – 30 %, facilitating their ability to accomplish their missions, and reducing the total number of personnel rotating in and out of the contaminated area. AFRRRI focuses on countermeasure candidates with clear paths to licensure, including appropriate consideration of routes of administration, durations of efficacy, and toxicity. A number of AFRRRI candidates have been tested successfully in large animal models for safety and survival enhancement, and have been demonstrated to be safe in preliminary clinical trials. A continuing roadblock is the lack of funding available to small biotechnology companies for expanded large animal testing, multi-center clinical safety trials and other aspects of advanced drug development required for regulatory approval. AFRRRI is not funded for advanced development. Some funding is available for advanced development from civilian U.S. government agencies, but this does not address the military requirements of administration times before or shortly after radiation exposure. This report highlights recent activities of AFRRRI’s research program on mechanisms of injury and recovery, a novel animal model (mini-pig), and current promising MedCM efforts. MedCM against pure radiation (gamma rays and mixed neutrons/gamma rays) and radiation combined with other injury (Combined Injury, RCI) are discussed.

1.3.3.1 Mechanisms of Radiation Injury and Recovery

AFRRI's investigations of the mechanisms of radiation injury and recovery are exemplified by Dr. Mang Xiao's program on signaling pathways. Her work has shown that NF-kappaB is a radiation-induced prosurvival factor in human osteoblastic cells [267]. NF-kappaB was found to be necessary for the hematopoietic niche function of these cells in supporting hematopoietic stem and progenitor cells [267]. Osteoblast cells are protected from radiation-induced senescence by the stress response gene REDD1, as shown by small interfering RNA (siRNA) knockdown experiments [139]. MicroRNA (miRNA) arrays revealed that radiation upregulated miRNA-30c (miR-30c) in hematopoietic cells, but miR-30c was downregulated in osteoblasts. Transfecting cells with miR-30c precursor (pre-miR-30c) suppressed REDD1 in both hematopoietic cells and osteoblasts [138]. This REDD1 suppression by miR-30c enhanced cell death in the osteoblasts. Inhibition of miR-30c protected hematopoietic progenitors from gamma radiation [138]. The group also demonstrated that protection of murine and human hematopoietic cells by Delta-Tocotrienol (DT3) is mediated by pathways involving Erk1/2 and mTOR [137].

In a study of Human Umbilical Vein Endothelial Cells (HUVECs) and immortalized T lymphocytes (Jurkat cells) cultured individually and in co-culture after exposure to mixed neutron/gamma fields, it was shown that radiation-induced higher levels of phosphorylated Mitogen-Activated Protein Kinases (MAPKs) p38 and Erk1/2 in HUVEC, in addition to elevated IL-6, IL-8, G-CSF, Platelet Derived Growth Factor (PDGF) and Angiopoietin 2 (ANG2) [5]. Alterations in HUVEC gene expression were observed after exposure to mixed fields and/or co-culture with Jurkat cells. Co-culture with HUVEC also influenced the function of Jurkat cells. Non-irradiated Jurkat cells showed an increase in proliferation when co-cultured with non-irradiated HUVEC, and a decrease in proliferation when co-cultured with irradiated HUVEC. Additionally, non-irradiated Jurkat cells incubated in media from irradiated HUVEC exhibited a marked decrease in proliferation and upregulation of activated caspase 3. Irradiation of Jurkat cells caused a G2/M arrest and increased adherence to HUVEC. When co-cultured with HUVEC, irradiated Jurkat cells exhibited G0/G1 arrest and increased apoptosis. The data indicate that gene expression and cell function of endothelial cells and hematopoietic cells are influenced by radiation and by interactions between the two cell types. These phenomena may affect the success of therapies for ARS and cancer [45].

1.3.3.2 Mini-Pig Model of Acute Radiation Syndrome (ARS)

Animal models are required for efficacy testing of radiation countermeasures, and must be well-characterized. So far, the only large animal models well-characterized for Acute Radiation Syndrome (ARS) are the canine and the Non-Human Primate (NHP). Multiple animal models are needed because no individual model is optimal for every drug and every radiation injury. The Gottingen mini-pig appears to be very promising as an alternate large animal model for radiation countermeasures, based on the work of Dr. Maria Moroni at AFRRI. Advantages of the mini-pig compared to rhesus macaque are that mini-pigs are cheaper, easier to handle (less training of personnel), safer, and raise fewer ethical concerns on the part of staff and the public. Disadvantages are that the mini-pig is not as well-developed a model, and displays a steep survival vs radiation dose curve. The steep survival curve was a concern at first, because it was felt that different labs or even the same lab at different times might find it hard to reproduce survival data. If the radiation dose or animal susceptibility varies even a little from experiment to experiment, wouldn't that shift the curve too much? In actuality, AFRRI has been getting rock solid survival curves for 6 years [155], [156], [158], [159], and 3 additional independent institutions funded by BARDA have obtained almost identical survival curves with Gottingen mini-pigs [62]. We actually find radiation survival data easier to reproduce with mini-pigs than with mice. The LD50 for the hematopoietic syndrome is about half that of humans; the LD50 for rhesus macaques is about twice that of humans. Both models are similar to human in terms of anatomy and physiology. Swine are a popular model for drug pharmacology/toxicology testing for other indications. The mini-pig is a good model for both the hematopoietic and the GI syndromes [61], [155], [156], [158]. G-CSF (Neupogen®) administration enhances survival during the hematopoietic syndrome to an almost identical degree to what was found in rhesus [159]. In addition, an accelerated hematopoietic syndrome

involving Systemic Inflammatory Response Syndrome (SIRS) was found in mini-pigs at radiation doses intermediate between those causing the hematopoietic and GI syndromes [157] similar to what has been observed in mice and humans. Swine are recognized as the best animal model for skin.

1.3.3.3 Medical Countermeasures (MedCM)

1.3.3.3.1 Pure Gamma Rays (Low Linear Energy Transfer (LET))

The countermeasure efforts of AFRRRI mainly focus on hematopoietic ARS in animals exposed to pure gamma rays in our high-level cobalt facility. Some current MedCM in active development in collaborations between AFRRRI and corporate sponsors are the:

- Tocotrienols (delta (GT3) and gamma (GT3));
- Onconova's Ex-Rad®;
- Genistein (BIO 300, Humanetics); and
- CDX-301 (Celldex).

These have been selected for advanced development because of their efficacy and low toxicity. In the cases of the tocotrienols and genistein, AFRRRI did the early work on characterizing their use as radiation countermeasures and recruited biotechnology companies as sponsors. For Ex-Rad® and CDX-301, AFRRRI was recruited at early stages of development by companies to explore their efficacy as radiation countermeasures.

GT3 and DT3 exhibit a Dose Reduction Factor (DRF) of about 1.25 when administered sc 24 hours before irradiation, and are similar in efficacy and toxicity [229]. They are also effective (DRF ~1.1) when given 2 hours post-irradiation. AFRRRI holds a patent on the use of GT3 as a radiation countermeasure. The tocots (Vitamin E compounds, including tocopherols and tocotrienols) were originally of interest because of their anti-oxidant activity. However, the mechanisms of action of these agents as radiation countermeasures are not clear. Ongoing activities include signaling pathways mediating beneficial effects [137], testing formulations and routes of administration, and testing efficacy in non-human primates.

Onconova's Ex-Rad® (Recilisib, ON 01210.Na, 4-carboxystyryl-4-chlorobenzylsulfone, sodium salt) enhances survival during hematopoietic ARS and inhibits apoptotic pathways when given sc before irradiation by reducing levels of p53, p21 and Bax [83]. The DRF is about 1.2 and protective effects are also observed in GI tissue [82]. Ex-Rad® administered post-exposure can reduce DNA damage and increase clonogenic survival of bone marrow cells [227]. Oral administration confers protection comparable to the sc route [226]. AFRRRI is examining efficacy and biomarkers in non-human primates treated with Ex-Rad®. Ex-Rad® does not exhibit significant side effects in clinical trials [167]. The Food and Drug Administration (FDA) granted Investigational New Drug (IND) status to Ex-Rad® in 2008.

Genistein (Humanetics BIO 300) is a soy isoflavone with anti-oxidant, free radical scavenging, estrogenic, anti-microbial, anti-inflammatory and protein kinase inhibitory properties [128]. It also displays a DRF of about 1.2 when given sc prior to irradiation [129]. Part of the mechanism of action is induction of hematopoietic stem cell quiescence, making the cells less sensitive to radiation [53]. Current studies involve variations in route of administration and formulation [88]. Oral administration is also effective at enhancing survival after irradiation of mice [128]. Clinical safety trials indicate BIO 300 is well tolerated in humans [107]. BIO 300 has FDA IND status as of 2007.

CDX-301 is soluble, recombinant human FMS-like tyrosine kinase-3 Ligand (Flt3L) [46] that is well tolerated in human safety trials [14]. AFRRRI is investigating the efficacy of CDX-301 as a radiation countermeasure that can be given subcutaneously either before or after exposure. Survival enhancement has been observed in both situations (unpublished data).

1.3.3.3.2 *Mixed Neutron/Gamma Ray Fields (Mixed High/Low LET)*

After detonation of a nuclear device, a portion of the population that survives the effects of blast and burns will receive doses of mixed neutron/gamma radiation threatening survival [162], [163] (Kyle Millage and Carl Curling, personal communications). Although radiation countermeasures generally have been studied in subjects exposed to pure photons (gamma- or X-rays), the mechanisms of injury of these low Linear Energy Transfer (LET) radiations are different from those of high-LET radiation such as neutrons. For example, high LET radiations produce local clustered lesions in DNA that are more difficult to repair than those caused by low LET radiations. In recent studies, AFRRRI tested more than eight agents that were successful against pure gamma against mixed neutron/gamma fields (neutron/gamma dose 2:1) used for total body irradiation in mouse survival studies (hematopoietic ARS). Only G-CSF [44] and CDX-301 (unpublished data) showed promise in the mixed field environment. AFRRRI is currently extending the studies on CDX-301.

1.3.3.3.3 *Combined Injury (CI)*

A high proportion of radiation casualties in a mass casualty scenario are likely to receive additional injuries in the form of wounds, burns, or hemorrhage [71]. Research at AFRRRI and elsewhere has shown that there is a marked synergy between radiation and other injuries in causing morbidity and moribundity [120]. A number of countermeasures effective against pure radiation have been found to be ineffective against various forms of combined injury at AFRRRI. Interestingly, Ciprofloxacin (CIPRO), an FDA-approved fluoroquinolone anti-microbial, shows efficacy as a CI mitigator, acting via mechanisms other than anti-microbial activity [77], [78], [119]. In fact, CIPRO enhanced survival to a greater degree in CI mice than in mice exposed to radiation alone, indicating this agent may be valuable tool to investigate the mechanisms of synergy between radiation and other injuries. Positive findings by another group using ghrelin as a CI countermeasure [115] have also been confirmed at AFRRRI (unpublished data).

1.3.4 **Attenuation of Radiation-Induced Gastrointestinal Damage by Epidermal Growth Factor and Bone Marrow Transplantation in Mice**

Abstract

We examined the effect of Epidermal Growth Factor (EGF) and Bone Marrow Transplantation (BMT) on gastrointestinal damage after high-dose irradiation of mice. C57Black/6 mice were used. Two survival experiments were performed (12 and 13 Gy; ⁶⁰Co, 0.59 – 0.57 Gy/min). To evaluate BMT and EGF action, 5 groups were established:

- 0 Gy;
- 13 Gy;
- 13 Gy + EGF (2 mg/kg, first dose 24 hours after irradiation and then every 48 hours);
- 13 Gy + BMT (5×10^6 cells from Green Fluorescent Protein (GFP) syngenic mice, 4 hours after irradiation); and
- 13 Gy + BMT + EGF.

Survival data, blood cell counts, gastrointestinal and liver parameters and GFP positive cell migration were measured. BMT and EGF (3 doses, 2 mg/kg, administered 1, 3 and 5 days after irradiation) significantly increased survival (13 Gy). In blood, progressive cytopenia was observed with BMT, EGF or their combination having no improving effect early after irradiation. In gastrointestinal system, BMT, EGF and their combination attenuated radiation-induced atrophy and increased regeneration during first week after irradiation with the combination being most effective. Signs of systemic inflammatory reaction were observed 30 days after irradiation. Our data indicate that BMT together with EGF is a promising strategy in the treatment of high-dose whole-body irradiation damage.

1.3.4.1 Introduction

Acute Gastrointestinal Radiation Syndrome (AGRS) is a major life-threatening situation that develops after high-dose whole-body exposure to ionizing radiation. Its pathogenesis lies in severe damage to and denudation of Gastrointestinal (GI) epithelium leading to fluid and electrolyte imbalance as well as translocation of GI pathogens and toxins. Additionally, the clinical condition is worsened by impaired haematopoiesis and the development of acute Hematopoetic Radiation Syndrome (HRS) [69]. Although HRS can be treated by cytokines and/or Bone Marrow Transplantation (BMT), currently, there is no satisfactory treatment for rescuing patients from AGRS-related death [67], [97], [270].

To treat whole-body irradiation by doses higher than 9 – 10 Gy, employment of BMT is necessary to counteract irreversible bone marrow damage [67], [242], [269]. BMT may also attenuate GI damage [231], although, more recently, Leibowitz *et al.* [135] reported a very limited, if any, role of BM-derived cells in acute GI injury. Therefore, growth factors such as Epidermal Growth Factor (EGF) may play a significant role. Lee *et al.* [130] utilized recombinant human (rh) EGF to recover GI injury after abdominal irradiation by 15 Gy. In their model, the regeneration of villi was noticeable in mice treated with more than 0.2 mg/kg rhEGF, and the villi recovered fully in mice treated with the dose higher than 1 mg/kg rhEGF. Oh *et al.* [165] investigated rhEGF effect in mice after whole body irradiation by 10 Gy. They found that rhEGF suppresses apoptosis, supports recovery of villi and improves weight loss and survival following radiation (animals in rhEGF-treated group died within 17 days after irradiation vs. 13 days in irradiated and rhEGF non-treated mice).

The aim of this study is to evaluate the effect of BMT, EGF and their combination on gastrointestinal damage after high-dose whole-body irradiation.

1.3.4.2 Material and Methods

1.3.4.2.1 Animals

Female C57Black/6 (C57BL/6) mice aged 12 – 16 weeks and weighing 19.5 – 24.0 g (Velaz, Unetice, Czech Republic) were kept in an air-conditioned room ($22 \pm 2^\circ\text{C}$ and $50 \pm 10\%$ relative humidity, with lights from 7:00 to 19:00 h) and allowed access to standard food (Velaz) and tap water *ad libitum*. Experimental animals were handled under supervision of the Ethics Committee (Faculty of Military Health Sciences, Hradec Kralove, Czech Republic).

1.3.4.2.2 Irradiation (IR)

For IR treatments, the animals were kept in a Plexiglas box (VLA JEP, Hradec Kralove, Czech Republic) and were irradiated using a ^{60}Co unit (Chirana, Prague, Czech Republic) at a dose rate of 0.59 – 0.57 Gy/min with a target distance of 1 m. Dosimetry was performed using an ionization chamber (Dosemeter PTW Unidos 1001, Serial No. 11057, with ionization chamber PTW TM 313, Serial No. 0012; RPD Inc., Albertville, MN, USA).

1.3.4.2.3 Experimental Set-Ups

Altogether, 3 experiments were performed. In the first experiment, 6 groups of mice (10 animals per group) were used:

- 0 Gy;
- 12 Gy ($0.59 \text{ Gy}\cdot\text{min}^{-1}$);
- 12 Gy + BMT;
- 13 Gy;

- 13 Gy + BMT; and
- 13 Gy + BMT + EGF.

In all experiments, BMT was performed by injecting 5×10^6 Green Fluorescent Protein positive (GFP⁺) syngenic bone marrow cells from GFP⁺ mice (LFUK, Hradec Králové, Czech Republic) into a tail vein 4 hours after irradiation. EGF (ProSpec-Tany Technogene Ltd., East Brunswick, NJ, USA) was administered subcutaneously at a dose of 2 mg/kg. The first dose was given 24 hours after irradiation and then every 48 hours. In the second experiment, 4 groups of mice (10 animals per group) were used:

- 0 Gy;
- 13 Gy ($0.57 \text{ Gy} \cdot \text{min}^{-1}$);
- 13 Gy + BMT; and
- 13 Gy + BMT + EGF.

EGF was administered subcutaneously at a dose of 2 mg/kg 24, 72 and 120 hours after irradiation. Finally, 5 groups of mice were used in the third experiment:

- 0 Gy (18 mice);
- 13 Gy ($0.57 \text{ Gy} \cdot \text{min}^{-1}$; 12 mice);
- 13 Gy + BMT (12 mice);
- 13 Gy + EGF (12 mice); and
- 13 Gy + BMT + EGF (22 mice).

EGF was administered subcutaneously at a dose of 2 mg/kg 24, 72 and 120 hours after irradiation.

1.3.4.2.4 Sample Collection

Mice were euthanized by cervical dislocation. Samples from jejunum (5 – 6 cm from the pyloric ostium), ileum and colon ascendens (both 1 – 2 cm from ileocecal valve), liver, Peyer's patches, lung, and bone marrow were collected 2 and 4 days after irradiation (Experiment 3). Jejunum, ileum, colon ascendens and liver were also collected 7 (Experiment 3) and 30 days (Experiment 2) after irradiation.

1.3.4.2.5 Jejunum, Ileum, Colon Ascendens and Liver – Staining

Samples were fixed with 10% neutral buffered formalin (Chemapol, Prague, Czech Republic), embedded into paraffin (Paramix, Holic, Czech Republic), and tissue sections 5- μm thick were cut (Microtome model SM2000 R, Leica, Heidelberg, Germany). Staining with hematoxylin and eosin (both Merck, Kenilworth, NJ, USA) and immunohistochemical detection of activated (cleaved at aspartic acid-175) caspase-3 using rabbit monoclonal antibody (1:200) and Green Fluorescent Protein (GFP) using rabbit monoclonal antibody (1:100; both Biotech, Prague, Czech Republic) by a standard peroxidase technique published previously [173] were done.

1.3.4.2.6 Evaluation of Acute Inflammatory Infiltration

In jejunum, ileum and colon ascendens, acute inflammatory infiltration was evaluated at 400 \times magnification using a BX-51 microscope (Olympus Czech Group, Prague, Czech Republic) and semi-quantitative criteria:

- 0 – Not present;
- 1 – Infiltration in lamina propria mucosa (at least 1 microscopic field with ≥ 10 granulocytes);

- 2 – Additional infiltration in crypts (at least 1 crypt with ≥ 1 granulocytes) or in lamina submucosa (at least 1 microscopic field with ≥ 10 granulocytes); and
- 3 – Infiltration in all three compartments.

In liver, different criteria were used:

- 0 – Not present;
- 1 – At least 1 microscopic field with ≥ 10 granulocytes; and
- 2 – At least 1 microscopic field with ≥ 50 granulocytes.

To evaluate round cell in liver, we counted the amount of nodules (≥ 10 cells) per microscopic field (in 10 fields) at 200 \times magnification.

1.3.4.2.7 Microcolony Assay

The number of surviving crypts per circumference was counted in a section at 400 \times magnification. Only transversely sectioned crypts of 10 or more epithelial cell (excluding Paneth cells) were counted [264].

1.3.4.2.8 Morphometric Analysis

For morphometric analysis, samples of jejunum, ileum and colon ascendens were evaluated using a BX-51 microscope and the ImagePro 5.1 computer image analysis system (Media Cybernetics, Bethesda, MD, USA). The length of 20 randomly selected crypts and 20 randomly selected villi was measured per animal under 200 \times magnification.

1.3.4.2.9 Evaluation of Mitotic and Apoptotic Activities

In crypts, mitotic (hematoxylin-eosin) and apoptotic activity (activated caspase-3 stained samples) were measured under 400 \times magnification. Crypts were selected for scoring if they represented good longitudinal sections containing crypt lumen. Total number of apoptotic and mitotic cells was measured in enterocytes on both sides of 50 longitudinal crypt sections up to the 14th position starting at the midpoint at the base of the crypt. Number of apoptotic cells was judged subjectively by the size and number of closely adjacent apoptotic fragments. An apoptotic cell could be judged as a single large fragment approximately the size of a neighbouring cell or a cluster of at least 3 closely associated small fragments. Data were expressed as apoptotic and mitotic index, where apoptotic index = (total number of apoptotic cell in 50 crypts \times 100) / (50 \times 28) and mitotic index = (total number of mitotic cells in 50 crypts \times 100) / (50 \times 28). In jejunum and ileum, we also evaluated villar apoptotic activity representing % of apoptotic cell positive villi. An apoptotic cell positive villus was considered a one with ≥ 1 apoptotic cells starting at the tip down to the 10th position. In colon ascendens, apoptotic cells were evaluated in 1000 enterocytes at the luminal surface and in liver, the amount of apoptotic cells per microscopic field (in 10 fields) was calculated under 400 \times magnification.

1.3.4.2.10 Amount of GFP⁺ Cells

In jejunum, ileum and colon ascendens, we evaluated the amount of GFP⁺ cells per microscopic field (in 10 fields) under 400 \times magnification in the cryptal compartment of lamina propria mucosa and per villus at the same magnification. GFP⁺ cells were also counted per microscopic field (in 10 fields) under 400 \times magnification in liver.

1.3.4.2.11 Blood

Venous blood was collected into heparinized tubes (Scanlab Systems, Prague, Czech Republic) and analyzed using ABX Pentra 60C+ haemoanalyser (Trigon-Plus, Prague, Czech Republic).

1.3.4.2.12 *GFP⁺ Cells in Blood, Bone Marrow, Peyers' Patches, Lung*

Single cell suspensions from liver, lung and Peyers' patches were isolated by teasing tissue into cold Phosphate-Buffered Saline (PBS, pH 7.2; Sigma, St. Louis, MO, USA). Small pieces of tissue were sedimented at 1 g (1 min) and the supernatant was filtered through Nylon sifter (70 µm pore; Servis Centrum, Brno, Czech Republic).

Bone marrow was flushed from femoral bone using cold PBS. Suspensions from liver, lung, Peyers' patches, bone marrow and heparinized blood were incubated in EasyLyse solution (according the manufacturer's instructions; Dako, Glostrup, Denmark) to remove the red cells. The remaining cells were centrifuged (280 g force, 4°C, 5 min using Hettich Universal 32R centrifuge; Gemini BV, Apeldorn, Netherlands); the pellets were resuspended and washed twice in cold PBS containing 0.2% gelatin from cold water fish skin and 0.1% sodium azide (both from Sigma). Propidium iodide (Sigma) was added at a final concentration of 0.1 µg/ml immediately prior to acquisition to discern dead cells. A total of 5×10^6 cells from each sample were analysed using CyAn flowcytometer with Summit software 4.2 (both from Dako).

1.3.4.2.13 *Statistical Analysis*

The Mann-Whitney test and Kaplan-Meier Survival Analysis using SigmaStat 3.1 software (Systat Software Inc., Erkhart, Germany) were used for the statistical analysis. The differences were considered significant when $p \leq 0.05$.

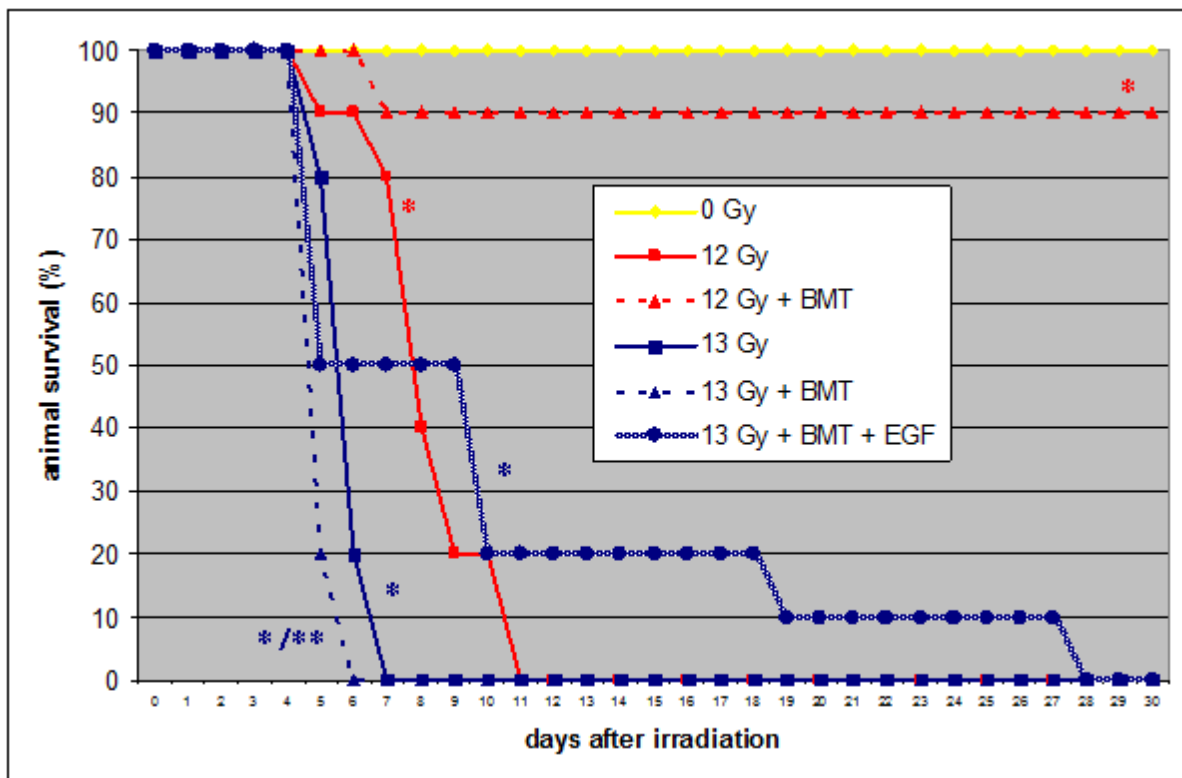
1.3.4.3 **Results**

1.3.4.3.1 *Effect of BMT on Animal Survival After Irradiation by 12 Gy*

All animals died 5 – 11 days after irradiation by 12 Gy (Median Survival (MS) = 8 days). Bone marrow transplantation significantly increased survival ($p \leq 0.001$) with only one death 7 days after irradiation (MS > 30 days). (Figure 1-10).

1.3.4.3.2 *Effect of BMT and Application of EGF (up to 14 Doses) on Animal Survival After Irradiation by 13 Gy*

All mice died 5 – 7 days after irradiation by 13 Gy (MS = 6 days). After bone marrow transplantation, all animals died 5 – 6 days after irradiation. Median Survival (MS = 5 days) significantly decreased by 17% ($p = 0.007$). Bone marrow transplantation combined with application of EGF (2 mg/kg) starting 24 hours after irradiation and then every 48 hours did not improve survival when compared with irradiated and non-treated counterparts ($p = 0.115$). The whole group died 5 – 28 days after irradiation (MS = 8.5 days) (Figure 1-10).

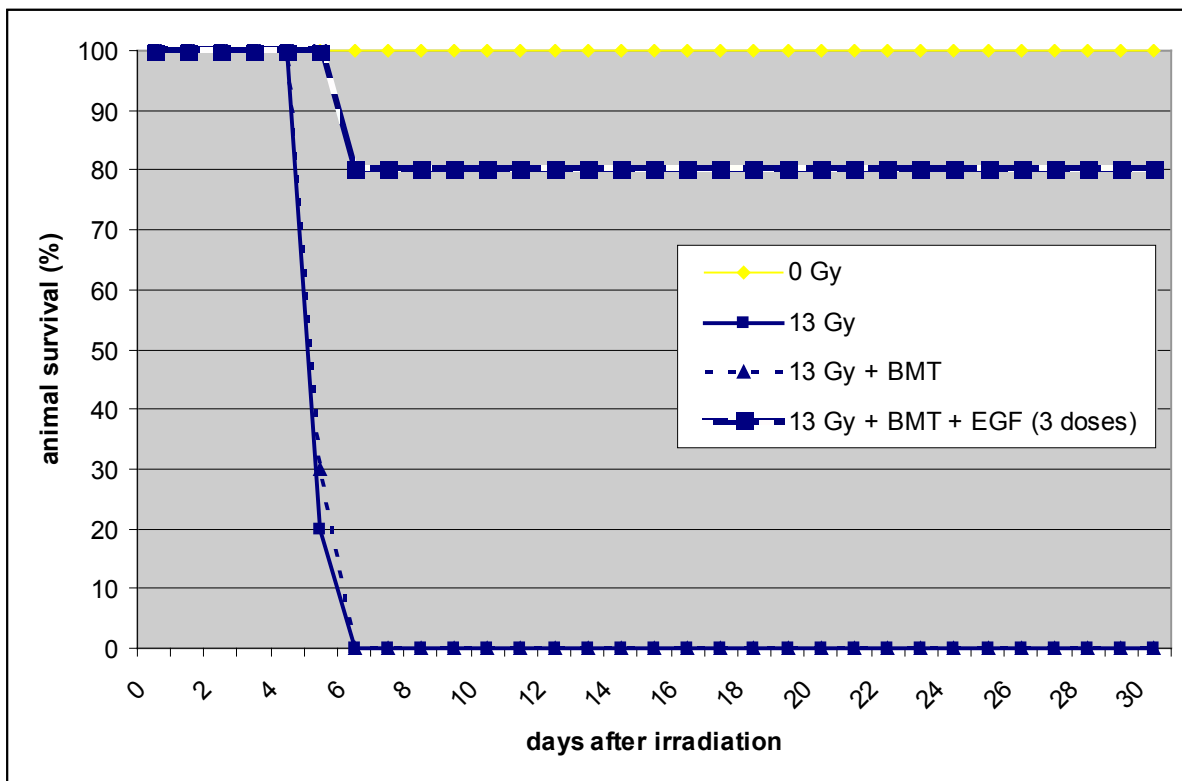


- For BMT, 5×10^6 GFP⁺ syngenic bone marrow cells were injected into a tail vein 4 hours after irradiation. EGF was applied subcutaneously at a dose of 2 mg/kg. First dose was given 24 hours after irradiation and then every 48 hours till the death of the last mouse.
- Significant differences between non-irradiated and irradiated groups: * $p \leq 0.05$.
- Significant differences between irradiated/non-treated and irradiated/treated groups: ** $p \leq 0.05$.

Figure 1-10: Effect of Bone Marrow Transplantation (BMT) and Epidermal Growth Factor (EGF) on Animal Survival of C57BL/6 Mice After Whole Body Irradiation by 12 and 13 Gy.

1.3.4.3.3 Effect of BMT and 3 Doses of EGF on Animal Survival After Irradiation by 13 Gy

In this experiment, the whole non-treated group died 5 – 6 days after irradiation (MS = 5 days). Bone marrow transplantation did not affect survival rate (MS = 5 days, $p = 0.615$). Additional administration of EGF (2 mg/kg) 1, 3 and 5 days after irradiation significantly improved survival rate (MS > 30, $p \leq 0.001$) with 8 animals surviving 30-day interval. (Figure 1-11).



- For BMT, 5×10^6 GFP⁺ syngenic bone marrow cells were injected into a tail vein 4 hours after irradiation. EGF was applied subcutaneously 2 mg/kg 1, 3 and 5 days after irradiation.
- Significant differences between non-irradiated and irradiated groups: * $p \leq 0.05$.
- Significant differences between irradiated/non-treated and irradiated/treated groups: ** $p \leq 0.05$.

Figure 1-11: Effect of Bone Marrow Transplantation (BMT) and 3 Doses of Epidermal Growth Factor (EGF) on Animal Survival of C57BL/6 Mice After Whole Body Irradiation by 13 Gy.

1.3.4.3.4 Effect of BMT and EGF on Jejunum, Ileum, Colon Ascendens, Liver, Blood and Migration of GFP⁺ Cells

No animal died before sample collection 2 and 4 days after irradiation. For the 7-day interval, 6 control animals and 10 irradiated mice treated with combination of BMT and EGF were kept. Five of 10 irradiated mice died before sample collection.

1.3.4.3.5 Inflammatory Infiltration

Jejunum

Two days after irradiation by 13 Gy, we found acute inflammatory infiltration in all mice with the maximum at the base of crypts ($p = 0.002$). In the 4-day interval, the infiltration was observed in 3 of 6 animals and its intensity significantly dropped compared with the 2-day interval ($p = 0.004$). EGF, BMT or their combination did not affect this parameter 2 and 4 days after irradiation. In the group treated with the combination of EGF and BMT, the inflammatory reaction was also evaluated in the later time points. In comparison with control animals, no infiltration was measured 7 days after irradiation but was present in all mice 30 days after irradiation ($p = 0.01$). The maximum was observed at the base of crypts and submucosal layer. (Table 1-10).

Ileum

We found acute inflammatory infiltration in all mice with the maximum at the base of crypts 2 and 4 days after the irradiation ($p = 0.002$). EGF, BMT or their combination did not affect the inflammatory reaction 2 and 4 days after irradiation. The acute inflammatory infiltration was also evaluated in the group treated with the combined therapy in the 7- and 30-day intervals. In comparison with control animals, no infiltration was measured 7 days after irradiation but reappeared in 2 of 4 mice 30 days after irradiation (no statistical difference). (Table 1-10).

Colon

In colon ascendens, we observed acute inflammatory infiltration only in 1 of 4 mice 30 days after irradiation (no statistical difference when compared with control group). (Table 1-10).

Table 1-10: Inflammatory Infiltration in Jejunum, Ileum and Colon Ascendens Expressed as the Median Value of Positive Findings (of Values ≥ 1) or 0 (No Positive Finding in the Group) and the Amount of Affected Animals in the Group (in brackets).

Days after IR		0 Gy	13 Gy	13 Gy + EGF	13 Gy + BMT	13 Gy + BMT + EGF
Jejunum	2	0 (0 of 6)	3 (6 of 6) ¹	3 (6 of 6) ¹	3 (6 of 6) ¹	3 (6 of 6) ¹
	4	0 (0 of 6)	1 (3 of 6)	1 (3 of 6)	1 (3 of 6)	2 (2 of 6)
	7	0 (0 of 6)	N/A	N/A	N/A	0 (0 of 5)
	30	0 (0 of 6)	N/A	N/A	N/A	2 (4 of 4) ¹
Ileum	2	0 (0 of 6)	3 (6 of 6) ¹	3 (6 of 6) ¹	3 (6 of 6) ¹	3 (6 of 6) ¹
	4	0 (0 of 6)	2 (6 of 6) ¹	2.5 (6 of 6) ¹	2 (6 of 6) ¹	2.5 (6 of 6) ¹
	7	0 (0 of 6)	N/A	N/A	N/A	0 (0 of 5)
	30	0 (0 of 6)	N/A	N/A	N/A	2 (2 of 4)
Colon	2	0 (0 of 6)	0 (0 of 6)	0 (0 of 6)	0 (0 of 6)	0 (0 of 6)
	4	0 (0 of 6)	0 (0 of 6)	0 (0 of 6)	0 (0 of 6)	0 (0 of 6)
	7	0 (0 of 6)	N/A	N/A	N/A	0 (0 of 5)
	30	0 (0 of 6)	N/A	N/A	N/A	2 (1 of 4)

- Inflammatory infiltration: 0 – none, 1 – in lamina propria mucosae, 2 – additionally in either crypts or lamina submucosa, 3 – in all three compartments.
- Significant differences between non-irradiated and irradiated groups: ¹ $p \leq 0.05$.
- N/A = Not Available.

1.3.4.3.6 *Microcolony Assay*

Jejunum

The amount of viable crypts significantly decreased 2 and 4 days after irradiation reaching 15% and 23% (both $p = 0.002$) of control values, respectively. EGF or BMT did not improve cryptal viability. The combined therapy significantly increased amount of viable crypts 1.4-fold compared to irradiated and non-treated group in the 4-day interval ($p = 0.041$; 32% of control value). In this group, the parameter remained significantly decreased 7 and 30 days after irradiation (58% and 88% of control values, $p = 0.004$ and 0.038, respectively). (Table 1-11).

Ileum

The amount of viable crypts significantly decreased 2 and 4 days after irradiation reaching 16% and 19% ($p = 0.002$) of control values, respectively. EGF or BMT did not affect cryptal viability in ileum. In comparison to irradiated and non-treated group, the combined therapy significantly increased amount of viable crypts 1.6-fold in the 4-day interval ($p = 0.026$; 30% of control value). In this group, the parameter remained significantly decreased 7 days after irradiation (56% of control values, $p = 0.004$) and it returned to the control level 30 days after irradiation. (Table 1-11).

Colon

The amount of viable crypts significantly decreased 2 and 4 days after irradiation reaching 75% ($p = 0.026$) and 49% ($p = 0.002$) of control values, respectively. Compared to irradiated and non-treated group, EGF and combination of BMT and EGF increased amount of viable crypts 1.5- and 1.3-fold ($p = 0.009$ and $p = 0.015$, 75% and 65% of control value) 4 days after irradiation, respectively. In group treated with the combination of BMT and EGF, the parameter remained also decreased 7 and 30 days after irradiation (53% and 71% of control values, $p = 0.004$ and 0.038, respectively). (Table 1-11).

Table 1-11: Average Values for Microcolony Assay in Jejunum, Ileum and Colon Ascendens $\pm 2 \times$ Standard Error of Mean for N = 6 Animals Except for * N = 5 and ** N = 4 Animals.

Days after IR		0 Gy	13 Gy	13 Gy + EGF	13 Gy + BMT	13 Gy + BMT + EGF
Jejunum	2	135 \pm 7	20 \pm 7 ¹	25 \pm 7 ¹	23 \pm 4 ¹	23 \pm 5 ¹
	4	132 \pm 4	30 \pm 7 ¹	35 \pm 12 ¹	29 \pm 7 ¹	42 \pm 8 ^{1a}
	7	138 \pm 11	N/A	N/A	N/A	79 \pm 10 ^{1*}
	30	130 \pm 6	N/A	N/A	N/A	114 \pm 7 ^{1**}
Ileum	2	118 \pm 4	19 \pm 3 ¹	18 \pm 4 ¹	19 \pm 3 ¹	24 \pm 6 ¹
	4	115 \pm 9	22 \pm 7 ¹	25 \pm 7 ¹	38 \pm 16 ¹	35 \pm 6 ^{1a}
	7	116 \pm 7	N/A	N/A	N/A	65 \pm 9 ^{1*}
	30	120 \pm 5	N/A	N/A	N/A	129 \pm 9 ^{**}
Colon	2	463 \pm 32	347 \pm 69 ¹	351 \pm 75 ¹	320 \pm 68 ¹	354 \pm 61 ¹
	4	417 \pm 37	203 \pm 39 ¹	313 \pm 45 ^{1a}	200 \pm 48 ¹	274 \pm 19 ^{1a}
	7	406 \pm 42	N/A	N/A	N/A	214 \pm 46 ^{1*}
	30	405 \pm 32	N/A	N/A	N/A	288 \pm 40 ^{1**}

- Significant differences between non-irradiated and irradiated groups: ¹ $p \leq 0.05$.
- Significant differences between irradiated/non-treated and irradiated/treated groups: ^a $p \leq 0.05$.
- N/A = Not Available.

1.3.4.3.7 Length of Crypts and Height of Villi

Jejunum

Length of crypts and height of villi decreased 1.2-fold ($p < 0.001$) 2 days after irradiation and 1.1- and 1.3-fold ($p < 0.001$) 4 days after irradiation, respectively. When compared with irradiated and non-treated group, we observed effect in all treated groups. In comparison to irradiated and non-treated animals,

EGF application increased length of crypts and height of villi 1.2- and 1.3-fold ($p < 0.001$) 2 days after the irradiation and 1.2- and 1.1-fold ($p = 0.002$ and 0.007) 4 days after the irradiation, respectively. BMT affected the length of crypts solely in the 4-day interval increasing 1.2-fold ($p < 0.001$). The height of villi increased 1.1- and 1.2-fold ($p < 0.001$ and 0.003) 2 and 4 days after the irradiation, respectively. In combined therapy group, the length of crypts and height of villi were both 1.2-fold ($p < 0.001$) higher 2 days after the irradiation and 1.3- and 1.1-fold ($p < 0.001$) higher 4 days after the irradiation, respectively. In this group, both parameters were evaluated in the later time points. In comparison with control values, the length of crypts increased 1.2- and 1.4-fold ($p < 0.001$) 7 and 30 days after the irradiation, respectively. The height of villi of increased 1.2-fold in the 7-day interval ($p < 0.001$), while no change was found in the 30-day interval. (Table 1-12).

Ileum

In ileum, length of crypts and height of villi decreased 1.2- and 1.8-fold ($p < 0.001$) 4 days after irradiation, respectively. In comparison to irradiated and non-treated animals, we found significant differences in all treated groups. Length of crypts and height of villi increased 1.1- and 1.2-fold ($p = 0.005$ and 0.004) in EGF applied mice 4 days after irradiation, respectively. BMT increased height of villi 1.1-fold ($p = 0.002$) 2 days after irradiation and both length of crypts and height of villi 1.4- and 1.3-fold ($p < 0.001$), respectively, 4 days after irradiation. Combination of BMT and EGF increased height of villi 1.3-fold ($p < 0.001$) 2 days after irradiation and both length of crypts and height of villi 1.2- and 1.3-fold ($p < 0.001$), respectively, 4 days after irradiation. (Table 1-12).

Colon

After irradiation by 13 Gy, the length of crypts decreased 1.2-fold ($p < 0.001$) in the 4-day interval. EGF, BMT and their combination affected this radiation-induced outcome with values being 1.1-, 1.1- and 1.2-fold ($p = 0.002$, 0.028 and < 0.001), respectively, than in irradiated and non-treated group. (Table 1-12).

Table 1-12: Average Values for Length of Crypts and Height of Villi in Jejunum, Ileum and Colon Ascendens $\pm 2 \times$ Standard Error of Mean for N = 6 Animals Except for * N = 5 and ** N = 4 Animals.

Days after IR		0 Gy	13 Gy	13 Gy + EGF	13 Gy + BMT	13 Gy + BMT + EGF	
Length of Crypts, μm	Jejunum	2	100 \pm 5	82 \pm 5 ¹	97 \pm 5 ^a	81 \pm 4 ¹	96 \pm 5 ^a
		4	99 \pm 4	87 \pm 8 ¹	104 \pm 10 ^a	106 \pm 9 ^a	112 \pm 11 ^a
		7	100 \pm 5	N/A	N/A	N/A	120 \pm 10 ^{1*}
		30	102 \pm 4	N/A	N/A	N/A	146 \pm 13 ^{1**}
	Ileum	2	119 \pm 10	118 \pm 4	110 \pm 10	115 \pm 5	123 \pm 5
		4	123 \pm 5	99 \pm 8 ¹	111 \pm 7 ^{1a}	137 \pm 18 ^a	123 \pm 8 ^a
		7	113 \pm 10	N/A	N/A	N/A	105 \pm 7 [*]
		30	121 \pm 5	N/A	N/A	N/A	121 \pm 7 ^{**}
	Colon	2	113 \pm 6	119 \pm 5	118 \pm 5	113 \pm 5	117 \pm 5
		4	122 \pm 6	100 \pm 5 ¹	112 \pm 5 ^{1a}	109 \pm 6 ^{1a}	117 \pm 5 ^a
		7	124 \pm 7	N/A	N/A	N/A	129 \pm 7 [*]
		30	110 \pm 5	N/A	N/A	N/A	117 \pm 9 ^{**}

Days after IR		0 Gy	13 Gy	13 Gy + EGF	13 Gy + BMT	13 Gy + BMT + EGF	
Height of Villi, μm	Jejunum	2	379 \pm 21	317 \pm 16 ¹	399 \pm 18 ^a	357 \pm 18 ^a	396 \pm 20 ^a
		4	360 \pm 27	271 \pm 23 ¹	296 \pm 29 ^{1a}	324 \pm 40 ^{1a}	306 \pm 33 ^{1a}
		7	363 \pm 16	N/A	N/A	N/A	438 \pm 48 ^{1*}
		30	378 \pm 31	N/A	N/A	N/A	396 \pm 34 ^{**}
	Ileum	2	198 \pm 10	202 \pm 10	194 \pm 11	226 \pm 10 ^{1a}	255 \pm 10 ^{1a}
		4	203 \pm 10	112 \pm 8 ¹	129 \pm 8 ^{1a}	147 \pm 10 ^{1a}	151 \pm 9 ^{1a}
		7	191 \pm 9	N/A	N/A	N/A	193 \pm 18 [*]
		30	199 \pm 7	N/A	N/A	N/A	190 \pm 18 ^{**}

- Significant differences between non-irradiated and irradiated groups: ¹ $p \leq 0.05$.
- Significant differences between irradiated/non-treated and irradiated/treated groups: ^a $p \leq 0.05$.
- N/A = Not Available.

1.3.4.3.8 Mitotic and Apoptotic Activities

Jejunum

Two days after the irradiation by 13 Gy, the mitotic activity decreased 25.0-fold ($p = 0.002$), while the apoptotic activity in crypts increased 14.2-fold ($p = 0.002$) compared to the control. The apoptotic activity in the villar compartment was not changed. Four days after the irradiation, the mitotic index returned to the control level. The cryptal apoptotic index was increased 2.5-fold ($p = 0.002$), while the villar apoptotic parameter decreased 1.7-fold ($p = 0.002$). EGF, BMT or their combination significantly decreased radiation-induced apoptosis in crypts with values being 1.2-, 1.1- and 1.4-fold lower ($p = 0.041$, 0.026 and 0.002) 2 days after the irradiation and 2-, 2- and 1.7-fold lower ($p = 0.041$, 0.009 and 0.035) 4 days after the irradiation, respectively. The combined therapy also increased mitotic index 1.4-fold ($p = 0.014$) compared to the irradiated and non-treated animals in the 4-day interval. Mitotic and apoptotic activities were also measured 7 and 30 days after the irradiation in the group treated with combined therapy. Compared to the control values, we observed 1.4- and 2.6-fold increase ($p = 0.030$ and 0.004) in mitotic and apoptotic activity in crypts, respectively, while the villar apoptotic parameter remained 1.6-fold decreased ($p = 0.030$) 7 days after the irradiation. In the 30-day interval, the only affected parameter was cryptal apoptotic activity being 1.6-fold higher ($p = 0.038$) than in the control group. (Table 1-13).

Ileum

Two days after the irradiation by 13 Gy, the mitotic activity declined 11.5-fold ($p = 0.002$), while the cryptal apoptotic index increased 4.4-fold ($p = 0.002$). The apoptotic activity in the villar compartment did not change. Four days after the irradiation, the mitotic index returned to the control level. The cryptal apoptotic index was increased 1.7-fold ($p = 0.004$), whereas the villar apoptotic parameter decreased 2.2-fold ($p = 0.015$). In comparison to irradiated and non-treated group, EGF, BMT and their combination showed significant effects. EGF increased mitotic index 1.5-fold ($p = 0.026$) 4 days after irradiation. BMT suppressed radiation-induced apoptosis in crypts 1.3-fold ($p = 0.015$) and decreased villar apoptotic parameter 2.4-fold ($p = 0.026$) 2 days after irradiation and stimulated mitotic activity 1.5-fold ($p = 0.030$) 4 days after irradiation. The combined therapy decreased apoptotic activity in crypts 1.3-fold ($p = 0.009$) and villar apoptotic parameter 2.2-fold ($p = 0.004$) 2 days after irradiation. It also increased mitotic activity 1.5-fold ($p = 0.015$), while decreased apoptotic activity in crypts 1.5-fold ($p = 0.035$) 4 days after irradiation. In this group, we also measured stimulated mitotic activity and apoptotic activity 1.5- and 1.4-fold ($p = 0.050$ and 0.017), respectively, while the villar apoptotic activity parameter remained suppressed 1.9-fold ($p = 0.017$) 7 days after irradiation. (Table 1-13).

Colon

In colon ascendens, we found increased apoptotic activity in crypts (2.8-fold, $p = 0.002$), whereas mitotic activity and apoptotic activity at the luminal surface decreased both 5.5-fold ($p = 0.002$) 2 days after irradiation. Four days after irradiation, mitotic and apoptotic index in crypts returned at the control level. Apoptotic index at the luminal surface remained suppressed (1.5-fold, $p = 0.002$). In comparison to irradiated and non-treated group, EGF treatment significantly increased mitotic activity 2.0- and 1.3-fold ($p = 0.015$) 2 and 4 days after irradiation, respectively. BMT did not affect radiation-induced changes. Similarly to EGF-treated group, combination of BMT and EGF increased mitotic activity 1.5- and 1.2-fold ($p = 0.026$ and 0.009) 2 and 4 days after irradiation, respectively. In this group, mitotic index was 1.3-fold ($p = 0.009$) higher, while apoptotic index at the luminal surface was 2-fold ($p = 0.050$) lower than in control group in the 7-day interval. (Table 1-13).

Table 1-13: Average Values for Cryptal Mitotic and Apoptotic Index and Villar Apoptotic Activity or Apoptotic Index at the Luminal Surface in Jejunum, Ileum and Colon Ascendens $\pm 2 \times$ Standard Error of Mean for N = 6 Animals Except for * N = 4 and ** N = 5 Animals.

Days after IR		0 Gy	13 Gy	13 Gy + EGF	13 Gy + BMT	13 Gy + BMT + EGF	
Mitotic Index in Crypts, %	Jejunum	2	2.5 \pm 0.3	0.1 \pm 0.1 ¹	0.2 \pm 0.1 ¹	0.2 \pm 0.1 ¹	0.2 \pm 0.1 ¹
		4	2.4 \pm 0.3	2.1 \pm 0.4	2.6 \pm 0.5	2.6 \pm 0.5	3.0 \pm 0.4 ^{1a}
		7	2.2 \pm 0.2	N/A	N/A	N/A	3.0 \pm 0.4 ^{1*}
		30	2.3 \pm 0.3	N/A	N/A	N/A	2.4 \pm 0.3 ^{**}
	Ileum	2	2.3 \pm 0.2	0.2 \pm 0.1 ¹	0.4 \pm 0.1 ¹	0.3 \pm 0.1 ¹	0.3 \pm 0.0 ¹
		4	2.2 \pm 0.1	2.4 \pm 0.4	3.3 \pm 0.4 ^{1a}	3.3 \pm 0.5 ^{1a}	3.3 \pm 0.4 ^{1a}
		7	2.0 \pm 0.2	N/A	N/A	N/A	2.8 \pm 0.4 ^{1*}
		30	2.2 \pm 0.1	N/A	N/A	N/A	2.3 \pm 0.2 ^{**}
	Colon	2	1.1 \pm 0.3	0.2 \pm 0.1 ¹	0.4 \pm 0.1 ^{1a}	0.1 \pm 0.0 ¹	0.3 \pm 0.1 ^{1a}
		4	0.9 \pm 0.2	0.9 \pm 0.1	1.2 \pm 0.1 ^{1a}	0.8 \pm 0.1	1.1 \pm 0.1 ^a
		7	0.9 \pm 0.1	N/A	N/A	N/A	1.2 \pm 0.1 ^{1*}
		30	1.0 \pm 0.2	N/A	N/A	N/A	1.3 \pm 0.2 ^{**}
Apoptotic Index in Crypts, %	Jejunum	2	0.6 \pm 0.1	8.5 \pm 0.6 ¹	7.2 \pm 0.6 ^{1a}	7.6 \pm 0.2 ^{1a}	6.2 \pm 0.8 ^{1a}
		4	0.4 \pm 0.1	1.0 \pm 0.2 ¹	0.5 \pm 0.3 ^a	0.5 \pm 0.3 ^a	0.6 \pm 0.2 ^a
		7	0.5 \pm 0.1	N/A	N/A	N/A	1.3 \pm 0.2 ^{1*}
		30	0.5 \pm 0.1	N/A	N/A	N/A	0.8 \pm 0.1 ^{1**}
	Ileum	2	1.2 \pm 0.2	5.3 \pm 0.6 ¹	4.9 \pm 0.2 ¹	4.1 \pm 0.6 ^{1a}	4.1 \pm 0.2 ^{1a}
		4	1.3 \pm 0.2	2.2 \pm 0.5 ¹	1.9 \pm 0.6	1.8 \pm 0.4	1.5 \pm 0.2 ^a
		7	1.0 \pm 0.2	N/A	N/A	N/A	1.4 \pm 0.1 ^{1*}
		30	1.0 \pm 0.2	N/A	N/A	N/A	1.0 \pm 0.1 ^{**}
	Colon	2	0.4 \pm 0.1	1.1 \pm 0.1 ¹	1.0 \pm 0.2 ¹	1.1 \pm 0.2 ¹	1.3 \pm 0.3 ¹
		4	0.4 \pm 0.1	0.6 \pm 0.1	0.6 \pm 0.2	0.5 \pm 0.1	0.4 \pm 0.1
		7	0.4 \pm 0.1	N/A	N/A	N/A	0.5 \pm 0.2 [*]
		30	0.5 \pm 0.1	N/A	N/A	N/A	0.5 \pm 0.1 ^{**}

Days after IR		0 Gy	13 Gy	13 Gy + EGF	13 Gy + BMT	13 Gy + BMT + EGF	
Villar Apoptotic Activity (Jejunum, Ileum) and Apoptotic Index at the Surface (Colon), %	Jejunum	2	46 ± 11	40 ± 15	47 ± 14	43 ± 11	37 ± 9
		4	54 ± 4	31 ± 4 ¹	30 ± 4 ¹	28 ± 4 ¹	27 ± 5 ¹
		7	46 ± 5	N/A	N/A	N/A	28 ± 5 ^{1*}
		30	44 ± 8	N/A	N/A	N/A	44 ± 12 ^{**}
	Ileum	2	22 ± 4	28 ± 9	23 ± 11	9 ± 4 ^{1a}	10 ± 2 ^{1a}
		4	26 ± 5	12 ± 5 ¹	15 ± 2 ¹	17 ± 2 ¹	18 ± 4 ¹
		7	25 ± 6	N/A	N/A	N/A	13 ± 2 ^{1*}
		30	22 ± 5	N/A	N/A	N/A	20 ± 5 ^{**}
	Colon	2	1.1 ± 0.3	0.2 ± 0.1 ¹	0.3 ± 0.1 ¹	0.2 ± 0.1 ¹	0.3 ± 0.1 ¹
		4	0.9 ± 0.1	0.6 ± 0.1 ¹	0.6 ± 0.2 ¹	0.5 ± 0.2 ¹	0.4 ± 0.2 ¹
		7	1.0 ± 0.3	N/A	N/A	N/A	0.5 ± 0.1 ^{1*}
		30	1.1 ± 0.2	N/A	N/A	N/A	1.2 ± 0.1 ^{**}

- Significant differences between non-irradiated and irradiated groups: ¹ p ≤ 0.05.
- Significant differences between irradiated/non-treated and irradiated/treated groups: ^a p ≤ 0.05.
- N/A = Not Available.

Liver

Acute inflammatory Infiltration

We did not observe any inflammatory reaction in liver 2 and 4 days after irradiation by 13 Gy. No infiltration was observed in EGF, BMT or the combination therapy treated groups with just one exception. We observed inflammation in 1 of 4 mice 30 days after irradiation (no statistical difference when compared with control group). (Table 1-14).

Round Cell Infiltration (Lymphocyte)

In comparison with control group, we did not observe any lymphatic nodule (≥ 10 cells) in liver tissue 2 and 4 days after irradiation by 13 Gy. EGF, BMT or their combination did not affect this radiation-induced outcome with just one exception. We observed increased lymphatic infiltration in 1 of 4 mice 30 days after irradiation (no statistical difference when compared with control group). (Table 1-14).

Apoptotic Activity

Increased apoptotic activity was measured only in the group treated with both BMT and EGF 30 days after irradiation with value being 2.8-fold (p < 0.001) higher than in the control group. (Table 1-14).

Table 1-14: Inflammatory Infiltration in Liver Expressed as the Median Value of Positive Findings (of Values ≥ 1) or 0 (No Positive Finding in the Group) and the Amount of Affected Animals in the Group (in brackets). Round cell infiltration and amount of apoptotic cells per microscopic field in liver $\pm 2 \times$ standard error of mean for $n = 6$ animals except for * $n = 5$ and ** $n = 4$ animals.

Days after IR	0 Gy	13 Gy	13 Gy + EGF	13 Gy + BMT	13 Gy + EGF + BMT
Acute Inflammatory Infiltration					
2	0 (0 of 6)	0 (0 of 6)	0 (0 of 6)	0 (0 of 6)	0 (0 of 6)
4	0 (0 of 6)	0 (0 of 6)	0 (0 of 6)	0 (0 of 6)	0 (0 of 6)
7	0 (0 of 6)	N/A	N/A	N/A	0 (0 of 5)
30	0 (0 of 6)	N/A	N/A	N/A	1 (4 of 4) ¹
Round Cell Infiltration					
2	3 \pm 3	0 \pm 0 ¹			
4	3 \pm 1	0 \pm 0 ¹			
7	5 \pm 2	N/A	N/A	N/A	0 \pm 0 ^{1*}
30	3 \pm 2	N/A	N/A	N/A	12 \pm 4 ^{1**}
Amount of Apoptotic Cells per Microscopic Field (at 400\times Magnification)					
2	1.2 \pm 0.4	0.9 \pm 0.3	0.9 \pm 0.3	1.1 \pm 0.3	1.1 \pm 0.3
4	1.0 \pm 0.3	0.8 \pm 0.2	1.2 \pm 0.3	1.0 \pm 0.2	0.8 \pm 0.3
7	1.2 \pm 0.3	N/A	N/A	N/A	1.1 \pm 0.3 [*]
30	1.1 \pm 0.3	N/A	N/A	N/A	3.1 \pm 0.7 ^{1**}

- Significant differences between non-irradiated and irradiated groups: ¹ $p \leq 0.05$.
- N/A = Not Available.

Blood

In irradiated and non-treated animals, we found significantly decreased amount of lymphocytes in peripheral blood 2 days after irradiation reaching 25% of the control value ($p = 0.002$). Their decline intensified 4 days after irradiation reaching 9% of the control value ($p = 0.002$), which was accompanied with monocytes and thrombocytes decreasing to 25% and 79% of their control values ($p = 0.004$ and 0.049), respectively. We did not find any improvement using EGF, BMT or combined therapy treatment. On the other hand, EGF, both alone and in combination with BMT, amplified neutropenia in the 4-day interval with values at undetectable level ($p = 0.002$). (Table 1-15).

Table 1-15: Average Values for Blood Lymphocytes, Monocytes, Neutrophil Granulocytes and Thrombocytes $\pm 2 \times$ Standard Error of Mean for N = 6 Animals.

Days after IR	0 Gy	13 Gy	13 Gy + EGF	13 Gy + BMT	13 Gy + EGF + BMT
Lymphocytes per 1 μL					
2	2550 \pm 510	630 \pm 110 ¹	430 \pm 150 ¹	470 \pm 90 ¹	480 \pm 290 ¹
4	1500 \pm 260	130 \pm 70 ¹	140 \pm 20 ¹	240 \pm 120 ¹	110 \pm 30 ¹
Monocytes per 1 μL					
2	110 \pm 40	100 \pm 60	70 \pm 30	140 \pm 130	70 \pm 30
4	40 \pm 20	10 \pm 10 ¹	10 \pm 10 ¹	10 \pm 10 ¹	0 \pm 0 ¹

Days after IR	0 Gy	13 Gy	13 Gy + EGF	13 Gy + BMT	13 Gy + EGF + BMT
Neutrophil Granulocytes per 1 μ L					
2	190 \pm 80	110 \pm 80	60 \pm 30 ¹	40 \pm 20 ¹	110 \pm 70
4	140 \pm 60	80 \pm 50	0 \pm 0 ^{1a}	50 \pm 10 ¹	0 \pm 0 ^{1a}
Thrombocytes per 1 mL					
2	870 \pm 120	910 \pm 90	790 \pm 40	840 \pm 40	950 \pm 60
4	900 \pm 70	710 \pm 50 ¹	870 \pm 70	980 \pm 120	810 \pm 60

- Significant differences between non-irradiated and irradiated groups: ¹ p \leq 0.05.
- Significant differences between irradiated/non-treated and irradiated/treated groups: ^a p \leq 0.05.

1.3.4.3.9 *GFP⁺ Cells in Blood, Bone Marrow, Peyers' Patches, Lung*

We did not measure any significant effect of EGF. In both BMT and combined therapy treated group, the relative representation of GFP⁺ cells significantly decreased in blood (p = 0.002) during 2- to 4-day interval reaching non detectable values, whereas it increased in bone marrow (p = 0.015) and Peyers' patches 6.0- and 22.0-fold (p = 0.041). (Table 1-16).

Table 1-16: Average Values for Relative Representation of GFP⁺ Cells in Blood, Bone Marrow, Peyers' Patches, and Lung \pm 2 \times Standard Error of Mean for N = 6 Animals.

Group	13 Gy + BMT		13 Gy + BMT + EGF	
	2	4	2	4
Blood	0.2 \pm 0.1	0.0 \pm 0.0 ¹	0.4 \pm 0.1	0.0 \pm 0.0 ¹
Bone Marrow	0.0 \pm 0.0	1.0 \pm 0.6 ¹	0.0 \pm 0.0	0.5 \pm 0.3 ¹
Peyers' Patches	0.2 \pm 0.1	1.2 \pm 1.2 ¹	0.1 \pm 0.2	2.2 \pm 2.3 ¹
Lung	0.0 \pm 0.0	0.0 \pm 0.0	0.0 \pm 0.0	0.0 \pm 0.0

- Significant differences between 2- and 4-day intervals: ¹ p \leq 0.05.

1.3.4.3.10 *GFP⁺ Cells in Jejunum, Ileum, Colon Ascendens, and Liver*

We did not observe any significant effect of EGF on migration of GFP⁺ cells into jejunum, ileum, colon ascendens, or liver. Differences were found only between particular time points. In both BMT and combined therapy treated group, the amount of GFP⁺ cells increased 9.0- and 3.0-fold (p = 0.003 and p = 0.042) in the jejunal cryptal compartment and 3.0- and 3.3-fold (p = 0.033 and p = 0.015) in ileal cryptal compartment during 2- to 4-day interval, respectively. The migration of GFP⁺ cells was also evaluated in combined therapy treated group 7 and 30 days after irradiation. The amount of GFP⁺ cells increased 20.0-, 3.1- and 13.9-fold (p = 0.003, 0.001 and < 0.001) in both cryptal and villar jejunal compartment and liver during 4 – 7-day interval and 88.8-, 24.2-, 35.0-, 19.8-, 10.4- and 16.2-fold (p < 0.001) in cryptal and villar jejunal compartment, cryptal and villar ileal compartment, colon ascendens and liver in 7 – 30-day interval after irradiation, respectively. (Table 1-17).

Table 1-17: Average Values for GFP⁺ Cells in Jejunum, Ileum, Colon Ascendens, and Liver $\pm 2 \times$ Standard Error of Mean for N = 6 Animals Except for * N = 5 and ** N = 4 Animals.

Days after IR		2	4	7	30
13 Gy + BMT					
Jejunum	Villy	0.0 \pm 0.0	0.0 \pm 0.0	N/A	N/A
	Crypts	0.1 \pm 0.1	0.9 \pm 0.4 ¹	N/A	N/A
Ileum	Villy	0.0 \pm 0.0	0.0 \pm 0.0	N/A	N/A
	Crypts	0.3 \pm 0.2	0.9 \pm 0.4 ¹	N/A	N/A
Colon Ascendens		0.0 \pm 0.0	0.0 \pm 0.1	N/A	N/A
Liver		0.6 \pm 0.2	0.7 \pm 0.3	N/A	N/A
13 Gy + BMT + EGF					
Jejunum	Villy	0.0 \pm 0.0	0.0 \pm 0.0	0.4 \pm 0.3 ^{1*}	35.5 \pm 5.8 ^{1**}
	Crypts	0.3 \pm 0.2	0.9 \pm 0.4 ¹	2.8 \pm 1.3 ^{1*}	67.7 \pm 20.2 ^{1**}
Ileum	Villy	0.0 \pm 0.0	0.0 \pm 0.0	0.1 \pm 0.1 [*]	3.5 \pm 0.6 ^{1**}
	Crypts	0.4 \pm 0.2	1.3 \pm 0.7 ¹	0.9 \pm 0.3 [*]	17.8 \pm 6.2 ^{1**}
Colon Ascendens		0.1 \pm 0.1	0.1 \pm 0.1	0.5 \pm 0.4 [*]	5.2 \pm 1.6 ^{1**}
Liver		0.5 \pm 0.2	0.8 \pm 0.5	11.1 \pm 3.4 ^{1*}	180.1 \pm 13 ^{1**}

- Significant difference against the previous time point: ¹ p \leq 0.05.
- N/A = Not Available.

1.3.4.4 Discussion

In this study, we evaluated the effect of BMT, EGF and their combination on GI damage in C57BL/6 mice after high-dose whole-body irradiation. Our results show that doses of 12 and 13 Gy are absolutely lethal. BMT improved short-term prognosis after irradiation by 12 Gy but was ineffective after irradiation by 13 Gy. EGF was utilized to change this outcome. At first, EGF was applied in BMT-treated mice at a dose of 2 mg/kg starting 24 hours after irradiation by 13 Gy and then every 48 hours. This treatment did not significantly affect animal survival. Nevertheless, the survival curve showed that 5 of 10 BMT-treated mice lived after 7-day interval, in which the death could be related to acute GRS [150]. These animals died 10 to 28 days after irradiation. In this period, HRS plays a very significant role. Thus, tissue damage caused by subcutaneous route of administration in immuno-suppressed mice could have significantly contributed to the lethality [120].

The existing findings led to the adjustment of the therapeutical regimen in the second experiment. EGF was applied only to cover GRS critical phase, i.e., 3 doses of EGF (2 mg/kg) were administered 1, 3 and 5 days after the irradiation by 13 Gy. This therapy was efficient and 80% of mice survived 30 days after the irradiation.

The effectivity of the combined BMT and EGF treatment led us to the third experiment. To elucidate the mechanisms of BMT, EGF and combined therapy action, we evaluated different parameters in jejunum, ileum, colon ascendens, liver and peripheral blood.

1.3.4.4.1 Jejunum

Our results show progressive cell loss and atrophy induced by increased apoptotic activity (2 and 4 days after irradiation) and suppressed proliferation (2 days after irradiation) in jejunum. Signs of regeneration (renewed

mitotic activity 4 days after irradiation) were also found. Inflammation accompanied these changes. Its intensity decreased 4 days after irradiation, which correlated with drop of neutrophil granulocyte in peripheral blood.

Administration of EGF decreased ionizing radiation-induced apoptotic activity in crypts 2 and 4 days after irradiation. The mechanism likely contributed to the preservation of average cryptal length at the control level and supported cell flow into the villar compartment in both time intervals since the length of villi did not change 2 days after irradiation and its shortening was reduced 4 days after irradiation.

Similarly to EGF, BMT reduced ionizing radiation-induced apoptotic activity in crypts 2 and 4 days after irradiation. Since it did not prevent the decrease in length of crypts and height of villi in the 2-day interval, BMT effect appears delayed. Four days after irradiation, all parameters were comparable with those in EGF-treated group. This indicates that BMT stimulates jejunal epithelial regeneration more effectively than EGF during the 2- to 4-day interval. The mechanism underlying this finding remains unknown, but might be explained by short EGF plasma half-life (1.5 min in humans), whereas we may presume progressive increase in GFP endocrine and paracrine activity after the transplantation correlating with increasing amount of GFP⁺ cells in jejunum [122], [151].

Combination of BMT and EGF modulated ionizing radiation-induced changes in the extent observed in EGF-treated group 2 days after irradiation. This confirms delayed BMT action in jejunum. In the 4-day interval, BMT intensified EGF effects. Thus, beside changes that were also measured in EGF- and BMT-treated group, we found increased amount of viable crypts and higher mitotic activity when compared with irradiated and non-treated group. This indicates that the combined therapy not only reduces cell loss but also accelerates jejunal regeneration. We also evaluated later time points in this group. No inflammatory infiltration was found 7 days after irradiation, which most likely reflected the depletion of neutrophil granulocytes observed in the peripheral blood 4 days after irradiation. Morphometric parameters indicate continuing regeneration in jejunum. Increased mitotic activity seems to support formation of new crypts, their elongation and the flow of new cells into the villi, which, together with the compensatory attenuation of apoptotic activity in this compartment, prolonged their length over the control values. Increased mitotic activity might also explain a second (late) wave of apoptosis in crypts. Restoration of proliferation in cells with residual DNA damage may cause improper distribution of chromosomes during mitosis and activate mitotic catastrophe [247]. In the 30-day interval, the status of jejunal mucosa improved but still, its parameters did not reach pre-exposure levels. The inflammatory reaction resumed and correlated with higher apoptotic activity in crypts. Dysregulation of cellular kinetics (increased apoptosis not compensated with increased proliferation) is a potential risk. If not treated, it may impair the integrity of GI epithelium and possibly support the development of radiation-induced systemic inflammatory response syndrome and subsequent multiple organ failure [85], [109], [268].

1.3.4.4.2 Ileum

Ileum is more radio-resistant than jejunum [23]. This corresponds with our results showing lower apoptotic activity in the cryptal compartment, which possibly helped to preserve the average length of remaining crypts and height of villi at the control level 2 days after irradiation. Other changes were similar to what we found in jejunum.

Administration of EGF did not affect any parameter 2 days after irradiation but modulated ionizing radiation-induced changes 4 days after irradiation. Compared to jejunum, EGF treatment seems to exhibit later onset, which might be linked to lower EGF receptor expression in ileum [80]. The effect of this therapy also differed. Our results show that the increased cellularity in both compartments was due to stimulation of mitotic activity instead of reducing ionizing radiation-induced apoptotic activity in crypts as observed in jejunum. Possible explanation for that may lie in different expression of genes regulating cell cycle and apoptosis in different parts of small intestine [65].

BMT significantly mitigated radiation-induced apoptotic activity in both compartments 2 days after irradiation. Reduced enterocyte loss accompanied with mucosal oedema (unpublished data) increased length of villi above the control level in the same interval. In the 4-day interval, it also seems to support increased proliferation to attenuate shortening of villi and crypts since this outcome was more profound in BMT- than in EGF-treated group. The mechanism regulating earlier onset of BMT effect in ileum than in jejunum is not known. Given the similar amount of GFP⁺ cells in both parts of small intestine, mucosal GFP⁺ cells do not appear to affect this outcome. Thus, we may only speculate that different expression of growth factor receptors and/or close relation of terminal ileum to Peyer's patches, which support epithelial regeneration, may play a more significant role [176], [206], [230], [257].

The combined therapy modulated ionizing radiation-induced changes in the extent observed in BMT-treated group 2 days after irradiation. This confirms delayed action of EGF in ileum. In the 4-day interval, EGF intensified BMT effects. On the top of changes that were found in EGF- and BMT-treated group, combined therapy stimulated mitotic activity, which significantly increased amount of viable crypts. Similarly to jejunum, the results show that the combination of EGF and BMT not only reduces cell loss, but also accelerates regeneration in ileum. The regeneration also continued in the later time point. Seven days after irradiation, no inflammation was found and the amount of viable crypts further increased. Similarly to jejunum, increased mitotic and apoptotic activity were measured in crypts. The villar compartment was morphologically restored. The only change observed in this compartment was reduced apoptotic activity in apical enterocyte as a sign of prolonged generation time. The results show that the regeneration in ileum progressed faster than in jejunum and 30 days after irradiation, no difference in morphometric parameters, mitotic and apoptotic activity was measured. The only change found in this time interval was inflammation in 2 (of 4) animals. The mechanism triggering this response remains unknown. In contrast to jejunum, the inflammatory infiltration did not correlate with alteration of tissues morphology. We may only speculate that persisting DNA damage and/or dysregulation of intra- and intercellular communication might have been involved [114], [172], [259].

1.3.4.4.3 Colon Ascendens

Colon ascendens is the most resistant of the three evaluated parts of GI tract [23], [43]. The dose of 13 Gy led to the lowest increase in apoptotic activity, which correlated with the smallest loss of enterocytes (as expressed by micro-colony assay in the context of cryptal length data). Interestingly, amount of viable crypts in colon ascendens further decreased 4 days after irradiation indicating more pronounced cell loss than in small intestine during the 2- to 4-day interval.

Administration of EGF stimulated proliferation, which subsequently increased amount of viable crypts and their length. Thus, EGF seems to accelerate regeneration in colon ascendens. Moreover, this response (stimulation of mitotic activity with no impact on apoptotic activity) appears similar to the action of EGF in ileum.

BMT showed minimal impact. It significantly affected only one parameter being increased length of crypts in the 4-day interval. The mechanism underlying this outcome remains unknown, since we did not observe any modulation of mitotic or apoptotic activity. On the other hand, the difference between BMT- and irradiated and non-treated group was small. Therefore, it might actually reflect the biological variability of animals in groups with low number of tested subjects (6 mice per group in this case).

The effect of combined therapy resembled changes found in EGF-treated group 2 and 4 days after irradiation. It confirms low or possibly none effect of BMT in colon ascendens. We also evaluated later time points in this group. Similarly to small intestine, increased proliferation in crypts and decreased apoptotic activity at the luminal surface were found 7 days after irradiation. On the other hand, we did not observe any increase in apoptotic activity in the cryptal compartment and the amount of viable crypts further decreased. Both phenomena might have same explanation. Proliferating enterocytes express less pro-apoptotic tumor

suppressor p53 targets in large intestine than in small intestine, which correlates with relatively low caspase-3 activity detected in the presence of DNA damage [65], [103]. Wang *et al.* [259] showed that bone marrow stem cells may alternatively enter senescence after irradiation. In large intestine, senescent cells may help to preserve tissue integrity at first but their presence might become problematic. Crypts without a single cell capable of self-renewal will eventually collapse (in contrast to small intestine, the amount of viable crypts was decreasing in colon ascendens during 2 – 7-day interval). However, the presence of such cells will preserve the crypts [42], [205], [243]. The question is how much their functions and adaptive mechanism will be altered if both proliferating as well as senescent cells are present. For instance, defective branching and formation of new crypts could explain persisting decrease of viable crypts 30 days after irradiation. Senescence may also associate with inflammation, which was found in colon ascendens in 1 (of 4) animals in the same interval [74].

1.3.4.4.4 Liver

Lymphoid accumulations were found in the liver tissue of control animals (physiological norm; Ref. [39]). The accumulations disappeared after irradiation, which correlated with the loss of lymphocytes from the peripheral blood circulation. Other parameters (granulocyte infiltration and apoptosis) were not affected.

EGF, BMT and their combination did not modulate ionizing-radiation induced changes in liver 2 and 4 days after irradiation. In the combined therapy-treated group, the parameters were also evaluated in the later time points. We found increased acute inflammatory and lymphoid infiltration 30 days after irradiation, which correlated with increased apoptotic activity suggesting an active process [258].

1.3.4.4.5 Peripheral Blood Cells

The irradiation by 13 Gy leads to irreversible bone marrow damage [67], [242], [269]. This corresponds with our findings in the peripheral blood.

EGF, BMT or their combination did not prevent ionizing radiation-induced changes. To the contrary, EGF significantly decreased amount of neutrophil granulocytes in the 4-day interval reaching undetectable values. Lewkowitz *et al.* [136] and Uddin *et al.* [239] reported that EGF stimulates homing of neutrophil granulocyte under inflammatory conditions. Thus, EGF seems to accelerate neutrophil granulocyte loss from the circulation. This mechanism might also prolong granulocytopenia and contribute to higher lethality of repetitive EGF application (Experiment 1) when compared with 3 dose regimen (Experiment 2).

1.3.4.4.6 GFP⁺ Cells

The results show that GFP⁺ cells persist in peripheral blood circulation of supralethally irradiated mice at least 44 hours after the transplantation but are not measurable using flow cytometry in the 92-hour interval. The disappearance of GFP⁺ cells from blood indirectly correlated with their migration into bone marrow, Peyer's patches, jejunum and ileum. Due to undetectable values of GFP⁺ cells in bone marrow in the 44-hour interval and the length of bone marrow transit times [70], GFP⁺ cells seem to migrate into these tissues directly from the circulation. Myelogenic production becomes significant later. It appears to play its role 7 days after irradiation since the amount of GFP⁺ cells increased in jejunum and liver. In the 30-day interval, the amount of GFP⁺ cells further increased and the highest values were found in jejunum reflecting the intensity of inflammatory reaction in tissues with most profound histopathological alterations.

EGF did not affect the migration of transplanted GFP⁺ cells early after transplantation.

1.3.4.5 Conclusion

Both bone marrow transplantation and epidermal growth factor attenuate gastrointestinal damage and/or support regeneration in mice after whole-body irradiation by 13 Gy. Their combination is most effective.

Bone marrow transplantation was performed 4 hours after irradiation via i.v. administration of bone marrow cells into the venous system. Such a therapy is highly unlikely for victims of mass casualty radiological or nuclear incident but may find its use for rescuers or other personnel conducting operations in an environment with a risk of high-dose ionizing radiation exposure.

Epidermal growth factor showed efficiency in bone marrow-transplanted mice when applied at a dose of 2 mg/kg 1, 3 and 5 days after irradiation. Application of epidermal growth factor after the critical phase for gastrointestinal sub-syndrome of acute radiation syndrome lacks foundation. First, we found significant regeneration of gastrointestinal mucosa 7 days after irradiation. Second, EGF might significantly prolong granulocytopenia. And finally, there is an infection/sepsis risk of parenteral administration in immunosuppressed individuals.

1.3.5 EGF Attenuates Delayed Ionizing Radiation-Induced Tissue Damage in Bone Marrow Transplanted Mice

Abstract

We examined the effect of epidermal growth factor in bone marrow transplanted mice after whole-body irradiation by 11 Gy. C57BL/6 mice were divided into 3 groups:

- 0 Gy;
- 11 Gy (⁶⁰Co, single dose, 0.51 Gy/min) + bone marrow transplantation (5×10^6 bone marrow cells isolated from green fluorescent protein syngenic mice, 3 – 4 hours after irradiation); and
- 11 Gy + bone marrow transplantation + epidermal growth factor (2 mg/kg applied subcutaneously 1, 3 and 5 days after irradiation).

Survival data were collected. Bone marrow, peripheral blood count and cytokines, gastrointestinal, and liver parameters and migration of green fluorescent protein positive cells were evaluated 63 days after irradiation. Epidermal growth factor increased survival of irradiated and bone marrow transplanted animals from 10.7 to 85.7% 180 days after irradiation. In bone marrow transplanted group, we found changes in differential bone marrow and blood counts, plasma cytokine levels, gastrointestinal tissues, and liver 63 days after irradiation. These alterations were completely or in some parameters at least partially restored by epidermal growth factor. Epidermal growth factor significantly improves long-term prognosis of bone marrow transplanted mice.

1.3.5.1 Introduction

High-doses whole-body irradiation induces a wide variety of cellular and tissue damage, which clinically manifests as Acute Radiation Syndrome (ARS). Three different sub-syndromes are classified within ARS depending on dose-dependent involvement of early reacting systems including [59]:

- Haematopoietic (H-ARS; >2 Gy);
- Gastrointestinal (G-ARS; >10 Gy); and
- Neurovascular sub-syndrome (>30 Gy).

Whereas the H-ARS is treatable using cytokines, blood component transfusion or even Bone Marrow Transplantation (BMT), the G-ARS has poor prognosis [67], [97], [270]. To treat whole-body irradiation by doses higher than 9 – 10 Gy, cell therapy counteracting severe H-ARS combined with effective mitigators to prevent development of G-ARS seems therefore necessary to improve the outcome [67], [242], [269].

So far, different mitigators have been used to modulate ionizing radiation-induced gastrointestinal damage including growth factors. One of them is Epidermal Growth Factor (EGF). EGF was found to stimulate

regeneration of villi after abdominal irradiation by 15 Gy and it suppresses apoptosis, supports villi recovery and promotes animal survival of mice after whole-body irradiation by 10 Gy [130], [165]. Recently, we have also proved that administration of EGF is compatible with Bone Marrow Transplantation (BMT). Combination of BMT and EGF significantly stimulated intestine regeneration and increased 30-day survival of mice after whole-body irradiation by 13 Gy [174]. On the other hand, we failed to improve long-term prognosis since the majority of animals died during the second month after irradiation (unpublished data). This was probably related to the delayed inflammatory response, which is associated with Multiple Organ Dysfunction Syndrome / Multiple Organ Failure (MODS/MOF) [109], [174].

The aim of this study is to evaluate the effect of EGF in bone marrow-transplanted mice after whole-body irradiation. To improve the long-term prognosis of solely transplanted animals the dose was reduced to 11 Gy.

1.3.5.2 Materials and Methods

1.3.5.2.1 Animals

Female C57BL/6 mice aged 12 – 16 weeks and weighing 19.0 – 23.5 g (Velaz, Unetice, Czech Republic) were kept in an air-conditioned room ($22 \pm 2^\circ\text{C}$ and $50 \pm 10\%$ relative humidity, with lights from 7:00 to 19:00 h) and allowed access to standard food (Velaz) and tap water ad libitum. Experimental animals were handled in accredited facility (accreditation number: c.j. 25895/2010-17210) and approved by the Ethics Committee (Faculty of Military Health Sciences, Hradec Kralove, Czech Republic).

1.3.5.2.2 Irradiation (IR)

For IR treatments, the animals were kept in a Plexiglas box (VLA JEP, Hradec Kralove, Czech Republic) and were irradiated using a ^{60}Co unit (Chirana, Prague, Czech Republic) at a dose rate of 0.51 (first model) and 0.37 Gy/min (second model) with a target distance of 1 m. Dosimetry was performed using an ionization chamber (Dosemeter PTW Unidos 1001, Serial No. 11057, with ionization chamber PTW TM 313, Serial No. 0012; RPD Inc., Albertville, MN, USA).

1.3.5.2.3 Experimental Set-Ups

In the first model, mice were randomly divided into 3 groups. The first, a control group (22 mice) treated with physiologic solution applied in volumes and routes equivalent to BMT and EGF treatment. The second, a group (34 mice) irradiated by a single dose of 11 Gy and treated with BMT 3 – 4 hours after irradiation. BMT was performed by injecting 5×10^6 Green Fluorescent Protein positive (GFP^+) syngenic bone marrow cells from GFP^+ mice (LF UK, Hradec Kralove, Czech Republic) in 0.5 ml Phosphate-Buffered Saline (PBS, pH 7.2; Sigma, St. Louis, MO, USA) into a tail vein 4 hours after irradiation as previously described by Filip *et al.* [68] and adjusted. Physiologic solution was applied in a volume and a route equivalent to EGF treatment. Finally, a group (34 mice) irradiated by 11 Gy and treated with BMT 3 – 4 hours after irradiation and EGF (BioVision Inc., Milpitas, CA, USA) 24, 72 and 120 hours after irradiation. EGF was administered subcutaneously in a dose of 2 mg/kg.

The second model was designed to demonstrate the effect of EGF in animals treated without BMT. In this model, mice were randomly divided into 2 groups. First, a group (10 mice) irradiated by a single dose of 11 Gy receiving physiologic solution in a volume and a route equivalent to EGF treatment. And second, a group (10 mice) administered with EGF 24, 72 and 120 hours after irradiation.

1.3.5.2.4 Sample Collection

Six mice from each group of the first experimental model were randomly selected and euthanized by cervical dislocation 63 days after irradiation. Blood and samples from jejunum (5 – 6 cm from the pyloric ostium),

ileum (1 – 2 cm from ileocecal valve), colon transversum (3 – 4 cm from ileocecal valve), liver, lung, bone marrow, spleen, and thymus were collected.

1.3.5.2.5 Jejunum, Ileum, Colon Transversum and Liver – Staining

Samples from jejunum, ileum, colon transversum and liver (left lateral lobe) were fixed with 10% neutral buffered formalin (Chemapol, Prague, Czech Republic), embedded into paraffin (Paramix, Holic, Czech Republic), and tissue sections 5- μ m thick were cut (Microtome model SM2000 R, Leica, Heidelberg, Germany). Staining with hematoxylin and eosin (both Merck, Kenilworth, NJ, USA) and immunohistochemical detection of activated caspase-3 (cleaved at aspartic acid-175) using rabbit monoclonal antibody (1:200, clone 5A1E; Biotech, Prague, Czech Republic) by a standard peroxidase technique published previously [173] were done.

1.3.5.2.6 Evaluation of Histopathological Changes

Histopathological changes were evaluated in hematoxylin-eosin stained samples according to semi-quantitative criteria presented in tables II, VI and VIII using a BX-51 microscope (Olympus Czech Group, Prague, Czech Republic).

1.3.5.2.7 Amount of Crypts and Villi

The number of crypts and villi were evaluated per circumference in hematoxylin-eosin stained samples at 400 \times magnification. As a crypt, we considered a crypt-like structure with ≥ 3 Paneth cells (small intestine) or ≥ 5 enterocytes (large intestine) in close proximity to lamina muscularis mucosae. As a villus, we considered a villus-like mucosal prominence exceeding at least 5 times the length of its enterocytes.

1.3.5.2.8 Length of Crypts and Villi

To measure the length of crypts and villi, hematoxylin-eosin stained samples were evaluated using a BX-51 microscope and the ImagePro 5.1 computer image analysis system (Media Cybernetics, Bethesda, MD, USA). The length of 20 randomly selected crypts and 20 randomly selected villi was measured per animal under 200 \times magnification.

1.3.5.2.9 Evaluation of Mitotic and Apoptotic Activities

In crypts, mitotic (hematoxylin-eosin) and apoptotic activity (activated caspase-3) were measured under 400 \times magnification. Crypts were selected for scoring if they represented good longitudinal sections containing crypt lumen. Total number of apoptotic and mitotic cells was measured in enterocytes on both sides of 50 longitudinal crypt sections up to the 20th position starting at the midpoint at the base of the crypt. Number of apoptotic cells was judged subjectively by the size and number of closely adjacent apoptotic fragments. An apoptotic cell could be judged as a single large fragment approximately the size of a neighbouring cell or a cluster of at least 3 closely associated small fragments. Data were expressed as apoptotic and mitotic index, where apoptotic index = (total number of apoptotic cell in 50 crypts \times 100) / (50 \times 40) and mitotic index = (total number of mitotic cells in 50 crypts \times 100) / (50 \times 40). In jejunum and ileum, we also evaluated villar apoptotic activity representing % of apoptotic cell positive villi. An apoptotic cell positive villus was considered a one with ≥ 1 apoptotic cells starting at the tip down to the 10th position. In colon ascendens, apoptotic index was evaluated in 1000 enterocytes at the luminal surface. In liver, the amount of apoptotic cells per microscopic field (in 10 fields) was calculated under 400 \times magnification.

1.3.5.2.10 Cell Counts and Cytokines in Peripheral Blood Plasma

Venous blood was collected into heparinized tubes (Scanlab Systems, Prague, Czech Republic) and kept on ice until all samples from the whole group (6 mice) were collected.

To measure peripheral blood cell count, 120 µl of heparinized blood was evaluated using ABX Pentra 60C+ analyser (Trigon-Plus, Prague, Czech Republic).

To assess cytokines in peripheral blood plasma, the rest of blood was transferred into centrifuge tubes (TPP, Trasadingen, Switzerland) and centrifuged (2000 g, 4°C, 20 minutes using Jouan BR4i multi-function centrifuge; Thermo Electron Corporation, Waltham, MA, USA). The supernatants were collected and assayed specific targets using Custom Quantibody Array technology (RayBiotech, Inc., Norcross GA, USA) following the manufacturer's protocol. Levels of cytokines were determined by RayBiotech using Quantibody service. For publication, only proteins, whose calibration curve correlation coefficients were ≥ 0.99 , were selected, including:

- Intercellular adhesion molecule-1 (ICAM-1);
- Interleukin 4 (IL-4);
- Interleukin 6 (IL-6);
- Interleukin 10 (IL-10); and
- Leptin.

Tumor Necrosis Factor alpha (TNF- α) was measured using quantitative mouse TNF- α ELISA Kit (Alpha Diagnostic International, Inc., San Antonio, TX, USA) according to the manufacturer's protocol.

1.3.5.2.11 Colony-Forming Unit-Granulocyte/Macrophage (CFU-GM) Assay

For CFU-GM assay, bone marrow was harvested from left femoral bone using 1 ml of Iscove's modified Dulbecco's medium supplemented with 1% glutamin and 4% fetal bovine serum (both from Sigma) under sterile conditions. Bone marrow cells (5×10^4 per 35 mm dish; TPP) were planted in Methocult methylcellulose-based medium supplemented with recombinant cytokines and erythropoietin for mouse cells (StemCell Technologies Inc., Vancouver, BC, Canada). Only aggregates with more than 40 cells were considered colonies and were scored with light microscopy using Olympus CKX41 microscope (Olympus Czech Group) 12 – 14 days after incubation at 37°C in 5% CO₂ fully humidified atmosphere in Galaxy 170R incubator (Eppendorf, Inc., Enfield, CT, USA).

1.3.5.2.12 Bone Marrow Differential Count

Bone marrow was flushed from right femoral bone using 1 ml cold PBS (pH 7.2) under non-sterile conditions. Resuspended cells were transferred into centrifuge tubes (TPP) and centrifuged (130 g, 37°C, 5 minutes using Thermo CL30 centrifuge; Thermo Electron Corporation). The supernatants were discarded. The pellets were resuspended and used to prepare smears onto clean microscopic slides (P-lab, Prague, Czech Republic). The smears were left to air dry at laboratory temperature. Next day, the smears were stained with May-Grünwald (10 minutes) and Romanowsky-Giemsa solution (10 – 15 minutes; both from Penta, Prague, Czech Republic). The differential count was evaluated in 300 cell at 1000 \times magnification using Olympus BX41 microscope (Olympus Czech Group).

1.3.5.2.13 Analysis of GFP⁺, B Lymphocytes (CD19⁺CD3⁻), T Lymphocytes (CD19⁻CD3⁺), and Stem Cells (Lin⁻CD117⁺Sca1⁺) in Bone Marrow

The rest of cells harvested from left femoral bone were used for the flow cytometry analysis. Suspensions from bone were incubated in EasyLyse solution (according the manufacturer's instructions; Dako, Glostrup, Denmark) to remove the red blood cells. The remaining cells were centrifuged (280 g, 4°C, 5 minutes using Hettich Universal 32R centrifuge; Gemini BV, Apeldorn, Netherlands), the pellets were resuspended and washed twice in cold washing buffer (PBS containing 0.2% gelatin from cold water fish skin and 0.1% sodium azide; all from Sigma).

For stem cell and GFP cell analysis, 5×10^5 cells (100 μ l) were incubated with biotinylated anti-mouse lineage depletion cocktail (4 μ l, a cocktail of anti-mouse CD3e [clone 145-2C11], anti-mouse CD11 [clone M1/70], anti-mouse CD45R/B220 [clone RA3-6B2], anti-mouse Ly-6G and Ly-6C [clone RB6-8C5], and anti-mouse TER-119/Erythroid Cells [clone TER-119] antibodies; (BD Biosciences, San Jose, CA, USA) and anti-mouse CD117 PerCP-Cy5.5 (3 μ l, clone 2B8; BD Biosciences) and anti-mouse Ly-6A/E-APC (Stem cell antigen 1 [Sca1], 1 μ l, clone D7; SouthernBiotech, Birmingham, AL, USA) antibodies at 8°C for 15 minutes. After the incubation, the cells were washed twice in cold washing buffer and incubated with V450 Streptavidin at 8°C for 15 min. The cells were then washed twice in cold washing buffer. Propidium iodide (Sigma) was added at a final concentration of 0.1 μ g/ml immediately prior to acquisition to discern dead cells. The cells from each sample were analysed using CyAn flow cytometer with Summit software 4.2 (both from Dako).

For B and T lymphocyte analysis, 5×10^5 cells (100 μ l) were incubated with anti-mouse CD3 PE-Cy7 (clone 145-2C11) and anti-mouse CD19 APC-H7 antibodies (clone ID3; both from BD Biosciences) at 8°C for 15 minutes. After the incubation, the cells were washed twice in cold washing buffer. Propidium iodide (Sigma) was added at a final concentration of 0.1 μ g/ml immediately prior to acquisition to discern dead cells. The cells from each sample were analysed using CyAn flow cytometer with Summit software 4.2 (both from Dako).

1.3.5.2.14 *Weight of Spleen*

After sample collection, spleen was weighed using KERN EG 620-3NM (Vahy-Tep Skoricka, Teplice, Czech Republic).

1.3.5.2.15 *GFP⁺ Cells in Liver, Lung, Spleen and Thymus*

Single-cell suspensions from liver (right lateral lobe), lung, spleen and thymus were isolated by teasing tissue into cold PBS. Small pieces of tissue were sedimented at 1 g (1 min) and the supernatant was filtered through Nylon sifter (70 μ m pore; Servis Centrum, Brno, Czech Republic). As for bone marrow, the rest of cells flushed from left femoral bone were used for the analysis. Suspensions from liver, lung, spleen and thymus were incubated in EasyLyse solution (according the manufacturer's instructions; Dako) to remove the red cells. The remaining cells were centrifuged (280 g, 4°C, 5 min using Hettich Universal 32R centrifuge; Gemini BV), the pellets were resuspended and washed twice in cold washing buffer. Propidium iodide (Sigma) was added at a final concentration of 0.1 μ g/ml immediately prior to acquisition to discern dead cells. A total of 5×10^6 (1 ml) cells from each sample were analysed using CyAn flowcytometer with Summit software 4.2 (both from Dako).

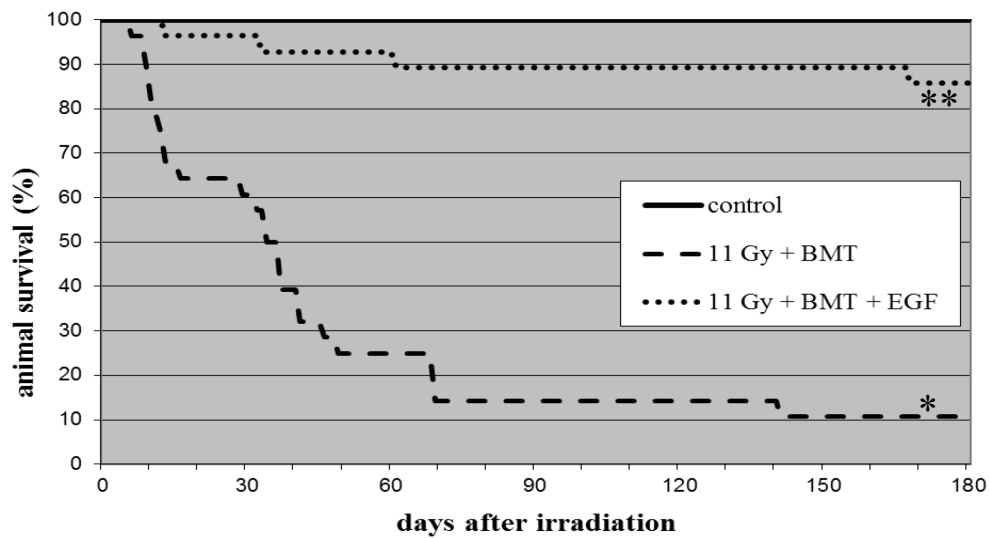
1.3.5.2.16 *Statistical Analysis*

The Mann-Whitney test and Kaplan-Meier Survival Analysis using SigmaStat 3.1 software (Systat Software Inc., Erkhart, Germany) were used for the statistical analysis. The differences were considered significant when $p \leq 0.05$.

1.3.5.3 **Results**

Effect of EGF on survival of BMT-treated mice after irradiation by 11 Gy.

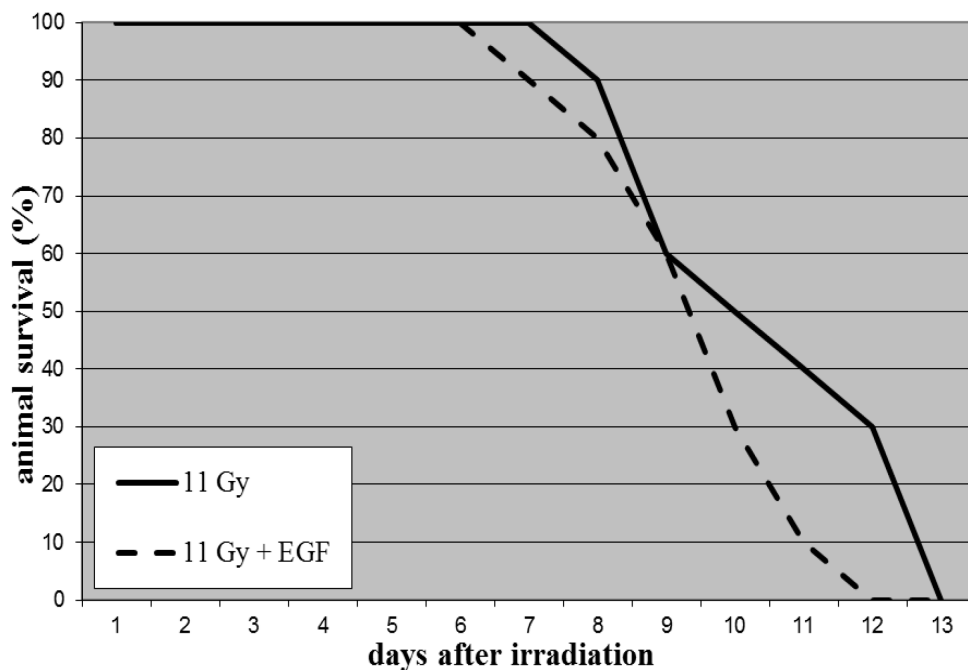
After censoring the 6 mice, whose samples were taken from each group (first model) 63 days after irradiation, no death was observed in control group during 180-day interval. In BMT-treated group, 25 (of 28) animals died with the median survival (39.5 days) significantly decreased compared to the control ($p \leq 0.001$). In BMT- and EGF-treated group, only 4 (of 28) mice died with the median survival being > 180 days. Compared to BMT-treated group, administration of EGF significantly increased the survival from 10.7 to 85.7% ($p \leq 0.001$) 180 days after irradiation reaching the level of control animals ($p = 0.12$). (Figure 1-12).



- For BMT, 5×10^6 GFP⁺ syngenic bone marrow cells were injected into a tail vein 3 – 4 hours after irradiation. EGF was applied subcutaneously 2 mg/kg 1, 3 and 5 days after irradiation.
- * Statistically significant compared to non-irradiated control group ($p \leq 0.05$).
- ** Statistically significant compared to irradiated BMT-treated EGF-non-treated group ($p \leq 0.05$).

Figure 1-12: Effect of Bone Marrow Transplantation (BMT) and Epidermal Growth Factor (EGF) on Animal Survival of C57BL/6 Mice After Whole Body Irradiation by 11 Gy.

Without BMT (second model), no mice survived longer than 13 days after irradiation by 11 Gy. Administration of EGF did not affect survival of animals (median = 9 days) compared to animals receiving no treatment (median = 10 day, $p = 0.114$). (Figure 1-13).



- EGF was applied subcutaneously 2 mg/kg 1, 3 and 5 days after irradiation.

Figure 1-13: Effect of Epidermal Growth Factor (EGF) on Animal Survival of C57BL/6 Mice After Whole Body Irradiation by 11 Gy.

1.3.5.3.1 Histopathological Changes in Jejunum

We found significant changes in jejunum of 5 BMT-treated mice including cystic dilatation of crypts, granulocyte infiltration, mucosal and submucosal oedema (all $p = 0.15$) 63 days after irradiation. Compared to this group, administration of EGF significantly attenuated cystic dilatation of crypts, which was found in 2 animals ($p = 0.026$) and mucosal and submucosal oedema ($p = 0.026$ and 0.41 , respectively) present in 1 of the 2 mice. (Table 1-18).

Table 1-18: Histopathological Changes in Jejunum Expressed as the Median Value of Positive Findings (of Values ≥ 1) or 0 (No Positive Finding in the Group) and the Amount of Affected Animals in the Group (in brackets). The changes were evaluated 63 days after irradiation.

Group		0 Gy	11 Gy + BMT	11 Gy + BMT +EGF
Epithelial Continuity		0 (0 of 6)	0 (0 of 6)	0 (0 of 6)
Cystic Crypts		0 (0 of 6)	2 (5 of 6) ^a	1 (2 of 6) ^b
Oedema	Cellular	0 (0 of 6)	0 (0 of 6)	0 (0 of 6)
	Mucosal	0 (0 of 6)	4 (5 of 6) ^a	3 (1 of 6) ^b
	Submucosal	0 (0 of 6)	1 (5 of 6) ^a	1 (1 of 6) ^b
Granulocyte Infiltration		0 (0 of 6)	1 (5 of 6) ^a	1 (2 of 6)
Fibrotisation		0 (0 of 6)	0 (0 of 6)	0 (0 of 6)

- Epithelial continuity: 0 – no change, 1 – erosion, 2 – ulceration.
- Cystic dilation of crypts: 0 – not present, 1 – $\leq 10\%$ of crypts, 2 – $\leq 50\%$ of crypts, 3 – $\leq 80\%$ of crypts, 4 – $> 80\%$ of crypts.
- Cellular oedema: 0 – not present, 1 – present.
- Mucosal oedema: 0 – not present, 1 – present without sub-epithelial component, 2 – sub-epithelial oedema in $\leq 10\%$ of villi, 3 – sub-epithelial oedema in $\leq 50\%$ of villi, 4 – sub-epithelial oedema in $\leq 80\%$ of villi, 5 – sub-epithelial oedema in $> 80\%$ of villi.
- Submucosal oedema: 0 – not present, 1 – present.
- Granulocyte infiltration: 0 – not present, 1 – in lamina propria mucosae (at least 1 microscopic field with ≥ 10 granulocytes at $400\times$ magnification), 2 – additionally in either crypts (at least 1 crypt with ≥ 1 granulocytes at $400\times$ magnification) or lamina submucosa (at least 1 microscopic field with ≥ 10 granulocytes at $400\times$ magnification), 3 – in all three compartments.
- Fibrotisation: 0 – not present, 1 – present.
- ^a Significant differences between non-irradiated and irradiated groups: $p \leq 0.05$.
- ^b Significant differences between irradiated BMT-treated EGF-non-treated group and irradiated BMT-treated EGF-treated group: $p \leq 0.05$.

1.3.5.3.2 Morphometric Parameters, Apoptotic and Mitotic Activity in Jejunum

Compared to controls (0 Gy), we measured significantly decreased amount of crypts (1.5-fold, $p < 0.001$), length of villi (1.1-fold, $p < 0.001$) and villar apoptotic activity (1.3-fold, $p = 0.045$) and significantly increased length of crypts (1.8-fold, $p < 0.001$), apoptotic (2.6-fold, $p = 0.009$) and mitotic activity in crypts (1.6-fold, $p = 0.015$) in BMT-treated mice. Compared to this group, administration of EGF significantly attenuated changes of all these parameters ($p = 0.015$, < 0.001 , 0.009 , < 0.001 , 0.015 , and 0.009 , respectively) to the control levels. (Table 1-19).

Table 1-19: Average Values of Morphometric Parameters, Apoptotic and Mitotic Activity in Jejunum $\pm 2 \times$ Standard Error of Mean. Parameters and activities were evaluated 63 days after irradiation.

Group	0 Gy	11 Gy + BMT	11 Gy + BMT +EGF
Crypts			
Amount of Crypts	144 \pm 6	98 \pm 13 ^a	140 \pm 26 ^b
Length, μ m	103 \pm 3	184 \pm 13 ^a	99 \pm 5 ^b
Mitotic Index, %	2.7 \pm 0.5	4.2 \pm 0.6 ^a	2.8 \pm 0.4 ^b
Apoptotic Index, %	0.7 \pm 0.1	1.8 \pm 0.5 ^a	0.8 \pm 0.2 ^b
Villi			
Amount of villi	52 \pm 4	56 \pm 8	60 \pm 12
Length, μ m	378 \pm 18	329 \pm 13 ^a	370 \pm 14 ^b
Villar Apoptotic Activity, %	82 \pm 9	63 \pm 10 ^a	87 \pm 5 ^b

- ^a Significant differences between non-irradiated and irradiated groups: $p \leq 0.05$.
- ^b Significant differences between irradiated BMT-treated EGF-non-treated group and irradiated BMT-treated EGF-treated group: $p \leq 0.05$.

1.3.5.3.3 Histopathological Changes in Ileum

We did not observe any significant changes of histopathological parameters in ileum of BMT and combined therapy treated group 63 days after irradiation. The only findings (statistically insignificant) were the presence of cystic dilatation and granulocyte infiltration in 2 mice accompanied with mucosal oedema in one of them. (Table 1-20).

Table 1-20: Histopathological Changes in Ileum Expressed as the Median Value of Positive Findings (of Values ≥ 1) or 0 (No Positive Finding in the Group) and the Amount of Affected Animals in the Group (in brackets). The changes were evaluated 63 days after irradiation.

Group	0 Gy	11 Gy + BMT	11 Gy + BMT +EGF
Epithelial Continuity	0 (0 of 6)	0 (0 of 6)	0 (0 of 6)
Cystic Crypts	0 (0 of 6)	1 (2 of 6)	0 (0 of 6)
Oedema	Cellular	0 (0 of 6)	0 (0 of 6)
	Mucosal	0 (0 of 6)	4 (1 of 6)
	Submucosal	0 (0 of 6)	0 (0 of 6)
Granulocyte Infiltration	0 (0 of 6)	1 (2 of 6)	0 (0 of 6)
Fibrotisation	0 (0 of 6)	0 (0 of 6)	0 (0 of 6)

- For each parameter's scale see Table 1-18.

1.3.5.3.4 Morphometric Parameters, Apoptotic and Mitotic Activity in Ileum

In BMT-treated mice, we found significantly increased length of crypts (1.3-fold, $p < 0.001$), length of villi (1.3-fold, $p < 0.001$) and mitotic activity in crypts (1.6-fold, $p = 0.041$). Compared to this group, administration of EGF significantly attenuated length of crypts and villi (both $p < 0.001$) to the control levels. (Table 1-21).

Table 1-21: Average Values of Morphometric Parameters, Apoptotic and Mitotic Activity in Ileum $\pm 2 \times$ Standard Error of Mean. Parameters and activities were evaluated 63 days after irradiation.

Group	0 Gy	11 Gy + BMT	11 Gy + BMT +EGF
Crypts			
Amount of Crypts	128 \pm 13	101 \pm 26	116 \pm 21
Length, μ m	96 \pm 4	126 \pm 6 ^a	94 \pm 4 ^b
Mitotic Index, %	2.0 \pm 0.4	3.1 \pm 0.7 ^a	2.2 \pm 0.3
Apoptotic Index, %	1.0 \pm 0.1	1.2 \pm 0.3	1.1 \pm 0.1
Villi			
Amount of Villi	44 \pm 7	55 \pm 10	40 \pm 10
Length, μ m	153 \pm 8	200 \pm 11 ^a	157 \pm 8 ^b
Villar Apoptotic Activity, %	43 \pm 10	53 \pm 5	40 \pm 13

- ^a Significant differences between non-irradiated and irradiated groups: $p \leq 0.05$.
- ^b Significant differences between irradiated BMT-treated EGF-non-treated group and irradiated BMT-treated EGF-treated group: $p \leq 0.05$.

1.3.5.3.5 Histopathological Changes in Colon Transversum

We did not observe any significant changes of histopathological parameters in colon transversum of BMT and combined therapy treated groups 63 days after irradiation. The only finding (statistically insignificant) was the presence of cystic dilatation of crypts in 1 animal. (Table 1-22).

Table 1-22: Histopathological Changes in Colon Transversum Expressed as the Median Value of Positive Findings (of Values ≥ 1) or 0 (No Positive Finding in the Group) and the Amount of Affected Animals in the Group (in brackets). The changes were evaluated 63 days after irradiation.

Group	0 Gy	11 Gy + BMT	11 Gy + BMT +EGF
Epithelial Continuity	0 (0 of 6)	0 (0 of 6)	0 (0 of 6)
Cystic Crypts	0 (0 of 6)	2 (1 of 6)	0 (0 of 6)
Oedema	Cellular	0 (0 of 6)	0 (0 of 6)
	Mucosal	0 (0 of 6)	0 (0 of 6)
	Submucosal	0 (0 of 6)	0 (0 of 6)
Granulocyte Infiltration	0 (0 of 6)	0 (0 of 6)	0 (0 of 6)
Fibrotisation	0 (0 of 6)	0 (0 of 6)	0 (0 of 6)

- For each parameter's scale see Table 1-22 caption except for mucosal eodema: 0 – not present, 1 – present without sub-epithelial component, 2 – present with sub-epithelial component.

1.3.5.3.6 Morphometric Parameters, Apoptotic and Mitotic Activity in Colon Transversum

In colon transversum, we measured significantly decreased length of crypts (1.3-fold, $p < 0.001$). Application of EGF did not mitigate this change. (Table 1-23).

Table 1-23: Average Values of Morphometric Parameters, Apoptotic and Mitotic Activity in Colon Transversum $\pm 2 \times$ Standard Error of Mean. Parameters and activities were evaluated 63 days after irradiation.

Group	0 Gy	11 Gy + BMT	11 Gy + BMT +EGF
Crypts			
Amount of Crypts	166 \pm 23	151 \pm 18	192 \pm 51
Length, μ m	207 \pm 10	157 \pm 9 ^a	165 \pm 8 ^b
Mitotic Index, %	1.2 \pm 0.1	1.3 \pm 0.4	1.0 \pm 0.2
Apoptotic Index, %	0.9 \pm 0.1	0.9 \pm 0.3	0.7 \pm 0.1
Luminal surface			
Apoptotic Index, %	2.1 \pm 0.2	2.1 \pm 0.4	2.4 \pm 0.2

- ^a Significant differences between non-irradiated and irradiated groups: $p \leq 0.05$.
- ^b Significant differences between irradiated BMT-treated EGF-non-treated group and irradiated BMT-treated EGF-treated group: $p \leq 0.05$.

1.3.5.3.7 *Histopathological Changes and Apoptotic Activity in Liver*

In liver of BMT-treated group, granulocyte infiltration was present in 5 mice ($p = 0.015$), whereas fatty degenerative changes were significantly diminished and present only in 1 animal ($p = 0.009$). Round cell infiltration and apoptotic activity significantly increased 6.5- and 1.8-fold ($p = 0.015$, $p < 0.001$), respectively. Compared to this group, EGF administration significantly attenuated changes of all these parameters ($p = 0.041$, 0.041 , 0.026 , and 0.003 , respectively) to the control levels. (Table 1-24).

Table 1-24: Histopathological Changes in Liver Expressed as the Median Value of Positive Findings (of Values ≥ 1) or 0 (No Positive Finding in the Group) and the Amount of Affected Animals in the Group (in brackets). Round cell infiltration and apoptotic activity $\pm 2 \times$ standard error of mean. All parameters were evaluated 63 days interval after irradiation.

Group	0 Gy	11 Gy + BMT	11 Gy + BMT +EGF
Degenerative Changes	1 (6 of 6)	1 (1 of 6) ^a	1 (5 of 6) ^b
Granulocyte Infiltration	0 (0 of 6)	2 (5 of 6) ^a	1 (2 of 6) ^b
Round Cell Infiltration	1.0 \pm 0.7	6.5 \pm 3.1 ^a	1.5 \pm 1.0 ^b
Fibrotisation	0 (0 of 6)	0 (0 of 6)	0 (0 of 6)
Apoptotic Activity	1.1 \pm 0.4	2.0 \pm 0.5 ^a	1.2 \pm 0.4 ^b

- Degenerative changes: 0 – not present, 1 – microvesicular changes, 2 – mixed microvesicular and slight macrovesicular changes.
- Granulocyte infiltration: 0 – not present, 1 – 1 microscopic field with ≥ 10 neutrophil granulocytes in 10 randomly selected microscopic fields at 400 \times magnification, 2 – ≥ 2 microscopic field with ≥ 10 neutrophil granulocytes in 10 randomly selected microscopic fields at 400 \times magnification.
- Round cell infiltration: amount of mononuclear nodules (with ≥ 10 cells) per microscopic field at 200 \times magnification (measured in 10 microscopic fields per animal).
- Fibrotisation: 0 – not present, 1 – present.
- Apoptotic activity: amount of apoptotic cells per microscopic field at 400 \times magnification (measured in 10 microscopic fields per animal).
- ^a Significant differences between non-irradiated and irradiated groups: $p \leq 0.05$.
- ^b Significant differences between irradiated BMT-treated EGF-non-treated group and irradiated BMT-treated EGF-treated group: $p \leq 0.05$.

1.3.5.3.8 Cytokines in Peripheral Blood Plasma

In comparison with control mice, we measure significantly increased concentrations of ICAM-1 (2.3-fold, $p = 0.026$), IL-4 (28.7-fold, $p = 0.002$), IL-6 (113.3-fold, $p = 0.002$), and IL-10 (1673.3-fold, $p = 0.015$) in plasma of BMT-treated mice, whereas the concentration of leptin significantly decreased 11.7-fold ($p = 0.004$). In EGF- and BMT-treated group, only IL-6 levels were increased (854.4-fold, $p = 0.002$) compared to control (there was no significant difference compared to BMT-treated group, $p = 0.589$). (Table 1-25).

Table 1-25: Average Values of Plasma Cytokine Levels (pg/ml) $\pm 2 \times$ Standard Error of Mean. Cytokine concentrations were evaluated 63 days after irradiation.

Group	0 Gy	11 Gy + BMT	11 Gy + BMT +EGF
ICAM-1	400 \pm 142	900 \pm 310 ^a	518 \pm 110
IL-4	0.0 \pm 0.0	1.0 \pm 0.5 ^a	0.0 \pm 0.0 ^b
IL-6	0.8 \pm 1.4	89 \pm 38 ^a	670 \pm 1144 ^a
IL-10	0.0 \pm 0.0	21 \pm 12 ^a	6 \pm 6
Leptin	693 \pm 311	60 \pm 100 ^a	677 \pm 446 ^b
TNF- α	168 \pm 97	321 \pm 153	246 \pm 116

^a Significant differences between non-irradiated and irradiated groups: $p \leq 0.05$.

^b Significant differences between irradiated BMT-treated EGF-non-treated group and irradiated BMT-treated EGF-treated group: $p \leq 0.05$.

1.3.5.3.9 Bone Marrow

Compared to control, we found significantly decreased relative representation of hematopoietic stem cells (3.0-fold, $p = 0.017$), erythropoietic cells (3-fold, $p = 0.002$) and lymphocytes (1.9-fold, $p = 0.026$) associated with decrease in both B (5.0-fold, $p = 0.004$) and T lymphocyte lineage (5.0-fold, $p = 0.004$) in bone marrow of BMT-treated mice. Relative representation of mature granulocytes and monocytes significantly increased 1.3- and 2.3-fold ($p = 0.009$ and 0.015), respectively. In comparison with the BMT-treated group, EGF administration significantly affected total, B and T lymphocyte and monocyte relative numbers ($p = 0.015$, 0.015 , 0.026 , and 0.002 , respectively). No significant change was measured in this group when compared with control values except for monocytes, which relative representation decreased 4.0-fold ($p = 0.015$). (Table 1-26).

Table 1-26: Average Values of Bone Marrow Quantitative and Qualitative Parameters $\pm 2 \times$ Standard Error of Mean. All Parameters Were Evaluated 63 Days after Irradiation.

Group	0 Gy	11 Gy + BMT	11 Gy + BMT +EGF
Quantitative Parameters			
Amount of Cells in Femoral Bone Lavage (10^5 /ml)	227 \pm 22	163 \pm 51	221 \pm 30
CFU-GM	42 \pm 7	41 \pm 4	41 \pm 7
Qualitative Parameters, (%)			
Erythropoietic Cells	17.6 \pm 3.9	5.9 \pm 2.5 ^a	12.1 \pm 5.4
Immature Granulocytes	24.6 \pm 2.9	30.4 \pm 4.6	26.8 \pm 2.9
Mature Granulocytes	42.8 \pm 3.0	53.3 \pm 3.8 ^a	46.1 \pm 5.4

Group	0 Gy	11 Gy + BMT	11 Gy + BMT +EGF
Qualitative Parameters, (%) (cont'd)			
Eosinophilic Cells	6.9 ± 2.1	4.8 ± 2.4	5.5 ± 0.7
Lymphoreticular Cells	8.2 ± 2.0	5.5 ± 2.0	9.5 ± 2.9
Lymphocytes	7.4 ± 2.0	3.8 ± 2.1 ^a	9.3 ± 2.8 ^b
B Lymphocytes (CD19 ⁺ CD3 ⁻)	3.0 ± 0.9	0.6 ± 0.9 ^a	3.3 ± 1.5 ^b
T Lymphocytes (CD19 ⁻ CD3 ⁺)	0.5 ± 0.2	0.1 ± 0.0 ^a	0.5 ± 0.2 ^b
Monocytes	0.8 ± 0.2	1.8 ± 0.7 ^a	0.2 ± 0.2 ^{a, b}
Stem Cells (CD117 ⁺ Sca1 ⁺ Lin ⁻)	0.15 ± 0.04	0.05 ± 0.02 ^a	0.10 ± 0.13
GFP ⁺ Stem Cells	N/A	0.04 ± 0.02	0.09 ± 0.13
GFP ⁻ Stem Cells	N/A	0.01 ± 0.00	0.01 ± 0.01

- ^a Significant differences between non-irradiated and irradiated groups: $p \leq 0.05$.
- ^b Significant differences between irradiated BMT-treated EGF-non-treated group and irradiated BMT-treated EGF-treated group: $p \leq 0.05$.
- N/A = Not Available.

1.3.5.3.10 Peripheral Blood Cell Count and Weight of Spleen

Compared to controls, we found significantly decreased amount of erythrocytes (1.1-fold, $p = 0.041$), thrombocytes (1.3-fold, $p = 0.002$), granulocytes (8.6-fold, $p = 0.002$), lymphocytes (2.4-fold, $p = 0.002$), and monocytes (2.1-fold, $p = 0.015$) in peripheral blood, whereas the weight of spleen was not affected ($p = 0.132$) in BMT-treated animals. Compared to this group, administration of EGF significantly increased amount of erythrocytes to the control level ($p = 0.041$) and increased weight of spleen ($p = 0.015$). (Table 1-27).

Table 1-27: Peripheral Blood Cell Counts and Weight of Spleen ± 2 × Standard Error of Mean Evaluated 63 Days after Irradiation.

Group	0 Gy	11 Gy + BMT	11 Gy + BMT +EGF
Erythrocytes	7.5 ± 0.1	7.1 ± 0.2 ^a	7.6 ± 0.3 ^b
Thrombocytes	648 ± 44	482 ± 32 ^a	523 ± 48 ^a
Granulocytes	0.37 ± 0.41	0.04 ± 0.02 ^a	0.05 ± 0.01 ^a
Lymphocytes	3.9 ± 1.2	1.6 ± 0.2 ^a	1.9 ± 0.2 ^a
Monocytes	0.3 ± 0.1	0.1 ± 0.0 ^a	0.1 ± 0.0 ^a
Weight of Spleen (mg)	83 ± 8	69 ± 11	90 ± 8 ^b

- ^a Significant differences between non-irradiated and irradiated groups: $p \leq 0.05$.
- ^b Significant differences between irradiated BMT-treated EGF-non-treated group and irradiated BMT-treated EGF-treated group: $p \leq 0.05$.

1.3.5.3.11 GFP⁺ Cells in Bone Marrow, Liver, Lung, Spleen, and Thymus

When compared to BMT-treated group, combined therapy significantly decreased relative representation of GFP⁺ cells in liver (1.7-fold, $p = 0.030$), whereas their numbers significantly increased in thymus (341.4-fold, $p = 0.002$). (Table 1-28).

Table 1-28: Relative Representation (%) of GFP⁺ Cells in Different Tissues $\pm 2 \times$ Standard Error of Mean. Relative representations were measured 63 days after irradiation.

Group	11 Gy + BMT	11 Gy + EGF + BMT
Bone Marrow	82.9 \pm 4.3	81.4 \pm 4.8
Liver	4.3 \pm 0.9	2.5 \pm 0.6 ^a
Lung	0.8 \pm 0.1	0.9 \pm 0.3
Spleen	10.8 \pm 7.5	9.5 \pm 2.9
Thymus	0.14 \pm 0.05	47.8 \pm 10.9 ^a

- ^a Significant differences between irradiated BMT-treated EGF-non-treated group and irradiated BMT-treated EGF-treated group: $p \leq 0.05$.

1.3.5.4 Discussion

In this study, two experimental models were utilized. First model was designed to evaluate the effect of EGF in BMT-treated mice after whole-body irradiation by 11 Gy. EGF was administered in 3 doses (2 mg/kg) 1, 3 and 5 days after irradiation, which was previously demonstrated to improve short-term prognosis of irradiated (13 Gy) and BMT-treated mice [174]. The results show that EGF significantly increased 180-day survival. On the other hand, the effect of EGF was very limited without BMT treatment (second model). To further illuminate possible mechanisms of EGF- in BMT-treated mice, different parameters were evaluated in jejunum, ileum, colon ascendens, liver, peripheral blood, spleen, lung, and thymus 63 days after irradiation.

1.3.5.4.1 Intestine

Cystic crypts and inflammation were found in intestine of BMT-treated animals 63 days after irradiation. The intensity of these findings corresponded to the radio-sensitivity of intestinal tissues [24]. It also seems to reflect the extensity of morphometric and cellular changes although different outcomes were observed in jejunum, ileum and colon transversum. In jejunum, we found reduced amount of crypts. Proliferation increased in the remaining crypts and overcompensated for intensified apoptosis, which caused extension of crypts. It did not however compensate for higher apoptotic activity in the villar compartment, since the length of villi decreased. Increased mitotic activity inducing extension of crypts was also measured in ileum. In contrast to jejunum, no change in the apoptotic activity was found, thus, increased cellular output from crypts prolonged the villi. The mechanisms stimulating mitotic activity in small intestine remain unknown. We may only speculate that increased proliferation might be a reaction compensating for decreased amount of crypts (although slight and statistically insignificant in ileum) and/or an attempt to sustain sufficient cellular capacity of the cryptal compartment. On the other hand, increased apoptotic activity in jejunum could be related to the inflammatory response [207]. Modulation of the inflammation during this phase may therefore help mitigate the pathological changes. In colon transversum, the only parameter altered was the decreased length of crypts. The mechanism underlying this outcome is uncertain, since we did not observe any modulation of mitotic or apoptotic activity in the 63-day interval.

EGF therapy significantly mitigated ionizing radiation-induced intestinal damage with one exception. We measured decreased length of crypts in colon transversum analogous to what we observed in irradiated mice treated solely with BMT. This indicates that stimulation of regeneration early after irradiation does not affect this outcome. Possible explanation may lie in specific expression profile of colon enterocytes. Proliferating enterocytes express less pro-apoptotic tumor suppressor p53 targets in large intestine than in small intestine, which corresponds to relatively low caspase-3 activity detected in the presence of DNA damage [65], [103]. Damaged cells may alternatively enter senescence, which may subsequently alter tissue morphology [145], [259].

1.3.5.4.2 Liver and Cytokines

Lymphoid accumulations and fat infiltration (predominantly microvesicular) were found in the liver of control animals (physiological norm; Ref. [39]).

After irradiation, loss of fat and active inflammation occurred in the hepatic tissue of BMT-treated mice. Given rather multi-organ character of inflammation accompanied with increased concentrations of pro-inflammatory (ICAM-1, IL-6) as well as anti-inflammatory (IL-4 and IL-10) cytokines in blood, the presence of Systemic Inflammatory Response Syndrome (SIRS) is highly probable [31], [219], [237]. Since an excessive SIRS is associated with MODS (20), we may assume multi-organ failure to be the cause of death during this period (3 mice died in this group 69 days after irradiation). Moreover, SIRS is associated with loss of weight [220]. Mean body weight reached 68% of the initial value in this group compared to 105% and 95% in control and EGF-treated group, respectively (unpublished data). As circulating leptin is directly proportional to body fat mass, SIRS might also explain loss of fat infiltration in liver and decreased leptin level in blood.

Administration of EGF significantly attenuated ionizing radiation-induced changes in liver. Mild granulocyte infiltration was observed only in 2 mice (the same mice with inflammation present in ileum) and mean cytokine concentrations resembled control levels except for IL-6. Since the highest IL-6 value was not found in the 2 affected animals, it seems that IL-6 does not correspond to the inflammatory status in mice 63 days after irradiation. On the other hand, Hayashi *et al.* (measured increased IL-6 in survivors of the A-bomb long after the event and Fagiolo *et al.* found that aging and senescent fibroblasts secrete pro-inflammatory cytokines such as IL-6, higher levels of which are detected in cells from healthy, elderly people [64], [92]. Increased IL-6 blood concentration may therefore reflect the ionizing radiation-accelerated aging. Beside the above mentioned findings, no additional pathology was observed in one of the 2 affected mice suggesting rather local character of inflammation in organs. In the latter mouse, leptin concentration showed a very strong decrease (by two orders) from the remaining group values. Although it is difficult to estimate the inflammatory status in this animal, leptin decrease might precede other cytokine changes and may have prognostic value.

1.3.5.4.3 Bone Marrow

Significant loss of Hematopoietic Stem Cells (HSCs) was observed in bone marrow of BMT-treated mice 63 days after irradiation. The HSC population consisted of both GFP⁺ and GFP⁻ cells (80% and 20%, respectively). Stem cells are very radiosensitive and Flidner *et al.* suppose only 1 – 3 out of 1,000 stem cells to remain intact after an acute exposure to doses around 10 Gy [70]. In our model, GFP⁻ HSCs reached 6.7% of control value and HSC GFP⁺/GFP⁻ ratio resembled GFP⁺/GFP⁻ ratio of bone marrow cells. This indicates active participation of recipient's HSCs in bone marrow regeneration creating the genetic mosaicism. As for the outcome of the regeneration, no quantitative but qualitative differences represented by intensified granulo-monocytopoiesis were detected. Pronounced granulocytosis is a feature characteristic for the regeneration phase [209].

EGF administration in BMT-treated mice accelerated bone marrow recovery. Both quantitative and qualitative parameters were similar to the control values with one exception. We found decreased amount of cells in the monocytic cell line, which may be an overcompensation of the regeneration phase bone marrow monocytosis.

1.3.5.4.4 Blood Count and Weight of Spleen

Although bone marrow displayed quantitative regeneration, pancytopenia was found in peripheral blood of BMT-treated mice 63 days after irradiation.

EGF treatment supported red cell recovery, which correlates with bone marrow qualitative findings. EGF also seems to accelerate regeneration of spleen. Since the GFP cells analysis did not show any

differences between both irradiated groups, it might be an outcome of red cell recovery and red pulp requirements.

1.3.5.4.5 GFP Cells Analysis

The relative representation of GFP⁺ cells was evaluated in bone marrow, liver, lung, spleen, and thymus of transplanted animals. Significant differences were measured in liver and thymus.

In liver, higher amount of GFP⁺ cells was found in the group treated solely with BMT, which corresponded with the present inflammation.

In thymus, amount of GFP⁺ cells was lower in this group than in the combined therapy treated animals. Thymus is a radiosensitive organ [117], [180]. A very low relative representation of GFP⁺ cells (0.14%) in our model indicates persisting atrophy and explains decreased amount of T-lymphocytes found in bone marrow. Although thymic decline is of minimal consequence to healthy individuals, the reduced efficacy of the immune system has direct etiological linkages with an increase in diseases including opportunistic infections, autoimmunity, and incidence of cancer and might contribute to the increased mortality of irradiated and transplanted mice [246].

After EGF administration, we found increased amount of GFP⁺ cells in thymus. EGF receptors are present at the surface of thymic epithelial cells (30). EGF thus seems to attenuate damage to and/or accelerate regeneration of epithelial stroma, which subsequently support migration of lymphocytes into the organ [181], [228].

1.3.5.5 Conclusion

The increasing risk of acute large-scale radiation exposure of population (arising from nuclear energetics, radiation accidents, terroristic attack, military conflict, etc.) implies the development of novel and effective countermeasures in order to attenuate negative health effects of ionizing radiation. Here we report that epidermal growth factor administered at the dose of 2 mg/kg 1, 3 and 5 days after irradiation improves long-term prognosis and mitigates epithelial tissue damage in bone marrow transplanted mice exposed to high-dose radiation. Taken together, our data underline the concept of combining EGF treatment together with BMT as a promising strategy to mitigate effects of whole-body irradiation.

1.4 MODELLING

Abstract

Health effect models, based on physiological mechanisms of radiation injury and treatment, can help integrate modern medical expertise and cutting-edge research into practical tools for developing planning guidance and recommendations for military commanders. The U.S. Defense Threat Reduction Agency contractor, ARA, Inc. has developed tools that use radiation injury models to predict probability of lethality, time to lethality, time-dependent severity of the signs and symptoms of acute radiation syndrome, and time-dependent performance decrement after acute radiation exposures and protracted exposures that may be encountered in a fallout field. We are updating these tools to incorporate models that predict additional clinical parameters and expanded to include models for additional injury types such as burn, trauma, and radiation combined injury. Physiologically-based models have also been developed for evaluating the efficacy of countermeasure treatment of internalized radionuclides. A brief overview of current models and tools we are developing will be provided. Selected cases will be presented to illustrate the utility of the model outputs and how this information may be applied. For example, these tools allow end-users to simulate a variety of insult scenarios and predict time-dependent patient flow, medical personnel requirements and

material resource needs, and may also be used to optimize treatment protocols in resource limited environments. The model outputs can also be used in further analysis, such as developing optimal work cycles or predicting medical transport needs. Physiologically-based mathematical models allow the translation of current biomedical research into practical recommendations for military commanders.

1.4.1 Scenarios and Urban Environments

Modern nuclear and radiological incident scenarios, such as an Improvised Nuclear Device (IND) scenario, involve complicated environments due to features of the urban setting. Urban settings afford shielding to radiation which can change the range of prompt radiation from an IND. The ratio of gamma and neutron radiation will be significantly different from open field scenarios due to the interaction of the prompt radiation with building materials. The radiation transport simulation shown in Figure 1-14 illustrates the shielding that can result in an urban environment. Urban structures can also shield thermal and blast effects; however, secondary effects may arise from the nuclear environment effects interaction with urban structures. For example, building collapse, glass shattering, fire initiation, and secondary explosions may result from such interactions. Collectively, nuclear effects in the urban environment create complex hazards that are likely to result in a spectrum of injuries that include many potentially survivable radiation exposures that are combined with trauma and/or burn injuries.

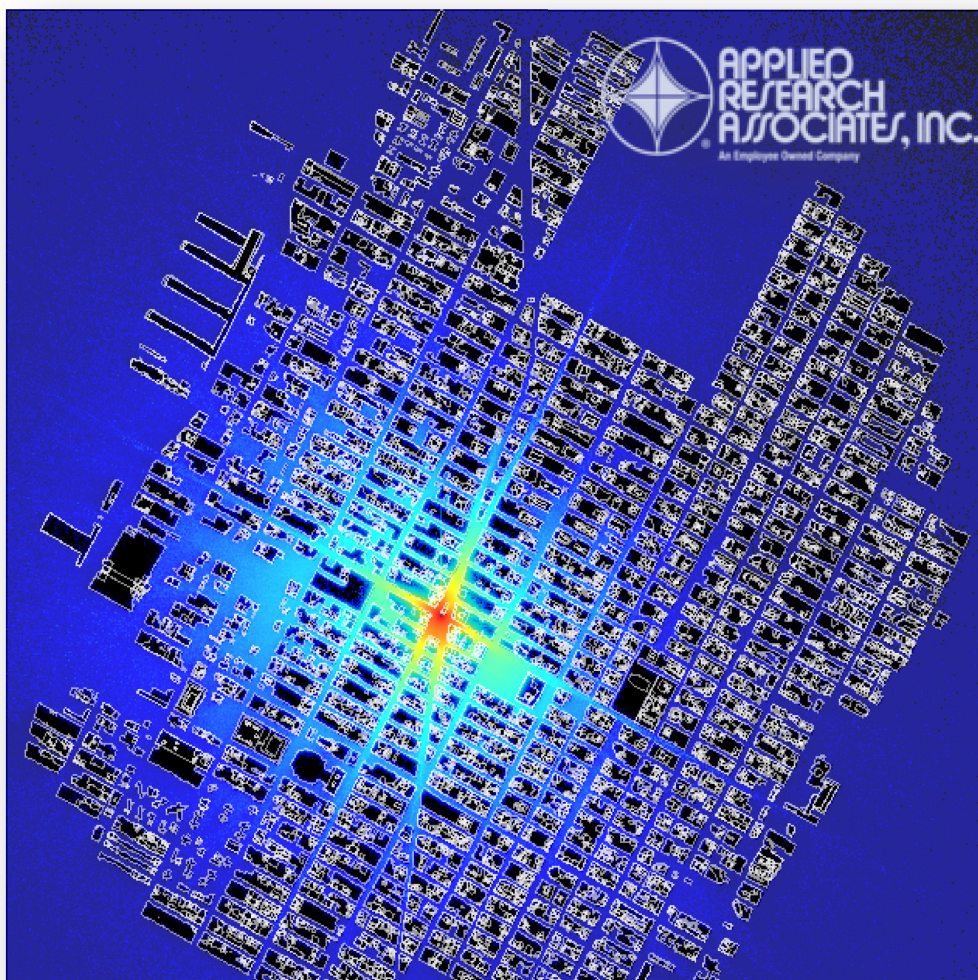


Figure 1-14: An Illustration of Radiation Shielding in the Urban Environment.

1.4.2 Physiological Modelling of Health Effects

Modern biomedical information on the pathophysiological mechanisms of injury can be integrated into biological models that help understand the impact of health effects. The models can be used to estimate the probability of consequences from complex injuries, such as those involving trauma or burn, combined with radiation. Mechanistic modelling of combined injury enables improved understanding and prediction of the synergistic interactions of combined injury. Physiological modelling also helps to predict the time to onset of signs and symptoms or outcomes. This type of information can be used to provide insight on time dependent patient streams and resource requirements.

1.4.3 Physiological Models of Radiation

1.4.3.1 Radiation-Induced Performance Decrement (RIPD)

Radiation-Induced Performance Decrement (RIPD) is a physiologically based model of acute radiation sickness that was originally designed in the 1990's. The model was incorporated into a U.S. Defense Threat Reduction Agency (DTRA) contractor ARA, Inc. software tool that has recently been computationally updated, RIPD 5.2. The tool may be used to predict probability and time to mortality, time-dependent symptom severity from prompt (neutron and gamma) and protracted exposures (gamma), and the resulting performance decrement.

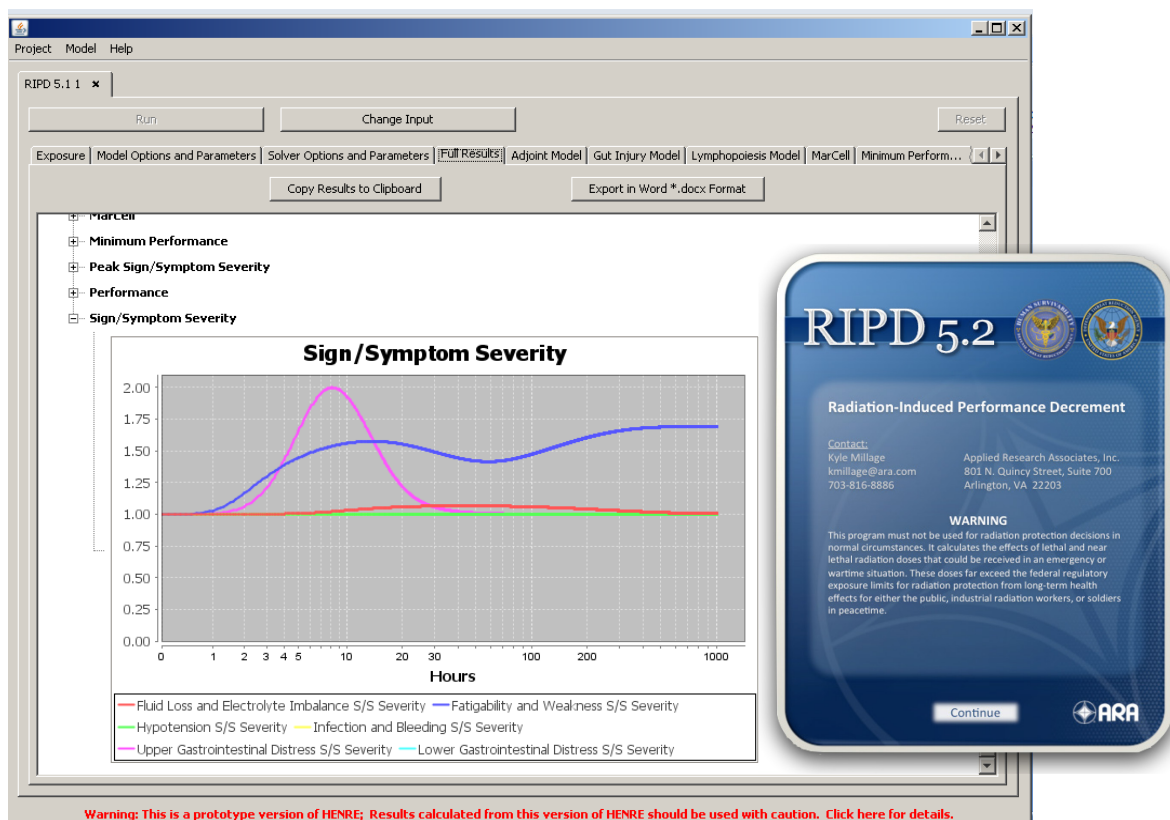


Figure 1-15: Radiation-Induced Performance Decrement Software – RIPD 5.2.

1.4.3.2 Physiological Models in RIPD

The physiological basis of RIPD involves four physiological models of acute radiation illness mechanisms. Lethality is estimated from a myelopoiesis model based on an idealized bone marrow cell kinetics model.

A lymphopoiesis model is used to predict fatigability and weakness. Upper Gastrointestinal (GI) effects are estimated from model based on humoral response to circulating neuroactive agents. Lower GI effects are estimated from a physiological cell kinetic model of the gut mucosal. The upper GI and lower GI models are used to estimate prodromal fluid loss. Subject-matter expert input was also used to develop empirical models for the time-dependent severity of manifest illness signs and symptoms which include:

- Infection and bleeding;
- Fluid loss;
- Upper GI effects; and
- Hypotension.

1.4.3.2.1 Concept of Equivalent Prompt Dose (EPD)

The idealized bone marrow cell kinetics models used in RIPD, MarCell, originally developed by Jones *et al.* [118] is the basis for estimating lethality from complex exposure scenarios. This mechanistic model uses a set of differential equations that describe the cell kinetics of radiation-induced cell killing and injury, sub-lethal repair, and repopulation as shown in Figure 1-16. Many of the calculations in RIPD use the minimal cell count in MarCell to determine lethality and time to observation of some signs and symptoms.

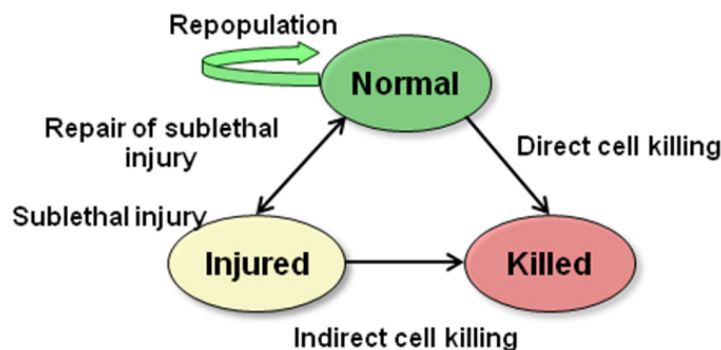


Figure 1-16: Structure of the Cell Kinetics Model, MarCell.

Cell kinetic rates in MarCell are dose rate dependent and the model can be used to determine the effect of doses delivered over a period of time. The minimal cell count from a dose delivered of over a period of time is equated to the effect of an Equivalent Prompt Dose (EPD). In this way, the effects of protracted exposures can be estimated.

1.4.3.3 Example Application of RIPD

RIPD may be used to examine a wide range of complex exposure scenarios. As an illustration, an IND scenario involving a location with free-in-air doses of 250 cGy gamma and 500 cGy neutron radiation is considered. At the time of the incident, the individual (or population) is inside a building that has a protection factor of 5. Therefore, the initial radiation is reduced by the shielding of the building. Dose to the marrow will also be somewhat reduced by the body, and the Relative Biological Effectiveness (RBE) of the neutron radiation is accounted for in the calculation of effects. The fallout field, immediately after the event at this location, is 500 cGy per hour. Note that the dose rate decline for fallout is dramatic in the initial hours and RIPD has algorithms that accounts for this decline in dose rate over time. The person (or population) remains in the building and shelters in place for 24 hours and then evacuates to a no fall out zone; however, the evacuation results in two hours of exposure without protection. The equivalent prompt dose to the marrow from the complex exposure scenario is estimated to be 213 cGy which is related to a 17% probability of lethality in 29 days. The resulting time-course of sign and symptom severity is provided in Figure 1-17.

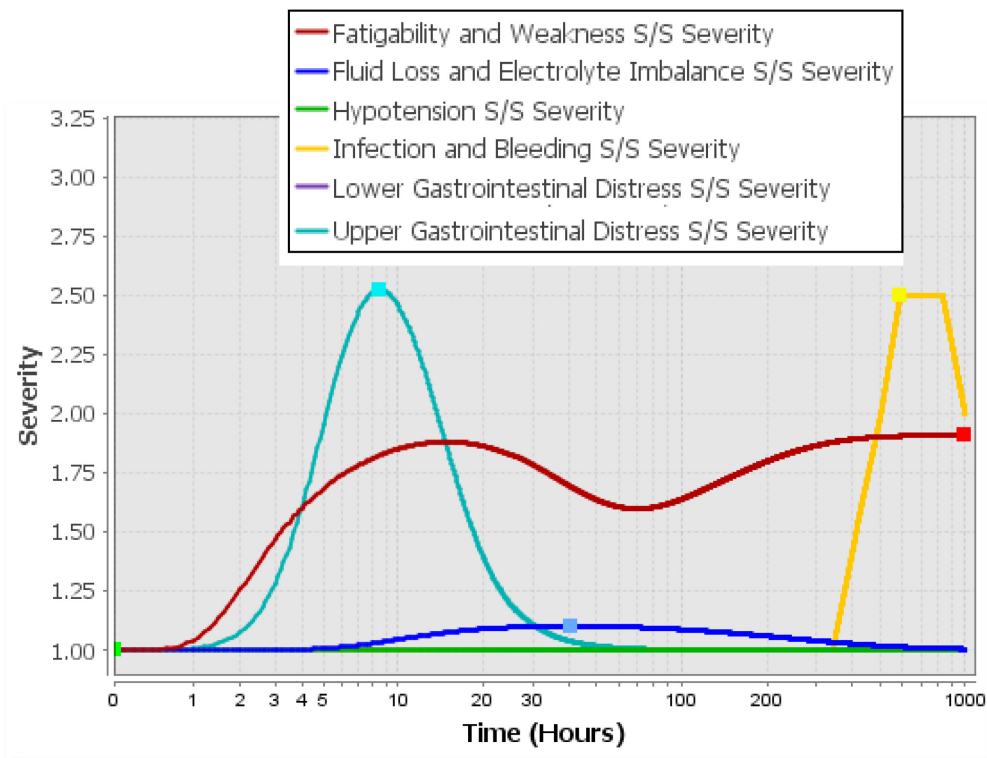


Figure 1-17: Time Course Severity of Signs and Symptoms After a Complex Radiation Exposure Scenario.

1.4.4 Health Effects from Nuclear and Radiological Environments (HENRE)

The next generation code, DTRA’s Health Effects from Nuclear and Radiological Environments or HENRE, has been developed so that additional features, outputs, and modules can be included along with the current RIPD capabilities. This code contains additional physiological models for radiation effects that provide outputs that include predictions of clinical parameters, such as time-dependent hematopoietic cell counts, following exposure to radiation. Additional insult modules for thermal, blast, and combined injuries are being incorporated with the intention of merging these models with radiation parameters to predict the effects of combined injury. The structure of the computational engine for HENRE is shown in Figure 1-18.

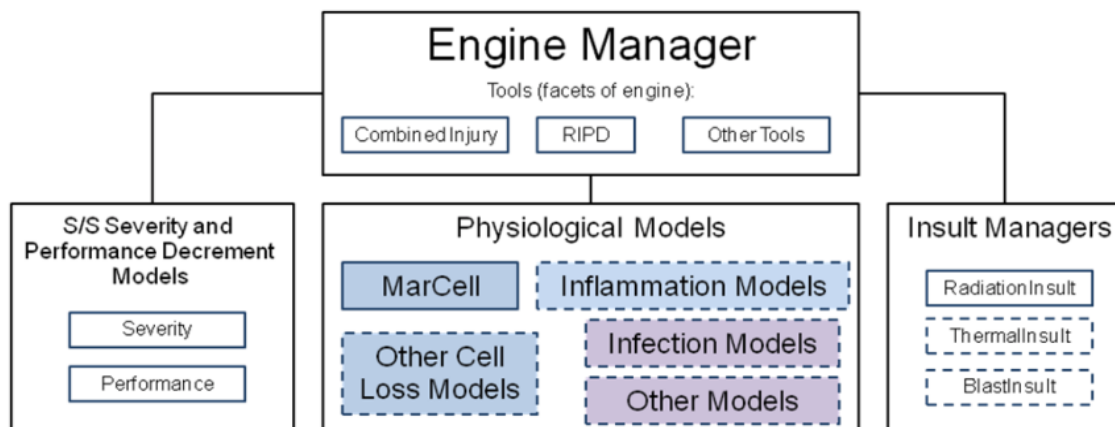


Figure 1-18: Structure of the Computational Engine for HENRE.

Currently, HENRE retains RIPD 5.2 but also includes a Prompt Injury module that incorporates a thermal injury model with radiation parameters for estimating the risk of 48-hour circulatory shock as well as more detailed hematopoietic models for radiation and burn. The input for thermal injury is the percent Total Body Surface Area (%TBSA) affected by burn. The HENRE 1.0 Graphical User Interface (GUI) with the Prompt Injury module illustrating the prompt for the burn input is shown in Figure 1-19.



Figure 1-19: HENRE 1.0 GUI with Prompt Injury Module.

1.4.4.1 Combined Injury Model Development

Combined injury is known to increase the probability of mortality and reduce the time to onset of signs and symptoms. Physiological modelling of underlying pathophysiological processes of the injuries is critical in understanding and predicting these effects. An effort has been made to map out the complex set of physiological processes involved in thermal injury combined with radiation as illustrated in Figure 1-20.

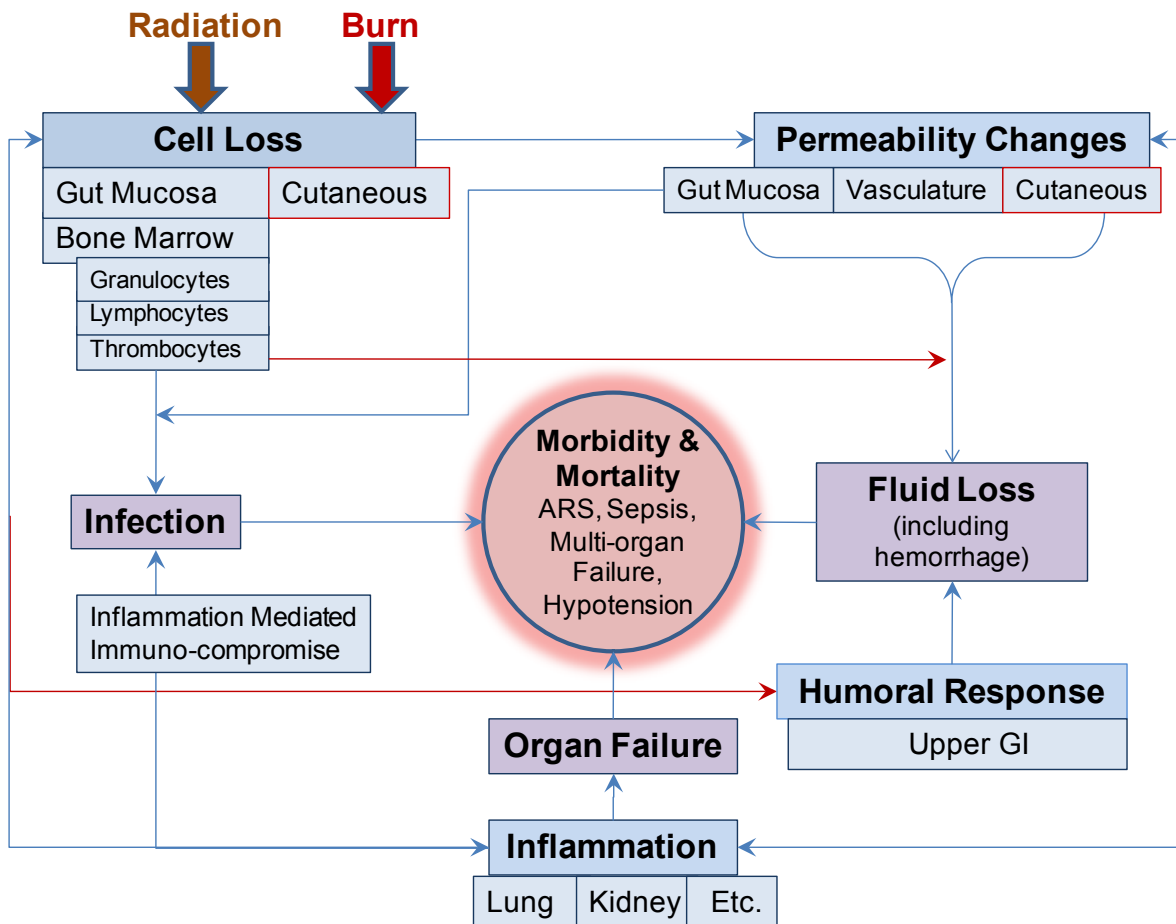


Figure 1-20: Pathophysiological Processes in Combined Radiation and Burn Injury.

The critical mechanisms for modelling the effects of combined injury are briefly described. Radiation impacts the hematopoietic system by direct cell killing, while thermal injury results in cutaneous cell loss. Thermal injury impacts hematopoietic cell kinetics through mediator-related mechanisms. Permeability changes in the GI tract, microvasculature, and cutaneous system arise from direct cell killing from radiation, but both radiation and burn can influence permeability changes via mediators released in the systemic circulation. Infection can arise from both injuries, in part, due to loss of neutrophils and, in part, due to inflammatory mediated immune-compromise. These complex and inter-related set of pathophysiological processes must be understood and mathematically described in order to accurately predict the synergistic effects of radiation combined with thermal injury.

1.4.4.2 Circulatory Shock

The first potentially fatal physiological mechanism encountered after severe injury is shock. Thermal injuries involving more than about 20% of the Total Body Surface Area (TBSA) are associated with risk of circulatory shock and increased risk of mortality. In part, due to loss of fluid from the burn wound site, and in part due, to mediator-related mechanisms resulting in significant swelling at the injury site, fluid fluctuation can be dramatic in the first 48 hours after burn injury. To understand, describe, and model the circulatory shock mechanism, we have studied and implemented a microvascular exchange model originally developed by Ampratwum *et al.* [13] and Bert *et al.* [28]. This model was developed to aid in establishing optimal fluid resuscitation regimes for burn. We relate critical endpoints such as loss of plasma volume to the risk of circulatory shock and increased probability of mortality in the first 48 hours after injury.

Figure 1-21 illustrates the movement of fluid and protein between injured and uninjured compartments. The red lines/arrows indicate where radiation impacts parameters of the model. Additional mechanisms for fluid loss unrelated to permeability changes (vomiting and diarrhea) must be considered with significant radiation exposure.

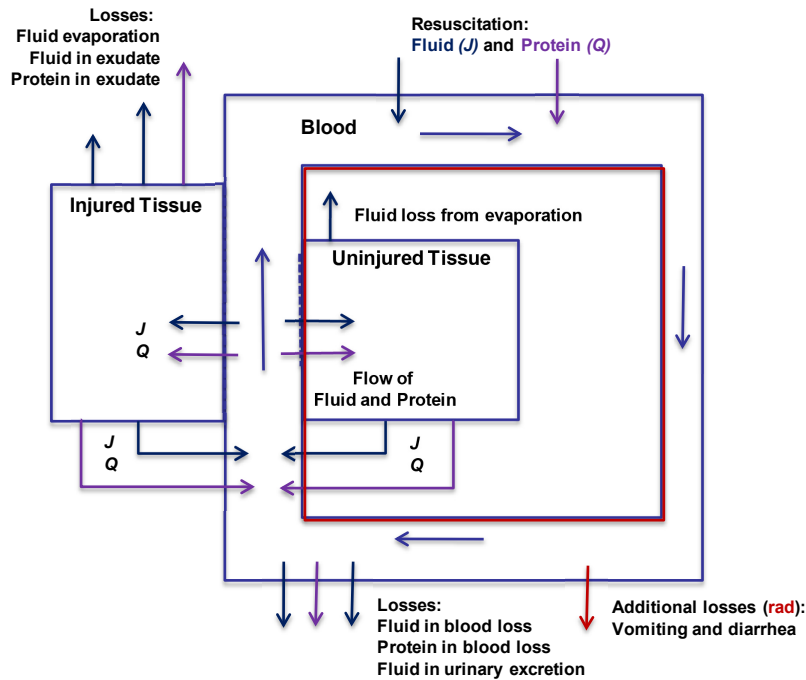


Figure 1-21: Model of Microvascular Exchange for Understanding the Circulatory Shock Mechanism (Adapted from Ref. [28]).

The microvascular exchange model may be used to examine the early changes (within the first 48 hours) in plasma volume, after different %TBSA burn insults, as illustrated in Figure 1-22. The simulations show that dramatic decreases can occur quite quickly with minimum levels resulting after about 12 hours. These early effects usually resolve within 48 hours after injury which is also illustrated in the simulations.

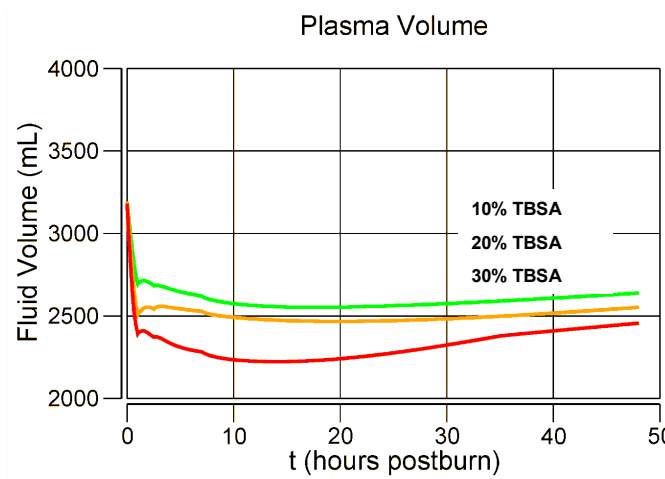


Figure 1-22: Plasma Volume Changes Over 48 Hours After 10, 20, and 30 %TBSA.

The minimum plasma fluid volume as a function of %TBSA burn can be examined as an output of the microvascular exchange model. This data is compared to the estimated probability of mortality from circulatory shock (mortality in the first 48 hours) in untreated burn.

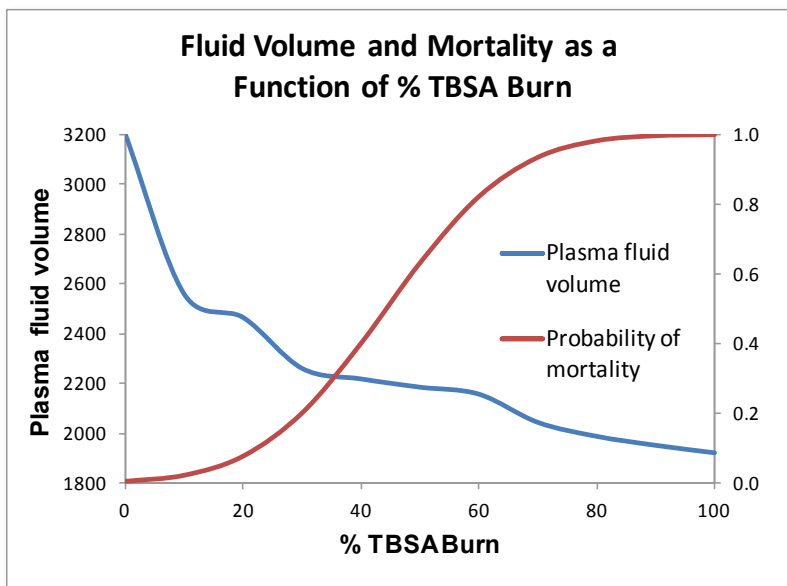


Figure 1-23: Predicted Value of Minimum Plasma Volume as a Function of %TBSA Burn and Associated Probability of Mortality.

Radiation as mentioned previously also impacts permeability. Using animal data, parameters have been developed to describe the impact of radiation and the permeability changes observed in the first 48 hours after exposure. The dose response relationship of radiation on permeability changes occurring within the first 48 hours after exposure was developed from the collective literature [63], [79], [91], [125], [161], [171], [217], [240] and was described in terms of relative change. The collective data evaluated and the resulting dose response relationship is illustrated in Figure 1-24.

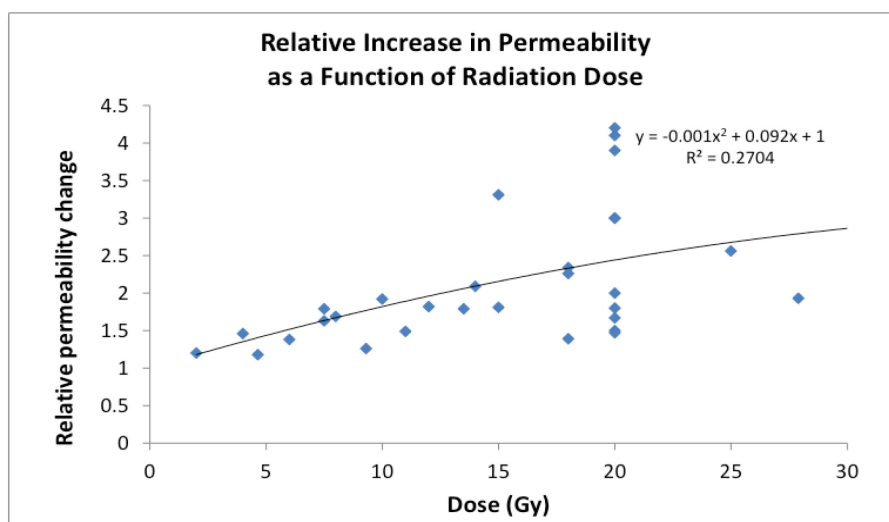


Figure 1-24: Early Permeability Changes Observed After Radiation. (Composite of 8 Studies – Refs. [63], [79], [91], [125], [161], [171], [217], [240]).

The dose response relationship illustrated in Figure 1-24 was adapted into radiation perturbation parameters that have been integrated into the microvascular exchange model to evaluate the risk of circulatory shock in combined injury. The resulting fluid shifts and associated decreases in plasma volumes can be related to risk of circulatory shock and categorized according to the criteria illustrated in Table 1-29.

Table 1-29: Relationship between Circulating Blood Volume Loss and Risk of Circulatory Shock from Hypovolemia [235].

% Blood volume loss	Plasma volume equivalent (mL)	Severity of shock	Response
normal	3200		
<15	2752	1	Compensated constriction of vascular bed
15-30	2720-2240	2	Decreased cardiac output, increased respiratory rate
31-40	2208-1920	3	Systolic blood pressure drop, marked tachycardia, altered mental status
>40	1888	4	Extreme tachycardia, significantly decreased blood pressure, and loss of consciousness

The revised model with the radiation parameters is used to predict 48-hour mortality based on plasma volume minimums that reach a category 4 of circulatory shock severity. Simulations can be run with different radiation doses and %TBSA thermal injuries. Table 1-30 presents the simulation results of several different combined injury combinations, along with the estimated percent of mortality anticipated from those exposures.

Table 1-30: 48-hr Mortality CI Predictions (in %) Based on Simulated Plasma Volume Minimums.

Radiation Dose Gy (FIA*)	%TBSA			
	0	20	40	60
0	0	7.2	38.5	80.9
1	0.5	9	57.7	90.1
2	0.5	12.3	79.9	99.1
3	0.5	12.7	96.9	99.9
4	0.6	60.3	99.9	99.9
5	1.7	95.3	99.9	99.9
6	9.4	99.9	99.9	99.9
7	12.6	99.9	99.9	99.9
8	89.2	99.9	99.9	99.9

* FIA is the free-in-air dose.

The simulated mortality predictions based on microvascular exchange model and plasma volumes are comparable with animal data model [12], [22]. Significant increases in mortality were observed in animals with combined radiation and burn injury in the first 48 hours due to circulatory shock.

1.4.4.3 Hematopoietic Cell Kinetic Models

Since the hematopoietic system is significantly impacted by radiation, in part by direct cell killing, and in part, due to mediator-related mechanisms, a number of critical time-dependent changes in blood cell kinetics

occur after significant radiation exposures. A series of hematopoietic cell models have been developed as detailed by Smirnova [212] to describe the effects of radiation on the cell kinetics of thrombocytes, erythrocytes, lymphocytes, and granulocytes. These models can help to understand the risks of hemorrhage, anemia, and infection after radiation exposure. The thrombopoiesis, granulopoiesis, and lymphopoiesis models have been adapted by integrating more biological parameters based on experimentally determined values [260]. The original mediator feedback loop was changed to reflect a stimulatory mechanism rather than an inhibitory mechanism. In some cases, additional compartments and delays in transition times were required. The models were optimized with blood cell kinetic data from persons exposed to a range of radiation doses, and then validated with human data not used in the optimizations. The structure of each of the hematopoietic models varies, but a general conceptual model for this work is shown in Figure 1-25. In general, the model considers heavily, moderately, and weakly radiation damaged cells which each have different rates in which they progress to cell death.

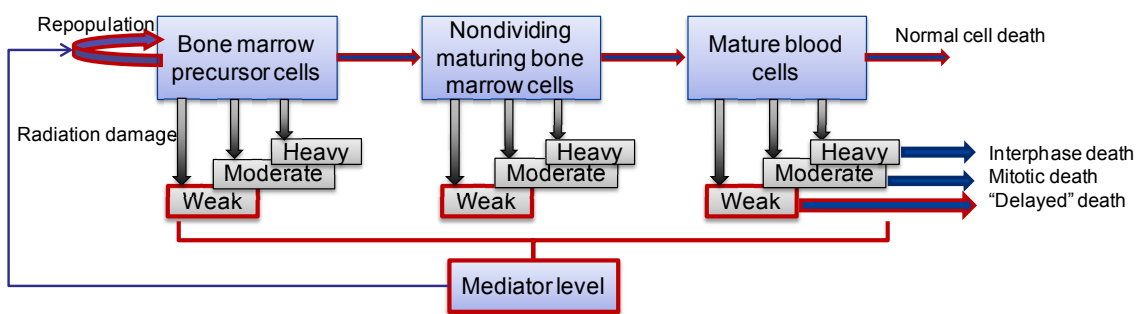


Figure 1-25: Hematopoietic Cell Kinetic Model Structure (Adapted from Ref. [212]).

The updated hematopoietic models allow simulation of a wide range of radiation doses to predict the circulating blood cell levels. The dynamics of the different blood cell lineages provide valuable clinical insight on the progression and resolution of radiation effects. For example, the time to and duration of the thrombocyte nadir can indicate risk of hemorrhage, when and how many platelet transfusions might be required, and when recovery is anticipated. These features are illustrated in the simulation shown in Figure 1-26.

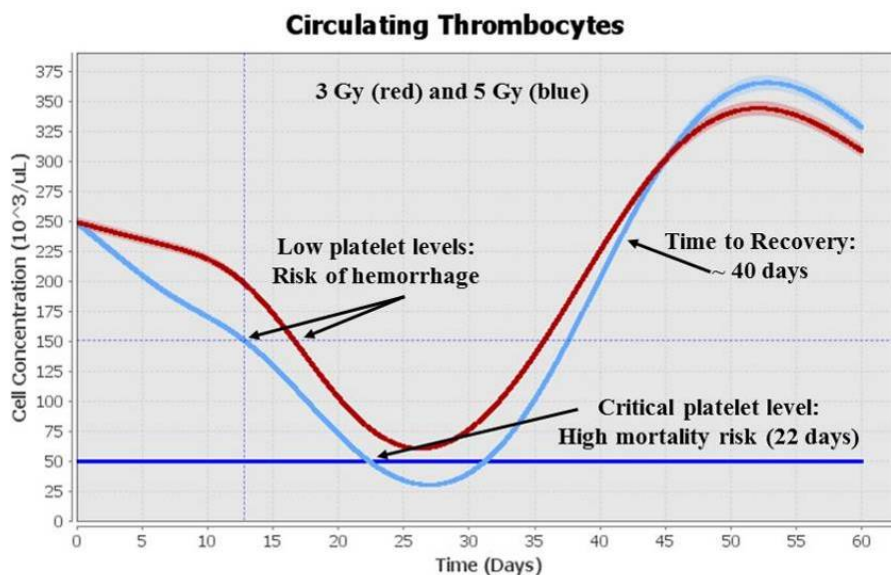


Figure 1-26: Simulated Thrombocyte Kinetics After 3 and 5 Gy Prompt Radiation.

The inclusion of the effect of the generic mediator level in the models, which regulate the repopulation rates, is an important feature that enables merging the model with other injury types. Thermal injury primarily impacts hematopoietic effects through mediator-related mechanisms. Parameters have been developed that estimate the influence of burn on the different hematopoietic processes and include the increased mediator levels resulting after thermal injury [261], [262]. The thermal injury models of hematopoiesis have been integrated into the radiation models to provide an avenue for evaluating and predicting the potential impact of radiation exposure combined with burn on hematopoietic cell kinetics.

Figure 1-27 provides a schematic description of the general hematopoietic model illustrating which parameters radiation and burn impact and how the two insults can be evaluated together to provide estimates of combined injury effects. The model tracks the concentration of cell populations in the different compartments by accounting for the number starting cell population size, and accounting for the proliferation rate and transition rates, etc., to ultimately estimate the cell levels in the circulation.

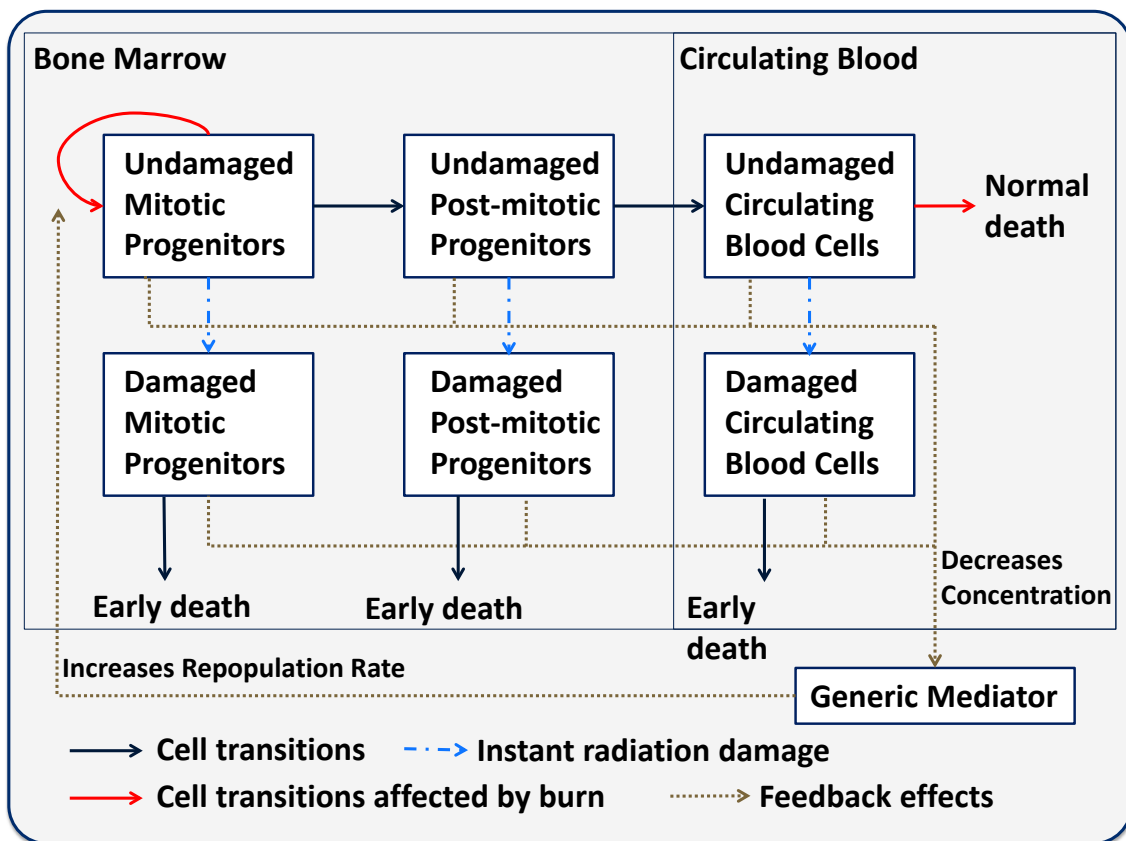


Figure 1-27: Radiation and Burn Combined Injury Hematopoietic Model.

Figure 1-28 provides an example simulation of thrombocyte kinetics after a combined injury scenario compared to single injury predictions, along with case study data (burn: Ref. [143]; radiation: Ref. [15]). In this example, the combined injury impact is predicted to be worse than burn alone, but improved as compared to radiation alone. The reason for the improvement from radiation alone is attributed to the stimulatory effect on proliferation after thermal injury. However, at higher radiation and burn levels, the impacts become more deleterious due to more dramatic cell killing by radiation and mediator response from burn. Therefore, the injury profiles change depending on the magnitude of each insult. The complex interaction of competing mechanisms after injury makes predictions non-intuitive and highlights the value of the models in understanding the interaction of these complex processes.

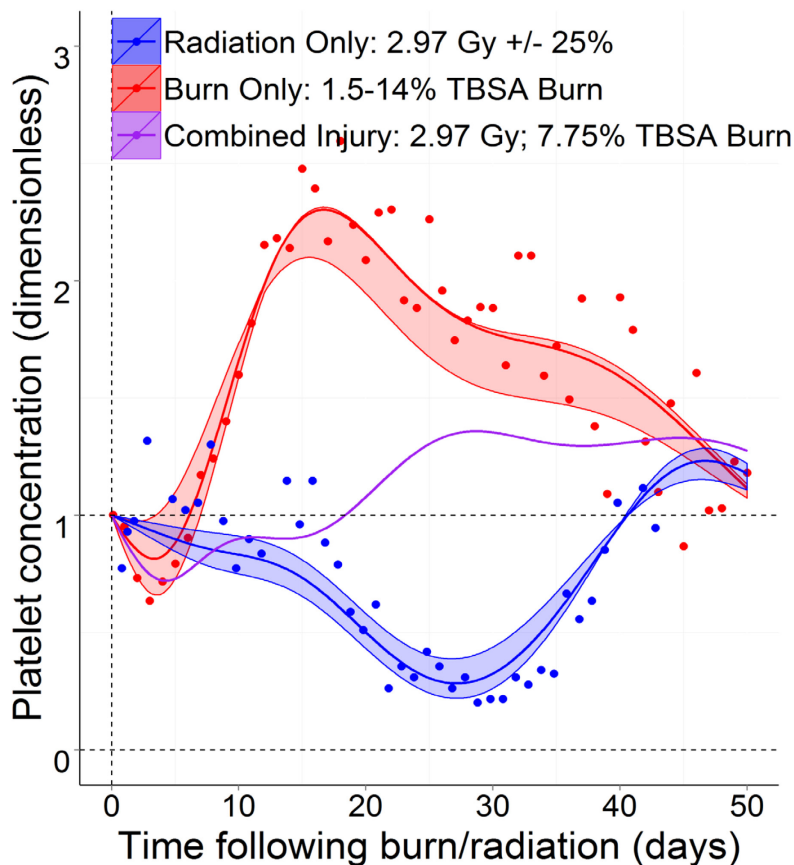


Figure 1-28: A Combined Radiation and Burn Injury Simulation Compared to Single Injury Predictions and Data.

Although a significant number of combined injuries were observed in A-bomb survivors, little to no clinical data is available on human radiation and burn combined injury. However, animal combined injury data (for example, Refs. [36], [54], [121] and [170]) indicates greatly increased mortality from combined injuries. Therefore, we developed murine model parameters for the radiation and burn hematopoietic models in order to compare and validate the combined injury predictions.

An example comparison used for validation of the combined injury simulations is shown in Figure 1-29. In this example, platelet data from rats exposed to 25%TBSA burn and/or ~1 Gy [170] are compared to simulated thrombocyte kinetics. The general trends observed after combined injury are captured by the models. In this example, the general decrease of platelets that follow radiation and combined injury exposure is captured. Likewise, the rebound of platelets in the combined injured animals to levels that are more comparable to that of the burned animals are illustrated in the simulations. Please note that the absolute response and precise time-dependent kinetics may in part vary in this example because the experimental data are derived from rats; however, the model parameters were developed in mice due to the availability of data.

Overall, analysis of combined injury data, with review of combined injury predictions in the three different blood cell lines, show that effects of combined injury are not simply exacerbated from what is observed with single injuries. In some instances, combined injury leads to a more severe nadir and/or a delayed recovery. In some cases, evidence suggests that combined injury could accelerate recovery relative to radiation injury alone. The models can be used to better understand complex interactions resulting in irregular injury profiles after combined injury. Future work will correlate model outputs with risk of infection, hemorrhage, and/or mortality.

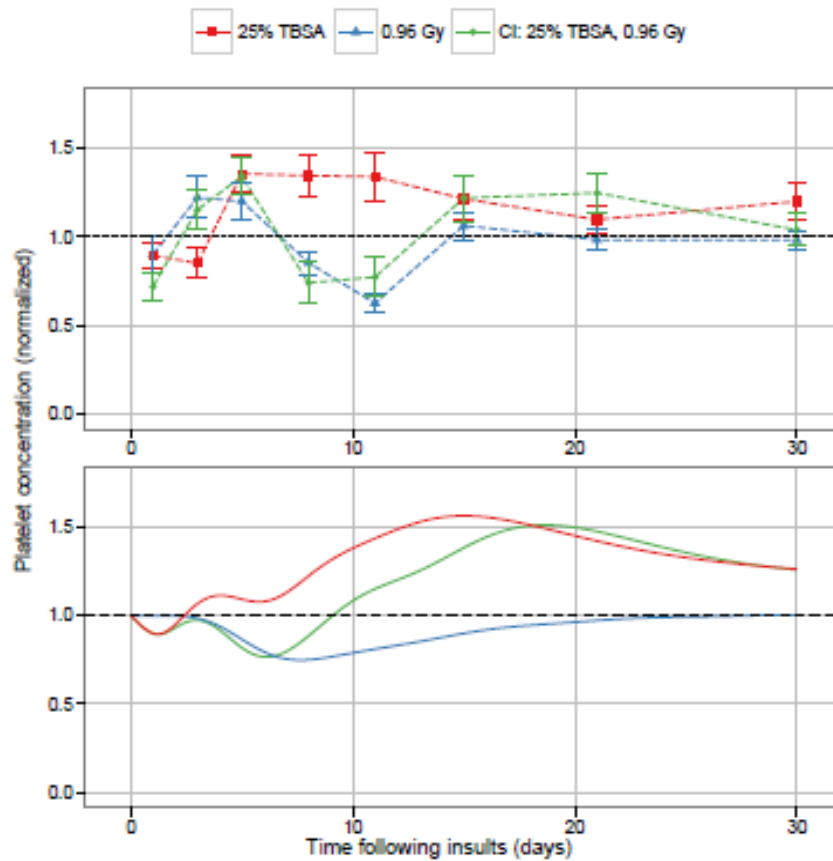


Figure 1-29: Platelet Concentration Following Combined Injury in Rats [54] Compared with Murine Model Simulations.

1.4.5 Treatment Models: Internalized Radionuclides

Physiological models for internalized radionuclides have been necessary for estimating the body burden of radionuclides over time, so that radiation dose absorbed by tissues can be estimated. The International Commission on Radiological Protection (ICRP) has developed biokinetic and dosimetric models for a number of radionuclides. These models enable estimation of radionuclide tissue distribution, retention, and excretion over time. Together, with radiation dosimetry models, the dose to critical organs, 50-year committed doses, and risk to health effects can be estimated.

Decorporation models have been adapted to the biokinetic models to mathematically estimate the sequestration and subsequent removal of radionuclides from relevant compartments during treatment. Coupled with the biokinetic and dosimetric models, reduction of nuclide burden, radiation dose, and risk may be examined with different treatment regimes.

1.4.5.1 Prussian Blue Decorporation of Cs-137

A decorporation model for Cesium-137 (Cs) with Prussian Blue (PB) was developed [222] by implementing the Cs biokinetic model [134] as shown in Figure 1-30 and then adding the impact of PB administration and subsequent sequestration of Cs. Since PB is insoluble, it is not absorbed into the circulation. It sequesters Cs in the small intestines as it moves through the GI tract. An effective transit time of 8 hours, in which all Cs is removed from the small intestines, accurately reflects the average observed excretion of Cs under PB treatment in humans.

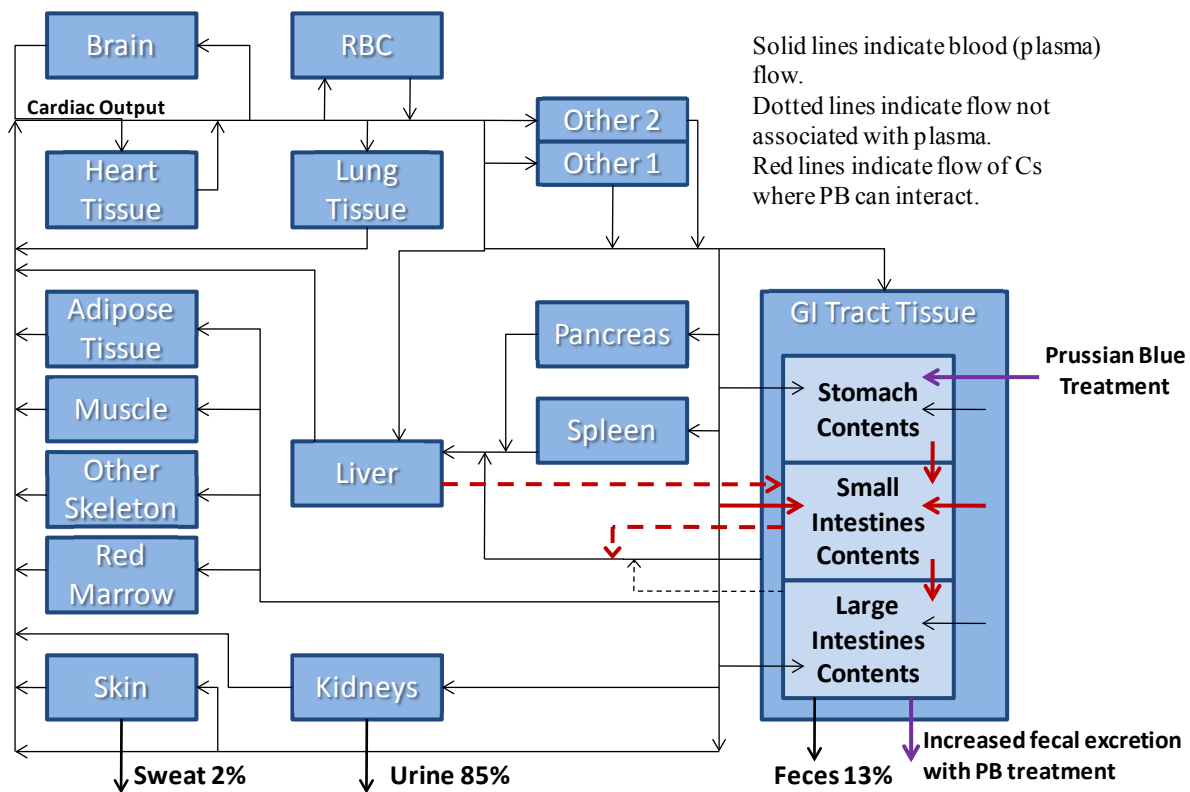


Figure 1-30: Decorporation Model for Cesium with Prussian Blue. (Adapted from Ref. [134]).

1.4.5.2 DTPA Decorporation of Am-241 and Pu-238/239

Decorporation models for Americium-241 (Am-241) and Plutonium-238/239 (Pu-238/239) with Diethylene Triamine Pentaacetic Acid (DTPA) were also developed [222], [223], [224]. First, the biokinetic models for americium [132] and plutonium [133] were implemented. Then, the removal of Am or Pu by DTPA was modelled by removing the amount of Am or Pu found in the blood compartment over the residence time of DTPA in the circulation after injection, which was effectively 24 hours. The predicted excretion rates of the radionuclides were compared to bioassay data of exposed persons. The basic structure of the biokinetic models, with the inclusion of DTPA treatment, is depicted in Figure 1-31.

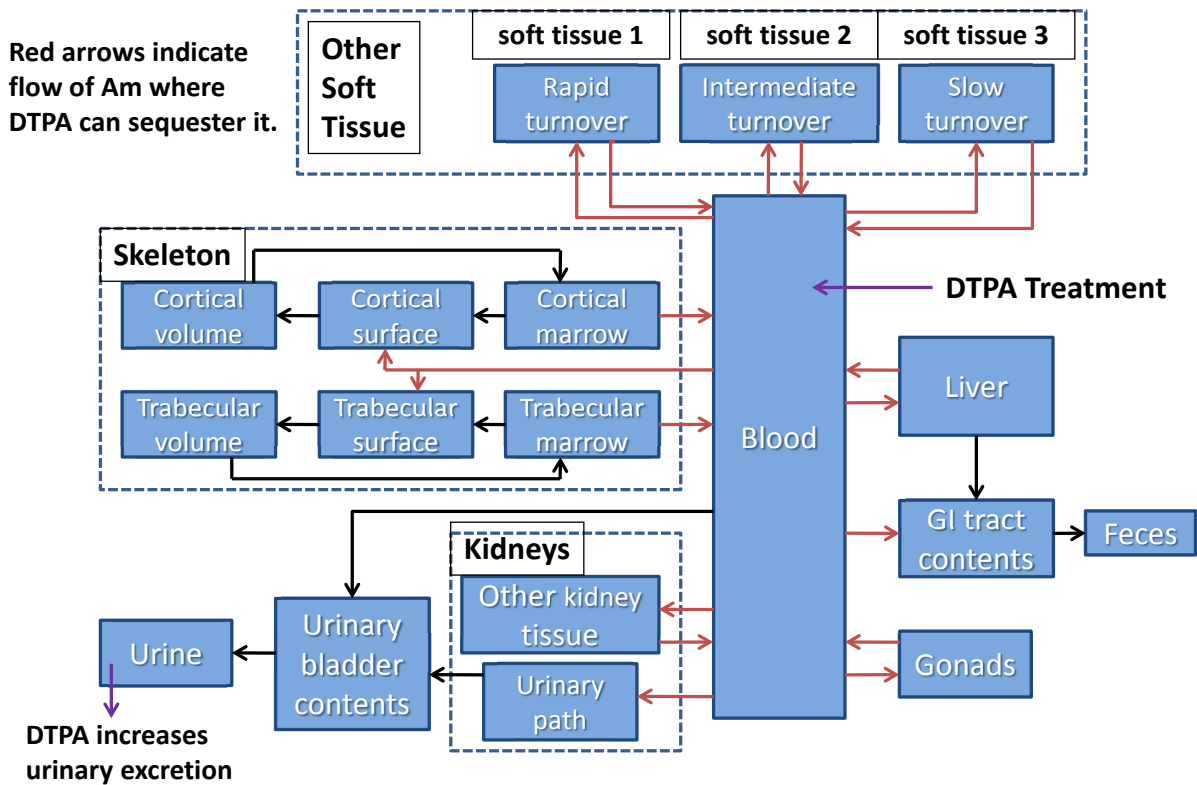


Figure 1-31: DTPA Decorporation Model for Am and Pu (Adapted from Refs. [132] and [133]).

In the case of Am, more of the radionuclide was removed than could be accounted for than that found in the circulation. Therefore, some Am in the interstitial space was assumed and the amount was included as a parameter fit to the bioassay data.

1.4.5.3 Application of Decorporation Models

Decorporation models may be used to evaluate different treatment regimens on radionuclide burden and reduction of radiation dose. Variable treatment initiation times and duration of treatments can be examined to inform treatment optimization when resources are limited. Table 1-31 illustrates the difference in efficacy in terms of dose reduction from different treatment initiation times and treatment durations times.

Table 1-31: Efficacy of Different Treatment Regimens of Cs-137 with Prussian Blue.

Duration of PB (days)	Treatment Initiation Times (days post exposure)			
	0	90	180	270
0	0	-	-	-
90	0.55	0.25	0.13	0.07
180	0.63	0.30	0.15	0.08
270	0.65	0.31	0.16	0.08

1.4.6 Summary

1.4.6.1 Additional Modelling Needs

Many factors can impact the casualties and outcomes anticipated after an IND type of event. Additional factors that are either under development or to be addressed in the near future are briefly described. A model for partial body exposures, using a similar mathematical approach as used for “equivalent prompt dose”, is being developed. The inflammation model for combined injury being developed for combined injury may provide a resource for estimating latent multi-organ failure. Medical treatment will be incorporated into the acute radiation syndrome models, first with standard care, and then for cytokine and advanced therapeutic treatments. Models for understanding radiation cutaneous injury from, for example, fallout particles, are needed. Finally, a large variability of response to injury is observed in the general population. Demographics such as age, gender, and co-morbidities can greatly influence individual response to injury and efforts are underway to model these factors.

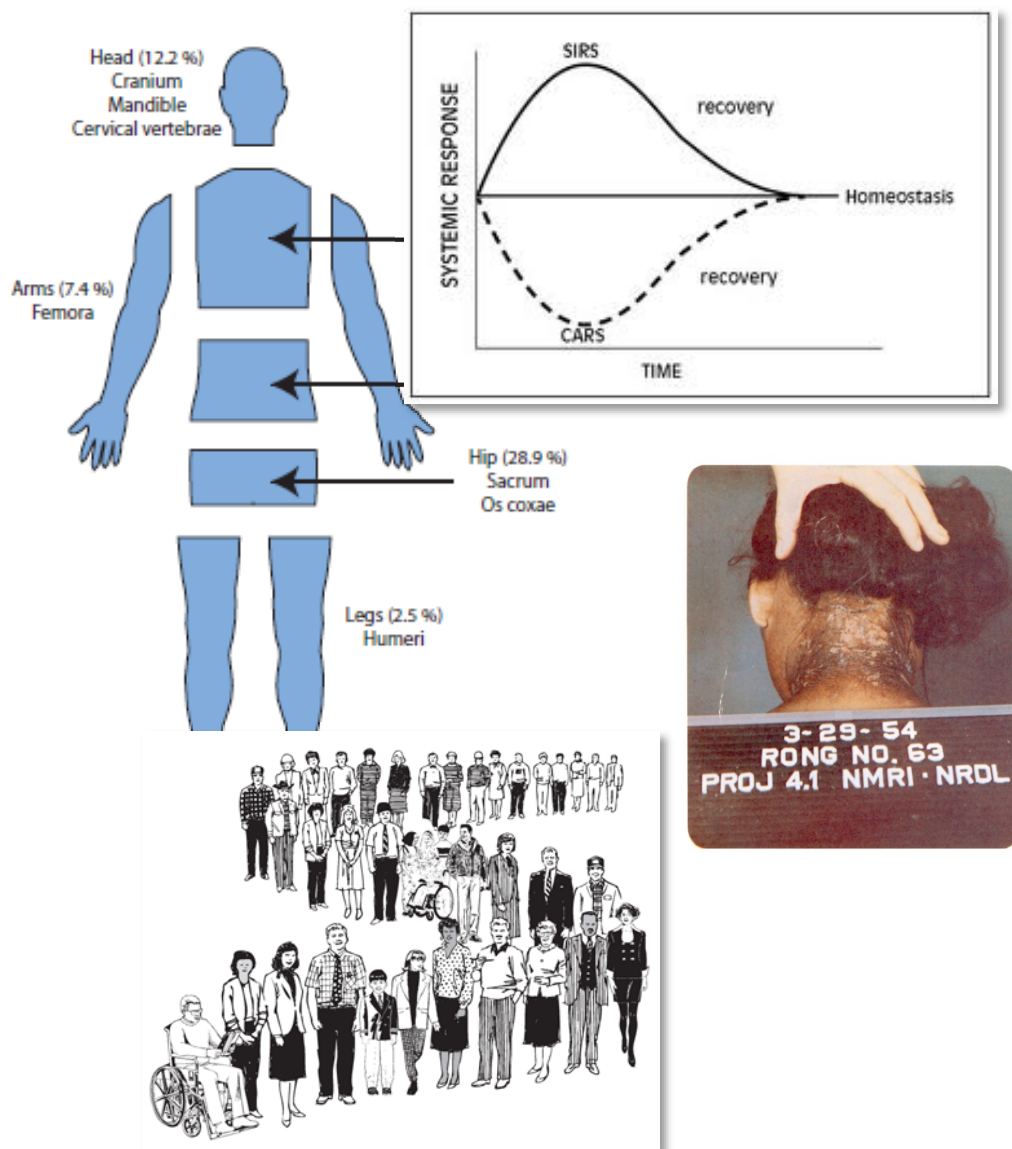


Figure 1-32: Development of Additional Models.

1.4.6.2 Spectrum of Modelling and Analysis

A spectrum of modelling and analysis as illustrated in Figure 1-33 is available to inform nuclear and radiological event preparedness planning. For example, for the IND scenario, modern nuclear environments modelling provide details concerning the thermal, blast, and radiation impacts in the urban environment. Injury criteria modelling translates the environment insults into the spectrum of injuries, such as %TBSA burn or number of blunt or penetrating traumatic injuries anticipated from those environments. Physiological modelling then translates the injuries into an anticipated timeline of casualties and outcomes, including time-course of signs, symptoms, and clinical parameters.

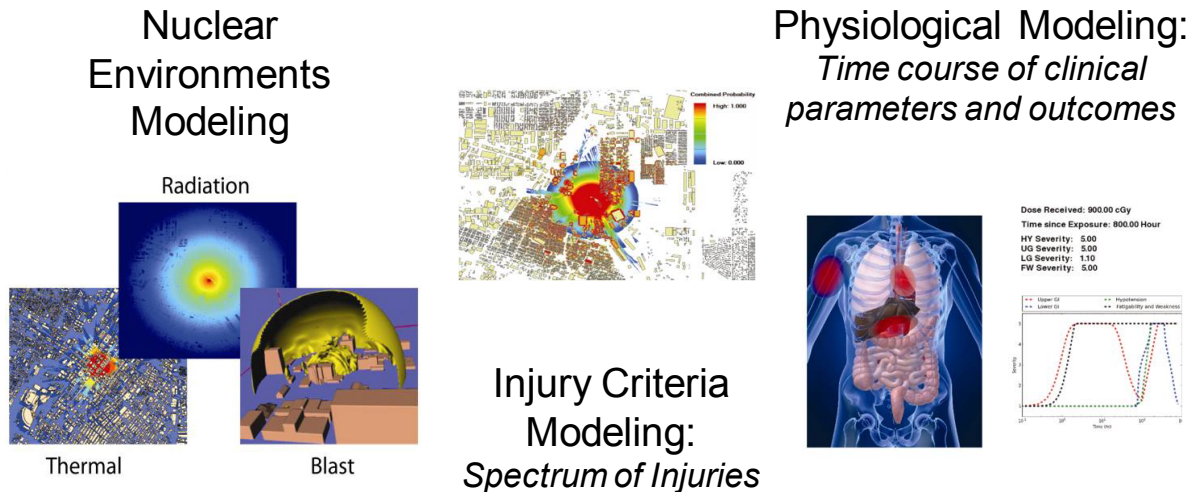


Figure 1-33: Spectrum of Modelling to Inform Operational Planning.

1.4.6.3 Informing Operational Planning

In summary, physiological modelling tools allow informed operation planning by enabling users to evaluate a wide range of complex exposure scenarios. Protection factor inputs for vehicles/buildings for prompt and fallout field exposures can be used. Different courses of action, such as shelter in place and evacuation strategies, can be compared in terms of dose and health effects resulting from those actions. The algorithms can be used to inform work cycle planning for search and rescue missions. The models enable improved consequence assessment estimates by accounting for the synergistic effects of combined injury. Physiological models also enable evaluation of the time-course of clinical parameters which can then be used to inform time-dependent patient flow and resource needs.

1.5 REFERENCES

- [1] Abend, M., Rothkamm, K., Romm, H., Badie, C., Balagurunathan, Y., Barnard, S., Bernard, N., Boulay-Greene, H., Brengues, M., De Amicis, A., De Sanctis, S., Greither, R., Hérodin, F., Jones, A., Knie, T., Kabacik, S., Kulka, U., Lista, F., Martigne, P. Missel, A., Moquet, J., Oestreicher, U., Peinnequin, A., Poyot, T., Roessler, U., Scherthan, H., Terbrueggen, B., Thierens, H., Valente, M., Vral, A., Zenhausem, F., Meineke, V., Little, M.P. and Beinke, C. NATO exercise 2011: Intra- and inter-assay comparison of established and emerging biodosimetry assays – preliminary results. NATO Science and Technology Organization Report STO-MP-HFM-223, 20, 1-8.
- [2] Adamiec, M., Adamus, J., Ciebiada, I., Denys, A. and Gebicki, J. Search for drugs of the combined anti-inflammatory and anti-bacterial properties: 1-methyl-N'-(hydroxymethyl)nicotinamide. Pharmacol Rep 2006;58:246-9.

- [3] Adaramoye, O.A., Okiti, O.O. and Olatunde Farombi, E. (2011). Dried fruit extract from *Xylopiya aethiopica* (Annonaceae) protects Wistar albino rats from adverse effects of whole body radiation. *Experimental and Toxicologic Pathology* 63, 635-643.
- [4] Ainsbury, E.A., Al-hafidh, J., Bajinskis, A., Barnard, S., Barquinero, J.F., Beinke, C., de Gelder, V., Gregoire, E., Jaworska, A., Lindholm, C., Lloyd, D., Moquet, J., Nylund, R., Oestreicher, U., Roch-Lefevre, S., Rothkamm, K., Romm, H., Scherthan, H., Sommer, S., Thierens, H., Vandevoorde, C., Vral, A. and Wojcik, A. (2014). Inter- and intra-laboratory comparison of a multibiodosimetric approach to triage in a simulated, large scale radiation emergency. *Int J Radiat Biol*, 90, 193-202.
- [5] Ainsbury, E.A., Barnard, S., Barrios, L., Fattibene, P., de Gelder, V., Gregoire, E., Lindholm, C., Lloyd, D., Nergaard, I., Rothkamm, K., Romm, H., Scherthan, H., Thierens, H., Vandevoorde, C., Woda, C. and Wojcik, A. (2014a). Multibiodose radiation emergency triage categorisation software. *Health Phys*, 107, 83-89.
- [6] Ainsbury, E.A., Bouffler, S., Cocker, M., Gilvin, P., Holt, E., Peters, S., Slack, K. and Williamson, A. (2014b). Public Health England survey of eye lens doses in the UK medical sector. *J Radiol Prot*, 34, 15-29.
- [7] Ainsbury, E.A. and Lloyd, D.C. Dose estimation software for radiation biodosimetry. *Health Phys* 2010;98: 290-295.
- [8] Ainsbury, E.A., Moquet, J., Rothkamm, K., Darroudi, F., Vozilova, A., Degteva, M., Azizova, T.V., Lloyd, D.C. and Harrison, J. (2014c). What radiation dose does the FISH translocation assay measure in cases of incorporated radionuclides for the Southern Urals populations? *Radiat Prot Dosimetry*, 159, 26-33.
- [9] Ainsbury, E.A., Vinnikov, V.A., Maznyk, N.A., Lloyd, D.C. and Rothkamm, K. (2013a). A comparison of six statistical distributions for analysis of chromosome aberration data for radiation biodosimetry. *Radiat Prot Dosimetry*, 155, 253-267.
- [10] Ainsbury, E.A., Vinnikov, V.A., Puig, P., Higuera, M., Maznyk, N.A., Lloyd, D.C. and Rothkamm, K. (2014d). Review of Bayesian statistical analysis methods for cytogenetic radiation biodosimetry, with a practical example. *Radiat Prot Dosimetry*, 162, 185-196.
- [11] Ainsbury, E.A., Vinnikov, V.A., Puig, P., Maznyk, N.A., Rothkamm, K. and Lloyd, D.C. (2013b). CytoBayesJ: Software tools for Bayesian analysis of cytogenetic radiation dosimetry data. *Mutat Res*, 756, 184-191.
- [12] Alpen, E.L. and Sheline, G.E. The combined effects of thermal burns and whole body X irradiation on survival time and mortality. *Ann Surg*. 1954;140(1):113-8.
- [13] Ampratwum, R.T., Bowen, B.D., Lund, T., Reed, R.K. and Bert, J.L. A model of fluid resuscitation following burn injury: formulation and parameter estimation. *Comput Methods Programs Biomed* 1995;47(1):1-19.
- [14] Anandasabapathy, N. A phase 1 trial of the hematopoietic growth factor CDX-301 (rhuFlt3L) in healthy volunteers. http://www.celldextherapeutics.com/docs/CLDX-301_BMT_2-12-2013pdf, 2013.
- [15] Andrews, G.A., Sitterson, B.W., Kretchmar, A.L. and Brucer, M. Criticality accident at the Y-12 plant. *Diagnosis and Treatment of Acute Radiation Injury*. 1961;27-48.

- [16] Anzai, K., Ikota, N., Ueno, M., Nyui, M. and Kagiya, T.V. Heat-treated mineral-yeast as a potent post-irradiation radioprotector. *J Radiat Res.* 2008;49: 425-30.
- [17] Badie, C., Kabacik, S., Balagurunathan, Y., Bernard, N., Brengues, M., Faggioni, G., Greither, R., Lista, F., Peinnequin, A., Poyot, T., Herodin, F., Missel, A., Terbrueggen, B., Zenhausem, F., Rothkamm, K., Meineke, V., Braselmann, H., Beinke, C. and Abend, M. (2013). Laboratory intercomparison of gene expression assays. *Radiat Res*, 180, 138-148.
- [18] Barnard, S., Ainsbury, E.A., Al-Hafidh, J., Hadjidekova, V., Hristova, R., Lindholm, C., Monteiro Gil, O., Moquet, J., Moreno, M., Rossler, U., Thierens, H., Vandevoorde, C., Vral, A., Wojewodzka, M. and Rothkamm, K. (2015). The first gamma-H2AX biodosimetry intercomparison exercise of the developing European biodosimetry network RENE. *Radiat Prot Dosimetry*, 164, 265-270.
- [19] Bartuś, M., Łomnicka, M., Kostogrys, R.B., Kaźmierczak, P., Watala, C., Słominska, E.M., Smoleński, R.T., Pisulewski, P.M., Adamus, J., Gębicki, J. and Chlopicki, S. 1-Methylnicotinamide (MNA) prevents endothelial dysfunction in hypertriglyceridemic and diabetic rats. *Pharmacol Rep* 2008;60:127-138.
- [20] Bassinet, C., Woda, C., Bortolin, E., Della Monaca, S., Fattibene, P., Quattrini, M., Bulanek, B., Ekendahl, D., Burbidge, C., Cauwels, V., Kouroukla, E., Geber-Bergstrand, T., Mrozik, A., Marczevska, B., Bilski, P., Sholom, S., McKeever, S., Smith, R., Veronese, I., Galli, A., Panzeri, L. and Martini, M. (2014). Retrospective radiation dosimetry using OSL of electronic components: Results of an inter-laboratory comparison. *Radiat Meas*, doi: 10.1016/j.radmeas.2014.03.016.
- [21] Bauchinger, M. (1995). Quantification of low-level radiation exposure by conventional chromosome aberration analysis. *Mut. Res.* 339, 177-189.
- [22] Baum, S.J. *The Pathophysiology of Combined Radiation Injuries: A Review and Analysis of the Literature on Non-Human Research*, DNA-TR-90-211, Defense Nuclear Agency, Alexandria, VA, USA, 1991.
- [23] Becciolini, A. (1987). Relative radiosensitivities of the small and large intestine. *Adv Radiat Biol* 121, 83-128.
- [24] Becciolini, A. Relative radiosensitivities of the small and large intestine. In: *Advances in radiation biology*. New York, USA: Academic, 1987.
- [25] Beinke, C., Barnard, S., Boulay-Greene, H., De Amicis, A., De Sanctis, S., Herodin, F., Jones, A., Kulka, U., Lista, F., Lloyd, D., Martigne, P., Moquet, J., Oestreicher, U., Romm, H., Rothkamm, K., Valente, M., Meineke, V., Braselmann, H. and Abend, M. (2013). Laboratory intercomparison of the dicentric chromosome analysis assay. *Radiat Res*, 180, 129-137.
- [26] Bender, M.A. and Gooch, P.C. (1963). Persistent chromosome aberrations in irradiated human subjects. II. Tree and one-half dependent mechanism. *Radiat. Res.* 18, 389-396.
- [27] Berbée, M., Fu, Q., Boerma, M., Wang, J., Kumar, K.S. and Hauer-Jensen, M. gamma-Tocotrienol ameliorates intestinal radiation injury and reduces vascular oxidative stress after total-body irradiation by an HMG-CoA reductase-dependent mechanism. *Radiat Res.* 2009;171:596-605.
- [28] Bert, J., Gyenge, C., Bowen, B., Reed, R. and Lund, T. Fluid resuscitation following a burn injury: implications of a mathematical model of microvascular exchange. *Burns* 1997;23(2):93-105.

- [29] Bertho, J.M., Demarquay, C., Frick, J., Joubert, C., Arenales, S., Jacquet, N., Sorokine-Durm, I., Chau, Q., Lopez, M., Aigueperse, J., Gorin, N.C. and Gourmelon, P. Level of Flt3-ligand in plasma: a possible new bio-indicator for radiation-induced aplasia. *Int J Radiat Biol.* 2001 Jun;77(6):703-12.
- [30] Bhardwaj, G., Murdoch, B., Wu, D. *et al.* Sonic hedgehog induces the proliferation of primitive human hematopoietic cells via BMP regulation. *Nat immunol.*2001;2:172-180.
- [31] Bhatia, M. Novel therapeutic targets for acute pancreatitis and associated multiple organ dysfunction syndrome. *Curr Drug Targets Inflamm Allergy.* 2002;1(4):343-51.
- [32] Blakely, W.F., Ossetrova, N.I., Whitnal, M.H., Sandgren, D.J., Krivokrysenko, V.I., Shakhov, A. and Feinstein, E. Multiple parameter radiation injury assessment using a nonhuman primate radiation model – Biodosimetry applications. *Health Phys.* 2010 Feb;98(2):153-9.
- [33] Blakely, W.F., Sandgren, D.J., Nagy, V., Kim, S.Y., Sigal, G.B. and Ossetrova, N.I. Further Biodosimetry Investigations Using Murine Partial-Body Irradiation Model. *Radiat Prot Dosimetry.* 2014 Jun;159(1-4):46-51. doi: 10.1093/rpd/ncu127.
- [34] Boerma, M., Kruse, J.J., van Loenen, M., Klein, H.R., Bart, C.I., Zurcher, C. and Wondergem, J. Increased deposition of von Willebrand factor in the rat heart after local ionizing irradiation. *Strahlenther Onkol* 2004;180:109-116.
- [35] Bolognesi, C., Balia, C., Roggieri, P., Cardinale, F., Bruzzi, P., Sorcinelli, F., Lista, F., D’Amelio, R. and Righi, E. Micronucleus test for radiation biodosimetry in mass casualty events.
- [36] Boudagov, R.S., Oulianova, L.P. and Tsyb, A.F. The pathogenesis and therapy of combined radiation injury. DTRA-TR-06-24, Defense Threat Reduction Agency, Fort Belvoir, VA, USA, 2006.
- [37] Bouffler, S., Ainsbury, E., Gilvin, P. and Harrison, J. (2012). Radiation-induced cataracts: the Health Protection Agency’s response to the ICRP statement on tissue reactions and recommendation on the dose limit for the eye lens. *J Radiol Prot.* 32(4), 479-88.
- [38] Bouffler, S.D., Peters, S., Gilvin, P., Slack, K., Markiewicz, E., Quinlan, R.A., Gillan, J., Coster, M., Barnard, S., Rothkamm, K. and Ainsbury, E. (2015). The lens of the eye: exposures in the UK medical sector and mechanistic studies of radiation effects. *Ann ICRP*, 44 (1 suppl.), 84-90.
- [39] Brayton, C. *Spontaneous Diseases in Commonly Used Mouse Strains / Stocks.* Baltimore: Johns Hopkins University, USA, 2009.
- [40] Bryniarski, K., Biedron, R., Jakubowski, A., Chlopicki, S. and Marcinkiewicz, J. Anti-inflammatory effect of 1-methylnicotinamide in contact hypersensitivity to oxazolone in mice; involvement of prostacyclin. *Eur J Pharmacol* 2008;578:332-8.
- [41] Brzozowski, T., Konturek, P.C., Chlopicki, S., Sliwowski, Z., Pawlik, M., Ptak-Belowska, A., Kwiecien, S., Drozdowicz, D., Pajdo, R., Slonimska, E., Konturek, S.J. and Pawlik, W.W. Therapeutic potential of 1-methylnicotinamide against acute gastric lesions induced by stress: role of endogenous prostacyclin and sensory nerves. *J Pharmacol Exp Ther* 2008;326:105-16.
- [42] Buske, P., Przybilla, J., Loeffler, M., Sachs, N., Sato, T., Clevers, H. and Galle, J. (2012). On the biomechanics of stem cell niche formation in the gut-modelling growing organoids. *FEBS J* 279:3475-3487.

- [43] Cai, W.B., Roberts, S.A., Bowley, E., Hendry, J.H. and Potten, C.S. (1997). Differential survival of murine small and large intestinal crypts following ionizing radiation. *Int J Radiat Biol* 71, 145-155.
- [44] Cary, L.H., Ngudiankama, B.F., Salber, R.E., Ledney, G.D. and Whitnall, M.H. Efficacy of radiation countermeasures depends on radiation quality. *Radiat Res*, 2012;177:663-675.
- [45] Cary, L.H., Noutai, D., Salber, R.E., Williams, M.S., Ngudiankama, B.F. and Whitnall, M.H. Endothelial cells and T Cells modulate responses to mixed neutron/gamma radiation. *Radiat Res*, 2014;181:592-604.
- [46] Celldex Therapeutics. CDX-301 – A Flt3L Clinical Program Focused First on Hematopoietic Stem Cell Transplantation. <http://www.celldex.com/pipeline/cdx-301.php>. Accessed August 22, 2014.
- [47] Chamberlain, G., Fox, J., Ashton, B. and Middleton, J. Concise review: mesenchymal stem cells: their phenotype, differentiation capacity, immunological features, and potential for homing. *Stem Cells*. 2007;25:2739-2749.
- [48] Chlopicki, S., Swies, J., Mogielnicki, A., Buczko, W., Bartus, M., Lomnicka, M., Adamus, J. and Gebicki, J. 1-Methylnicotinamide (MNA). a primary metabolite of nicotinamide. exerts anti-thrombotic activity mediated by a cyclooxygenase-2/prostacyclin pathway. *Br J Pharmacol* 2007;152:230-239.
- [49] Chua, M., Horn, S., Somaiah, N., Davies, S., Gothard, L., A'Hern, R., Yarnold, J. and Rothkamm, K. (2014). DNA double-strand break repair and induction of apoptosis in ex vivo irradiated blood lymphocytes in relation to late normal tissue reactions following breast radiotherapy. *Radiat Environ Biophys*, 53, 355-364.
- [50] Chua, M., Somaiah, N., Bourne, S., Daley, F., A'Hern, R., Nuta, O., Davies, S., Herskind, C., Pearson, A., Warrington, J., Helyer, S., Owen, R., Yarnold, J. and Rothkamm, K. (2011). Inter-individual and inter-cell type variation in residual DNA damage after in vivo irradiation of human skin. *Radiother Oncol*, 99, 225-230.
- [51] Chua, M.L. and Rothkamm, K. (2013). Biomarkers of radiation exposure: can they predict individual radiosensitivity? *Clin Oncol*, 25, 610-616.
- [52] Citrin, D., Cotrim, A.P., Hyodo, F., Baum, B.J., Krishna, M.C. and Mitchell, J.B. Radioprotectors and Mitigators of Radiation-Induced Normal Tissue Injury. *The Oncologist* 2010;15:360-371.
- [53] Davis, T.A., Mungunsukh, O., Zins, S., Day, R.M. and Landauer, M.R. Genistein induces radioprotection by hematopoietic stem cell quiescence. *Int J Radiat Biol*, 2008;84:713-726.
- [54] Davis, W.M., Davis, A.K., Lee, W. and Alpen, E.L. The combined effects of thermal burns and whole-body x-irradiation. III. Study of blood coagulation. *Ann Surg*. 1955;142(1):66-75.
- [55] Degteva, M.O., Shagina, N.B., Shishkina, E.A., Vozilova, A.V., Volchkova, A.Y., Vorobiova, M.I., Wieser, A., Fattibene, P., Della Monaca, S., Ainsbury, E., Moquet, J., Anspaugh, L.R. and Napier, B.A. (2015). Analysis of EPR and FISH studies of radiation doses in persons who lived in the upper reaches of the Techa River. *Radiat Environ Biophys*, 54, 433-444.
- [56] Docs NRPB. 1996; 7(3): 1–31. 10 United Nations Scientific Committee on the Effects of Atomic Radiation (UNSCEAR). Sources, Effects and Risks of Ionizing Radiation. UNSCEAR 1988 Report to the General Assembly, with Annexes. New York: United Nations, 1988.
- [57] Dörr, H.D. and Meineke, V. (2006). Appropriate radiation accident medical management: necessity of extensive preparatory planning. *Radiat. Environ. Biophys*. 45 (4), 237-244.

- [58] Drouet, M., Garrigou, P., Peinnequin, A. and Hérodin, F. Short term sonic hedgehog gene therapy to mitigate myelosuppression in highly irradiated monkeys: hype or reality? *Bone marrow transplant* 2014;49:304-309.
- [59] Drouet, M. and Hérodin, F. Radiation victim management and the haematologist in the future: time to revisit therapeutic guidelines? *Int J Radiat Biol.* 2010;86:636-648.
- [60] Drouet, M., Mourcin, F., Grenier, N. *et al.* Single administration of stem cell factor, flt-3 ligand, megakaryocyte growth and development factor and interleukin-3 in combination soon after irradiation prevents nonhuman primates from myelosuppression : long term follow-up of hematopoiesis. *Blood.* 2004;103:878-885.
- [61] Elliott, T.B., Deutz, N.E., Gulani, J., Koch, A., Olsen, C.H., Christensen, C., Chappell, M., Whitnall, M.H. and Moroni, M. Gastrointestinal acute radiation syndrome in Göttingen minipigs (*Sus scrofa domestica*). *Comp Med.* 2014 Dec;64(6):456-63.
- [62] Esker, J., Moyer, B., Rauli, R., Grace, M., Weber, W., Doyle-Eisele, M., Melo, D., Guilmette, R., Thrall, K., Lovaglio, J., Moroni, M., Bartholomew, A., Lindeblad, M. and Lyubimov, A. Natural history and biomarker results for radiation injury from multiple institutions using a harmonized model. Demonstration of reproducibility for regulatory acceptance. Abstracts, Radiation Research Society Annual Meeting, 2014.
- [63] Evans, M.L., Graham, M.M., Mahler, P.A. and Rasey, J.S. Changes in vascular permeability following thorax irradiation in the rat. *Radiat Res* 1986;107(2):262-271.
- [64] Fagiolo, U., Cossarizza, A., Scala, E., Fanales-Belasio, E., Ortolani, C., Cozzi, E. *et al.* Increased cytokine production in mononuclear cells of healthy elderly people. *Eur J Immunol.* 1993;23(9):2375-8.
- [65] Fei, P., Bernhard, E.J. and El-Deiry, W.S. Tissue-specific induction of p53 targets in vivo. *Cancer Res.* 2002;62(24):7316-27.
- [66] Fenech, M. The cytokinesis-block micronucleus technique and its application to genotoxicity studies in human populations. *Environ Health Perspect* 1993;101:101-107.
- [67] Filip, S., Mokřý, J., Vávřová, J., Cízková, D., Sinkorová, Z., Tosnerová, V. and Bláha, M. Homing of lin(-)/CD117(+) hematopoietic stem cells. *Transfus Apher Sci.* 2009;41(3):183-90.
- [68] Filip, S., Mokřý, J., Vávřová, J., Sinkorová, Z., Mičuda, S., Sponer, P., Filipová, A. *et al.* The peripheral chimerism of bone marrow-derived stem cells after transplantation: regeneration of gastrointestinal tissues in lethally irradiated mice. *J Cell Mol Med.* 2014;18(5):832-43.
- [69] Flidner, T.M., Friesecke, I. and Beyrer, K. (2001). *Medical Management of Radiation Accidents: Management of the Acute Radiation Syndrome.* London: The British Institute of Radiology.
- [70] Flidner, T.M., Graessle, D., Paulsen, C. and Reimers, K. Structure and function of bone marrow hemopoiesis: mechanisms of response to ionizing radiation exposure. *Cancer Biother Radiopharm.* 2002;17(4):405-426.
- [71] Flynn, D.F. and Goans, R.E. (2012). Triage and treatment of radiation and combined-injury mass casualties. In: *Textbook of Military Medicine: Medical Consequences of Nuclear Warfare.* Mickelson AB (ed.) Office of The Surgeon General, US Army & Borden Institute: Falls Church, VA & Fort Detrick, MD, USA, pp. 39-71.

- [72] Forcheron, F., Agay, D., Scherthan, H., Riccobono, D., Herodin, F., Meineke, V. and Drouet, M. Autologous adipocyte derived stem cells favour healing in a minipig model of cutaneous radiation syndrome. *PLoS One*. 2012;7(2):e31694. doi: 10.1371/journal.pone.0031694. Epub 2012 Feb 14.
- [73] François, S., Bensidhoum, M., Mouiseddine, M. *et al.* Local irradiation induces not only homing of human mesenchymal stem cells (huMSC) at exposed sites but promotes their widespread engraftment to multiple organs: a study of their quantitative distribution following irradiation damages. *Stem Cells*. 2006;24:1020-1029.
- [74] Freund, A., Orjalo, A.V., Desprez, P.Y. and Campisi, J. (2010). Inflammatory networks during cellular senescence: causes and consequences. *Trends Mol Med* 16, 238-246.
- [75] Friedenstein, A.J., Petrakova, K.V., Kurolesova, A.I. and Frolova, G.P. Heterotopic of bone marrow analysis of precursor cells for osteogenic and hematopoietic tissues, *Transplantation*. 1968, Vol. 6, No. 2, pp. 230-247.
- [76] Fu, Q., Berbée, M., Boerma, M., Wang, J., Schmid, HA. and Hauer-Jensen, M. The Somatostatin Analog SOM230 (Pasireotide) Ameliorates Injury of the Intestinal Mucosa and Increases Survival after Total-Body Irradiation by Inhibiting Exocrine Pancreatic Secretion. *Radiat Res* 2009;171:698-707 doi:10.1667/RR1685.1.
- [77] Fukumoto, R., Burns, T.M. and Kiang, J.G. Ciprofloxacin Enhances Stress Erythropoiesis in Spleen and Increases Survival after Whole-Body Irradiation Combined with Skin-Wound Trauma. *PLoS ONE*, 9(2): e90448. doi:90410.91371/journal.pone.0090448, 2014.
- [78] Fukumoto, R., Cary, L.H., Gorbunov, N.V., Lombardini, E.D., Elliott, T.B. and Kiang, J.G. Ciprofloxacin modulates cytokine/chemokine profile in serum, improves bone marrow repopulation, and limits apoptosis and autophagy in ileum after whole body ionizing irradiation combined with skin-wound trauma. *PLoS ONE*, 2013;8:e58389.
- [79] Gabryś, D., Greco, O., Patel, G., Prise, K.M., Tozer, G.M. and Kanthou, C. Radiation Effects on the Cytoskeleton of Endothelial Cells and Endothelial Monolayer Permeability. *Int J Radiat Onc Biol Phys* 2007;69(5):1553-1562.
- [80] Gallo-Payet, N., Pothier, P. and Hugon, J.S. (1987). Ontogeny of EGF receptors during postnatal development of mouse small intestine. *J Pediatr Gastroenterol Nutr* 6, 114-120.
- [81] Gebicki, J., Sysa-Jedrzejowska, A., Adamus, J., Woźniacka, A., Rybak, M. and Zielonka, J. 1-Methylnicotinamide: a potent anti-inflammatory agent of vitamin origin. *Pol J Pharmacol* 2003;55:109-12.
- [82] Ghosh, S.P., Kulkarni, S., Perkins, M.W., Hieber, K., Pessu, R.L., Gambles, K., Maniar, M., Kao, T.C., Seed, T.M. and Kumar, K.S. Amelioration of radiation-induced hematopoietic and gastrointestinal damage by Ex-RAD® in mice. *J Radiat Res*, 2012;53:526-536.
- [83] Ghosh, S.P., Perkins, M.W., Hieber, K., Kulkarni, S., Kao, T.C., Reddy, E.P., Reddy, M.V.R., Maniar, M., Seed, T. and Kumar, K.S. Radiation Protection by a New Chemical Entity, Ex-Rad Efficacy and Mechanisms. *Radiat Res* 2009;171:173-179.
- [84] Gilvin, P., Tanner, R., Bouffler, S., Ainsbury, E. and Harrison, J. (2013). Footnote to ‘Radiation-induced cataracts: the Health Protection Agency’s response to the ICRP statement on tissue reactions and recommendation on the dose limit for the eye lens’. *J Radiol Prot* 33, 703.

- [85] Gourmelon, P., Marquette, C., Agay, D., Mathieu, J. and Clarençon, D. (2005). Involvement of the central nervous system in radiation-induced multi-organ dysfunction and/or failure. *BJR Suppl* 27, 62-68.
- [86] Graupner, A., Eide, D.M., Brede, D.A., Ellender, M., Lindbo Hansen, E., Oughton, D.H., Bouffler, S.D., Brunborg, G. and Olsen, A.K. Genotoxic effects of high dose rate X-ray and low dose rate gamma radiation in *Apc^{Min/+}* mice. *Environ Mol Mutagen*. 2017 Oct;58(8):560-569. doi: 10.1002/em.22121. Epub 2017 Aug 30.
- [87] Grebenyuk, A., Zatsepin, V., Aksenova, N. and Timoshevsky, A. Effects of early therapeutic administration of interleukin-1 β on survival rate and bone marrow haemopoiesis in irradiated mice. *Acta Medica* 2010;53:221-224.
- [88] Ha, C.T., Li, X.H., Fu, D., Xiao, M. and Landauer, M.R. Genistein Nanoparticles Protect Mouse Hematopoietic System and Prevent Proinflammatory Factors after Gamma Irradiation. *Radiat Res*, 2013;180: 316-325.
- [89] Hall, E.J. and Giaccia, A.J. *Radiobiology for the radiobiologist*. Philadelphia, PA, USA: Lippincott Williams and Wilkins, 2006.
- [90] Harfouche, G. and Martin, M.T. Response of normal stem cells to ionizing radiation: A balance between homeostasis and genomic stability. *Mutat Res* 2010;704:167-174.
- [91] Harris, J.W. and Nonan, T.R. Early vascular permeability changes in whole-body x-irradiated rats. *Radiation Res* 1968;34(2):357-365.
- [92] Hayashi, T., Kusunoki, Y., Hakoda, M., Morishita, Y., Kubo, Y., Maki, M. *et al.* Radiation dose-dependent increases in inflammatory response markers in A-bomb survivors. *Int J Radiat Biol*. 2003;79(2):129-36.
- [93] Hayata, I., Kanda, R., Minamihisamatsu, M., Furukawa, M. and Sasaki, M.S. (2001). Cytogenetic dose estimation for 3 severely exposed patients in the JCO criticality accident in Tokaimura. *J. Radiat. Res.* 42, S149-155.
- [94] Henderson, B.W., Bicher, H.I. and Johnson, R.J. Loss of vascular fibrinolytic activity following irradiation of the liver-an aspect of late radiation damage. *Radiat Res* 1983;95:646-652.
- [95] Hérodin, F., Richard, S., Grenier, N., Arvers, P., Gérome, P., Baugé, S., Denis, J., Chaussard, H., Gouard, S., Mayol, J.F., Agay, D. and Drouet, M. Assessment of total- and partial-body irradiation in a baboon model: preliminary results of a kinetic study including clinical, physical and biological parameters. *Health Phys*. 2012 Aug;103(2):143-9.
- [96] Hérodin, F., Bourin, P., Mayol, J.F., Lataillade, J.J. and Drouet, M. Short-term injection of antiapoptotic cytokine combinations soon after lethal gamma irradiation promotes survival. *Blood*. 2003;101:2609-2616.
- [97] Hérodin, F. and Drouet, M. (2005). Cytokine-based treatment of accidentally irradiated victims and new approaches. *Exp Hematol* 33, 1071-1080.
- [98] Hérodin, F., Mestries, J.C., Janodet, D., Martin, S., Mathieu, J., Gascon, M.P., Pernin, M.O. and Ythier, A. Recombinant glycosylated human interleukin-6 accelerates peripheral blood platelet count recovery in radiation-induced bone marrow depression in baboons. *Blood*. 1992 Aug 1;80(3):688-95.

- [99] Hérodin, F., Roy, L., Vaurijoux, A. *et al.* Single injection of Stem Cell Factor, Flt-3 ligand, Thrombopoietin, interleukin-3 combined with Pegylated G-CSF mitigates myelosuppression in highly irradiated nonhuman primates. *Exp Hematol.* 2007;35:1172-1181.
- [100] Hérodin, F., Valente, M. and Abend, M. Useful radiation dose biomarkers for identification of early partial-body exposures. *Health Phys.* 2014 Jun;106(6):750-4.
- [101] Higuera, M., Puig, P., Ainsbury, E.A. and Rothkamm, K. (2015a). A new inverse regression model applied to radiation biodosimetry. *Proc R Soc A*, 471.
- [102] Higuera, M., Puig, P., Ainsbury, E.A., Vinnikov, V.A. and Rothkamm, K. (2015b) A new Bayesian model applied to cytogenetic partial body irradiation estimation. *Radiat Prot Dosimetry*, doi: 10.1093/rpd/ncv356.
- [103] Hong, M.Y., Turner, N.D., Carroll, R.J., Chapkin, R.S. and Lupton, J.R. Differential response to DNA damage may explain different cancer susceptibility between small and large intestine. *Exp Biol Med.* 2005;230(7):464-471.
- [104] Horn, S., Barnard, S., Brady, D., Prise, K. and Rothkamm, K. (2013). Combined analysis of gamma-H2AX/53BP1 foci and caspase activation in lymphocyte subsets detects recent and more remote radiation exposures. *Radiat Res*, 180, 603-609.
- [105] Hosoi, Y., Yamamoto, M., Ono, T. and Sakamoto, K. Prostacyclin production in cultured endothelial cells is highly sensitive to low doses of ionizing radiation. *Int J Radiat Biol* 1993;63:631-638.
- [106] Huchet, A., Belkacémi, Y., Frick, J., Prat, M., Muresan-Kloos, I., Altan, D., Chapel, A., Gorin, N.C., Gourmelon, P. and Bertho, J.M. Plasma Flt-3 ligand concentration correlated with radiation-induced bone marrow damage during local fractionated radiotherapy. *Int J Radiat Oncol Biol Phys.* 2003 Oct 1;57(2):508-15.
- [107] Humanetics Corporation. BIO 300: Development Programs. <http://www.humaneticscorp.com/development-programs>, Accessed August 22, 2014.
- [108] IAEA (2001). Cytogenetic Analysis of Radiation Dose Assessment: a Manual. International Atomic Energy Agency, Vienna, Austria. Technical Report 405.
- [109] Igaki, H., Nakagawa, K., Uozaki, H., Akahane, M., Hosoi, Y., Fukayama, M., Miyagawa, K., Akashi, M., Ohtomo, K. and Maekawa, K. Pathological changes in the gastrointestinal tract of a heavily radiation-exposed worker at the Tokai-mura criticality accident. *J Radiat Res (Tokyo)*. 2008;49(1):55-62.
- [110] International Atomic Energy Agency and World Health Organization (2000). How to recognize and initially respond to an accidental radiation injury, Vienna, Austria: IAEA 2000.
- [111] International Atomic Energy Agency. Cytogenetic analysis for radiation dose assessment A manual. Vienna: IAEA, Technical Report 2011.
- [112] International Organization for Standardization (2004). Radiation Protection e Performance Criteria for Service Laboratories Performing Biological Dosimetry by Cytogenetics. ISO, Geneva, Switzerland. ISO 19238.
- [113] International Organization for Standardization (2008). Radiation Protection – Performance Criteria for Laboratories Performing Cytogenetic Triage for Assessment of Mass Casualties in Radiological

- or Nuclear Emergencies – General Principles and Application to Dicentric Assay. ISO, Geneva, Switzerland. ISO 21243.
- [114] Jaafar, L., Podolsky, R.H. and Dynan, W.S. (2013). Long-term effects of ionizing radiation on gene expression in a zebrafish model. *PLoS One* 8, e69445.
- [115] Jacob, A., Shah, K.G., Wu, R. and Wang, P. Ghrelin as a novel therapy for radiation combined injury. *Mol Med*, 2010;16:137-143.
- [116] Jaworska, A., Ainsbury, E.A., Fattibene, P., Lindholm, C., Oestreicher, U., Rothkamm, K., Romm, H., Thierens, H., Trompier, F., Voisin, P., Vral, A., Woda, C. and Wojcik, A. (2015). Operational guidance for radiation emergency response organisations in Europe for using biodosimetric tools developed in EU Multibiodose project. *Radiat Prot Dosimetry*, 164, 165-169.
- [117] Johnson, S.E., Li, Z., Liu, Y., Moulder, J.E. and Zhao, M. Whole-body imaging of high-dose ionizing irradiation-induced tissue injuries using ^{99m}Tc-duramycin. *J Nucl Med*. 2013;54(8):139-403.
- [118] Jones, T.D., Morris, M.D. and Young, R.W. A mathematical model for radiation-induced myelopoiesis. *Radiat Res* 1991;128(3):258-266.
- [119] Kiang, J.G. and Fukumoto, R. Ciprofloxacin increases survival after ionizing irradiation combined injury: gamma-h2ax formation, cytokine/chemokine, and red blood cells. *Health Phys*, 2014;106: 720-726.
- [120] Kiang, J.G., Jiao, W., Cary, L.H., Mog, S.R., Elliott, T.B., Pellmar, T.C. and Ledney, G.D. (2010). Wound trauma increases radiation-induced mortality by activation of iNOS pathway and elevation of cytokine concentrations and bacterial infection. *Radiat Res* 173, 319-332.
- [121] Kiang, J.G., Zhai, M., Liao, P.-J., Bolduc, D.L., Elliott, T.B. and Gorbunov, N.V. (2014). Pegylated G-CSF inhibits blood cell depletion, increases platelets, blocks splenomegaly, and improves survival after whole-body ionizing irradiation but not after irradiation combined with burn. *Oxidative medicine and cellular longevity*, 481392.
- [122] Koffman, C.G., Elder, J.B., Ganguli, P.C., Gregory, H. and Geary, C.G. (1982). Effect of urogastone on gastric secretion and serum gastrin concentration in patients with duodenal ulceration. *Gut* 23, 951-956.
- [123] Kouroukla, E., Bailiff, I. and Terry, I. (2014). Emergency dosimetry using ceramic components in personal electronic devices. *Int J Mod Phys Conf Ser* 27, 1460155, doi 10.1142/S2010194514601550.
- [124] Kouroukla, E., Bailiff, I., Terry, I. and Bowen, L. (2014a). Luminescence characterisation of alumina substrates using cathodoluminescence microscopy and spectroscopy. *Radiat Meas*, doi 10.1016/j.radmeas.2014.03.018.
- [125] Krishnan, L., Krishnan, E.C. and Jewell, W.R. Immediate effect of irradiation on microvasculature. *Int J Radiat Onc Biol Phys* 1988;15(1):147-150.
- [126] Kulka, U., Ainsbury, L., Atkinson, M., Barnard, S., Smith, R., Barquinero, J.F., Barrios, L., Bassinet, C., Beinke, C., Cucu, A., Darroudi, F., Fattibene, P., Bortolin, E., Monaca, S.D., Gil, O., Gregoire, E., Hadjidekova, V., Haghdoost, S., Hatzl, V., Hempel, W., Herranz, R., Jaworska, A., Lindholm, C., Lumniczky, K., M'kacher, R., Mortl, S., Montoro, A., Moquet, J., Moreno, M., Noditi, M., Ogbazgh, A., Oestreicher, U., Palitti, F., Pantelias, G., Popescu, I., Prieto, M.J., Roch-Lefevre, S., Roessler, U., Romm, H., Rothkamm, K., Sabatier, L., Sebastia, N., Sommer, S.,

- Terzoudi, G., Testa, A., Thierens, H., Trompier, F., Turai, I., Vandevoorde, C., Vaz, P., Voisin, P., Vral, A., Ugletveit, F., Wieser, A., Woda, C. and Wojcik, A. (2015). Realising the European network of biodosimetry: RENEb - status quo. *Radiat Prot Dosimetry*, 164, 42-45.
- [127] Kulka, U., Ainsbury, L., Atkinson, M., Barquinero, J.F., Barrios, L., Beinke, C., Bognar, G., Cucu, A., Darroudi, F., Fattibene, P., Gil, O., Gregoire, E., Hadjidekova, V., Haghdoost, S., Herranz, R., Jaworska, A., Lindholm, C., Mkacher, R., Mörtl, S., Montoro, A., Moquet, J., Moreno, M., Ogbazghi, A., Oestreicher, U., Palitti, F., Pantelias, G., Popescu, I., Prieto, M.J., Romm, H., Rothkamm, K., Sabatier, L., Sommer, S., Terzoudi, G., Testa, A., Thierens, H., Trompier, F., Turai, I., Vandersickel, V., Vaz, P., Voisin, P., Vral, A., Ugletveit, F., Woda, C. and Wojcik, A. (2012). Realising the European Network of Biodosimetry (RENEb). *Radiat Prot Dosimetry*, 151, 621-625.
- [128] Landauer M.R. (2008). Radioprotection by the soy isoflavone genistein. In: *Herbal Radiomodulators: Applications in Medicine, Homeland Defense and Space*. Arora R (ed.) CABI Publishing: Wallingford, England, pp. 163-173.
- [129] Landauer, M.R., Srinivasan, V. and Seed, T.M. Genistein treatment protects mice from ionizing radiation injury. *J Appl Toxicol* 2003;23:379-385.
- [130] Lee, K.K., Jo, H.J., Hong, J.P., Lee, S.W., Sohn, J.S., Moon, S.Y., Yang, S.H., Shim, H., Lee, S.H., Ryu, S.H. and Moon, S.R. Recombinant human epidermal growth factor accelerates recovery of mouse small intestinal mucosa after radiation damage. *Int J Radiat Oncol Biol Phys*. 2008;71(4):1230-1235.
- [131] Lefaix, J.L. and Delanian, S. Le syndrome cutané radio-induit. *John Libbey Eurotext ed., ed. 1st 2005: montrouge*. 87-95.
- [132] Leggett, R.W. A retention-excretion model for americium in humans. *Health Phys* 1992;62(4): 288-310.
- [133] Leggett, R.W. *et al.* Mayak worker study: an improved biokinetic model for reconstructing doses from internally deposited plutonium. *Radiat Res* 2005;164(2):111-122.
- [134] Leggett, R.W., Williams, L.R., Melo, D.R. and Lipsztein, J.L. A physiologically based biokinetic model for cesium in the human body. *Sci. Total Environ* 2003;317(1-3):235-255.
- [135] Leibowitz, B.J., Wei, L., Zhang, L., Ping, X., Epperly, M., Greenberger, J., Cheng, T. and Yu, J. (2014). Ionizing irradiation induces acute haematopoietic syndrome and gastrointestinal syndrome independently in mice. *Nat Commun* 5, 3494.
- [136] Lewkowicz, P., Tchórzewski, H., Dytnerka, K., Banasik, M. and Lewkowicz, N. (2005). Epidermal growth factor enhances TNF-alpha-induced priming of human neutrophils. *Immunol Lett* 96, 203-210.
- [137] Li, X.H., Fu, D., Latif, N.H., Mullaney, C.P., Ney, P.H., Mog, S.R., Whitnall, M.H., Srinivasan, V. and Xiao, M. Delta-tocotrienol protects mouse and human hematopoietic progenitors from gamma-irradiation through extracellular signal-regulated kinase/mammalian target of rapamycin signaling. *Haematologica*, 2010;95:1996-2004.
- [138] Li, X.H., Ha, C.T., Fu, D. and Xiao, M. Micro-RNA30c Negatively Regulates REDD1 Expression in Human Hematopoietic and Osteoblast Cells after Gamma-Irradiation. *PLoS ONE*, 2012;7:e48700.
- [139] Li, X.H., Ha, C.T., Fu, D. and Xiao, M. REDD1 protects osteoblast cells from gamma radiation-induced premature senescence. *PLoS ONE*, 2012;7:e36604.

- [140] Lloyd, D.C. (1997). Chromosomal analysis to assess radiation dose. *Stem Cells* 15, 195-201.
- [141] Lloyd, D.C., Edwards, A.A., Moquet, J.E. and Guerrero-Carbajal, Y.C. (2000). The role of cytogenetics in early triage of radiation casualties. *Appl. Radiat. Isot.* 52, 1107-1112.
- [142] Manning, G. and Rothkamm, K. (2013). DNA damage-associated biomarkers of ionising radiation - current status and future relevance for radiology and radiation therapy. *Br J Radiol*, 86, 20130173.
- [143] Marck, R.E., Montagne, H.L., Tuinebreijer, W.E. and Breederveld, R.S. Time course of thrombocytes in burn patients and its predictive value for outcome. *Burns* 2013;39(4):714-22.
- [144] Markiewicz, E., Barnard, S., Haines, J., Coster, M., van Geel, O., Wu, W., Richards, S., Ainsbury, E., Rothkamm, K., Bouffler, S. and Quinlan, R.A. (2015). Nonlinear ionizing radiation-induced changes in eye lens cell proliferation, cyclin D1 expression and lens shape. *Open Biol*, 5, 150011.
- [145] Martin, K., Potten, C.S., Roberts, S.A. and Kirkwood, T.B. Altered stem cell regeneration in irradiated intestinal crypts of senescent mice. *J Cell Sci.* 1998;111(Pt 16):2297-303.
- [146] Maznyk, N.A., Wilkins, R.C., Carr, Z. and Lloyd, D.C. (2012). The capacity, capabilities and needs of the WHO BioDoseNet member laboratories. *Radiat Prot Dosimetry*, 151, 611-620.
- [147] McManus, L.M., Ostrom, K.K., Lear, C., Luce, E.B., Gander, D.L., Pinckard, R.N. and Redding, S.W. Radiation-induced increased platelet-activating factor activity in mixed saliva. *Lab Invest* 1993;68: 118-124.
- [148] McNamee, J.P., Flegel, F.N., Green, H.B., Marro, L. and Wilkins, R.C. Validation of the cytokinesis-block micronucleus (CBMN) assay for use as a triage biological dosimetry tool. *Radiat Prot Dosimetry* 2009;135:232-242.
- [149] Meijne, E.I., van der Winden-van Groenewegen, R.J., Ploemacher, R.E., Vos, O., David, J.A. and Huiskamp, R. The effects of x-irradiation on hematopoietic stem cell compartments in the mouse. *Exp Hematol* 1991;19:617-623.
- [150] Milligan, A.J., Katz, H.R. and Leeper, D.B. (1978). Effect of lucanthone hydrochloride on the radiation response of intestine and bone marrow of the Chinese hamster. *J Natl Cancer Inst* 60, 1023-1028.
- [151] Mizunaga, Y., Terai, S., Yamamoto, N., Uchida, K., Yamasaki, T., Nishina, H., Fujita, Y., Shinoda, K., Hamamoto, Y. and Sakaida, I. (2012). Granulocyte colony-stimulating factor and interleukin-1 β are important cytokines in repair of the cirrhotic liver after bone marrow cell infusion: comparison of humans and model mice. *Cell Transplant* 21, 2363-2375.
- [152] Moquet, J., Barnard, S.G. and Rothkamm, K. (2014). Gamma-H2AX biodosimetry for use in large scale radiation incidents: comparison of a rapid '96 well lyse/fix' protocol with a routine method. *PeerJ*, 2, 282.
- [153] Morgan, D., Said, B., Walsh, A., Murray, V., Clarke, S., Lloyd, D., Rothkamm, K. and Gent, N. (2010). Initial investigation and management of outbreaks and incidents of unusual illnesses, Version 5.0. Health Protection Agency.
- [154] Moriña, D., Higuera, M., Puig, P., Ainsbury, E.A. and Rothkamm, K. (2015). radir package: An R implementation for cytogenetic biodosimetry dose estimation. *J Radiol Prot*, 35, 557-569.

- [155] Moroni, M., Coolbaugh, T.V., Lombardini, E., Mitchell, J.M., Moccia, K.D., Shelton, L.J., Nagy, V. and Whitnall, M.H. Hematopoietic Radiation Syndrome in the Gottingen Minipig. *Radiat Res*, 2011;176:89-101.
- [156] Moroni, M., Coolbaugh, T.V., Mitchell, J.M., Lombardini, E., Moccia, K.D., Shelton, L.J., Nagy, V. and Whitnall, M.H. Vascular access port implantation and serial blood sampling in a Gottingen minipig (*Sus scrofa domestica*) model of acute radiation injury. *JAALAS*, 2011;50:65-72.
- [157] Moroni, M., Elliott, T.B., Deutz, N.E., Olsen, C.H., Owens, R., Christensen, C., Lombardini, E.D. and Whitnall, M.H. Accelerated hematopoietic syndrome after radiation doses bridging hematopoietic (H-ARS) and gastrointestinal GI-ARS acute radiation syndrome: Early hematological changes and systemic inflammatory response syndrome in minipig. *Int J Radiat Biol*, 2014;90:363-372.
- [158] Moroni, M., Lombardini, E., Salber, R., Kazemzadeh, M., Nagy, V., Olsen, C. and Whitnall, M.H. Hematological changes as prognostic indicators of survival: similarities between Gottingen minipigs, humans, and other large animal models. *PLoS ONE*, 2011;6:e25210.
- [159] Moroni, M., Ngudiankama, B.F., Christensen, C., Olsen, C.H., Owens, R., Lombardini, E.D., Holt, R.K. and Whitnall, M.H. The Gottingen minipig is a model of the hematopoietic acute radiation syndrome: G-Colony Stimulating Factor stimulates hematopoiesis and enhances survival from lethal total-body gamma-irradiation. *Int J Radiat Onc Biol Phys*, 2013;86:986-992.
- [160] Moulder, J.E. Pharmacological intervention to prevent or ameliorate chronic radiation injuries. *Semin Radiat Oncol* 2003;13:73-84.
- [161] Mount, D. and Bruce, W.R. Local Plasma Volume and Vascular Permeability of Rabbit Skin after Irradiation. *Radiat Res* 1964;23:430-445.
- [162] National Security Staff, Interagency Policy Coordination Subcommittee for Preparedness & Response to Radiological and Nuclear Threats (2010). Planning Guidance for Response to a Nuclear Detonation, 2nd Edition.
- [163] NATO (1996). NATO Handbook on the Medical Aspects of NBC Defensive Operations AMedP-6(B)).
- [164] Nuta, O., Moquet, J., Bouffler, S., Lloyd, D., Sepai, O. and Rothkamm, K. (2014). Impact of long term exposure to sodium arsenite on cytogenetic radiation damage. *Mutagenesis*, 29, 123-129.
- [165] Oh, H., Seong, J., Kim, W., Park, S., Koom, W.S., Cho, N.H. and Song, M. (2010). Recombinant human epidermal growth factor (rhEGF) protects radiation-induced intestine injury in murine system. *J Radiat Res* 51, 535-541.
- [166] Oliveira, M., Einbeck, J., Higuera, M., Ainsbury, E., Puig, P. and Rothkamm, K. Zero-inflated regression models for radiation-induced chromosome aberration data: A comparative study (2015) *Biom J*, doi: 10.1002/bimj.201400233.
- [167] Onconova Therapeutics. Recilisib (Ex-RAD®). <http://www.onconova.com/product-pipeline/recilisib.php>, Accessed August 22, 2014.
- [168] Ossetrova, N.I. and Blakely, W.F. Multiple blood-proteins approach for early-response exposure assessment using an in vivo murine radiation model. *Int J Radiat Biol*. 2009;85(10):837-50.

- [169] Ossetrova, N.I., Sandgren, D.J. and Blakely, W.F. C-reactive protein and serum amyloid A as early-phase and prognostic indicators of acute radiation exposure in nonhuman primate total-body irradiation model. *Radiat Maes.* 2011;46:1019-1024.
- [170] Palmer, J.L., Deburghgraeve, C.R., Bird, M.D., Hauer-Jensen, M. and Kovacs, E.J. (2011). Development of a combined radiation and burn injury model, *Journal of Burn Care & Research*, 32(2), 317-23.
- [171] Panés, J., Anderson, D.C., Miyasaka, M. and Granger, D.N. Role of Leukocyte-endothelial Cell Adhesion in Radiation-induced Microvascular Dysfunction in Rats. *Gastroenterology* 1995;108(6): 1761-1769.
- [172] Park, J.S., Lee, S.H., Na, H.J., Pyo, J.H., Kim, Y.S. and Yoo, M.A. (2012). Age- and oxidative stress-induced DNA damage in *Drosophila* intestinal stem cells as marked by Gamma-H2AX. *Exp Gerontol* 47, 401-405.
- [173] Pejchal, J., Novotný, J., Mařák, V., Osterreicher, J., Tichý, A., Vávrová, J., Sinkorová, Z., Zárbynická, L., Novotná, E., Chládek, J., Babicová, A., Kubelková, K. and Kuča, K. (2012). Activation of p38 MAPK and expression of TGF- β 1 in rat colon enterocytes after whole body γ -irradiation. *Int J Radiat Biol* 88, 348-358.
- [174] Pejchal, J., Tichý, A., Kmochová, A., Ďurišová, K., Kubelková, K., Pohanka, M. *et al.* Attenuation of radiation-induced gastrointestinal damage by epidermal growth factor and bone marrow transplantation in mice. *Int J Radiat Biol.* 2015;91(9):1-35.
- [175] Pernot, E., Hall, J., Baatout, S., Benotmane, M.A., Blanchardon, E., Bouffler, S., El Saghire, H., Gomolka, M., Guertler, A., Harms-Ringdahl, M., Jeggo, P., Kreuzer, M., Laurier, D., Lindholm, C., Mkacher, R., Quintens, R., Rothkamm, K., Sabatier, L., Tapio, S., de Vathaire, F. and Cardis, E. (2012). Ionizing radiation biomarkers for potential use in epidemiological studies. *Mutat Res Reviews*, 751, 258-286.
- [176] Pezeshki, A., Muench, G.P. and Chelikani, P.K. (2012). Short communication: expression of peptide YY, proglucagon, neuropeptide Y receptor Y2, and glucagon-like peptide-1 receptor in bovine peripheral tissues. *J Dairy Sci* 95, 5089-5094.
- [177] Phinney, D.G. and Prockop, D.J. Concise review: mesenchymal stem/multipotent stromal cells: the state of transdifferentiation and modes of tissue repair-current views, *Stem Cells.* 25:2896-2902, 2007.
- [178] Ploemacher, R.E., van Os, R., van Beurden, C.A. and Down, J.D. Murine haemopoietic stem cells with long-term engraftment and marrow repopulating ability are more resistant to γ -radiation than are spleen colony forming cells. *Int J Radiat Bio* 1992;61:489-499.
- [179] Pola, R., Ling, L.E., Silver, M. *et al.* The morphogen sonic hedgehog is an indirect angiogenic agent upregulating two families of angiogenic growth factors. *Nat Med.*2001;7:706-711.
- [180] Ponemone, V., Fayad, R., Gove, M.E., Pini, M. and Fantuzzi, G. Effect of adiponectin deficiency on intestinal damage and hematopoietic responses of mice exposed to gamma radiation. *Mutat Res.* 2010;690(1-2):102-7.
- [181] Popa, I., Zubkova, I., Medvedovic, M., Romantseva, T., Mostowski, H., Boyd, R. *et al.* Regeneration of the adult thymus is preceded by the expansion of K5+K8+ epithelial cell progenitors and by

- increased expression of Trp63, cMyc and Tcf3 transcription factors in the thymic stroma. *Int Immunol.* 2007;19(11):1249-60.
- [182] Poston Sr., J.W. and Sinclair, W.K. (2005). Keynote Address: current challenges in countering radiological terrorism. *Health Phys.* 89, 450-456.
- [183] Prasanna, P.G.S., Moroni, M. and Pellmar, T.C. (2010). Triage dose assessment for partial-body exposure: dicentric analysis. *Health Phys.* 98, 244-251.
- [184] Pyatkin, E.K., Nugis, V.Y. and Chrikov, A.A. (1989). Absorbed dose estimation according to the results of cytogenetic investigations of lymphocyte cultures of persons who suffered in the accident at Chernobyl atomic power station. *Radiation Medicine* 4, 52-58.
- [185] Riccobono, D., Agay, D., Forcheron, F. *et al.* Transient gene therapy to treat cutaneous radiation syndrome : development in minipig model. *Health Physics.*2014;106:713-719.
- [186] Riecke, A., Ruf, C.G. and Meineke, V. Assessment of radiation damage the need for a multiparametric and integrative approach with the help of both clinical and biological dosimetry. *Health Phys.* 2010;98:160-167.
- [187] Romm, H., Ainsbury, E., Bajinskis, A., Barnard, S., Barquinero, J.F., Barrios, L., Beinke, C., Puig-Casanovas, R., Deperas-Kaminska, M., Gregoire, E., Oestreicher, U., Lindholm, C., Moquet, J., Rothkamm, K., Sommer, S., Thierens, H., Vral, A., Vandersickel, V. and Wojcik, A. (2014). Web-based scoring of the dicentric assay, a collaborative biodosimetric scoring strategy for population triage in large scale radiation accidents. *Radiat Environ Biophys*, 53, 241-254.
- [188] Romm, H., Ainsbury, E., Bajinskis, A., Barnard, S., Barquinero, J.F., Beinke, C., Puig-Casanovas, R., Deperas-Kaminska, M., Gregoire, E., Kulka, U., Oestreicher, U., Lindholm, C., Moquet, J., Rothkamm, K., Sommer, S., Thierens, H., Vral, A., Vandersickel, V. and Wojcik, A. (2012). The dicentric assay in triage mode as reliable biodosimetric scoring strategy for population triage in large scale radiation accidents. *Proceedings of the 13th International Congress of the International Radiation Protection Association, TS2c.3.*
- [189] Romm, H., Ainsbury, E., Barnard, S., Barrios, L., Barquinero, J.F., Beinke, C., Deperas, M., Gregoire, E., Koivistoinen, A., Kulka, U., Lindholm, C., Moquet, J., Oestreicher, U., Puig, R., Rothkamm, K., Sommer, S., Thierens, H., Vandersickel, V., Vral, A. and Wojcik, A. (2013). Automatic scoring of dicentric chromosomes as a tool in large scale radiation accidents. *Mutat Res*, 756, 174-183.
- [190] Romm, H., Ainsbury, E., Barnard, S., Barrios, L., Barquinero, J.F., Beinke, C., Deperas, M., Gregoire, E., Koivistoinen, A., Lindholm, C., Moquet, J., Oestreicher, U., Puig, R., Rothkamm, K., Sommer, S., Thierens, H., Vandersickel, V., Vral, A. and Wojcik, A. (2014a). Validation of semi-automatic scoring of dicentric chromosomes after simulation of three different irradiation scenarios. *Health Phys*, 106, 764-771.
- [191] Romm, H., Bajinskis, A., Oestreicher, U., Thierens, H., Vral, A., Rothkamm, K., Ainsbury, E., Benderitter, M., Voisin, P., Fattibene, P., Lindholm, C., Barrios, L., Sommer, S., Woda, C., Scherthan, H., Beinke, C., Vojnovic, B., Trompier, F., Jaworska, A. and Wojcik, A. (2013a). Multibiodose: new development of multi-disciplinary biodosimetric tools to manage high-scale radiological casualty. *Future Security 2013 Proc*, 222-228.

- [192] Romm, H., Barnard, S., Boulay-Greene, H., De Amicis, A., De Sanctis, S., Franco, M. *et al.* Laboratory intercomparison of the cytokinesis-block micronucleus assay. *Radiat Res* 2013;180: 120-128.
- [193] Romm, H., Barnard, S. and Boulay-Greene, H. *et al.* (2013b). Comparison of the cytokinesis-block micronucleus assay among laboratories. *Radiat Res*, 180, 120-128.
- [194] Rossnerova, A., Spatova, M., Schunck, C. and Sram, R.J. Automated scoring of lymphocyte micronuclei by the Metasystems Metafer image cytometry system and its application in studies of human mutagen sensitivity and biodosimetry of genotoxin exposure. *Mut* 2011;26:169-175.
- [195] Rothkamm, K., Barnard, S., Ainsbury, E.A., Al-hafidh, J., Barquinero, J.F., Lindholm, C., Moquet, J., Perälä, M., Roch-Lefèvre, S., Scherthan, H., Thierens, H., Vral, A. and Vandersickel, V. (2013a). Manual versus automated gamma-H2AX foci analysis across five European laboratories: can this assay be used for rapid biodosimetry in a large scale radiation accident? *Mutat Res*, 756, 170-173.
- [196] Rothkamm, K., Barnard, S., Moquet, J., Ellender, M., Rana, Z. and Burdak-Rothkamm, S. (2015). DNA damage foci: meaning and significance. *Environ Mol Mutagen*, 56, 491-504.
- [197] Rothkamm, K., Beinke, C., Romm, H., Badie, C., Balagurunathan, Y., Barnard, S., Bernard, N., Boulay-Greene, H., Brengues, M., De Amicis, A., De Sanctis, S., Greither, R., Herodin, F., Jones, A., Knie, T., Kabacik, S., Kulka, U., Lista, F., Martigne, P., Missel, A., Moquet, J., Oestreicher, U., Peinnequin, A., Poyot, T., Roessler, U., Scherthan, H., Terbrueggen, B., Thierens, H., Valente, M., Vral, A., Zenhausern, F., Meineke, V., Braselmann, H. and Abend, M. (2013b). Comparison of established and emerging biodosimetry assays. *Radiat Res* 180, 111-119.
- [198] Rothkamm, K., Crosbie, J.C., Daley, F., Bourne, S., Barber, P.R., Vojnovic, B., Cann, L. and Rogers, P.A.W. (2012b). In situ biological dose mapping estimates the radiation burden delivered to 'spared' tissue between synchrotron X-ray microbeam radiotherapy tracks. *PLoS One*, 7, e29853.
- [199] Rothkamm, K., Horn, S., Pope, I., Barber, P.R., Barnard, S., Moquet, J., Tullis, I. and Vojnovic, B. (2012a). The gamma-H2AX assay as a high throughput triage tool: comparison of two prototype devices. *NATO Science and Technology Organization Report STO-MP-HFM-223*, 12, 1-13.
- [200] Rothkamm, K., Horn, S., Scherthan, H., Rößler, U., De Amicis, A., Barnard, S., Kulka, U., Lista, F., Meineke, V., Braselmann, H., Beinke, C. and Abend, M. (2013c). Laboratory inter-comparison on the gamma-H2AX foci assay. *Radiat Res*, 180, 149-155.
- [201] Rothkamm, K. and Lloyd, D. (2014). Established and emerging methods of biological dosimetry. In: *Comprehensive Medical Biophysics, Volume VII: Radiation Biology and Radiation Safety* (ed.: J Hendry). Elsevier.
- [202] Samarth, R.M. Protection against radiation induced hematopoietic damage in bone marrow of Swiss albino mice by *Mentha piperita* (Linn). *J Radiat Res*. 2007;48:523-8.
- [203] Samarth, R.M. and Kumar, A. Radioprotection of Swiss albino mice by plant extract *Mentha piperita* (Linn.). *J Radiat Res* 2003;44:101-9.
- [204] Sasaki, M.S., Hayata, I., Kamada, N., Kodama, N. and Kodama, S. (2001). Chromosome aberration analysis in persons exposed to low-level radiation from JCO criticality accident in Tokaimura. *J. Radiat. Res.* 42, S107-116.

- [205] Sato, T. and Clevers, H. (2013). Growing self-organizing mini-guts from a single intestinal stem cell: mechanism and applications. *Science* 340, 1190-1194.
- [206] Saxena, S.K., Thompson, J.S. and Sharp, J.G. (1997). Role of organized intestinal lymphoid aggregates in intestinal regeneration. *J Invest Surg* 10, 97-103.
- [207] Seidelin, J.B. and Nielsen, O.H. Epithelial apoptosis: cause or consequence of ulcerative colitis? *Scand J Gastroenterol.* 2009;44(12):1429-34.
- [208] Sevan'kaev, A.V. (2000). Results of cytogenetic studies of the consequences of the Chernobyl accident. *Radiat. Biol. Radioecol.* 40, 589-95.
- [209] Shcherbova, E.N. and Krapchatova, M.P. Bone marrow transplantation as a factor modifying the recovery processes of hematopoietic tissue in irradiated mice. *Radiobiologiya.* 1984;24(3):315-20.
- [210] Singh, P.K., Wise, S.Y., Ducey, E.J., Fatanmi, O.O., Elliott, T.B. and Singh, V.K. α -Tocopherol Succinate Protects Mice against Radiation-Induced Gastrointestinal Injury. *Radiat Res* 2012;177: 133-145.
- [211] Singh, V.K., Ducey, E.J., Fatanmi, O.O., Singh, P.K., Brown, D.S., Purmal, A., Shakhova, V.V., Gudkov, A.V., Feinstein, E. and Shakhov, A. CBLB613: A TLR 2/6 Agonist, Natural Lipopeptide of *Mycoplasma arginini*, as a Novel Radiation Countermeasure. *Radiat Res* 2012;177:628-642.
- [212] Smirnova, O.A. Environmental Radiation Effects on Mammals: A Dynamical Modeling Approach. 1st ed. Springer; New York, USA, 2010.
- [213] Smith, R.W., Eakins, J.S., Hager, L.G., Rothkamm, K. and Tanner, R.J. (2015). Development of a retrospective/fortuitous accident dosimetry service based on OSL of mobile phones. *Radiat Prot Dosimetry*, 164, 89-92.
- [214] Somaiah, N., Rothkamm, K. and Yarnold, J. (2015). Where do we look for markers of radiotherapy fraction size sensitivity? *Clin Oncol*, 27, 570-578.
- [215] Somaiah, N., Yarnold, J., Daley, F., Pearson, A., Gothard, L., Rothkamm, K. and Helleday, T. (2012). The relationship between homologous recombination repair and the sensitivity of human epidermis to the size of daily doses over a 5-week course of breast radiotherapy. *Clin Cancer Res*, 18, 5479-5488.
- [216] Somaiah, N., Yarnold, J., Lagerqvist, A., Rothkamm, K. and Helleday, T. (2013). Homologous recombination mediates cellular resistance and fraction size sensitivity to radiation therapy. *Radiother Oncol*, 108, 155-161.
- [217] Song, C.W., Anderson, R.S. and Tabachnick, J. Early Effects of Beta Irradiation on Dermal Vascular Permeability to Plasma Proteins. *Radiat Res* 1966;27(4):604-615.
- [218] Sotnik, N.V., Azizova, T.V., Darroudi, F., Ainsbury, E.A., Moquet, J.E., Fomina, J., Lloyd, D.C., Hone, P.A. and Edwards, A.A. (2015). Verification by the FISH translocation assay of historic doses to Mayak workers from external gamma radiation. *Radiat Environ Biophys*, 54, 445-451.
- [219] Sousa, A., Raposo, F., Fonseca, S., Valente, L., Duarte, F., Gonçalves, M. *et al.* Measurement of cytokines and adhesion molecules in the first 72 hours after severe trauma: association with severity and outcome. *Dis Markers.* 2015;2015:747036.

- [220] Steinstraesser, L., Burkhard, O., Fan, M.H., Jacobsen, F., Lehnhardt, M., Su, G. *et al.* Burn wounds infected with *Pseudomonas aeruginosa* triggers weight loss in rats. *BMC Surg.* 2005;5:19.
- [221] Stone, H.B., Moulder, J.E., Coleman, C.N., Ang, K.K., Anscher, M.S., Barcellos-Hoff, M.H., Dynan, W.S., Fike, J.R., Grdina, D.J., Greenberger, J.S., Hauer-Jensen, M., Hill, R.P., Kolesnick, R.N., MacVittie, T.J., Marks, C., McBride, W.H., Metting, N., Pellmar, T., Purucker, M., Robbins, M.E., Schiestl, R.H., Seed, T.M., Tomaszewski, J.E., Travis, E.L., Wallner, P.E., Wolperta, M. and Zaharevitza, D. Models for Evaluating Agents Intended for the Prophylaxis. Mitigation and Treatment of Radiation Injuries Report of an NCI Workshop. 3-4 December 2003 *Radiat Res* 2004;162:711-728.
- [222] Stricklin, D., Millage, K., Rodriguez, J. and McClellan, G. Cesium-137 decorporation model. DTRA-TR-15-01, Defense Threat Reduction Agency, Fort Belvoir, VA, USA, 2014a.
- [223] Stricklin, D., Millage, K., Rodriguez, J. and McClellan, G. Americium-241 decorporation model. DTRA-TR-15-02, Defense Threat Reduction Agency, Fort Belvoir, VA, USA, 2014b.
- [224] Stricklin, D., Millage, K., Rodriguez, J. and McClellan, G. Plutonium-238/239 decorporation model. DTRA-TR-15-03, Defense Threat Reduction Agency, Fort Belvoir, VA, USA 2014c.
- [225] Sugarman, S.L., Livingston, G.K., Stricklin, D.L., Abbott, M.G., Wilkins, R.C., Romm, H., Oestreicher, U., Yoshida, M.A., Miura, T., Moquet, J.E., Di Giorgio, M., Ferrarotto, C., Gross, G.A., Christiansen, M.E., Hart, C.L. and Christensen, D.M. (2014). The internet's role in a biodosimetric response to a radiation mass casualty event. *Health Phys* 106, S65-S70.
- [226] Suman, S., Datta, K., Doiron, K., Ren, C., Kumar, R., Taft, D.R., Fornace, A.J., Jr. and Maniar, M. Radioprotective effects of ON 01210.Na upon oral administration. *J Radiat Res*, 2012;53:368-376.
- [227] Suman, S., Maniar, M., Fornace, A.J., Jr. and Datta, K. Administration of ON 01210.Na after exposure to ionizing radiation protects bone marrow cells by attenuating DNA damage response. *Radiat Oncol*, 2012;7:6.
- [228] Sun, L., Serrero, G., Piltch, A. and Hayashi, J. EGF receptors on TEA3A1 endocrine thymic epithelial cells. *Biochem Biophys Res Commun.* 1987;148(2):60-8.
- [229] Swift, S.N., Pessu, R.L., Chakraborty, K., Villa, V., Lombardini, E. and Ghosh, S.P. Acute toxicity of subcutaneously administered vitamin E isomers, delta- and gamma-tocotrienol in mice. *Int J Tox*, In revision, 2014.
- [230] Tanaka, M., Nakao, N., Yamamoto, I., Tsushima, N. and Ohta, Y. (2013). Changes in expression levels of neurotensin precursor and receptor mRNA in chicken intestinal tissues and liver during late embryonic and early posthatching development. *Poult Sci* 92, 2765-2771.
- [231] Terry, N.H. and Travis, E.L. (1989). The influence of bone marrow depletion on intestinal radiation damage. *Int J Radiat Oncol Biol Phys.* 17, 569-573.
- [232] Thierens, H. and Vral, A. The micronucleus assay in radiation accidents. *Ann Ist Super Sanita* 2009;45:260-264.
- [233] Thierens, H., Vral, A., Vandevoorde, C., Vandersickel, V., de Gelder, V., Romm, H., Oestreicher, U., Rothkamm, K., Barnard, S., Ainsbury, E., Sommer, S., Beinke, C. and Wojcik, A. (2014). Is a semi-automated approach indicated in the application of the automated micronucleus assay for triage purposes? *Radiat Prot Dosimetry*, 159, 87-94.

- [234] Timins, J.K. and Lipoti, J.A. (2004). Radiological terrorism. *N. J. Med* 101 (9 Suppl), 66-75.
- [235] Tintinalli, J.E. *Emergency medicine: a comprehensive study guide*. 7th Ed. New York: McGraw-Hill Medical; 2011, 2120 p.
- [236] Tolar, J.K., Blanc, K., Keating, A. and Blazar, B.R. Concise review: hitting the right spot with mesenchymal stromal cells. *Stem Cells*. 2010;28:1446-1455.
- [237] Torre, D., Tambini, R., Aristodemo, S., Gavazzeni, G., Goglio, A., Cantamessa, C. *et al.* Anti-inflammatory response of IL-4, IL-10 and TGF-beta in patients with systemic inflammatory response syndrome. *Mediators Inflamm*. 2000;9(3-4):193-5.
- [238] Trott, K.R., van Luijk, P., Ottolenghi, A. and Smyth, V. Biological mechanisms of normal tissue damage: importance for the design of NTCP models. *Radiother Oncol*. 2012 Oct;105(1):79-85. doi: 10.1016/j.radonc.2012.05.008. Epub 2012 Jun 29.
- [239] Uddin, M., Lau, L.C., Seumois, G., Vijayanand, P., Staples, K.J., Bagmane, D., Cornelius, V., Dorinsky, P., Davies, D.E. and Djukanović, R. (2013). EGF-induced bronchial epithelial cells drive neutrophil chemotactic and anti-apoptotic activity in asthma. *PLoS One* 8, e72502.
- [240] Ullrich, R.L. and Casarett, G.W. Interrelationship between the early inflammatory response and subsequent fibrosis after radiation exposure. *Radiat Res* 1977;72(1):107-121.
- [241] Valente, M., Denis, J., Grenier, N., Arvers, P., Foucher, B., Desangles, F., Martigne, P., Chaussard, H., Drouet, M., Abend, M. and Hérodin, F. Revisiting Biomarkers of Total-Body and Partial-Body Exposure in a Baboon Model of Irradiation. *PloS One* 2015 Jul 15;10(7):e0132194.
- [242] Van der Meeren, A., Mouthon, M.A., Gaugler, M.H., Vandamme, M. and Gourmelon, P. (2002). Administration of recombinant human IL11 after supralethal radiation exposure promotes survival in mice: interactive effect with thrombopoietin. *Radiat Res* 157, 642-649.
- [243] van Es, J.H., Sato, T., van de Wetering, M., Lyubimova, A., Nee, A.N., Gregorieff, A., Sasaki, N., Zeinstra, L., van den Born, M., Korving, J., Martens, A.C., Barker, N. van Oudenaarden, A. and Clevers, H. (2012). Dll1+ secretory progenitor cells revert to stem cells upon crypt damage. *Nat Cell Biol* 14, 1099-1104.
- [244] Varga, D., Johannes, T., Jainta, S., Schuster, S., Schwarz-Boeger, U., Kiechle, M., Patino Garcia, B. and Vogel, W. An automated scoring procedure for the micronucleus test by image analysis. *Mut*. 2004;19:391-397.
- [245] Vaurijoux, A., Gruel, G., Pouzoulet, F., Gregoire, E., Martin, C., Roch-Lefevre, S., Voisin, P., Voisin, P. and Roy, L. (2009). Strategy for population triage based on dicentric analysis. *Radiat. Res*. 171, 541-548.
- [246] Ventevogel, M.S. and Sempowski, G.D. Thymic rejuvenation and aging. *Curr Opin Immunol*. 2013;25(4):516-22.
- [247] Vitale, I., Galluzzi, L., Castedo, M. and Kroemer, G. (2011). Mitotic catastrophe: a mechanism for avoiding genomic instability. *Nat Rev Mol Cell Biol* 12, 385-392.
- [248] Voisin, P., Ainsbury, L., Atkinson, M., Barquinero, J.F., Barrios, L., Beinke, C., Darroudi, F., Fattibene, P., Gil, O., Hadjidekova, V., Haghdoost, S., Herranz, R., Jaworska, A., Lindholm, C.,

- Mörthl, S., Montoro, A., Moreno, M., Oestreicher, U., Palitti, F., Pantelias, G., Popescu, I., Romm, H., Rothkamm, K., Sabatier, L., Sommer, S., Testa, A., Thierens, H., Trompier, F., Turai, I., Vaz, P., Vral, A., Woda, C., Wojcik, A. and Kulka, U. (2012). RENEb – Realising the European Network of Biodosimetry. NATO Science and Technology Organization Report STO-MP-HFM-223, 19, 1-10.
- [249] Voisin, P., Benderitter, M., Claraz, M., Chambrette, V., Sorokine-Durm, I., Delbos, M., Durand, V., Leroy, A. and Paillole, N. (2001). The cytogenetic dosimetry of recent accidental overexposure. *Cell Mol. Biol. (Noisy-le-grand)* 47, 557-564.
- [250] Vozilova, A.V., Shagina, N.B., Degteva, M.O., Edwards, A.A., Ainsbury, E.A., Moquet, J.E., Hone, P., Lloyd, D.C., Fomina, J.N. and Darroud, F. (2012). Preliminary FISH-based assessment of external dose for residents exposed on the Techa River. *Radiat Res*, 177, 84-91.
- [251] Vozilova, A.V., Shagina, N.B., Degteva, M.O., Moquet, J., Ainsbury, E.A. and Darroudi, F. (2014). FISH analysis of translocations induced by chronic exposure to Sr radioisotopes: second set of analysis of the Techa river cohort. *Radiat Prot Dosimetry*, 159, 34-37.
- [252] Vral, A., Fenech, M. and Thierens, H. The micronucleus assay as a biological dosimeter of in vivo ionising radiation exposure. *Mut* 2011;26:11-17.
- [253] Walchuk, M. (2007). Cytogenetic biodosimetry at the Armed Forces Radiobiology research Institute, an interview with Dr. Pataje Prasanna. *Health Phys. News XXXV* (11).
- [254] Wang, J., Boerma, M., Fu, Q. and Hauer-Jensen, M. Significance of endothelial dysfunction in the pathogenesis of early and delayed radiation enteropathy. *World J Gastroenterol* 2007;13:3047-3055.
- [255] Wang, J., Zheng, H., Ou, X., Albertson, C.M., Fink, L.M., Herbert, J.M. and Hauer-Jensen, M., Hirudin ameliorates intestinal radiation toxicity in the rat: support for thrombin inhibition as strategy to minimize side-effects after radiation therapy and as countermeasure against radiation exposure. *J Thromb Haemost* 2004;2:2027-2035.
- [256] Wang, J., Zheng, H., Ou, X., Fink, L.M. and Hauer-Jensen, M. Deficiency of microvascular thrombomodulin and up-regulation of protease-activated receptor-1 in irradiated rat intestine: possible link between endothelial dysfunction and chronic radiation fibrosis. *Am J Pathol* 2002;160:2063-2072.
- [257] Wang, L.H., Zhang, W., Gao, Q.X. and Wang, F. (2012). Expression of the luteinizing hormone receptor (LHR) gene in ovine non-gonadal tissues during estrous cycle. *Genet Mol Res* 11, 3766-3780.
- [258] Wang, P., Han, L., Shen, H., Wang, P., Lv, C., Zhao, G., Niu, J., Xue, L., Wang, Q.J., Tong, T. and Chen, J. (2014). Protein kinase D1 is essential for Ras-induced senescence and tumor suppression by regulating senescence-associated inflammation. *Proc Natl Acad Sci USA* 111, 7683-7688.
- [259] Wang, Y., Schulte, B.A. and Zhou, D. Hematopoietic stem cell senescence and long-term bone marrow injury. *Cell Cycle*. 2006;5(1):35-38.
- [260] Wentz, J., Oldson, D. and Stricklin, D. Mathematical Models of Human Hematopoiesis Following Acute Radiation Injury, DTRA-TR-14-31, Defense Threat Reduction Agency, Fort Belvoir, VA, USA, 2014a.
- [261] Wentz, J., Oldson, D. and Stricklin, D. Models of Hematopoietic Dynamics Following Burn for Use in Combined Injury Simulations, DTRA-TR-15-024, Defense Threat Reduction Agency, Fort Belvoir, VA, USA, 2015.

- [262] Wentz, J., Oldson, D. and Stricklin, D. (2014b). Modeling the thrombopoietic effects of burn, *Letters in Biomathematics*, 1(1), 111-126.
- [263] Willems, P., August, L., Slabbert, J., Romm, H., Oestreicher, U., Thierens, H. and Vral, A. Automated micronucleus (MN) scoring for population triage in case of large scale radiation events. *Int J Radiat Biol* 2010;86:2-11.
- [264] Withers, H.R. and Elkind, M.M. (1970). Microcolony survival assay for cells of mouse intestinal mucosa exposed to radiation. *Int J Radiat Biol Relat Stud Phys Chem Med* 17, 261-267.
- [265] Wojcik, A., Lloyd, D., Rom, H. and Roy, L. (2010). Biological dosimetry for triage of casualties in a large-scale radiological emergency: capacity of the EU member states. *Radiat Prot Dosimetry*, 138, 397-401.
- [266] Woźniacka, A., Wiczorkowska, M., Gebicki, J. and Sysa-Jedrzejowska, A. Topical application of 1-methylnicotinamide in the treatment of rosacea: a pilot study. *Clin Exp Dermatol* 2005;30:632-5.
- [267] Xiao, M., Inal, C.E., Parekh, V.I., Li, X.H. and Whitnall, M.H. Role of NF-kappaB in hematopoietic niche function of osteoblasts after radiation injury. *Exp Hematol*, 2009;37:52-64.
- [268] Xu, D.Z., Zaets, S.B., Chen, R., Lu, Q., Rajan, H., Yang, X., Zhang, J., Feketova, E., Bogdan, N., Deitch, E.A. and Cao, Y. (2009). Elimination of C5aR prevents intestinal mucosal damage and attenuates neutrophil infiltration in local and remote organs. *Shock* 31, 493-499.
- [269] Zhang, C., Ni, J., Li, B.L., Gao, F., Liu, H., Liu, W., Huang, Y.J. and Cai, J.M. (2013). CpG-Oligodeoxynucleotide Treatment Protects against Ionizing Radiation-Induced Intestine Injury. *PLoS One* 8, e66586.
- [270] Zhang, L., Sun, W., Wang, J., Zhang, M., Yang, S., Tian, Y., Vidyasagar, S., Peña, L.A., Zhang, K., Cao, Y., Yin, L., Wang, W., Zhang, L., Schaefer, K.L., Saubermann, L.J., Swarts, S.G., Fenton, B.M., Keng, P.C. and Okunieff, P. (2010). Mitigation effect of an FGF-2 peptide on acute gastrointestinal syndrome after high-dose ionizing radiation. *Int J Radiat Oncol Biol Phys* 77, 261-268.



Chapter 2 – LOW-LEVEL RADIATION BIOEFFECTS

2.1 GENERAL INTRODUCTION

Low-level radiation is defined by the Commander's Operational radiation Risk Management and Tracking Tool superseding STANAG 2083 and STANAG 2473 as radiation levels above natural background levels resulting from any man-made cause other than the initial nuclear radiation and subsequent radioactive fallout from a deliberate and successful wartime detonation of a nuclear weapon.

In this chapter we address aspects such as the detection of low radiation exposure which can occur shortly after exposure or with a latency of years or even decades after exposure due to the delayed chronic health effects occurring after exposure. Andrea De Amicis *et al.* from the Italian Army Medical and Veterinary Research Centre provided preliminary data on a retrospective study employing FISH chromosome painting translocation in a cohort of Italian soldiers with past deployments in the Balkan Area. Stefania de Sanctis from the same group introduced a pilot dog model for biomonitoring of chemicals/radiation exposures in operational theatres using the micronucleus assay in acute exposure scenarios. Dogs are considered as animal sentinels providing information about chemicals/radiation environmental exposure with potential adverse health effects for their conductors.

Radiation-induced effects such as cancerogenesis represent a well-known threat associated with low-level radiation exposure. Dr. Alexandra Miller from Armed Forces Radiobiology Research Institute, USA, reported about the importance of low-dose radiation research and introduced models and mechanisms to develop biomarkers, countermeasures, and improved risk assessment. Prof. Dr. Marek and its group from Military Institute of Hygiene and Epidemiology, Poland provided an insight into the effect of low doses of low-LET radiation on the innate anti-tumor reactions in radio-resistant and radio-sensitive mice. This work was complemented by another study where the same group examined the effect of internal contamination with tritiated water on the innate anti-tumor and inflammatory reactions in radio-resistant and radio-sensitive mice.

Besides late effects such as cancer development the society becomes more and more alert about chronic non-cancer diseases. Several epidemiological reports suggest an increased risk for developing atherosclerosis after ionizing radiation, but target genes are so far unknown. Michael Abends group from the Bundeswehr Institute of Radiobiology, Germany examined gene expression changes in radiation exposed cohorts such as Chernobyl and the Russian Mayak worker. They not only focused on cancerogenesis, but also considered e.g., atherosclerosis.

2.2 BIOMARKERS OF EXPOSURE AND EFFECTS

2.2.1 Gene Expression Changes Observed in Radiation Exposed Cohorts – Health Risk After Low-Level Radiation

Abstract

Background: *In different irradiated cohorts we examined whether radiation-induced gene expression changes might be detectable many years after exposure and whether they are associated with the occurrence of chronic non-cancer diseases.*

Material and Methods: *Total RNA was isolated from 63 papillary thyroid cancer biopsies and associated normal thyroid tissues (Chernobyl victims) as well as from 150 blood samples derived from Mayak workers exposed to external-gamma rays and internal plutonium incorporation. According to a 2-phase study design,*

we divided the samples for screening of the whole genome in Phase I and validation of selected candidate genes in Phase II using qRT-PCR.

Results: *We observed in both cohorts persistent and significant gene-dose associations of genes (similar in 30%) up to 2 decades after radiation exposure which partly correlated significantly with, e.g., atherosclerotic diseases.*

Conclusion: *Identifying persistent radiation-induced genes in different cohorts, using different methods and materials might provide a hint for a new kind of diagnostic and therapeutic regimen, thus changing classic radiobiology from risk predictions to intervention.*

2.2.1.1 Introduction

The tumor mortality increases with rising radiation dose. This effect can be detected in adults' with statistical significance at 100 – 200 mSv and higher doses. Nowadays it is unclear whether a health risk in adults after exposures below 100 mSv might exist. This uncertainty is caused by the high prevalence of tumor diseases. Due to that large cohorts have to be followed over many decades. For instance, in order to detect an increased risk for developing a breast carcinoma after an exposure of 8 mSv (corresponding to one mammography) about 100,000,000 women suffering from a breast cancer and about the same number of controls have to be examined over decades [118]. Using classical radioepidemiology low risk at these exposures and large cohorts such as that examined over decades cannot be accomplished. In the absence of those studies the linear no-threshold model was established. It extrapolates the radiation-associated risk examined after high-radiation dose to low doses assuming a linear association and no-threshold.

In the absence of sufficient data for risk estimates at low doses using classical epidemiological methodology the question about alternative approaches rises, e.g., by combining molecular biology with epidemiology. A successful approach has to meet the following prerequisites:

- 1) Biological changes should be specific for radiation exposure in order to discriminate the majority of spontaneously occurring diseases from a few radiation-induced diseases. For instance, about 97% of all tumors are caused by exposures other than natural radiation, e.g., smoking (30%) or alimentation/overweight (30%).
- 2) Due to the long latency between the exposure and the event persistent biological changes occurring ahead of the diseases would be required.
- 3) A detected exposure-to-target molecule (gene, RNA-species, protein) relationship does not necessarily imply a target molecule-to-effect (disease) relationship. Showing both association strengthen the causal relationship and the assumed causal pathway starting with the exposure which induces certain biological changes which finally causes a disease.

Relationships such as that have been already identified. For instance, different environmental factors (temperature in plants [34]) can induce a modification in reading of the genome (transcriptional changes). Such modifications can be induced permanently (DNA-methylation) and can be forwarded to the next cell generation and even to the next generation [34]. Processes like that are called epigenetic modification, since the genomic sequence of the bases is not altered, but the activation/regulation of genes is newly adjusted. It is like a switch arrested in a new position after the exposure which finally helps the organisms to adjust to varied environmental conditions.

Clearly, radiation is an environmental factor. Assumed a radiation-specific and permanent new adjustment of the genome on different genes would take place, so that this signature could be detected even years after exposure this signature could be regarded as an indicator of an earlier radiation exposure. Occupational or accidental exposures which might happen, e.g., during out-of-area services of soldiers could be identified and compensation request due to a later occurring disease could be judged on an individual base. Moreover,

early detection of modified genes associated with a later occurring disease could be targeted. Hence, molecules altered after radiation exposure could serve as a **biomarker of exposure for risk prediction**, but due to its relationship with the disease it could also become a **biomarker of effect** and at this point it could become a target molecule **for therapeutic intervention** (Figure 2-1).

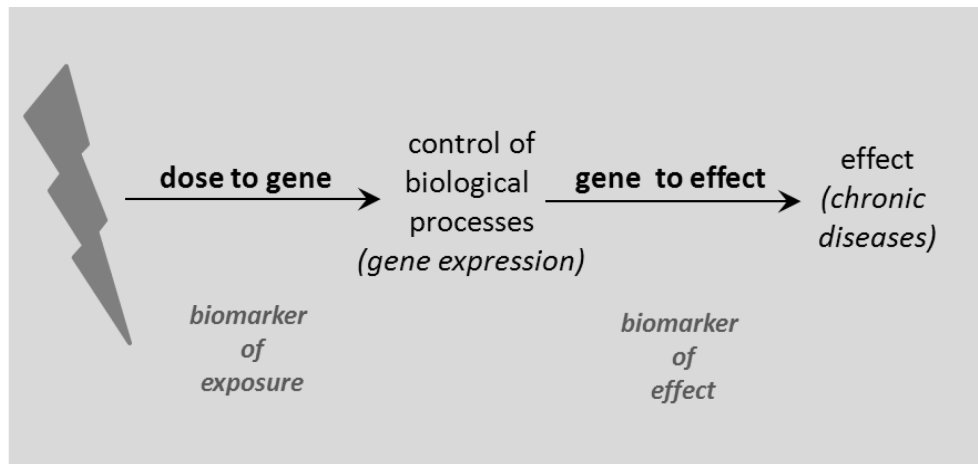


Figure 2-1: The Causal Pathway Depicts Genes Newly Adjusted After Radiation Exposure which Over a Latency of Decades are Involved in the Later Occurring Disease/Effect. Molecules identified along the causal pathway can be utilized for dose estimation (biomarker of exposure) or the prediction of the effect (biomarker of effect).

It was the aim of our studies performed on irradiated human cohorts to:

- 1) Search for persistent changes in gene expression after radiation exposure; and
- 2) Examine whether these changes are of harm and associated with certain chronic diseases.

We examined victims of the Chernobyl power plant accident (single dose exposure) and Mayak worker who got chronically exposed to protracted doses (external gamma and internal Plutonium) during the development of the Russian nuclear atomic bomb program. A two stage study design allowed us to screen the whole mRNA transcriptome and large quantities of the microRNA post-transcriptome (only Mayak worker). One part of the biological samples was used for this screening approach and the remainder samples were used for validation purposes of candidate genes from Phase I utilizing qRT-PCR. Those genes surviving the validation were examined for their association with chronic non-cancer diseases available for the Mayak worker only.

2.2.1.2 Materials and Methods

The “Chernobyl Tissue Bank” provided 63 RNA sample pairs from the thyroid tissue and corresponding histologically normal tissues from 63 children/juveniles exposed to I-131 during the Chernobyl power plant accident. RNA-samples were isolated from cryopreserved biopsies (Figure 2-2).

Chernobyl radiation victims

Inclusion/exclusion criteria	N
Thyroid cancers from Ukrainian-American cohort study::	110
Papillary thyroid cancers: (excluded 5 follicular and 1 medullary thyroid cancer)	104
RNA specimens from Chernobyl Tissue Bank (30 RNA specimens not available)	74
RNA specimen sample pairs (excluded 11 RNA samples without matched tumor/normal or failed QC ¹)	63

Phase I (two stage study design)

Random allocation to split sample set (Phase I 32/ Phase II 30)
 Screening set with 32 normal and 32 tumor RNA samples employing Whole Genome Microarray (~20,000 genes)

- running bioinformatic approach (PANTHER & DAVID) on genes significantly associated with dose in tumor (n=2,233) & normal tissues (n=3,099, p<10⁻⁶)
- selection of 95 gene candidates² going forward to Phase II for validation

Phase II (two stage study design)

Independent validation set with 28 normal and 30 tumor tissue samples employing qRT-PCR³ 74/79⁴ normal/tumor genes) → **8/6 normal/tumor genes**

PLOS One 2012; BJC 2013

Laboratory Technique Validation

Comparison of phase I whole genome microarray data (32 normal and 32 tumor RNA samples) with Phase II qRT-PCR data (28/30 normal/tumor tissue samples) using 95 genes

Mayak worker (Ozyorsk residents)

Inclusion/exclusion criteria	external γ-ray only	external γ-ray & internal Pu	N
• # exposed Ozyorsk residents	3,803	5,584	9,387
• total dose >0.5 Gy/>1.01 Gy + >0.7 kBq ¹	1,514	579	2,093 (100%)
• known vital status (May-June 2011)	1,469	579	2,048 (97.8%)
• alive & living in Ozyorsk during the study	301	153	454 (21.7%)
• # exposed residents involved in our study	18	82	100 (4.8%)
• # unexposed residents involved in our study			± 50 150

Phase I (whole genome screening for radiation-associated genes)

1. random split sample set: Phase I 40² / Phase II 110
2. screening set with 4x10 RNA samples comprising an unexposed (control) group and 3 exposure groups³
3. examining
 - transcriptional changes (whole genome microarray, 19,586 genes)
 - ~ 500 mRNA (335 genes)⁴
 - gene enrichment analysis (PANTHER)
 - 95 mRNA for phase II
 - post-transcriptional changes (qRT-PCR, ~ 667 microRNA)
 - 45 microRNA⁵ for phase II

Health Physic Journal 2014

Phase II (validation of radiation-associated genes on remaining samples)

1. independent validation set with 92 samples⁶
2. employing 6 statistical models separately for each exposure type and gene⁷
3. adjusting significantly associated candidates (25 mRNA, 20 microRNA) with 26 confounders → 15 mRNA and 15 microRNA survived
4. perform non parametric Kruskal Wallis test (3df) on the surviving candidate genes
5. examine mRNA-microRNA relationship
6. analytically determine association of final mRNA/microRNA candidates with blood cell counts
7. Laboratory technique validation on 40 samples used for the whole genome microarray (phase I) with qRT-PCR data from 92 samples (phase II)

RadRes, 2014

Phase III (examining phase II genes and their association with chronic non-cancer diseases)

1. selection of chronic diseases and clinical parameter used for analysis⁸ → 15 chronic diseases & 3 clinical parameter
2. employing 2 statistical models to examine radiation dose – gene – effect (chronic diseases/clin. Parameter) association for 15 mRNA, 15 microRNA and 18 chronic diseases/clinical parameter⁹
3. adjusting models for collinearity among diseases where needed⁹
4. calculate OR for models with persistent significant radiation-gene and effect-gene relationships¹⁰
5. examine disease dependent mRNA-microRNA relationships

RadRes, 2015

Figure 2-2: Overview on the Study Design of the Chernobyl (left-side) and the Mayak Worker Study (right-side). Shown are inclusion and exclusion criteria, the 2-phase study design with additional analysis performed at the Mayak group (Phase III) as well as the methodological validation. Further details of the study are provided in the cited literature shown in the flow diagram (right corner).

During Phase I, the whole mRNA transcriptome was screened using microarrays (Figure 2-3). Between 10 – 12 samples were summed up to three exposure groups comprising doses such as ≤ 0.3 Gy, 0.3 – 1.0 Gy and > 1.0 Gy. In the absence of an unexposed control group we used the lowest dose group as the reference (calibrator) for calculating the differential gene expression of quintil-normalized log₂-transformed gene expression data. Bioanalysis was performed using PANTHER or DAVID databases for differentially expressed genes which appeared over- or underrepresented when examined relative to, e.g., certain biological processes they are coding for. Significantly and ≥ 2 -fold deregulated genes (either up- or down-regulated) were selected for validation on the remaining samples and instead of utilizing the less precise microarray methodology we employed the gold standard for gene expression measurements namely qRT-PCR using TaqMan chemistry (Figure 2-3). For methodological validation of the microarray data in comparison with qRT-PCR we calculated the mean gene expression values of differentially expressed genes detected on the microarray and compared it with the corresponding differential gene expression data generated with qRT-PCR using other biological samples. The agreement between both methods was 93% ($r^2 = 0.86$) among up- and down-regulated genes examined with both methods.

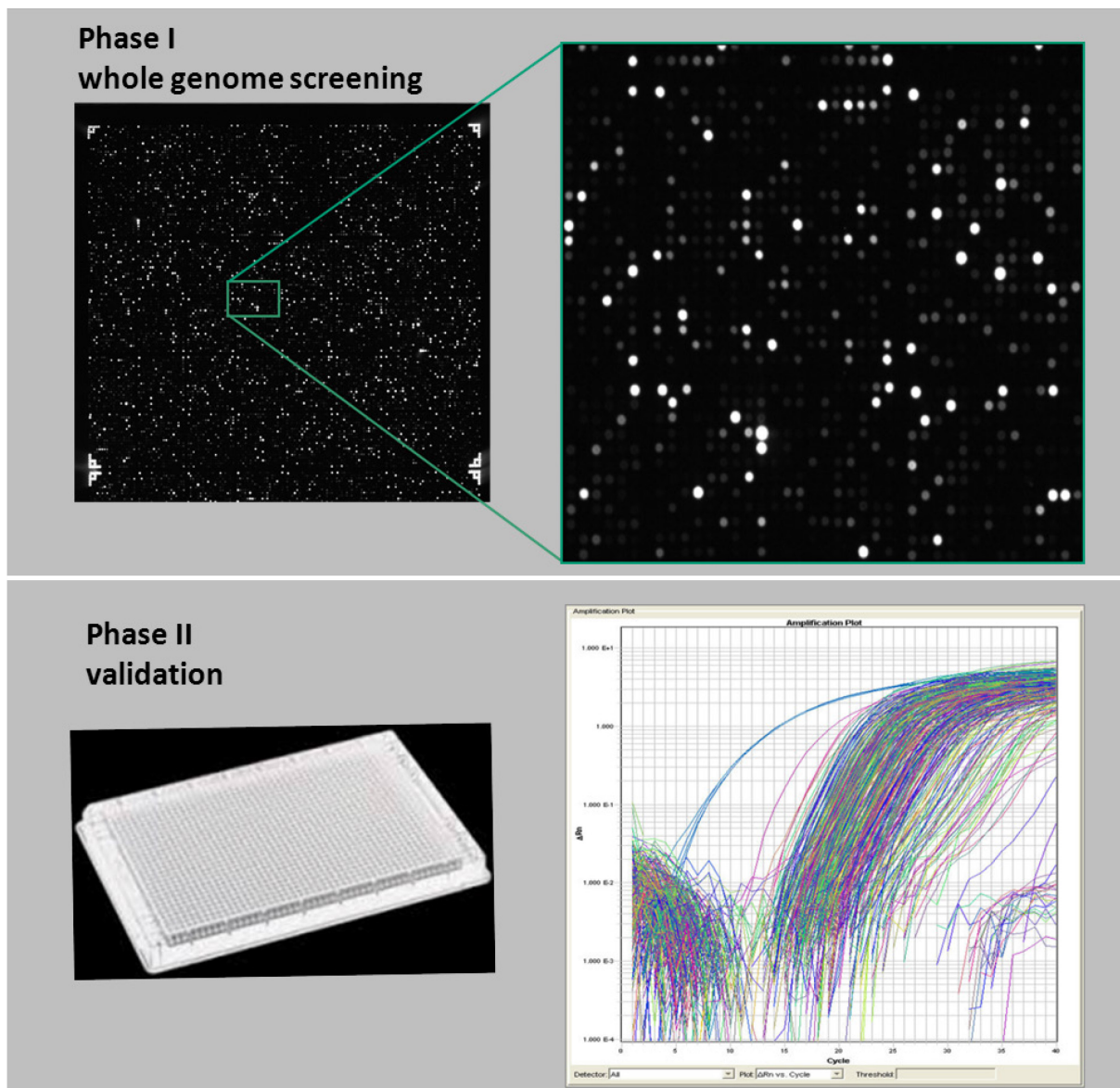


Figure 2-3: Phase I – Whole Genome Screening (upper part); Phase II – Validation (lower part).

A whole genome microarray was used for whole genome screening of radiation-associated changes in gene expression (Phase I – upper part of the figure). The magnification (left side) shows dot-like hybridization products consisting of labeled (chemoluminescence) template cRNA isolated from the samples and their hybridization with immobilized complementary nucleotide sequences. Each dot represents one gene and the intensity correlates with the mRNA copy number. The lower part of the figure (Phase II – validation) shows a validation of candidate genes using qRT-PCR and a 384 well platform (left side). So-called amplification plots (right side) allow a very specific and sensitive quantification of mRNA copy numbers for each desired gene.

The association of the qRT-PCR data with the exposure height was finally statistically examined (for details see Refs. [4] and [5]).

The second study was performed on 100 blood samples from radiation exposed Mayak worker who lived in a town (Oszerk) close to the Mayak production side. Another 50 blood samples were collected from

unexposed individuals living in Oszerk, who served as a reference group/control (for details see Refs. [1], [2], [3] and Figure 2-2). Mayak worker were exposed to chronic protracted external gamma exposure which lasted about 2 decades. They were also contaminated with internalized Plutonium. Phase I was conducted very similar to the Chernobyl study. However, in addition to the whole mRNA transcriptome this time 667 from about 1.200 miRNA were examined as well. After identification of radiation-associated target genes in Phase I and validation in Phase II these genes became forwarded to Phase III for further examination of the gene’s association with chronic non-cancer diseases such as atherosclerosis or diabetes (Figure 2-2 and Ref. [3]). Those clinical data were eligible for Mayak worker only. Tumor bearing individuals were excluded from analysis and could not be analyzed within this study.

2.2.1.3 Results

Using whole genome microarrays allowed the simultaneous detection of about 42.545 transcripts and 19.596 genes. Number of genes significantly associated with exposure was about 800 – 1.000 in both studies (Phase I). Based on certain criteria, e.g., strength of association, altogether 95 candidate genes were selected for further validation on the remainder samples using qRT-PCR (Phase II). The Chernobyl study validated 8 from these 95 genes in the normal tissue and 6 genes in the tumor tissue as significantly associated with dose (for details see Refs. [4] and [5]).

Bioinformatic analysis revealed altered biological processes taking place in the normal as well as the tumor tissue such as RNA binding and nucleic-acid metabolism, while other processes related to proliferation (FGF and EGF signal transduction pathways) and repair (p53) appeared over-represented in tumor tissues only (Figure 2-4).

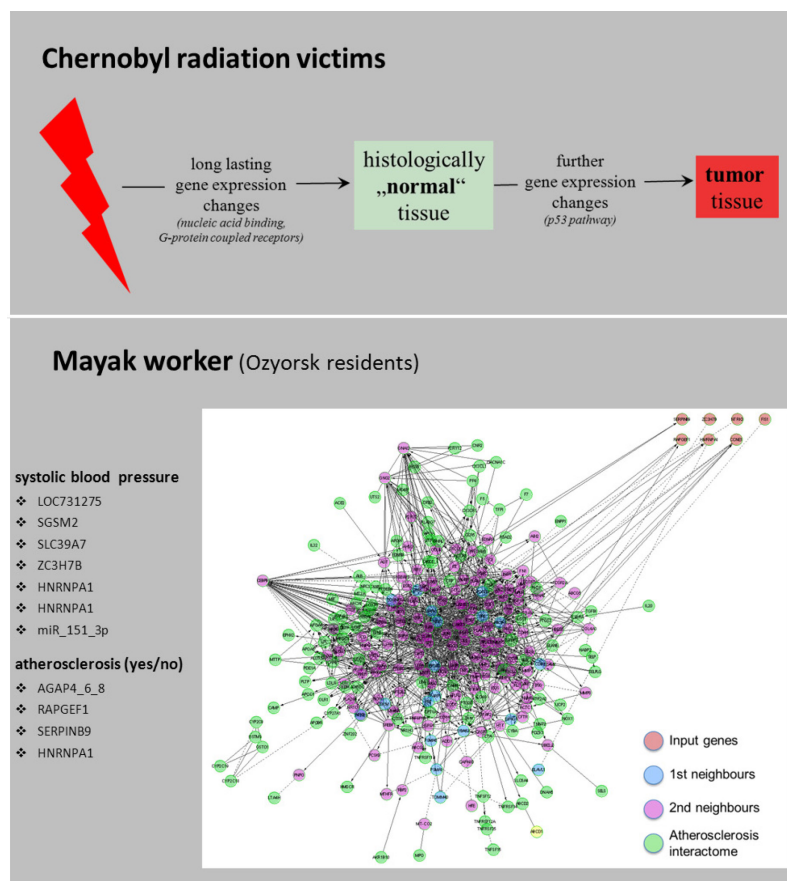


Figure 2-4: Examinations on the Chernobyl Radiation Victims and the Mayak Workers.

The upper part (Chernobyl victims) reveals biological processes already altered in histologically normal tissue, indicating that the genome became newly adjusted after radiation exposure. Further gene expression changes are probably associated with the development of tumors. The lower part (Mayak worker) depicts radiation-induced gene expression changes and their association with chronic non-cancer diseases. The atherosclerosis-interactom (right) is shown as an example. The graph represents known genes associated with atherosclerosis (green) and the known interactions among these genes. Seven of these radiation-associated genes (left) were identified in the context of the Mayak examination. Shown are first (blue) and second neighbors (pink) along their signal-transduction pathway.

After screening the mRNA transcriptome of the Mayak worker and after validation with qRT-PCR finally 15 mRNA and 15 miRNA species remained. These exposure-to-gene associations could be detected in both studies decades after exposure. The genes detected in the Mayak worker were partly detected in the Chernobyl study as well. However, in the Mayak study most dose-to-gene associations were related to the Plutonium incorporation, but associations to external gamma exposure were also detected (for details see Refs. [1] and [2]).

Some of the radiation-associated genes were also associated to thyroid diseases, the chronic radiation syndrome as well as increased blood pressure and atherosclerotic processes (Phase III, Figure 2-4, Ref. [3]).

2.2.1.4 Discussion

In vivo gene expression studies performed on two radiation exposed cohorts revealed the following findings:

- 1) Decades after exposures with external gamma rays or β -rays (incorporation of I-131) or incorporated alpha emitter (Plutonium) dose dependent gene expression changes in thyroid tumor tissues as well as in the peripheral blood of individuals could be detected.
- 2) Radiation associated changes in gene expression can be already found in histological normal thyroid tissues.
- 3) Some of these radiation-associated genes are also significantly associated with atherosclerotic processes.

Finding exposure-to-gene associations' decades after radiation exposure could be interpreted as an indication for a causal relationship (Bradford Hill criteria for causation) – however, it is not a proof.

Interesting, even after different exposures types (see above) about 30% of radiation-associated genes or gene groups found in the thyroid cancer tissues (Chernobyl study) could be also detected in the peripheral blood of the Mayak worker who also suffered from thyroid diseases. This could be interpreted as an indication of the blood bearing a certain communication matrix and serving as a source for information about biological processes, e.g., diseases going on at a certain location within the body. The blood somehow mirrors what is happening in the body. This thinking was recently confirmed and exosomes or microvesicles released from normal and tumor cells were identified as structures containing gene signatures (in particular small RNAs) which represent a copy of their original source (e.g., tumor cells). Indeed, both normal and diseased cells continuously shed vesicles into extracellular space, and these vesicles carry molecular signatures and effectors of both health and disease [136]. These microvesicles are currently identified as promising markers for individual therapeutic intervention and opened a new avenue of examinations on the so-called “liquid biopsies”. Interesting, most of our validated genes (Mayak project) were not associated with number of peripheral blood cell counts, which indicates that they are presenting molecules released at other locations within the body but not by the peripheral blood cell types themselves.

Gene expression changes were examined at different points in time for each exposed individual. This covers up to 3 decades after exposure. We interpret this as a hint for persisting changes in gene expression taking

place in a sub-set of genes; otherwise the exposure-to-gene associations would have been not detected. It is a limitation of our studies that we did not have access to sequential individual blood samples taken at different points in time. With our question and our analysis we – as a side effect – selectively searched for those genes. Noteworthy, in the context of another study on primates we could detect persisting changes in gene expression at 7 different points in time and up to 150 days after irradiation (data not published so far) which corroborates our findings in humans.

As another finding of the Chernobyl study significant dose-to-gene associations were identified in histologically normal thyroid tissues [5]. These changes could be interpreted as early diagnostic criteria for the later developing tumor. Further examinations in this regard might confirm it. Irrespective of that these changes in gene expression are very much in line with the idea of tumorigenesis as a multi-step process.

Beside chronic diseases such as cancer it was possible to examine gene-to-disease associations on the Mayak worker since clinical data on non-cancer chronic diseases such as atherosclerosis were available. Based on radioepidemiological studies on the same cohort [8], [9] and on others [74], an increased atherosclerosis risk has been already shown. However, our studies for the first time provide a hint to the radiation-induced genes involved in the development of those diseases which might become a gene target in future targeted therapies. Still, these findings have to be validated with larger studies.

Our studies bear certain limitations such as the number of samples examined, uncertainties in the dose estimates and examinations on prevalent cases in the absence of gene expression data taken before the onset of the diseases. Due to that further examinations on larger groups and a prospective study design are needed.

2.2.1.5 Acknowledgment

The studies summarized above were performed in collaboration with the partners as follow:

Chernobyl Study:

- 1) Biostatistics Branch, Division of Cancer Epidemiology and Genetics, NCI, Bethesda, Maryland, USA: R.M. Pfeiffer.
- 2) Radiation Epidemiology Branch, Division of Cancer Epidemiology and Genetics, NCI, Bethesda, Maryland, USA: A.V. Brenner, M. Hatch and K. Mabuchi.
- 3) State Institution “V.P. Komissarenko Institute of Endocrinology and Metabolism of Academy of Medical Sciences of Ukraine”, Kiev, Ukraine: T.I. Bogdanova and M.D. Tronko.
- 4) Bundeswehr Institute of Radiobiology, Munich, Germany: C. Ruf and J. Hartmann.

Mayak Study:

- 1) Southern Urals Biophysics Institute (SUBI), Russian Federation: T. Azizova, G. Rusinova, I. Glazkova and N. Vyazovskaya.
- 2) Research Unit of Radiation Cytogenetics, Integrative Biology Group, Helmholtz Center, Munich, Germany: D. Schmidl and K. Unger.
- 3) Bundeswehr Medical Office, Department F, CBRN Med Defence, Munich, Germany: H. Kreppel.
- 4) Bundeswehr Institute of Radiobiology affiliated to the University of Ulm, Munich, Germany: K. Müller, H. Dörr and S. Doucha-Senf.

2.2.2 Retrospective Study by FISH Chromosome Painting Translocation in a Cohort of Italian Soldiers with Past Deployments in the Balkan Area: Preliminary Data

Abstract

Stable chromosome aberrations, as translocations, persist over time after genotoxic exposure and then, they may be used for evaluating past exposure and chronic exposure. Quantitative measurements of translocation using fluorescence in situ hybridization (FISH) whole-chromosome painting method are a valid assay for retrospective biodosimetry. As regards to the open question about health risk for military personnel employed in the Balkans, it is often supposed an association with potential genotoxic exposure in this area. The aim of this study is to assess translocation frequencies by FISH chromosome painting in a cohort of Italian soldiers with past deployments in the Balkan area, to investigate a potential past genotoxic exposure in this operating theatre and compare these results with those obtained from control subjects similar to these soldiers for gender, age, place of origin and life-style, particularly with regard to smoker status.

FISH translocation analysis was performed using home-made probes. Blood samples were analyzed by FISH whole chromosome painting by labelling simultaneously chromosomes 1, 2, 4 in red and 3, 5, 6 in green. This set of chromosome pairs represents the 58.4% of the whole genome. Translocations were scored in 1000 well-spread metaphases and expressed per 100 Cells Equivalents (CE) per subject. The results from the analysis of the control subject are reported.

2.2.2.1 Introduction

It is known that chromosome aberrations are a biological marker of clastogenic exposure and of cancer susceptibility [17], [20], [57], [115]. Cancer cells often contain chromosomes with large structural rearrangements, including deletions, duplications, inversion, isochromosomes, ring structures and marker chromosomes, unbalanced and balanced translocations. Although it remains unknown if the majority of these structural rearrangements have a causative role in solid tumours, or if they are merely the result of decreased DNA damage checkpoints, DNA repair pathways, and/or mitotic segregations error [128], a number of observations support the idea that translocations may be the most relevant cytogenetic endpoint for assessing cancer risk.

Genotoxic agents, such as chemical and physical agents, induce chromosomal aberrations including translocations. *In vivo* and *in vitro* studies using mouse models and human blood lymphocytes to determine the persistence of chromosome aberrations following radiation exposure [59], [60], [79], [81] have demonstrated that stable chromosome translocations produced by ionizing radiation persist long after exposure. This opens up the possibility of using translocations as a biomarker many years after medical, accidental or occupational exposure [129]. Fluorescence *In Situ* Hybridization (FISH) using whole chromosome painting allows the rapid detection of reciprocal and non-reciprocal translocations in addition to dicentrics, rings and fragments [95], [97], [119], [120], [131]. Chromosome painting application in human cytogenetic population monitoring [112], [130] has opened new knowledge into the aberration spectrum generated by genotoxic agents in exposed populations [51], [99]. FISH-based translocation assay has the potential to assess acute as well as chronic exposure in cases of accidental and occupational exposure to mutagen, either immediately following exposure, or retrospectively by defining cumulative effects to red bone marrows.

The aim of this study is to assess translocation frequencies by FISH chromosome painting in a cohort of Italian soldiers with past deployments in the Balkan area to investigate a potential past exposure to mutagen substances in this operating theatre. In 2000, the international and national media reported on cases of leukaemia among Balkan deployed soldiers or peacekeepers which some attributed to presumed exposure to Depleted Uranium (DU), originating from DU-containing ammunition used by NATO Forces, leading to great public concern about hazard from depleted uranium [7]. Few epidemiological studies of cancer

incidence among UN personnel serving in the Balkan area have been published so far [47], [56], [91], [109], [127]. These studies did not demonstrate an increased incidence of all cancers or leukaemia among Balkan veterans compared to their national rates for the general population of comparable age and sex. To date, an excess of Hodgkin's lymphoma has been reported only among Italian troops involved in Bosnia and Kosovo [47]. Assessments of dose and risk showed that no negative health effects were to be expected, either from the radiological or from the toxicological properties of depleted uranium, and the short latency from the start of exposure was not consistent with a causative role for depleted uranium [113]. However, it was noted that the follow-up period in these studies was still short compared to the latency time of cancer development in association with ionizing radiation. Moreover, other potential cancer hazards have also been present in the environment in the Balkans, such as organic solvents, lubricants, and motor exhaust [56].

2.2.2.2 Results

As preliminary results of this study 47 healthy male control subjects were analyzed for chromosome translocations. Their age ranged from 20 to 47 years old (mean age of 26) and 32% of them were from central Italy, 55% from southern and 13% from northern.

In Table 2-1 are summarized data obtained from the examined population. For each subject we scored about 1,000 metaphases. A total of 49,704 metaphases were scored, corresponding to 14,028 CEs.

We detected 138 translocated cells for a total of 270 translocations, ranging from 0 to 18 translocations for subject. For each individual we calculated the aberration frequency per 100 CEs. The translocation frequency ranged from 0.00 to 3.28 per 100 CEs. Furthermore, other structural aberrations were detected as deletions, insertions and aneuploidies, many of which were due to the loss of one painted chromosomes. In Figure 2-5 the type of aberrations scored are shown.

Table 2-1: Chromosomes Aberrations and Relative Frequencies Observed in the Control Population Analysed.

	Age	Analysed cells	Traslocated cells	Total traslocations	Translocation frequency	Analysed Cell Equivalent	Translocation frequency (CE)	Translocation frequency (100CE)
1	20	1472	0	0	0.0000	860	0.00	0.00
2	20	671	2	4	0.0060	392	0.01	1.02
3	20	1087	3	5	0.0046	635	0.01	0.79
4	20	1125	2	4	0.0036	657	0.01	0.61
5	20	1024	0	0	0.0000	598	0.00	0.00
6	20	1486	0	0	0.0000	868	0.00	0.00
7	20	1034	2	4	0.0039	604	0.01	0.66
8	21	1010	3	5	0.0050	590	0.01	0.85
9	21	940	3	6	0.0064	549	0.01	1.09
10	21	1251	2	4	0.0032	731	0.01	0.55
11	21	1004	0	0	0.0000	586	0.00	0.00
12	21	1084	2	4	0.0037	633	0.01	0.63
13	22	1051	2	4	0.0038	614	0.01	0.65
14	22	1254	0	0	0.0000	732	0.00	0.00
15	23	1020	3	5	0.0049	596	0.01	0.84
16	23	1149	3	7	0.0061	671	0.01	1.04
17	23	1031	2	4	0.0039	602	0.01	0.66
18	23	918	1	2	0.0022	536	0.00	0.37
19	23	1425	2	4	0.0028	832	0.00	0.48
20	24	1017	4	7	0.0069	594	0.01	1.18
21	24	866	4	8	0.0092	506	0.02	1.58
22	24	1102	1	2	0.0018	644	0.00	0.31
23	25	1068	0	0	0.0000	624	0.00	0.00
24	25	960	1	2	0.0021	561	0.00	0.36
25	25	1024	9	18	0.0176	598	0.03	3.01
26	25	1118	0	0	0.0000	653	0.00	0.00
27	26	904	2	3	0.0033	528	0.01	0.57
28	27	1009	4	9	0.0089	589	0.02	1.53
29	27	1042	4	8	0.0077	609	0.01	1.31
30	27	1037	3	6	0.0058	606	0.01	0.99
31	28	1107	3	6	0.0054	646	0.01	0.93
32	29	1008	4	8	0.0079	589	0.01	1.36
33	29	1294	4	7	0.0054	756	0.01	0.93
34	30	1007	2	4	0.0040	588	0.01	0.68
35	30	1028	4	8	0.0078	600	0.01	1.33
36	30	701	0	0	0.0000	409	0.00	0.00
37	30	1451	4	8	0.0055	847	0.01	0.94
38	31	910	2	4	0.0044	531	0.01	0.75
39	31	900	3	6	0.0067	526	0.01	1.14
40	32	1004	2	4	0.0040	586	0.01	0.68
41	35	1025	7	13	0.0127	599	0.02	2.17
42	36	1025	5	10	0.0098	599	0.02	1.67
43	38	912	7	14	0.0154	533	0.03	2.63
44	38	1080	7	13	0.0120	631	0.02	2.06
45	39	1013	5	10	0.0099	592	0.02	1.69
46	47	1012	5	10	0.0099	591	0.02	1.69
47	47	1044	10	20	0.0192	610	0.03	3.28
Total		49704	138	270	0.0054	14028	0.02	1.92

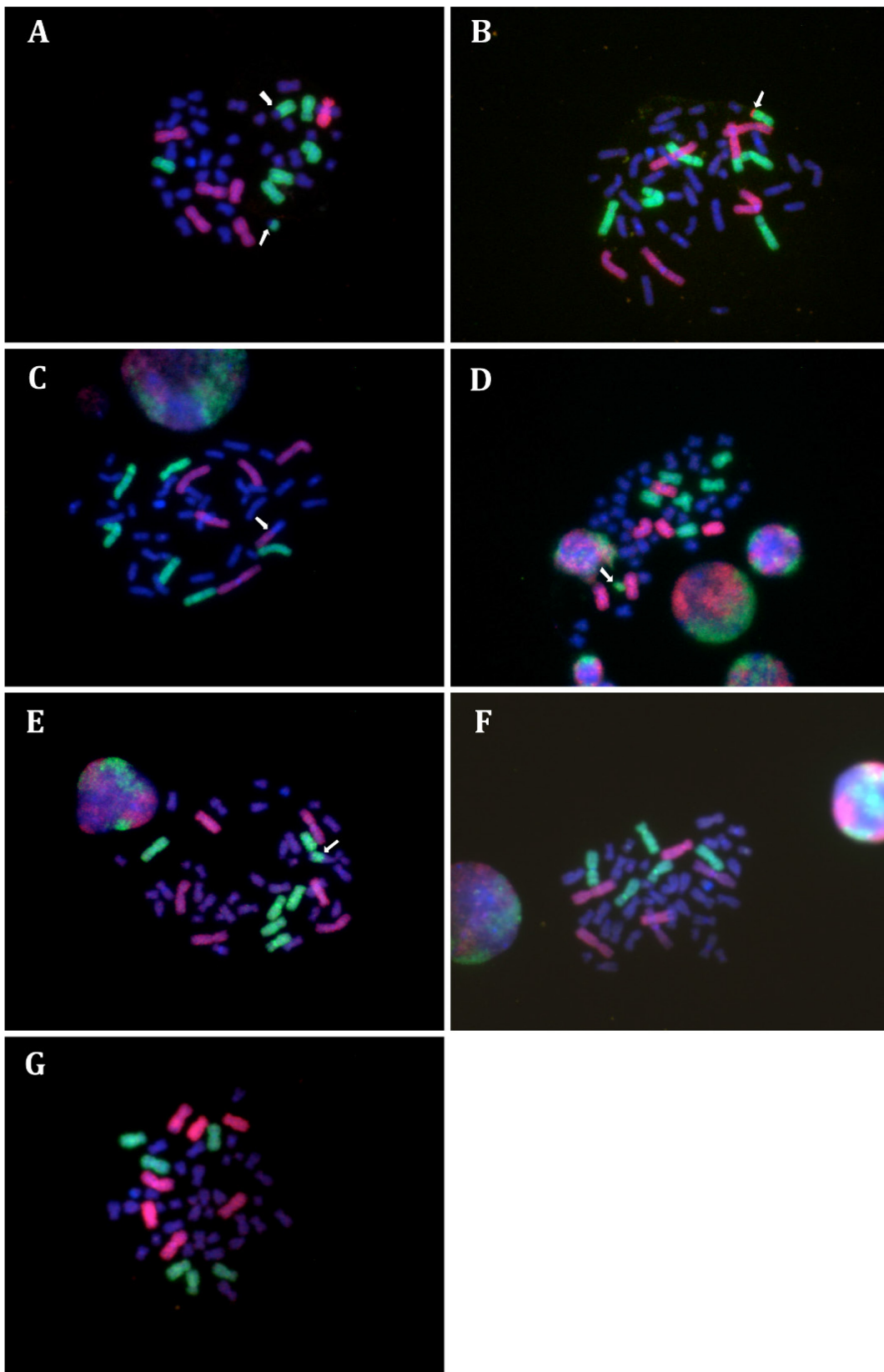


Figure 2-5: Chromosome Aberrations Scored – Two-Way Translocation (A and B); One-Way Translocation (C); Deletion (D); Insertion (E); Loss and Gain of One Chromosome (F and G respectively). Chromosomes 1, 2 and 4 are painted red; Chromosome 3, 5, and 6 are painted green.

From the analysis of overall translocations we have observed less one-way than two-way translocations; the latter amount to 260 (0.92 translocations per 100 CEs) while the one-way amount to 10 (0.03 per 100 CEs) with a significant statistical difference ($p < 0.0001$) in translocation frequency (Figure 2-6).

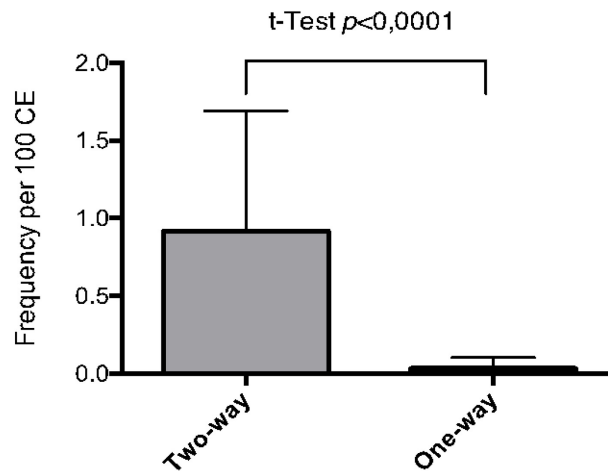


Figure 2-6: Comparison Between Two-Way and One-Way Translocation Frequencies. The difference between the two types of translocations is statistically significant ($p < 0,0001$).

We have determined whether translocations frequencies could be associated with age and geographical origin. Figure 2-7 illustrates the relationship between translocations frequencies and age. An increase of translocations with age is readily apparent, with a translocation frequency of:

- 0.64 in 20 – 25 age interval;
- 0.96 in 26 – 30 age interval;
- 1.19 in 31 – 35 age interval; and
- 2.17 in 36 – 47 age interval.

Figure 2-8 shows the translocations frequencies in associations with age and geographical origin of the subjects analyzed. The translocation frequencies amount to 1.04 for northern Italy, 0.85 for center Italy and 1.00 for southern Italy.

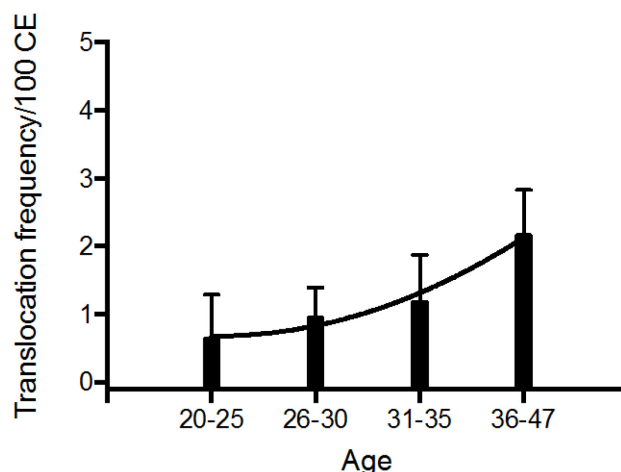


Figure 2-7: Translocation Frequencies per 100 Cell Equivalentents for the Different Age Intervals.

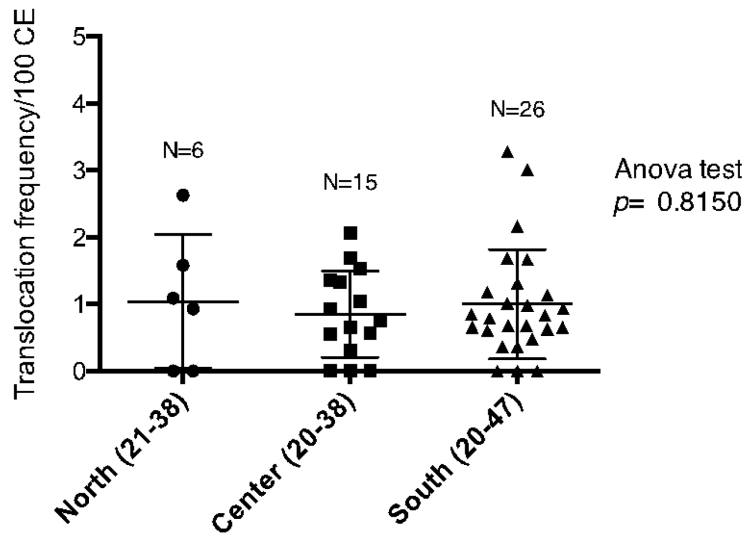


Figure 2-8: Translocation Frequencies per 100 Cell Equivalents by Age and Geographic Region.

To test the goodness of translocation frequencies with the age of the subjects we compared our data with values reported in a previous study by Sigurdson *et al.* [124]. We have converted the number of two-way translocations as a single event to adapt our data with those of Sigurdson and co-authors. We have observed a good correlation between the data using t-test with a p-value of 0.55. The results of this correlation are reported in Figure 2-9.

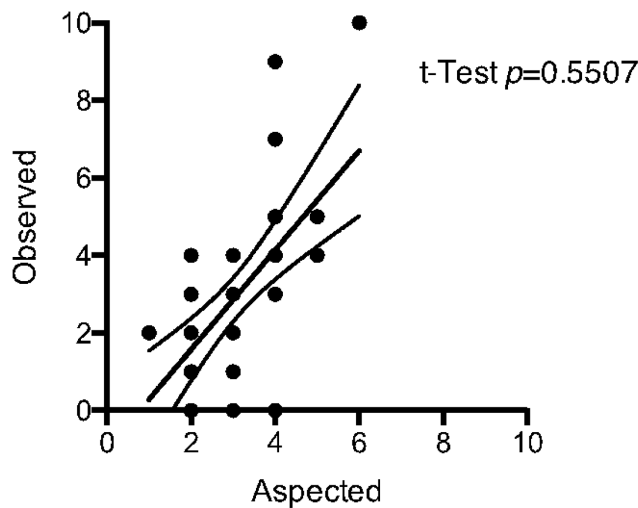


Figure 2-9: Comparison Between the Frequencies of Translocations Observed in this Study and the Frequency of Translocations Reported by Sigurdson *et al.* [124].

2.2.2.3 Discussion

The use of FISH with whole chromosomes probes provides an efficient approach for detecting structural chromosome aberrations in human lymphocytes. This rapid and sensitive technique is an effective tool for quantifying chronic exposure to environmental agents, which may result in an accumulation of cytogenetic

damage with age. Chromosome painting offers several distinct advantages over conventional cytogenetic techniques. First of all, the speed of analysis provides the ability to score large numbers of cells, thereby substantially increasing the statistical power that is needed to detect the possible effects that lifestyle and adverse environmental exposure may have on aberration frequencies. Secondly, the resolution of chromosome painting is such that rearrangement that can be detected is either too small or too difficult to resolve by conventional banding techniques. Finally, for routine aberration analysis, personnel require comparatively less training because aberration detection is based on visualizing colour changes between painted and unpainted chromosomes. When all these advantages are considered together, it is apparent that chromosome painting enables greater sensitivity towards the detection of environmental influences that may impact human health [114]. The use of chromosome painting has been also criticized because of its limitations, one of which is the inability to detect every chromosome exchange [119]. The fraction of all possible exchanges detected by painting depends on the amount of genome targeted [82]. It has been shown that the quality of the used chromosomes libraries, the choice of paints and the number of differentiated chromosomes within one metaphase are technical endpoints to be considered [16]. In the present study we painted, using home-made probes, Chromosomes 1, 2 and 4 in red and Chromosomes 3, 5 and 6 in green. This combination of probes gave us the advantage to detect 58.4% of all chromosomes exchanges. Moreover, the use of homemade probes led us to a substantial economic saving compared to the use of commercially available directly labelled probes.

FISH technologies can provide data only from a part of the genome so thousands of metaphases have to be analyzed to reduce the overall uncertainty. To address this issue, an automated system for an efficient detection and recording of fluorescent stained metaphases and their interactive analysis would therefore be highly desirable. In order to facilitate the scoring of the large number of cells needed for this study, we decided to use, for the microscope analysis, a semi-automatic scoring system. We performed this analysis using Metafer4 (MetaSystem GmbH, Germany) fluorescence scanning system. This computer-assisted metaphase scoring is a reliable alternative to manual scoring and led us to a considerable time-saving.

This is one of the first studies that aims to evaluate past exposure to genotoxic agents in Italian soldiers with past deployments in the Balkan area using FISH methodology to assess the cytogenetic damage. Here we reported preliminary data obtained from the analysis of the translocation frequencies of 47 healthy male control subjects. Most retrospective *in vitro* studies on radiation-exposed peripheral blood lymphocytes, and also studies of people accidentally exposed to high-radiation doses, show a higher proportion of two-way in comparison to one-way translocations [21], [75]. From our results, we observed that stable aberrations were more frequent than unstable aberrations. In particular two-way translocations were more frequent compared with one-way translocations, with a statistically significant difference ($p < 0.0001$). This result is supported by another work published by Edwards *et al.* [48]. In this multi-center data review of translocations detected by FISH the authors agreed that, over time, one-way translocations decrease in frequency more rapidly than two-way translocations.

We have shown that chromosomes translocation frequencies (expressed per 100 CEs) in peripheral blood lymphocytes of these control group increase with increasing age. This observation is in agreement with many other studies, which have reported age as a strong predictor of translocations frequencies [80], [114], [124], [125], [130], [137]. Several age-related mechanisms may explain this observation. During the entire lifespan, a variety of adverse conditions cause damage to DNA; they include exposure to external damaging factors and endogenous factors, such as oxidative stress and replication or recombination errors, all these events in combination with a decline in DNA repair efficiency may be related with an increase in chromosomal aberrations. Although the number of samples examined is too small, our data didn't show any differences in translocation frequencies considering the geographical origin of the subjects.

Considerable attention and time have been devoted to the design of the study in order to isolate the variable of interest as far as possible and to set up the scoring methodology more convenient for our purpose. We confirmed FISH as a reliable and efficiency approach that greatly facilitated the detection of

chromosomes aberrations, and the use of Metafer4 as a really suitable and rapid system of aberration analysis. In summary, here we reported preliminary data regarding the control subjects involved in this study. These preliminary results on the frequency of translocations among the control groups are consistent with data from previous study showing that stable cytogenetic damage accumulates with age. In the future, based on the results presented, we will do further investigations to evaluate the cytogenetic findings regarding the control group study, and we will start with the analysis of the study group, in order to evaluate the translocation frequencies in subjects potentially exposed to mutagen substances.

2.2.3 Pilot Biomonitoring Study for Ionizing Radiation Exposure in Operational Theatres: Dog as Sentinel of Environmental Risk

2.2.3.1 Background

Cases of leukemia and lymphoma reported in 2001 among soldiers or peacekeepers deployed in Balkans raised the question on a possible exposure to depleted uranium in this area and many studies were performed on Balkans and Gulf war veterans [85], [87], [109], [121]. Then, Italian Ministry of Defence was concerned in identifying potential health risk associated with the exposure to chemical and physical genotoxic agents of the Italian soldiers deployed in *operational theatres*. A *biomonitoring study carried out* in the Italian Army military personnel deployed in Iraq did not detect any toxicologically relevant variation of DNA-damage biomarkers related to the exposure in the operational theatre [19].

The present study is related to a pilot project addressing the safeguard of Italian military personnel from health hazards associated with possible environmental risk in international areas.

For this aim we selected groups of soldiers and their army dogs. Military working dogs deployed in *operational theatres* could be considered as animal sentinels providing information about chemicals/radiation environmental exposure with potential adverse health effects for their conductors. Studies on cancer incidences in military working dogs deployed in Vietnam indicated the dog as useful bioindicator of carcinogenic risk to war veterans [84]. These working dogs may be even more exposed than their conductors mainly to the contaminants present in soil of the operational area and, as previously reported, they seem to be more sensitive to genotoxic damage than humans. In addition military dogs are free from some of the typical confounders such as lifestyle and specific dietary factors. This condition could reduce some uncertainty associated with predicting human risk in biomonitoring studies.

Pet dogs could be used as sentinels for human genotoxic exposure. Dogs have shown to be good predictor of the environmental exposure to various pollutants in humans and seem to have similar responses to specific contaminants [8], [52], [62], [63]. Although dogs live in the same environments of humans, they are more exposed to contaminants than humans because they are in close contact with soil and rummage in the ground. Moreover, these animals appear more sensitive to genotoxic damage than humans. Few studies have been performed on genotoxic effects in dog. A first biodosimetry study using Micronucleus (MN) test, as a biomarker of chromosomal damage, reported a dose-related increase of MN frequency in peripheral lymphocytes of dogs *in vitro* exposed to increasing doses of ionizing radiation and indicated canine lymphocytes to be more radiosensitive than human lymphocytes [24]. Donmez-Altuntas [42] showed an induction of MN in peripheral lymphocytes in dogs treated with cadmium, a human carcinogen. Higher frequencies of MN were also reported in peripheral blood of pet dogs living in areas highly contaminated by organochlorine pesticides [10].

Aim:

- To evaluate the effectiveness of using military working dogs as bioindicators for the environmental risk exposure to radiation and/or chemical genotoxic agents in *operational theatres*.
- To monitor military personnel deployed in *operational theatres*.

2.2.3.2 Study Design

- Standardization of the experimental protocol for Cytokinesis Block Micronucleus (CBMN) assay in peripheral lymphocytes of dogs.
- Establishment of Micronucleus dog calibration curves.
- Recruitment of a small group of soldier and dogs with no or at most two previous missions.
- Analysis for each soldier and dog pre-deployment and post-deployment:
 - Micronucleus (MN) test and Dicentric (DIC) assay on soldiers.
 - Micronucleus (MN) test on dogs.
- Comparative analysis between pre and post- deployment.

2.2.3.3 Methods

2.2.3.3.1 Study Groups

Object of this pilot study was a small group of Italian military soldiers and their dogs of the Army Veterinary Center of Grosseto (Italy) deployed in Lebanon.

2.2.3.3.2 Human and Dog Calibration Curves

A standardized protocol for CBMN assay was established in peripheral lymphocytes of dogs for the determination of chromosomal damage using the MN frequency.

Micronucleus dose-response calibration curves for seven doses (0 – 4 Gy) of gamma radiation have been established following standardized criteria for 6 dogs Belgian Malinois (3 males and 3 females; age 3 – 4 years) and compared with the calibration curves in humans [18], [38].

2.2.3.3.3 Biomonitoring Study

A pilot biomonitoring study was performed in a group of 5 couples of militaries (5 males; age 33) and dogs (4 females and 1 male; age 3 – 4 years). Blood samples collection was carried out in two samplings before the deployment (11/2/2014; 25/3/2014) and one after deployment, about two weeks after returning to Italy (28/10/2014). We performed MN test both in dogs and soldiers. Besides, dicentric assay was carried out on soldiers.

2.2.3.4 Results

Canine lymphocytes appear more radiosensitive than human lymphocytes showing a higher decrease of the proliferation index at increasing radiation doses (Figure 2-10 and Figure 2-11). The comparison of MN calibration curves in humans and dogs (Figure 2-12 and Figure 2-13) indicates a good agreement between the two curves but a higher baseline level of DNA damage and micronuclei frequency was observed in dogs compared with humans (22.9 ± 6.2 vs 6.6 ± 2.5 mean MN /1000 BNcells).

The results of our pilot biomonitoring study in 5 couples of Italian militaries and their working dogs before and after the deployment in Lebanon didn't show any increase of MN and DIC frequency in soldiers related to their mission in this operational theater (Figure 2-14 and Figure 2-16). Conversely in dogs a significant increase of MN frequency after the deployment was observed (29, 39 vs 18.8 and 14.9 Mean MN/1000 BN cells) (Figure 2-15).

LOW-LEVEL RADIATION BIOEFFECTS

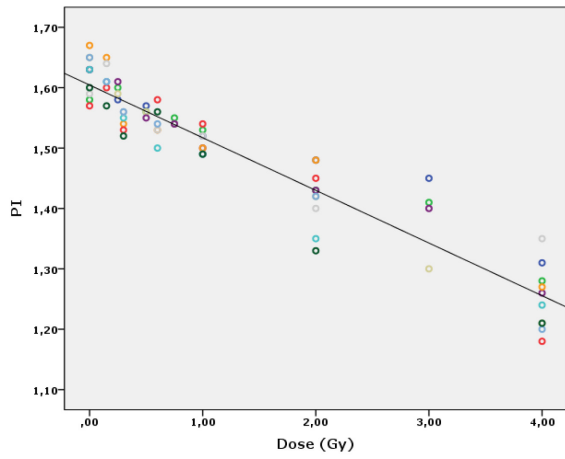


Figure 2-10: Proliferation Index (PI) Humans.

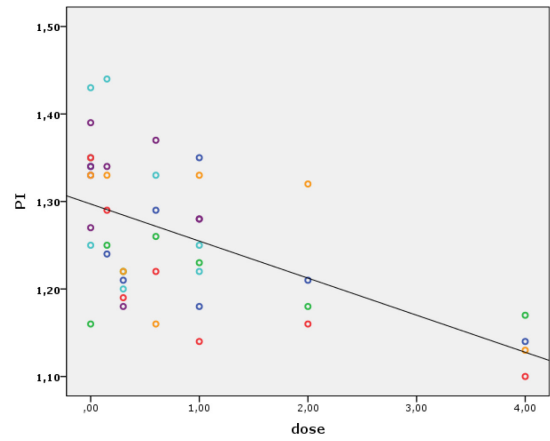


Figure 2-11: Proliferation Index (PI) Dogs.

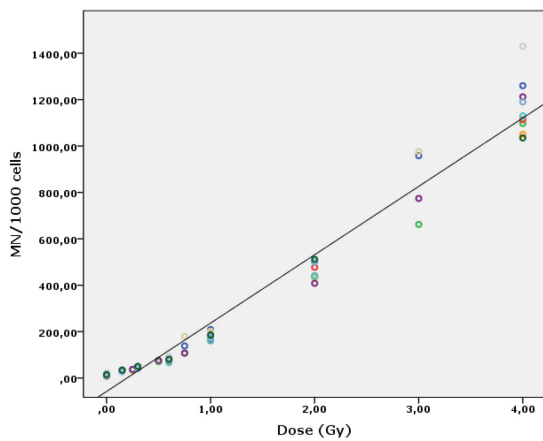
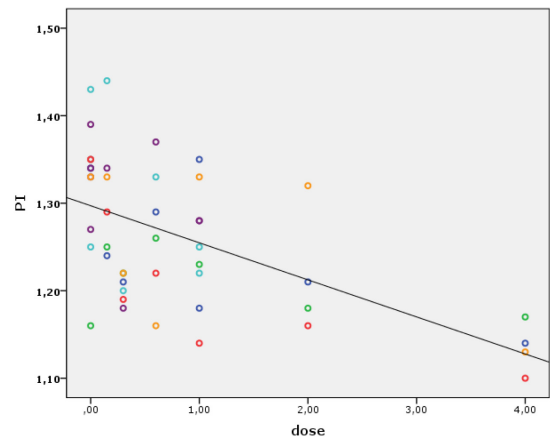
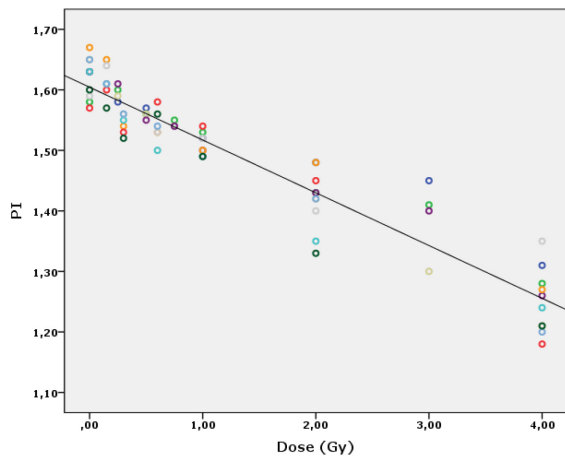


Figure 2-12: MN Dose-Response Curve (MN/1000 BN Cells) Humans.

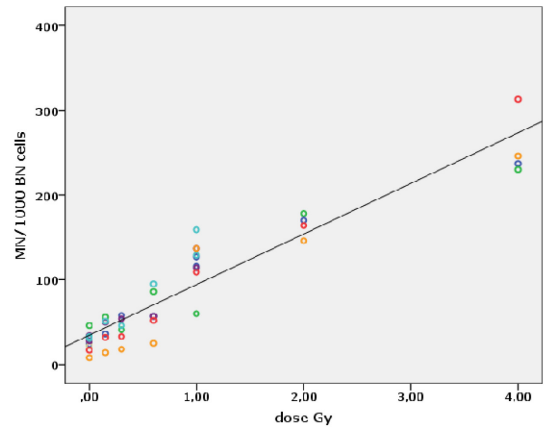


Figure 2-13: MN Dose-Response Curve (MN/1000 BN Cells) Dogs.

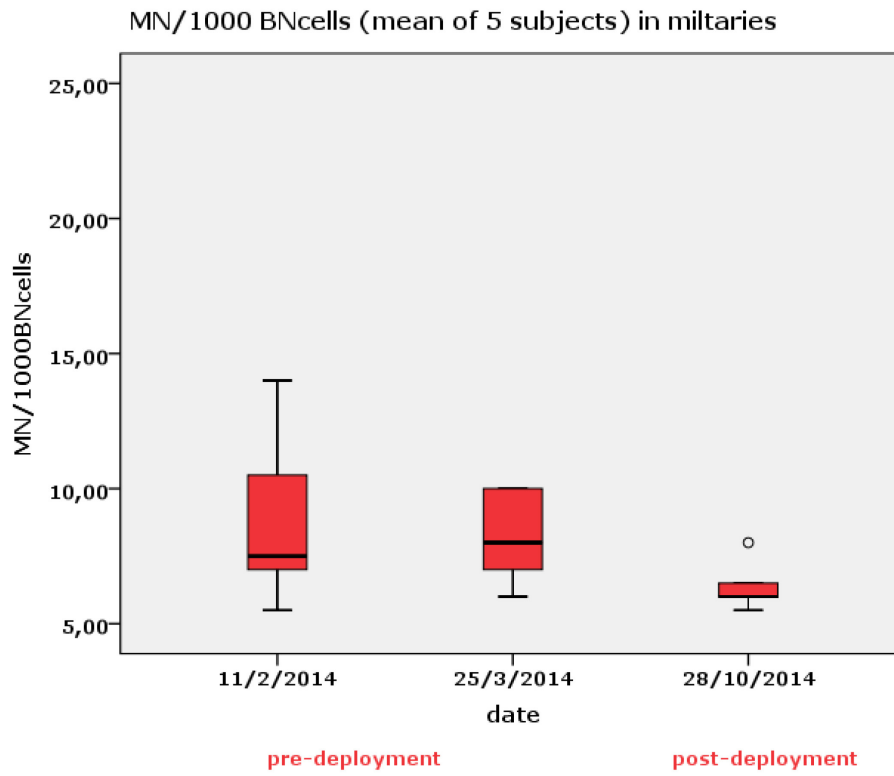


Figure 2-14: MN Frequency Pre- and Post-Deployment in Soldiers.

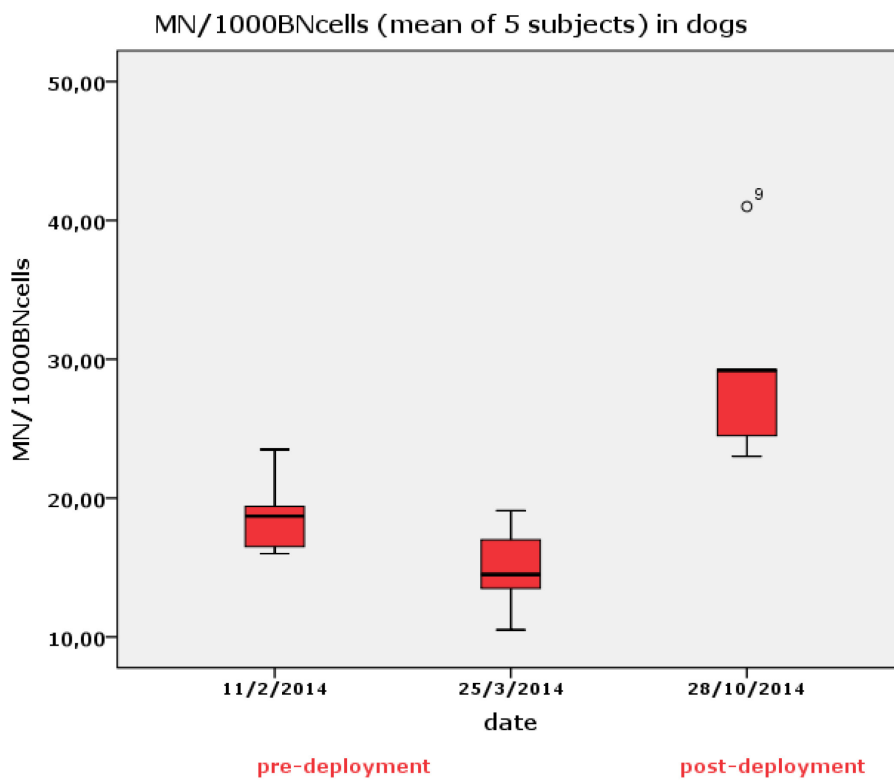


Figure 2-15: MN Frequency Pre- and Post-Deployment in Army Dogs.

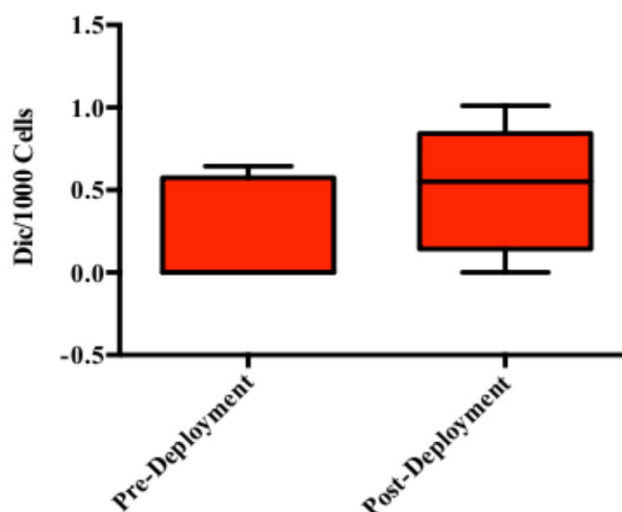


Figure 2-16: DIC Frequency Pre- and Post-Deployment in Soldiers.

2.2.3.5 Conclusions

The results obtained in this pilot study on soldiers and their army dogs deployed in Lebanon, are suggestive of agenotoxic damage in dogs associated with the period of stay in the *operational* theater. This animal appears more radiosensitive than human, confirming observations of other previous studies. Our results are promising to use micronucleus assay in this animal model as radiation indicator for biomonitoring of environmental genotoxic exposure, but for a reliable application of this biomarker the baseline frequency of micronuclei must be determined by increasing the number of dog samples. The induction of MN that we observed in army dogs deployed in Lebanon should be considered as a preliminary result and a greater number of samples of army dogs and soldiers deployed in this theater need to be examined. Finally, these data obtained in Lebanon deserve further investigations in other operational areas using also other genotoxicity biomarkers.

2.3 EARLY AND LATE EFFECTS

2.3.1 Evaluation of the Effect of Low Doses of Low-LET Radiation on the Innate Anti-Tumor Reactions in Radio-Resistant and Radio-Sensitive Mice

2.3.1.1 Introduction

In the present day military scenarios involving radiation exposure the majority of the personnel is likely to absorb low to intermediate doses of the predominantly low-LET¹ ionizing radiation [111]. Indeed, such doses will be incurred in areas of the enhanced radiation level due to the elevated natural background, contamination after explosions in nuclear installations or dispersal of radioactive material in the environment by other means (radiation dispersal devices) and even after detonations of tactical nuclear bombs. Absorption of such doses will not evoke any of the acute post-irradiation effects but can potentially be associated with a long-term risk of subsequent cancers. Interestingly, however, numerous experimental reports indicate that low-level exposures to low-LET ionizing radiation can retard the development of neoplasms in laboratory animals [22], [23], [25], [28], [61], [64], [66], [67], [70], [76], [92], [93], [100], [103], [107]. In these studies the animals were inoculated with tumor cells and the observed tumor-inhibitory effects of the exposures

¹ LET (Linear Energy Transfer) is a measure of the energy transferred to the material along the path of an ionizing particle. Typically, this measure is used to quantify the effects of ionizing radiation on biological specimens.

were generally detectable when whole bodies of the subjects were irradiated before the inoculations. In contrast, local irradiations of the growing tumor neither inhibited the inception of metastases nor stimulated lymphocyte migration to the neoplastic tissue [61], [117]. These findings suggest that reactions of the immune system may be involved in the anti-tumor effects of the exposures.

We have corroborated and extended some of the above results demonstrating that the development of the pulmonary tumor colonies in BALB/c mice intravenously (i.v.) injected with syngeneic L1 sarcoma cells was significantly inhibited after single Whole Body Irradiation (WBI) with 0.1 or 0.2 Gy X-rays [27], [28], [30], [68], [101], [106], [107]. Similarly, mice from the same strain exposed to 0.01, 0.02 or 0.1 Gy X-rays daily for ten days had markedly fewer induced ‘metastases’ in the lungs than their sham-irradiated counterparts [100]-[104]. These effects were accompanied by the significant up-regulation of the anti-tumor cytotoxic reactions of Natural Killer (NK) lymphocytes (mediated in part by the perforin and/or the Fas receptor ligand pathways) and/or activated macrophages (through the production of nitric oxide) [26]-[30], [68], [100], [102]-[107]. We further demonstrated that both single and fractionated irradiations of BALB/c mice at total absorbed doses of 0.1, 0.2 and 1.0 Gy X-rays significantly stimulated the production of IFN- γ and IL-2 by the NK cell-enriched and total splenocytes, respectively, as well as of IL-1 β , IL-12 and TNF- α by activated peritoneal macrophages [25], [26], [100], [102]-[104]. Collectively, our findings supported the notion that cooperation of macrophages and NK cells may be necessary for the efficient control of the development of both primary and secondary tumors *in vivo* [140].

All our previous examinations were performed on the relatively radiosensitive BALB/c mice.

Obviously, other results may be seen in strains of the differently determined immunological profile and/or radio-sensitivity. Hence, in the present study we also employed C57BL/6 mice which exhibit a Th1/M1 (Thlymphocyte/Macrophage; pro-inflammatory) response, are more radio-resistant, and develop fewer types of cancers following irradiation than BALB/c mice which express the Th2/M2 (anti-inflammatory) phenotype [71], [90], [108], [110], [126], [132], [133], [138]. Since the latter two differences may result from different responses of the immune systems of the two strains to radiation and in view of the important role of cytotoxic macrophages and/or NK cells in the innate anti-neoplastic immune system [6], [12], [50], [77], [94] the aim of our study was to evaluate the effects of fractionated low-level exposures of C57BL/6 and BALB/c mice to X-rays on the growth of induced tumor colonies and activities of cells involved in the innate anti-tumor immunity.

For the experiments, we used male BALB/c and C57BL/6 mice aged 6 – 8 weeks. Peritoneal macrophages (M ϕ) and NK cell-enriched splenocytes (NK cells) were collected from the animals exposed to fractionated (5 days/week for 2 weeks) irradiation to obtain the absorbed doses of 0.01, 0.02 or 0.1 Gy per mouse per fraction, so that total absorbed doses per mouse equalled to 0.1, 0.2 or 1.0 Gy, respectively. After the irradiations some mice were intravenously injected with syngeneic L1 sarcoma cells (BALB/c mice) or Louis Lang Carcinoma (LLC) cells (C57BL/6 mice), sacrificed fourteen days later and tumour colonies were counted on the surface of the removed lungs. In the separated cell populations the following assays were carried out:

- a) Cytotoxic activity;
- b) Blockade of the selected mechanisms of cytotoxicity; and
- c) Secretion of cytotoxic factors such as Nitric Oxide (NO), IL-1 β , IL-2, IL-12, IFN- γ or TNF- α .

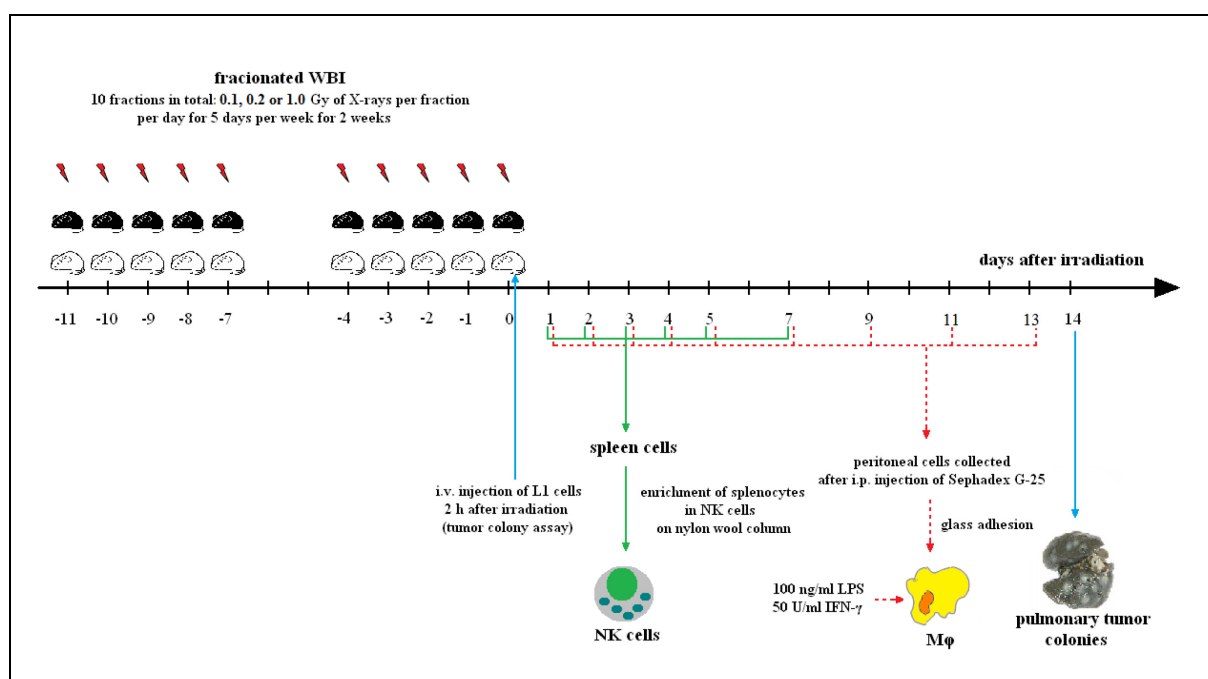


Figure 2-17: Experimental Protocol for Studying of the Effect of Low Doses of Low-LET Radiation on the Innate Anti-Tumor Reactions in Radio-Resistant and Radio-Sensitive Mice.

2.3.1.2 Results

The results demonstrated that ten daily exposures of BALB/c and C57BL/6 mice to 0.01, 0.02 or 0.1 Gy X-rays significantly stimulated anti-neoplastic functions of the NK cell-enriched splenocytes and the *in vitro* activated macrophages obtained from both strains and that such effects coincided with the radiation-induced suppression of the induced tumor colonies in the lungs of the animals. There were, however, few differences in reactions of the BALB/c and C57BL/6 mice to the exposures: the post-exposure reduction in the numbers of the tumor colonies in the lungs was more pronounced in BALB/c than C57BL/6 mice and the effect appeared to be dose-independent, whereas in the latter mice the reduction was less marked (especially following the lowest dose) and clearly increased with the rise of the absorbed dose.

As shown in Figure 2-18A, WBI of BALB/c mice with 10 daily doses of 0.01, 0.02, and 0.1 Gy X-rays prior to i.v. injection of L1 cells resulted in the significantly reduced number of the developed tumor colonies in the lungs (expressed as percentages of the control values obtained in the sham-exposed animals). Since in all the irradiated groups of the mice there was an approx. Forty-five (45) % reduction in the number of the colonies, the effect seemed to be dose-independent.

In contrast, although ten daily exposures of C57BL/6 mice to 0.01, 0.02, or 0.1 Gy of X-rays (Figure 2-18B) also markedly inhibited the development of the pulmonary tumor colonies produced by injection of the syngeneic LLC cells, the effect seemed to be dose-dependent – the strongest reduction was detected after irradiations of the mice at 0.1 Gy daily (about 34%), while in the animals exposed daily to 0.01 or 0.02 Gy the number of the colonies decreased by about 18% and 26%, respectively.

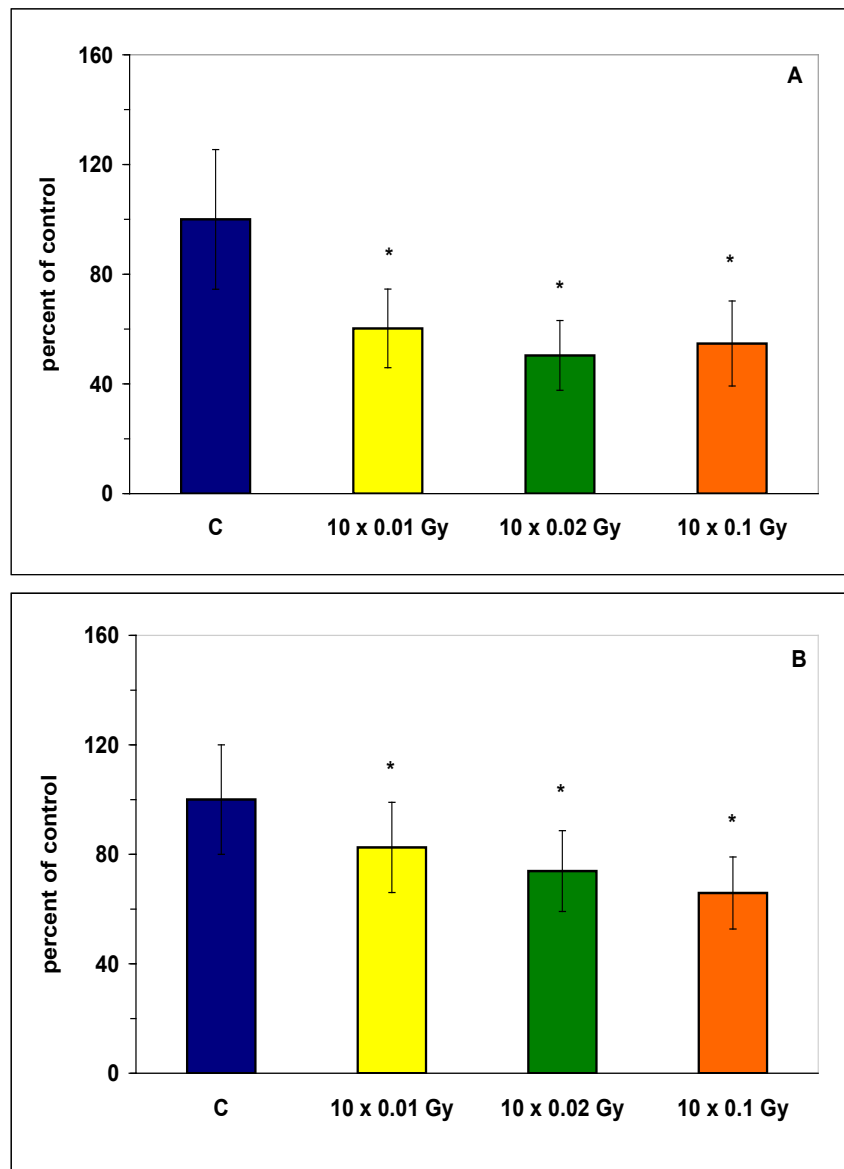


Figure 2-18: Development of Induced Metastases in the Lungs After Fractionated WBI of BALB/c (A) and C57BL/6 (B) Mice.

In terms of the cytotoxic activity of the NK cell-enriched splenocytes, in BALB/c mice stimulation of this activity occurred earlier after cessation of the irradiations, while in C57BL/6 mice similar effects were detectable later. As shown in Figure 2-19A, WBI of BALB/c mice with 10 daily doses of 0.01, 0.02 or 0.1 Gy X-rays led to the significant and comparable (i.e., dose-independent) enhancement of the cytolytic function of the NK cell-enriched splenocytes obtained from all the three groups of the exposed animals. This effect was pronounced already on the first day after cessation of the irradiations and occurred for four days after the exposure ended. Between the fifth and seventh days post-exposure the activity of the NK cell-enriched splenocytes declined to the control level.

Cytotoxic activity of NK cell-enriched splenocytes collected from C57BL/6 mice after ten daily irradiations with 0.01, 0.02, or 0.1 Gy X-rays was also significantly and comparably stimulated (Figure 2-19B). However, the kinetics of this activity was different from that demonstrated in BALB/c mice, i.e., the effect cropped up on the third day after cessation of the exposures and carried on for at least four days to follow.

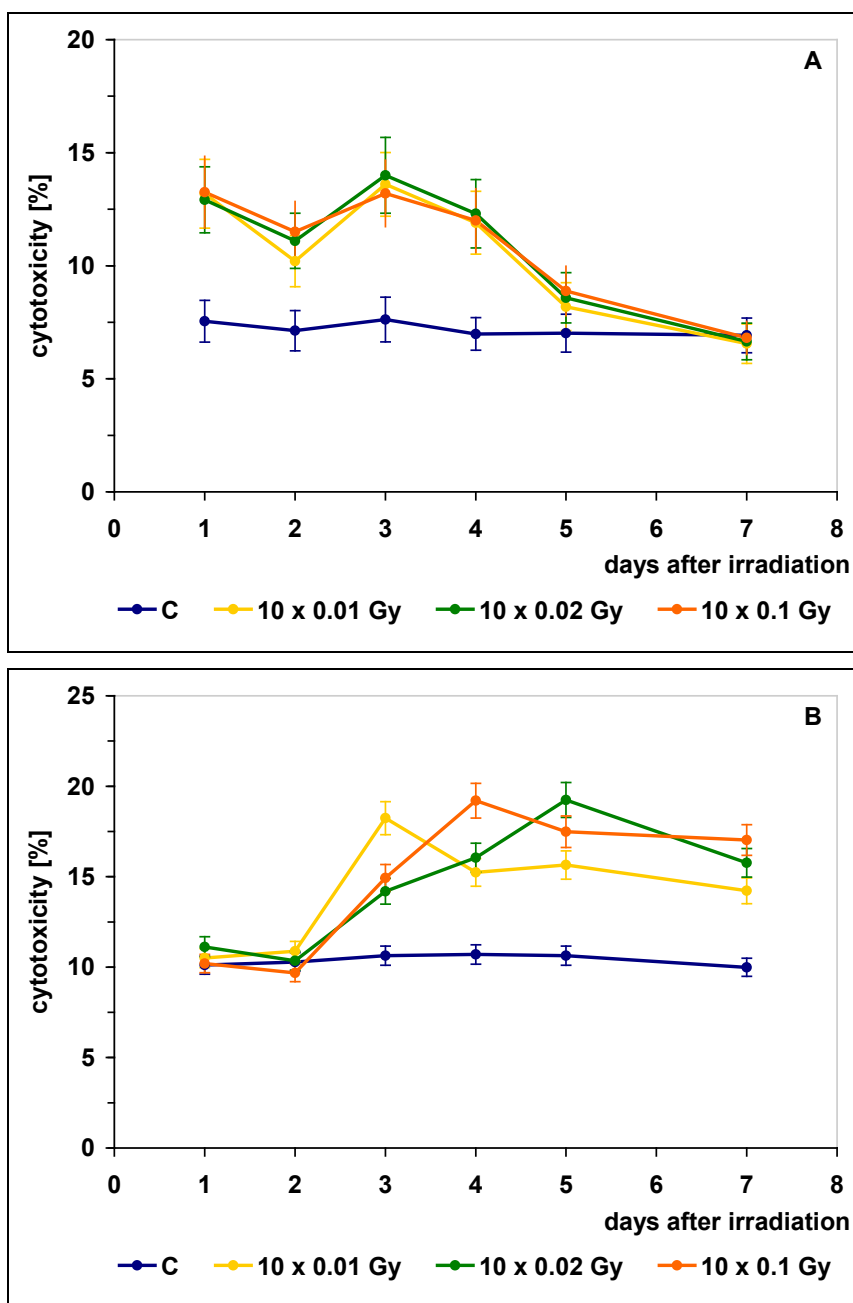


Figure 2-19: Cytotoxic Activity of NK Cells After Fractionated WBI of BALB/c (A) and C57BL/6 (B) Mice.

As shown in Figure 2-20, suppression of the perforin function by CMA markedly inhibited the cytolytic activity of the NK cell-enriched splenocytes collected from both irradiated and non-irradiated mice. The suppression was less, but still significantly, pronounced when the anti-FasL Ab was added to the incubation medium. Concurrent addition of the two blockers to the medium almost totally suppressed the cytotoxic function of the NK cell-enriched splenocytes collected from all the three groups of the irradiated animals. These results collectively indicate that both the perforin- and FasL-mediated cytolytic mechanisms are responsible, if to a different extent, for the enhanced cytotoxicity of the NK cell-enriched splenocytes demonstrated by us after cessation of the 10 low-level irradiations of mice with X-rays.

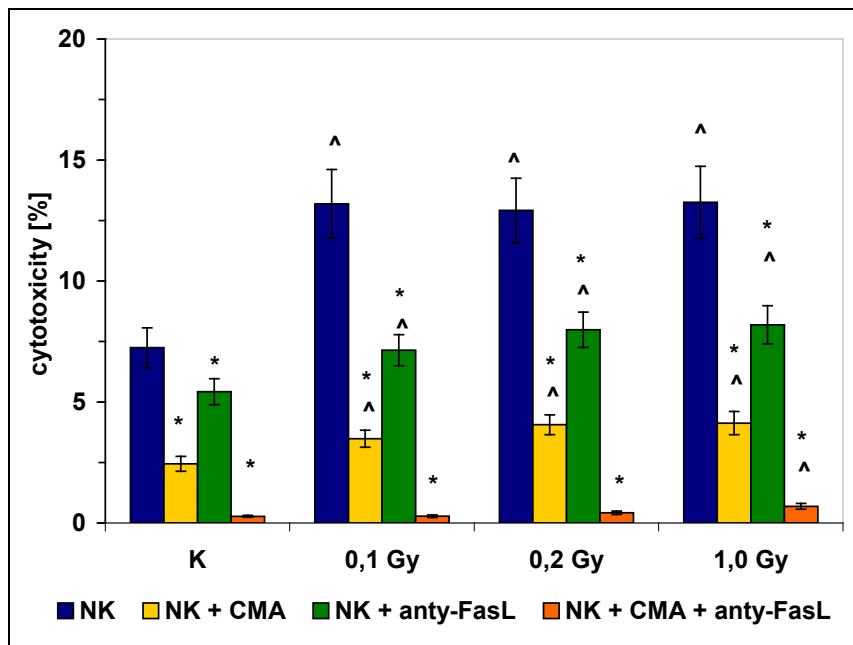


Figure 2-20: Inhibition of Cytotoxic Activity of NK Cells After Fractionated WBI of BALB/c Mice.

Our investigation also demonstrated that 10 repeated exposures of mice to 0.01, 0.02, or 0.1 Gy X-rays significantly stimulated the NK cell-enriched and total splenocytes to secrete IFN- γ (Figure 2-21A) and IL-2 (Figure 2-21B), respectively. IL-2 is a prominent activator of cytotoxic T and NK lymphocytes, whereas IFN- γ , although usually not directly cytotoxic for tumour cells stimulates cytolytic functions of macrophages and together with the macrophage-derived TNF- α and IL-1 β , can exert a strong anti-neoplastic effect. The stimulation was biphasic – in case of the former cytokine occurred already on the first day after cessation of the irradiations, and then after a transient decrease rose again between the third and fifth day, whereas in case of the latter cytokine, the stimulatory effect was detected between third and fourth days post-exposure, and after the decrease on day five, it rose again on the seventh day. Additionally the stimulation of the IL-2 production after ten daily exposures to 0.02 and 0.1 Gy of X-rays was slightly more pronounced than that of 0.01 Gy.

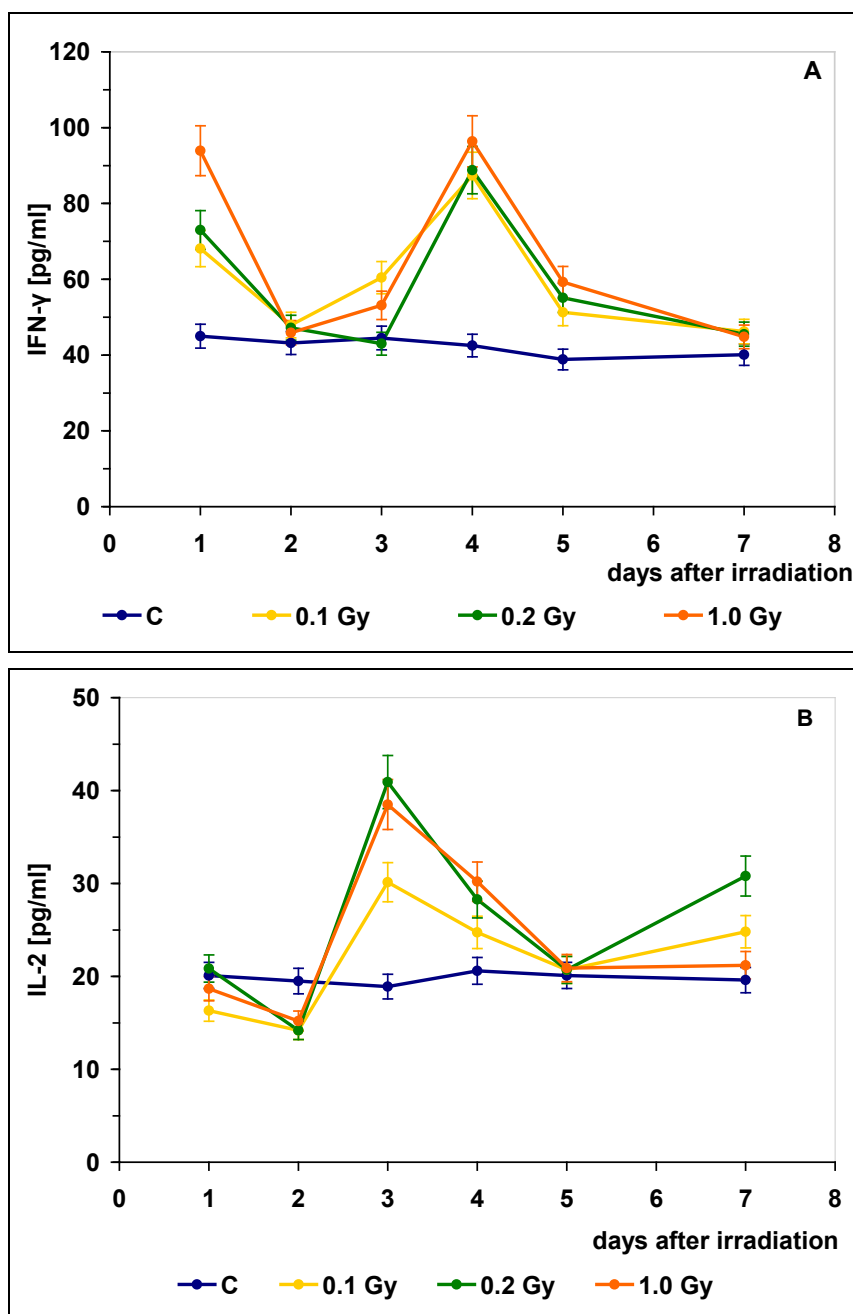


Figure 2-21: Production of IFN- γ by NK Cell-Enriched Splenocytes (A) and IL-2 by Splenocytes (B) After Fractionated WBI of BALB/c Mice.

In contrast to the cytotoxic activity of NK cell-enriched splenocytes, the low-level X-ray-induced up-regulation of the cytotoxicity of activated macrophages occurred earlier and was slightly more pronounced in the C57BL/6 compared to the BALB/c mice. As demonstrated in Figure 2-22A, WBI of BALB/c mice with 10 equal doses of 0.01, 0.02 or 0.1 Gy X-rays resulted in the significant, dose-independent (as indicated by the correlation analysis) stimulation of the cytolytic activity of activated against the P815 target cells. Enhanced cytotoxic function of the macrophages was detected on the second day after cessation of the exposures to X-rays, reached the highest values on the fourth (daily doses of 0.1 Gy) or fifth (daily doses of 0.01 or 0.02 Gy) days, and then, after a transient decline to the control level on the seventh day, was rising again until the 13th (at least) day post-exposure.

In turn, ten daily exposures of C57BL/6 mice to 0.01, 0.02, or 0.1 Gy of X-rays led to the significant and comparable stimulation of the cytotoxic activity of the activated macrophages, although the effect seemed to be slightly less pronounced after the daily irradiations with 0.02 Gy compared to 0.01 or 0.1 Gy (Figure 2-22B). As in BALB/c mice, the stimulation was also biphasic, with a transient decline to the control values on the seventh day, but the boosted cytotoxic function of the C57BL/6 macrophages was detectable already on the first day after cessation of the exposures and, past the seventh day nadir, was rising again only until the 11th day post-irradiation.

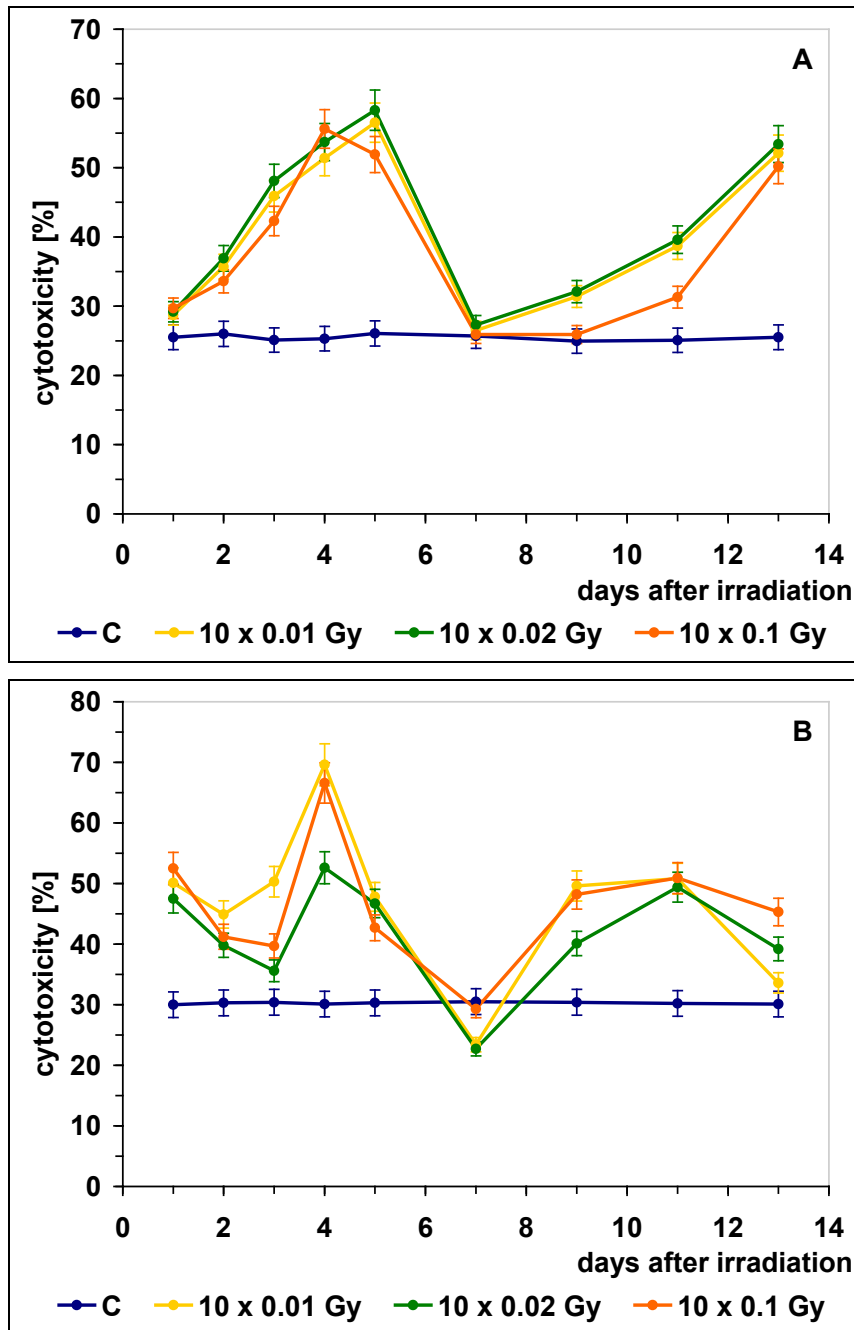


Figure 2-22: Cytotoxic Activity of Mφ After Fractionated WBI of BALB/c (A) or C57BL/6 (B) Mice.

As shown in Figure 2-23A, WBI of BALB/c mice with 10 daily doses of 0.01, 0.02 or 0.1 Gy X-rays resulted in the significant and kinetically comparable stimulation of the production of NO in macrophages incubated with IFN- γ and LPS. The enhanced secretion of NO was manifested already on the first day after cessation of the exposures, reached the highest levels on the fourth (daily doses of 0.1 Gy) or fifth (daily doses of 0.01 or 0.02 Gy) days post-exposure, declined to the control level on the seventh day (after irradiation with 0.1 Gy daily the decline below the control values occurred on days seventh and ninth post-exposure), and was rising again to the significantly increased levels until at least day 13 post-irradiation.

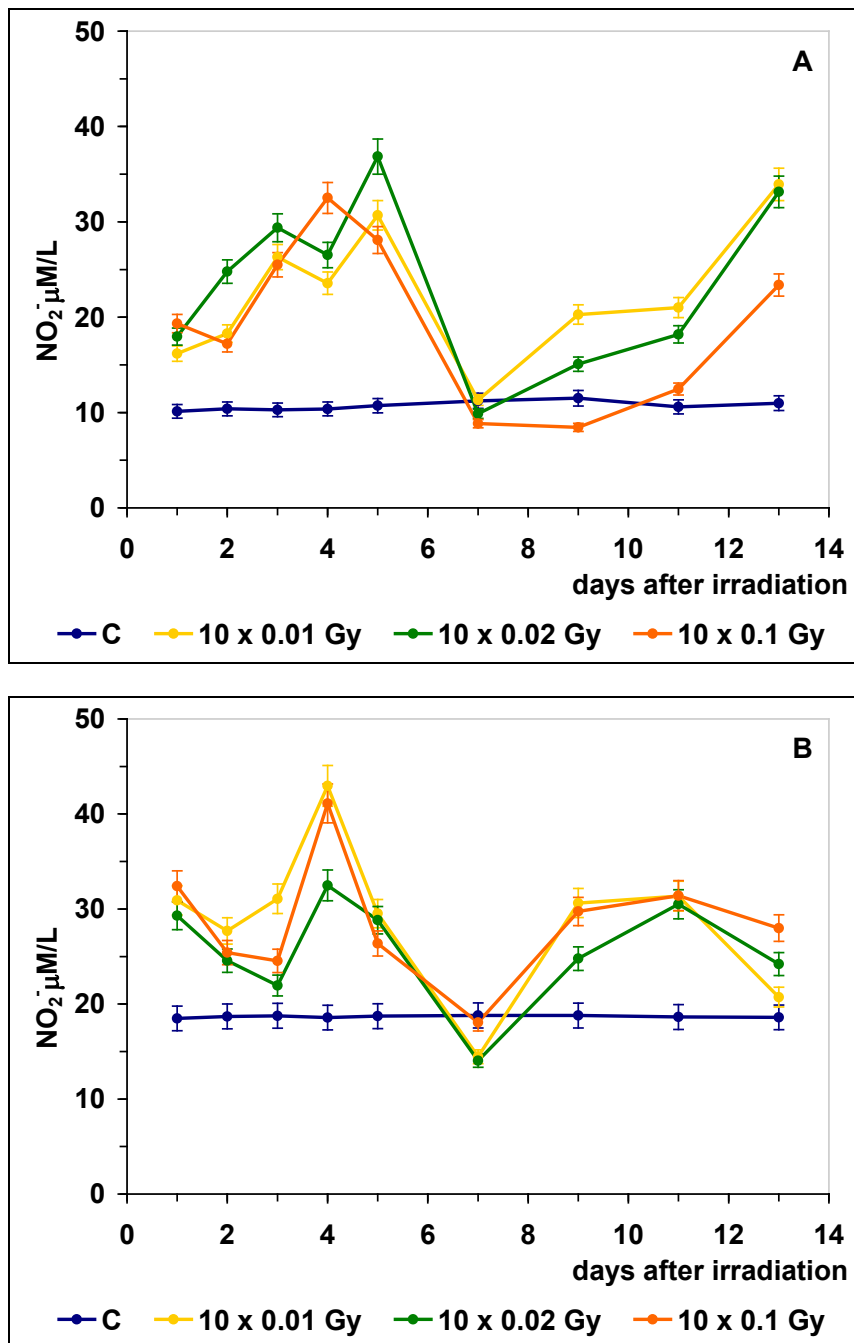


Figure 2-23: Production of NO by Mφ After Fractionated WBI of BALB/c (A) or C57BL/6 (B) Mice.

Likewise, ten daily exposures of C57BL/6 mice to 0.01, 0.02, or 0.1 Gy of X-rays led to the significant and stimulation of NO in the activated macrophages (Figure 2-23B). The effect was detectable already on the first day post-exposure and also followed the biphasic pattern – elevated secretion of NO reached the highest levels on the fourth day, declined to below the control levels on the seventh day, and then rose again to reach the second peak on the 11th day post-irradiation. Notably, in both strains of the mice, the kinetics of the stimulated production of NO in the activated macrophages closely followed the biphasic changes in the cytotoxic activities of these cells.

Decline of the boosted cytotoxicity of and NO synthesis in macrophages exactly at the same time (i.e., on the seventh day) post-irradiation followed by the second wave of stimulation observed in both strains is surprising and difficult to explain. Notably, very similar kinetics and similar differences between the BALB/c and C57BL/6 mice in terms of the production of NO by stimulated macrophages likely supports the described tumoricidal role of this molecule [35], [50], [69], [98], [139]. Based on the results of other authors [31], it can be speculated that the *in vivo* irradiations employed in the present study and/or the *in vitro* manipulations of the assayed cells might have caused shifts in the phenotypes of activated macrophages along the M1-M2 and the M2-M1 spectra.

We demonstrated previously that single exposures of BALB/c mice to low doses of X-rays significantly stimulated tumoricidal functions of activated macrophages and that the enhanced activity of these cells may, to an even larger extent than NK cells, may account for the tumor-inhibitory effect of such exposures [28], [107]. The present results demonstrate that both cell types may be responsible for the anti-metastatic effects of fractionated low-level exposures of both radio-sensitive (BALB/c) and radio-resistant (C57BL/6) mice to X-rays. Indeed, cooperation of macrophages, NK lymphocytes, and probably other cells of the anti-tumor surveillance system along with their cytotoxic factors is necessary for the efficient control of the development of both primary and secondary tumors *in vivo*. Thus, despite the fact that C57BL/6 and BALB/c mice vary in their Th phenotypes, transitions across the M1-M2 continuum of macrophage responses as well as other *in vivo* stimuli may explain the similar in the two strains final anti-tumor effect of the ten daily irradiations with low doses of X-rays.

In the present study we also demonstrated that multiple irradiations of BALB/c mice with total absorbed doses of 0.1, 0.2, or 1.0 Gy X-rays significantly stimulated macrophages to produce a number of cytokines with potential anti-neoplastic properties. These included IL-1 β , TNF- α , and IL-12. As indicated in Figure 2-24, irradiations of the mice with 10 equal doses of 0.01, 0.02 or 0.1 Gy X-rays also led to the significant enhancement of the production of IL-1 β , IL-12, and TNF- α by the activated macrophages. This effect was most pronounced on the fifth day after cessation of the exposures. Notably, in contrast to the rather dose-independent stimulation of the production of IL-1 β and IL-12, the enhanced synthesis of TNF- α was significantly more pronounced after the repeated irradiations with 0.01 and 0.02 Gy than with 0.1 Gy X-rays. Moreover, stimulation of the secretion of IL-12 and TNF- α by each of the three fractionated irradiations was much more pronounced than the same effect detected previously by us after single exposures to 0.1 or 0.2 Gy X-rays.

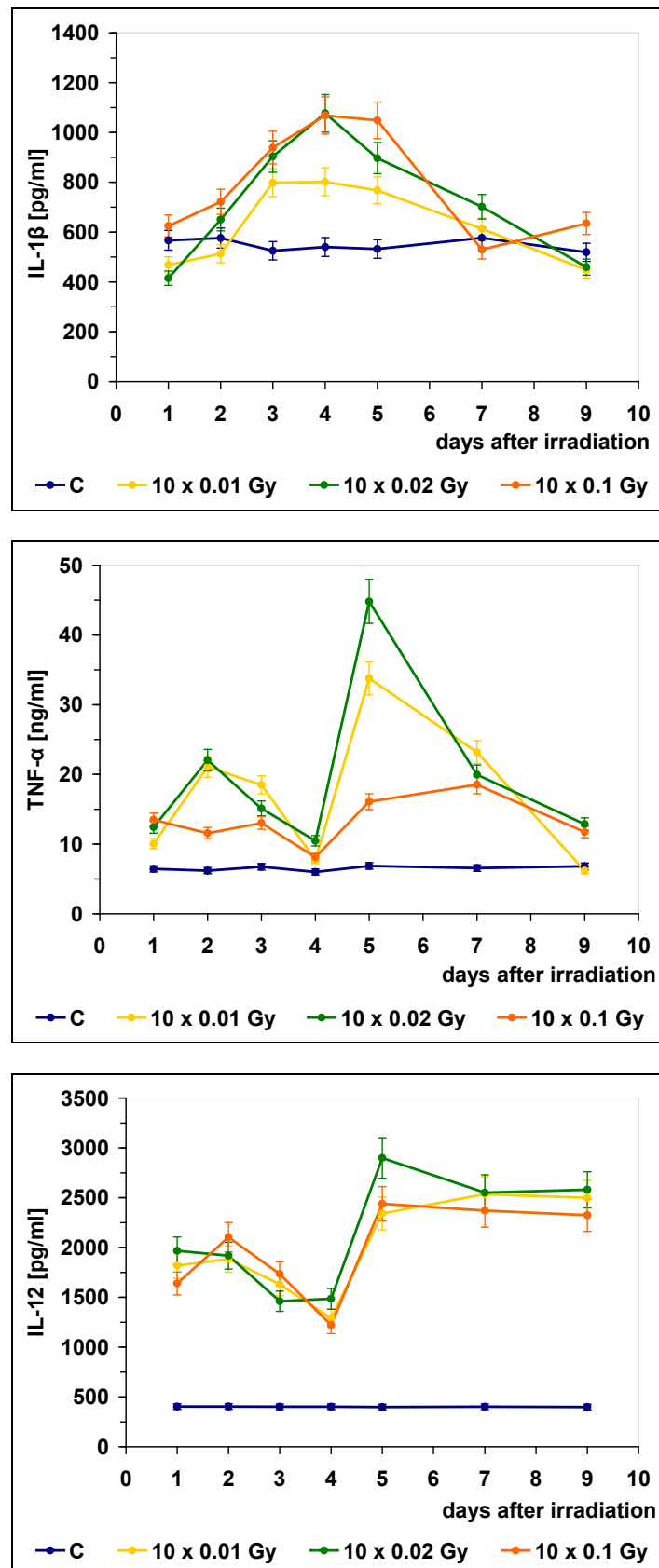


Figure 2-24: Production of IL-1 β , TNF- α and IL-12 by M ϕ After Fractionated WBI of BALB/c Mice.

2.3.1.3 Conclusions

The obtained data indicate that:

- 1) Despite some differences between radiosensitive BALB/c and radio-resistant C57BL/6 mice in the NK cell- and macrophage-mediated responses to repeated low-level irradiations at 0.01, 0.02 or 0.1 Gy X-rays, the final tumor-inhibitory effects of such exposures were comparable in the two strains.
- 2) Similar anti-metastatic immune mechanisms may operate in the irradiated BALB/c and C57BL/6 mice.
- 3) Whether or not observed variations in the kinetics and magnitude of the stimulation of the functions of macrophages and NK cells derived from BALB/c and C57BL/6 mice relate to the higher post-radiation tumor proneness of the former compared to the latter and/or to the differently genetically determined default M1/M2 phenotypes in the two strains remains to be elucidated in future studies.

2.3.2 Effect of Internal Contamination with Tritiated Water on the Innate Anti-Tumor and Inflammatory Reactions in Radio-Resistant and Radio-Sensitive Mice – A Preliminary Study

2.3.2.1 Introduction

People can be exposed today to low-level medical, occupational, and environmental ionizing radiation, the sources of which may be external (i.e., without contamination of the body) or internal, when radioactive material has deposited inside. Unlike the former, bio-medical effects of internal contamination are poorly characterized and understood. Hence, it was recently recommended that a review be conducted of the relevant risk of internal emitters [32]. One of the significant sources of internal radiation exposure of workers and members of the public is Tritium (T or ^3H), a radioactive isotope of hydrogen that binds with hydroxyl radicals to form tritiated water (HTO), which can be easily internalized by drinking, inhaling, or absorption through the skin. Naturally-occurring tritium is extremely rare, but it is a common by-product of nuclear reactors and is also used by a number of industries as well as for research and diagnostic purposes [134], [135]. Tritium decays to a stable atom of helium emitting an electron (β^- radiation), which has a mean energy of 5.7 keV and low-to-intermediate values of the Linear Energy Transfer (LET).

Initiation and progression of a malignant neoplasm depend on the composition and function of the environmental tumour niche [15]. In this milieu, an important role is played by cells of the immune system which generate both anti- and pro-neoplastic as well as anti- and pro-inflammatory responses [40], [41]. Diverse leukocyte populations found within growing tumours have been shown to adopt various phenotypes and bioeffector programmes that can differentially affect tumour progression [73], [86]. Most of these cells belong to innate immune system [41]. One of the recently recognized important function of this system is triggering and/or sustaining inflammation [11], which in turn promotes tumour growth, invasion, and metastases [86], [141].

Among cells which readily localize to sites of inflammation are monocytes/macrophages, which regulate local inflammatory responses [65], [78], [116], [141]. Tumour-associated macrophages consist of a spectrum of cell populations ranging from Type I (M1) macrophages (kill microorganisms and tumour cells, produce high levels of T- and NK-cell stimulatory cytokines and NO) to Type II (M2) macrophages (scavenge debris, promote cell proliferation and angiogenesis, repair damaged tissues) [11], [90]. Another cell population of the innate immune system that can bi-directionally interact with macrophages and dendritic cells are Natural Killer (NK) lymphocytes [39], [49], [58] which, depending on the context, produce either pro- (IFN- γ , TNF- α) or anti-inflammatory (TGF- β , IL-10) cytokines [33], [36], [37], [53].

Both activated macrophages and NK lymphocytes have long been recognized as the first line effectors of cytotoxicity aimed at neoplastic cells [49], [72]. Importantly, it was repeatedly demonstrated that low-dose

and low-dose-rate irradiations with X- and γ -rays result in suppression of both primary and secondary neoplasms in rodents and that the effects coexist with up-regulated cytotoxic function of NK lymphocytes and activated macrophages accompanied by the enhanced secretion by these cells of pro-inflammatory cytokines [22], [25], [28], [61], [67], [68], [70], [100], [102], [107]. On the other hand, many experiments have indicated that ionizing radiation stimulates tumour progression and activates pro-invasive and pro-metastatic activities of immune cells associated with inflammation in the tumour site (reviewed in Ref. [83]). Indeed, one of the manifestations of the inflammatory microenvironment is suppression of anti-tumour immunity [40]. Indeed, although it was shown that a high-dose (4 Gy) radiation promotes carcinogenesis by inducing a 'hospitable' tissue environment [13], [14], it is not clear whether such an effect can be instigated by low-level exposures to low-LET radiation and/or if the outcomes of the latter are qualitatively different from those of the higher dose irradiations.

The **concept** of the present investigation hinges on the assumptions that:

- a) One possibly underestimated health risk is internal contamination with tritium (mostly in the form of HTO).
- b) The most significant late effect of such a risk is cancer whose development is controlled by anti-tumour functions of the innate immune cells, which can also actively up-regulate the tumour-promoting inflammation.
- c) Virtually nothing is known about the effects of internal deposition of HTO on the immune and inflammatory responses related to malignancy.

In view of the above, the aim of the present study is to evaluate whether internal contamination of two strains of mice (which differ in their sensitivity to ionizing radiation and whose pro-inflammatory and macrophage-type responses are differently expressed) with HTO can modify the development of pulmonary tumour metastases and whether this effect can be associated with alterations in the anti- or pro-neoplastic functions of macrophages and NK lymphocytes.

In these investigations 6 – 8 week old BALB/c and C57BL/6 mice are intraperitoneally injected with tritiated water at total absorbed doses of:

- 0.01 Gy (a dose encountered in some occupational settings);
- 0.1 (upper limit of the low-dose region); and
- 1.0 Gy (a higher reference dose).

From Day 7, post-contamination with HTO (when almost all of the injected radioactivity was naturally removed from the body) on the selected days mice are anesthetized, blood, spleen, bone marrow, and peritoneal exudate are collected. As far, the following assays were conducted in the HTO-contaminated BALB/c and C57BL/6 mice:

- a) Production of nitric oxide by macrophages as a gauge of cytolytic function of these cells;
- b) Cytotoxic activity of NK lymphocytes;
- c) Peripheral blood counts; and
- d) Spleen and bone marrow cellularities.

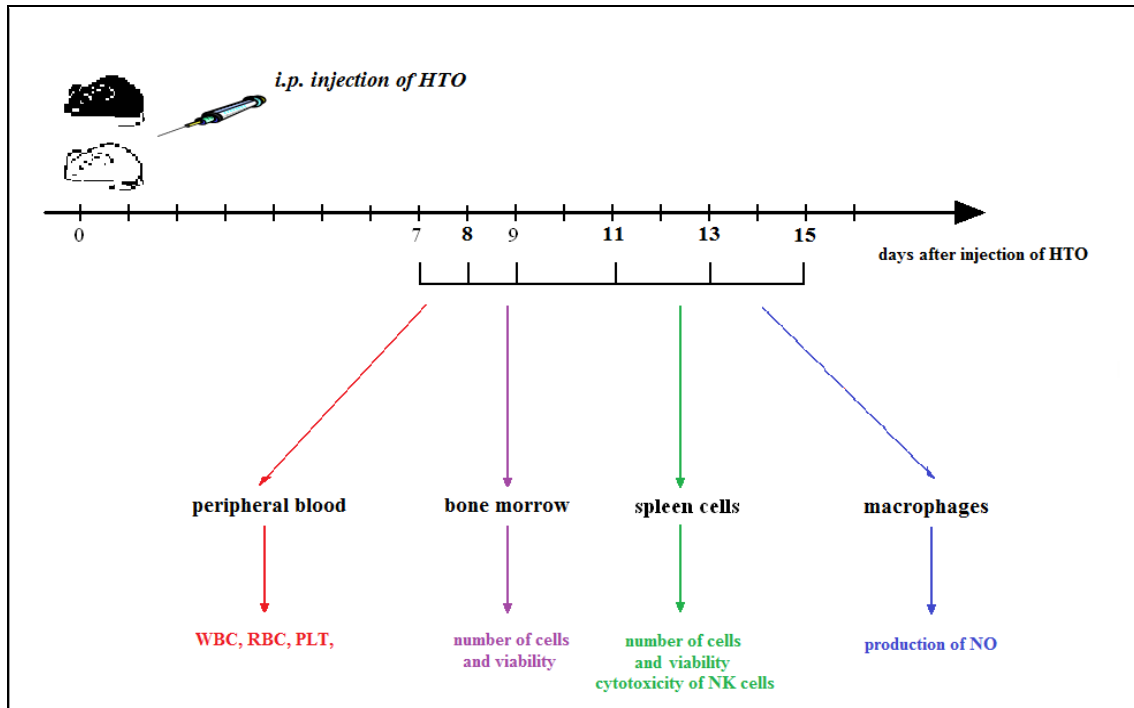


Figure 2-25: Experimental Protocol for Studying the Effect of Internal Contamination with Tritiated Water on the Innate Anti-Tumor and Inflammatory Reactions in Radio-Resistant and Radio-Sensitive Mice.

2.3.2.2 Results

As indicated in Figure 2-26, contamination of BALB/c mice with HTO at 0.1 Gy total dose stimulates cytotoxic activity of NK cells obtained from these animals; the effect was detected already on the first, second and fifth days post-contamination. When the total dose equals to 0.01 Gy the cytotoxic function of these cells is only slightly elevated. In turn, similar stimulation is recorded in C57BL/6 mice only on days 7 – 9 after their contamination with HTO at 0.01 Gy total dose (Figure 2-26).

As shown in Figure 2-27, contamination of BALB/c mice with HTO at 0.1 Gy total dose stimulates peritoneal macrophages obtained from these animals to produce elevated amounts of NO on Days 1 and 2 post-contamination and on Day 1 after their contamination with HTO at 0.01 Gy total dose. In turn, similar stimulation is detectable in C57BL/6 mice on days 1, 5 and 9 after their contamination with HTO at 0.01 Gy total dose as well as on Day 9 after their contamination with HTO at 0.1 Gy total dose (Figure 2-27).

As shown in Figure 2-28, exposure of BALB/c and C57BL/6 mice to HTO at doses of 0.01 or 0.1 Gy did not affect WBC, PLT or RBC counts. Moreover, the counts were comparable in both strains.

As indicated in Figure 2-29, significant alterations in bone marrow cells' numbers were detected in the two strains of mice after their contamination with HTO at 0.1 and 0.01 Gy total doses. Moreover, the numbers were comparable in both strains.

Similarly, no significant alterations in spleen cells' numbers were detected in the two strains of mice after their contamination with HTO at both total doses. However, the numbers were twice as high in BALB/c as in C57/BL6 mice.

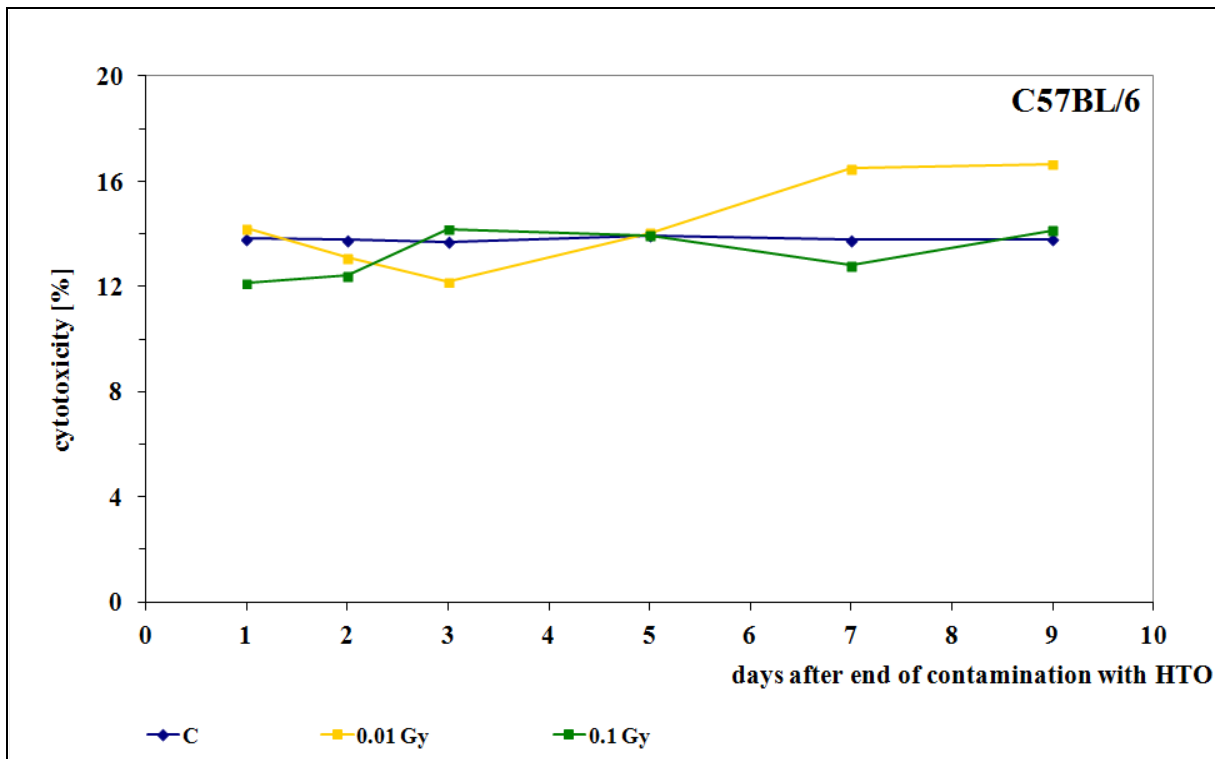
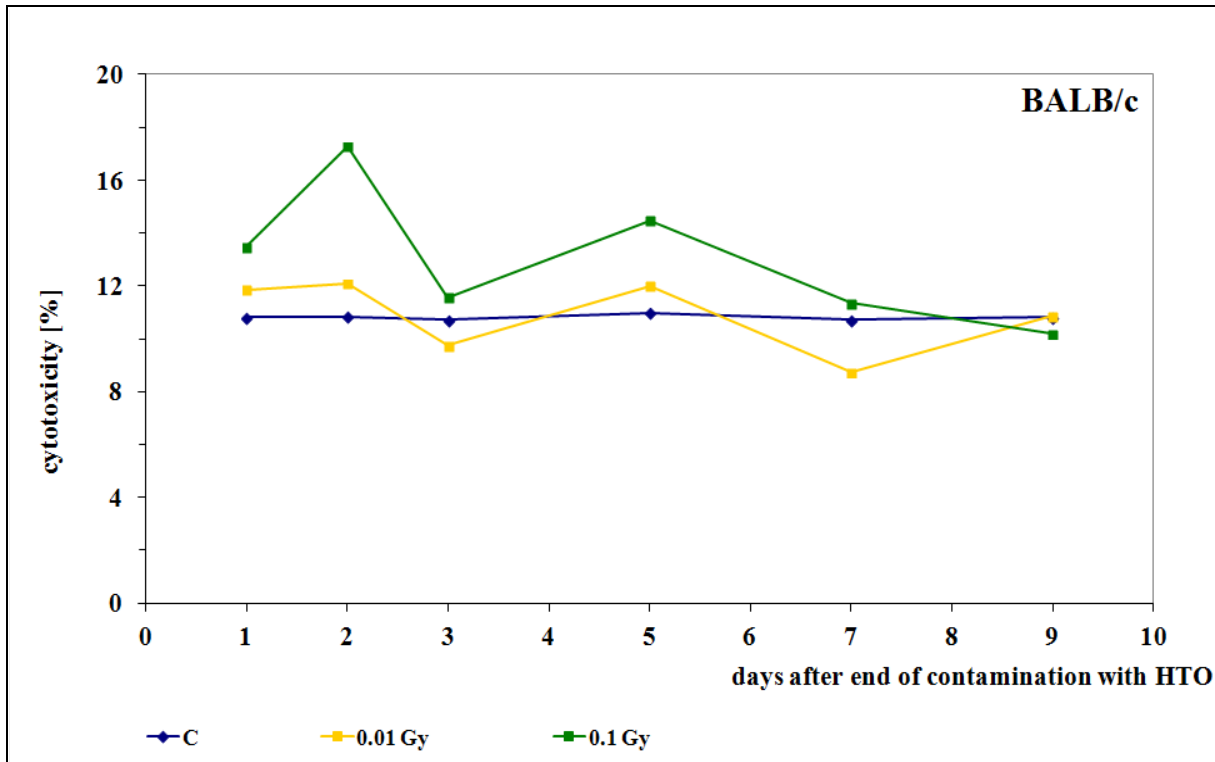


Figure 2-26: Cytotoxic Activity of NK Cells After Contamination with HTO of BALB/c or C57BL/6 Mice.

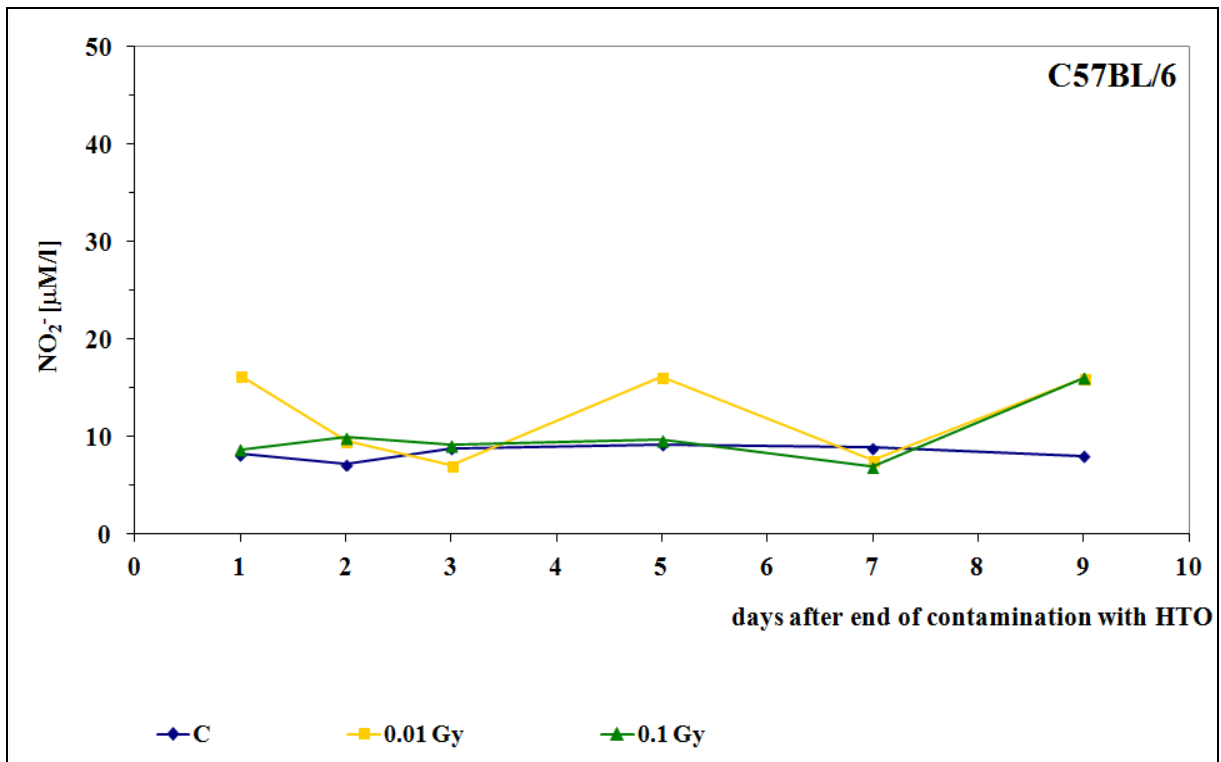
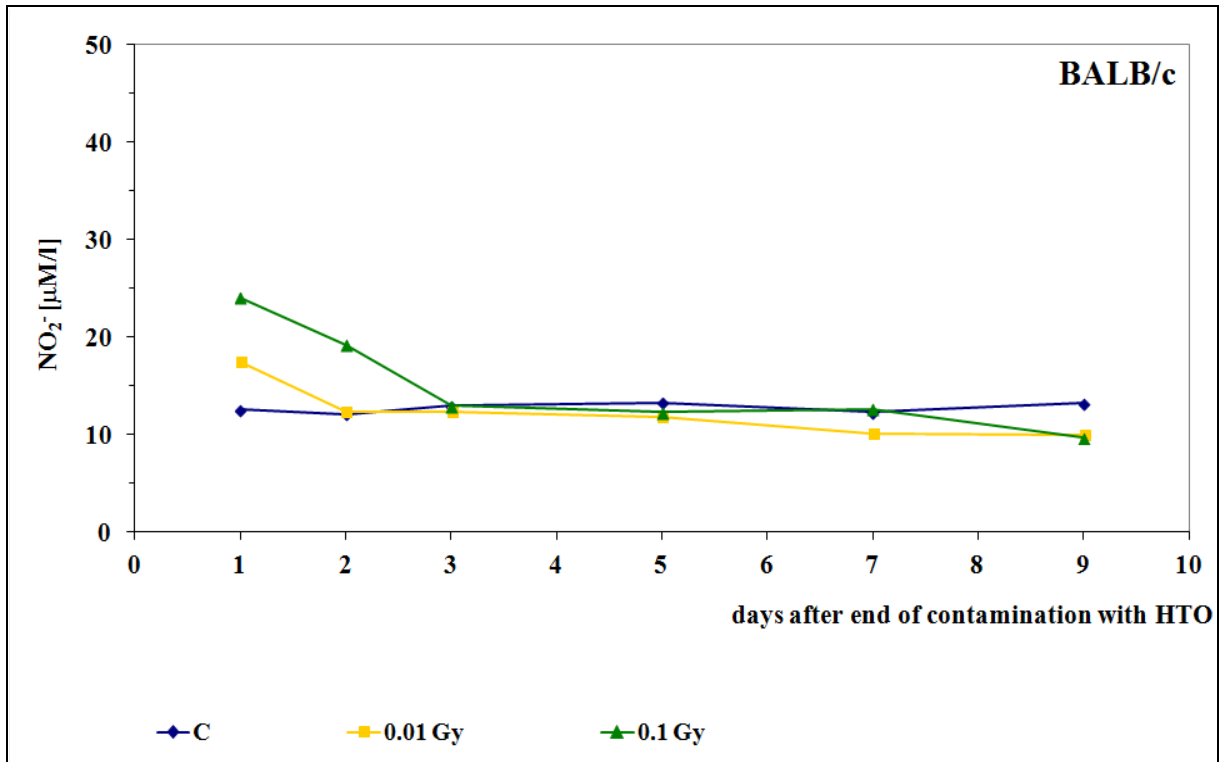


Figure 2-27: Production of NO by M ϕ Obtained from BALB/c or C57BL/6 Mice Contaminated with HTO.

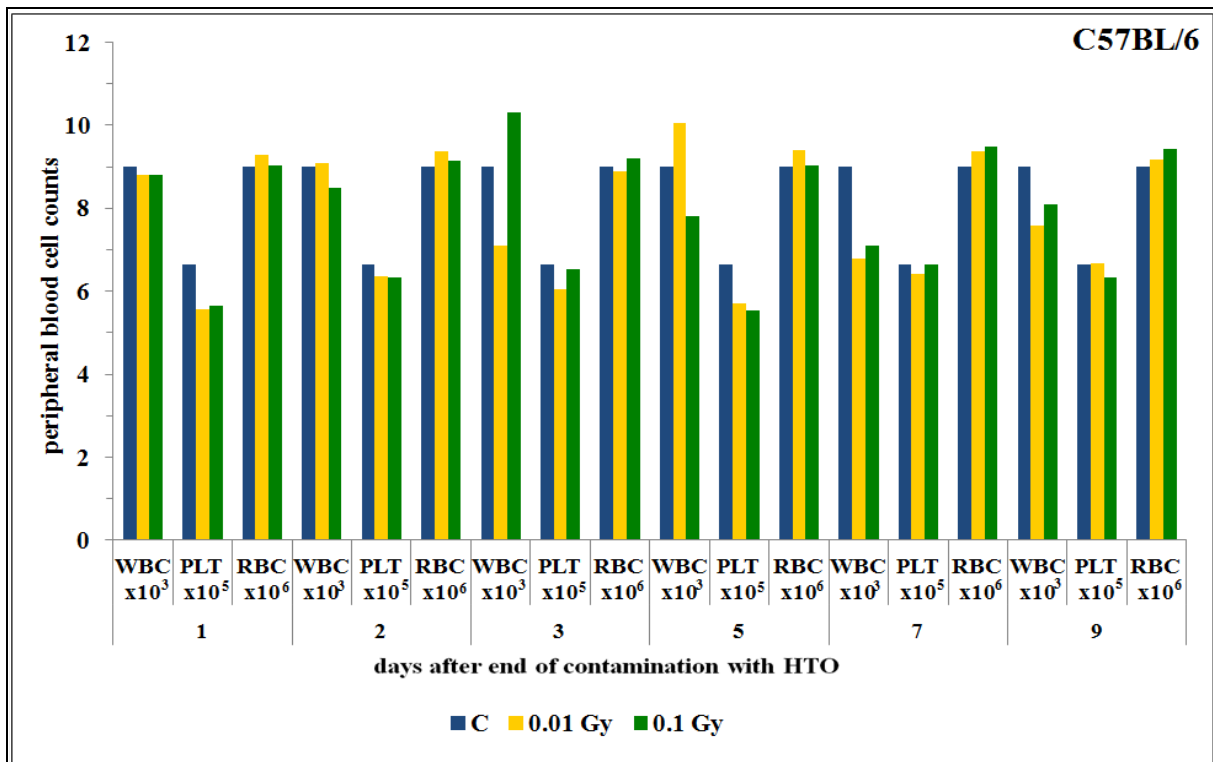
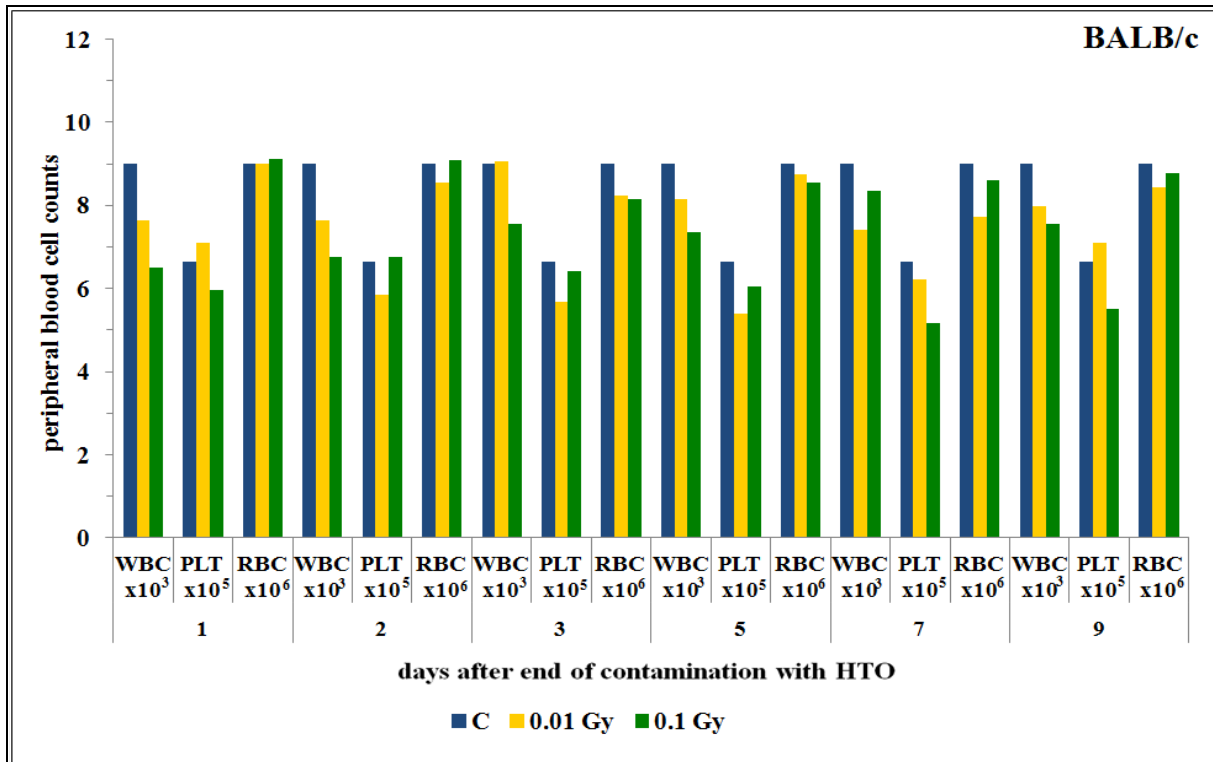


Figure 2-28: Blood Cell Counts in BALB/c or C57BL/6 Mice Contaminated with HTO.

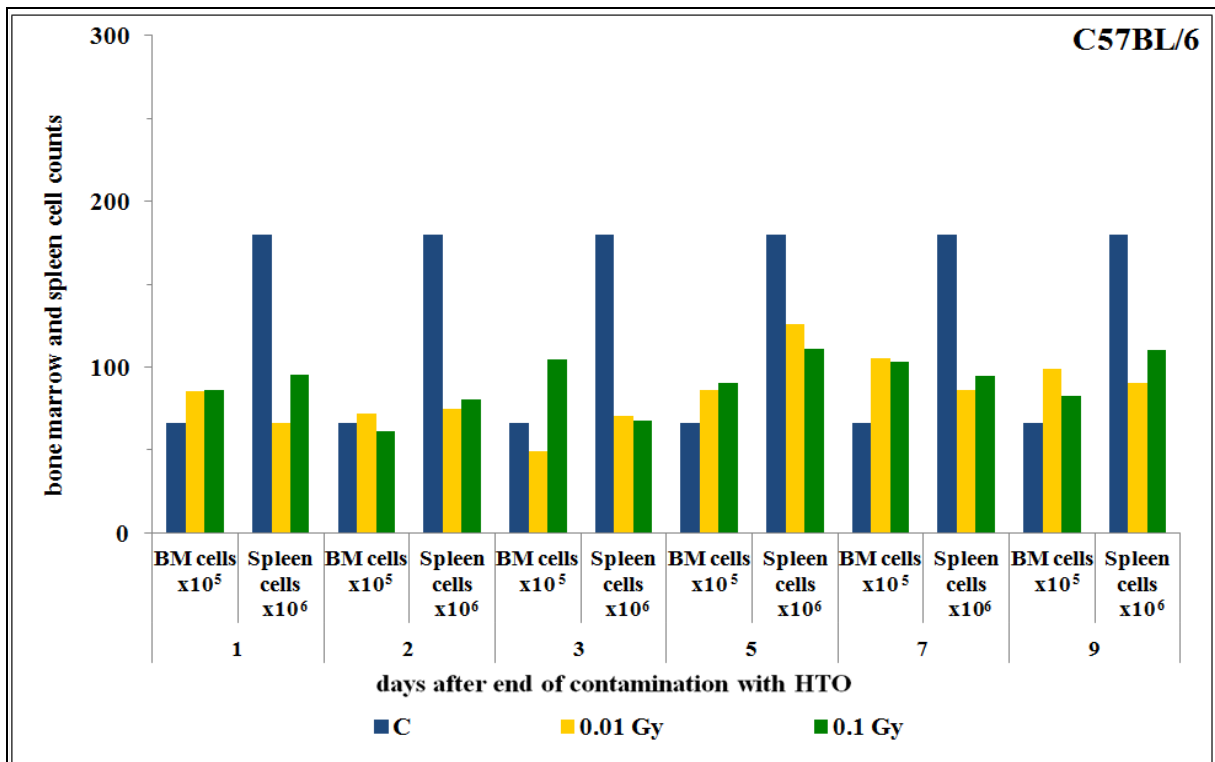
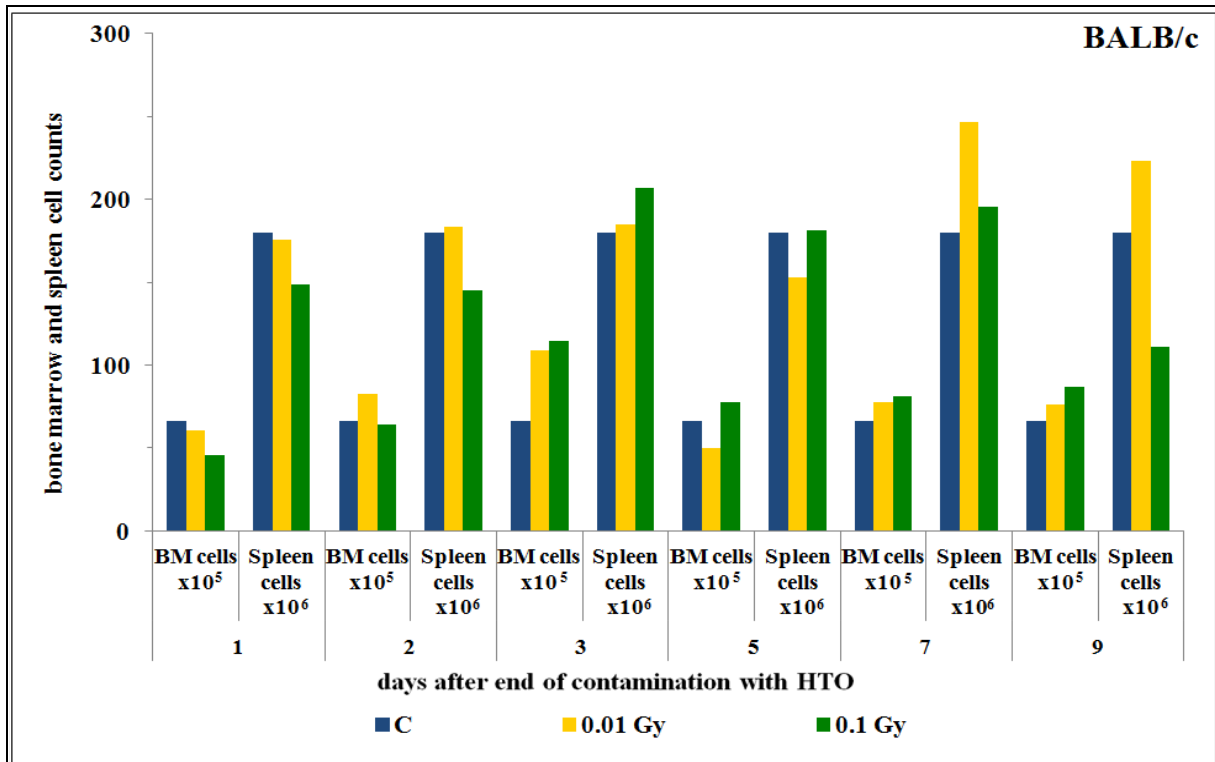


Figure 2-29: Spleen and Bone Marrow Cellularity in BALB/c or C57BL/6 Mice Contaminated with HTO.

2.3.2.2.1 *Summary of the Results*

- 1) Internal contamination of BALB/c and C57BL/6 mice with HTO stimulated cytotoxic activity of their spleen-derived NK cells, but:
 - a) In BALB/c mice the effect was demonstrable between the 2nd and 7th days post cessation of the contamination and only when the total dose to the body was 0.1 Gy; and
 - b) In C57BL/6 mice the effect occurred as late as 7 to 9 days post removal of HTO from the body and only when the total dose was 0.01 Gy.
- 2) Activated macrophages obtained from the HTO-contaminated BALB/c and C57BL/6 mice produced more NO than the counterpart cells obtained from uncontaminated mice, but:
 - a) In BALB/c mice the effect was demonstrable between the 1st and 2nd days post cessation of the contamination when the total doses to the body were 0.1 Gy and, to a lesser extent, 0.01 Gy; and
 - b) In C57BL/6 mice the effect occurred on the 1st, 5th and 9th days post removal of HTO from the body when the total dose was 0.01 Gy, and only on Day 9 post removal of HTO from the body when the total dose was 0.1 Gy.
- 3) Internal contamination of BALB/c and C57BL/6 mice with HTO at low (0.01 or 0.1 Gy) total doses did not affect:
 - a) Peripheral blood cell counts;
 - b) Spleen cells' numbers and viability; and
 - c) Bone marrow cells' numbers and viability.

2.3.3 The Importance of Low-Dose Radiation Research: Models and Mechanisms to Develop Biomarkers, Countermeasures, and Improved Risk Assessment

Abstract

Military and NATO personnel can potentially be exposed to external and internal radiation during military operations. The external radiation can occur via a nuclear weapons explosion or via the use of a "dirty bomb" by terrorists. Nuclear weapons exposure is a significant health hazard; while the damage due to radiation from a dirty bomb could be significantly lower, there is still a threat of some type of "late" radiation injury.

High-dose radiation exposure can cause significant acute health effects including radiation syndrome and potentially death. Late health effects caused by radiation are also a significant health hazard. These late effects include cancer, leukemia, fibrosis, cytogenetic effects, and transgenerational effects to offspring. While there is significant human and animal data regarding the induction of high-dose radiation-induced cancers, less attention has been paid to whether the unique military radiation exposures like internalized DU or low-dose radiation potentially from dirty bombs can cause late health effects like cancer and genetic effects. New biological models and a mechanistic understanding describing the role of genetic and epigenetic factors and cancer susceptibility in individuals are needed for improving radiation carcinogenesis risk estimates and countermeasure development in a low-dose scenario.

One of our goals is the development of new cutting edge approaches to understanding cancer risks for these military and NATO relevant exposures. To achieve this goal our laboratory emphasizes the application of mechanistic understanding to mammalian models to achieve significant reductions in the uncertainties in risk projections for cancer, to identify late effects biomarkers, and to develop more effective late effects countermeasures. For example, we use an in vivo leukemia model to study non-targeted radiation effects, epigenetic, and genetic effects.

This mechanistic and multi-parametric strategic research approach involving the progression from cellular studies to animal models has been applied to radiation and heavy-metal studies in our laboratory. These models are critical to improving the protection strategies and health of NATO personnel.

2.3.3.1 Introduction

Military and NATO personnel can potentially be exposed to external and internal radiation during military operations. The external radiation can occur via a nuclear weapons explosion; another scenario is the use of a “dirty bomb” by terrorists. Nuclear weapons exposure can be a significant health hazard causing development of the Acute Radiation Syndrome (ARS) or even possibly death. While the damage due to radiation from a dirty bomb could be significantly lower, there is still a threat of some type of radiation injury. In terms of internal radiation exposure to military personnel, the radioactive heavy metal Depleted Uranium (DU), used in military munitions is one possible type of exposure. Additionally, internalization of radioactive fallout could occur after the use of nuclear weapons or a nuclear incident like Fukushima. These types of “battlefield” radiation exposures are unique to military personnel and are different than the high-dose fractionated therapeutic exposures that the average civilian might be exposed to during their lifetime.

High-dose radiation exposure can cause significant acute health effects including radiation syndrome and potentially death. Late health effects caused by radiation are also a significant health hazard. These late effects include cancer, leukemia, cytogenetic effects, and transgenerational effects to offspring. It is well known that radiation exposure can lead to cancer development and in particular to development of leukemia [43], [54], [89], [122], [123]. While there is significant human and animal data regarding the induction of high-dose radiation-induced cancers, less attention has been paid to whether the unique military radiation exposures like internalized DU [88], [89] or low-dose radiation [43], [54], [122], [123] potentially from dirty bombs can cause late health effects like cancer and genetic effects. The recent nuclear event in Fukushima Japan highlighted the need for more information in the area of low-dose radiations exposures and induced health effects. The extent of the health effect of low-dose radiation exposures is a debated topic within the radiation biology community.

New biological models and a mechanistic understanding describing the role of genetic and epigenetic factors and cancer susceptibility in individuals are needed for improving radiation carcinogenesis risk estimates and countermeasure development in a low-dose scenario. To achieve this goal our approach is to emphasize the application of a mechanistic understanding to the mammalian models used in our laboratory to study cancer risk and the development of late-effects countermeasures. For example, we use an *in vivo* leukemia model to study non-targeted radiation effects, epigenetic, and genetic effects. With this mechanistic information, the leukemia model is then used to identify and test mechanism-responsive countermeasures like the epigenetic effector, Phenylbutyrate (PB).

This leukemia model is also effective to further study mechanisms as it is applicable as an *in vitro* / *in vivo* model. This novel *in vitro* / *in vivo* model has been used in my laboratory to explore the bone marrow microenvironment and radiation induction of leukemia [88], [89]; this model can be used to study Non-Targeted radiation Effects (NTEs) and in particular Radiation-Induced Bystander Effects (RIBEs) and low-dose radiation with an emphasis on understanding epigenetic mechanism like miRNAs. To study the process of radiation leukemogenesis, specifically from the standpoint of the hematopoietic microenvironment, we have used a novel murine model for the development Acute Myeloid Leukemia (AML) which allows an analysis of the indirect effects of irradiation separate from the direct radiation effects on hematopoietic cells [44]-[46]. In this NTE model, murine hematopoietic progenitor cells designated FDC-P1, consistently transform to AML when injected into DBA/2 mice irradiated with 1 to 3.5 Gy gamma radiation [44]-[46]. This leukemia model, in which non-tumorigenic immature hematopoietic cells are introduced into an irradiated bone marrow environment, and followed by the development of leukemia, characterizes it as a “non-targeted effects” leukemia model. The model is also novel since it can also be employed as an *in vitro* model system. Unirradiated FDC-P1 cells are co-cultured with directly irradiated murine bone marrow stromal cells (DBA/2-SC3) derived from DBA/ 2 mice. The FDC-P1 cells can be used for non-targeted

radiation exposure (co-cultured with irradiated DBA/2-SC3 cells) or targeted (directly irradiated). We have been using both the *in vivo* NTE leukemia model and the FDC-P1/DBA/2-SC3 *in vitro* model system to explore NTEs and epigenetic mechanisms focusing on DNA methylation (see preliminary data; Refs. [44]-[46]). This *in vitro* model provides an excellent means to examine a link between low-dose radiation, NTEs, and miRNAs; in an overarching objective these data would provide beneficial information relevant to low-dose risk assessment and to identification of miRNA signatures relevant to leukemic cell transformation. Furthermore, the proposed study could identify an miRNA signature during low-dose radiation-induced neoplastic transformation that could be used as a late radiation effects biomarker thus having a dual benefit.

2.3.3.2 Long-Term Goals

One of our goals in our laboratory is to employ new cutting-edge approaches to better understand the health effects of low-dose radiation. This information will assist in improving current risk standards, the development of biological countermeasures for cancer risks for these military and NATO relevant exposures, and the identification of novel biomarkers as predictors of low-dose radiation-induced late effects. The initial steps are to determine the mechanisms involved in radiation-leukemia development followed by the targeting of these mechanisms to better understand low-dose risk and identify biomarkers.

Specifically, the long-term research goals and benefits using the multi-parametric approach to understanding radiation cancer or leukemia risk are multi-fold. First, the evaluation of unique and potential carcinogenic exposures, i.e., radiation, DU, relevant to military personnel can be evaluated. Secondly, the development of non-toxic countermeasures to these radiation-induced cancers can be undertaken using multiple approaches. Thirdly, the potential discovery of biomarkers of exposure and disease development should be conducted simultaneously to the *in vitro* and *in vivo* cancer studies. The technical objectives of this approach include:

- 1) Development of *in vitro* models to study radiation-induced late effects and radiobiology mechanisms; and
- 2) Development of *in vivo* models to study radiation-induced late effects and evaluate efficacy of pharmacological countermeasures that are targeted to the newly-discovered specific radiation-induced mechanisms.

2.3.3.3 Research Progress

2.3.3.3.1 Targeted and Non-Targeted FDC-P1 Cell Response to Radiation: Radiation Quality Studies

Rationale: The purpose of these experiments was two-fold:

- 1) Was to demonstrate establishment of this *in vitro* model system as a model to study NTEs and neoplastic transformation at low doses; and
- 2) Was to determine if non-targeted radiation exposure of FDC-P1 cells results in transformation that was radiation quality dependent.

Experimental Design: Bone marrow stromal cells (DBA/2-SC3) and hematopoietic progenitor cells (FDC-P1) were used to evaluate NTEs on FDC-P1 cellular response to radiation quality differences. A bone marrow stromal cell line (adherent and fibroblastic) was derived in our laboratory from DBA/2 murine bone marrow (DBA/2-SC3) [44]-[46], [55], [96]. To determine the effects of Low-Dose Radiation (LDR) both high and low-LET radiations plateau-phase culture of DBA/2-SC3 cells were irradiated with X-rays (5, 50, 100 cGy, 68 cGy/min, 250 kVp) or alpha particles (5, 50, 100 cGy, 77 cGy/min, 120 MeV) and overlaid with 0.3% agar-containing medium and the target cell population, FDC-P1. Colony growth and malignant transformation of FDC-P1 cells following the same radiation exposure conditions were measured using the co-cultivation technique [55], [96]. These FDC-P1 cells were the non-targeted group. Cell growth and transformation were measured in the following groups:

- FDC-P1 (no radiation, no co- culture);
- DBA/2-SC3 (no radiation, no co-culture); and
- FDC-P1 + DBA/2-SC3 (no radiation, with co-culture).

In addition, another group was established in which FDC-P1 cells were irradiated directly (targeted group). Therefore, we established FDC-P1 groups that were non-targeted and targeted for comparison. We completed a series of radiation studies evaluating radiation quality effect on radiation-induced neoplastic transformation of FDCP-1 cells under targeted and non-targeted conditions.

Results: The Columbia University RARAF Singletron accelerator was used to produce the broad beam of 4He ions (alpha particles) and the RARAF X-ray source was used to produce X-ray exposures. The targeted FDC-P1 cells were irradiated and their growth and behavior in agar was monitored. Following radiation the irradiated FDC-P1 cells (targeted) or irradiated DBA/2-SC3 cells + unirradiated FDC-P1 (non-targeted) cells were overlaid in agar at a density of 1×10^5 . During transformation, FDC-P1 cells formed dense colonies, detected as early as four days after plating. Their growth rate and transformation frequency at Days 10 and 42 post-radiation were assessed. Table 2-2 shows the results from that series of radiation experiments (X-rays and alpha particles). The data demonstrated that direct or “targeted” alpha radiation exposure to FDC-P1 cells resulted in neoplastic transformation as expected at all three doses tested (transformation frequencies of $(43.2, 345, \text{ and } 655 \times 10^{-4}; 5, 50, 100 \text{ cGy, respectively})$. The transformation frequencies of non-targeted FDC-P1 cells were $(21.4, 345.1, \text{ and } 499.7 \times 10^{-4}; 5, 50, 100 \text{ cGy, respectively})$. These results show that alpha particle radiation caused a significant dose-dependent increase in neoplastic transformation of non-targeted FDC-P1 cells. A similar study was done with X-rays. The results indicate that at these low doses, X-rays did not induce significant increases in neoplastic transformation of targeted cells as expected nor did X-rays did not induce significant increases in non-targeted cell transformation. A nude mouse tumorigenicity study was done to determine whether the transformed clonal lines (at 10 and 42 days) were fully transformed to the tumorigenic phenotype as described [88]. Results are shown in Table 2-2.

Table 2-2: Effect of Alpha Particles and X-rays on Non-Targeted Radiation Population.

Treatment/Exposure	Growth (1×10^4) (in agar)		Transformation (1×10^{-4}) (in agar)		Tumor	
	Day 10 (Early stage)	Day 42 (Late stage)	Day 10 (Early stage)	Day 42 (Late Stage)	Day 10	Day 42
FDC-P1 (No Rad)	<0.1	<0.1	<0.1	<0.1	-	-
DBA/2-SC3 (No Rad)	<0.1	<0.1	<0.1	<0.1	-	-
FDC-P1 + DBA/2-SC3 (No Rad)	<0.1	<0.1	<0.1	<0.1	-	-
FDC-P1 (+Alpha Particles 120 keV) 5 cGy	5.0	14.2	11.5	43.2	1/10	6/10
FDC-P1 (+Alpha Particles 120 keV) 50 cGy	5.2	12.9	24.1	388	1/10	9/10
FDC-P1 (+Alpha Particles 120 keV) 100 cGy	5.7	17.2	36.6	655	2/10	10/10
DBA/SC-3 (+ Alpha Particles + FDC-P1 5 cGy	3.9	11.2	5.4	21.4	0/10	3/10
DBA/SC-3 (+ Alpha Particles + FDC-P1 50 cGy	4.1	10.2	19.2	345.1	1/10	10/10
DBA/SC-3 (+ Alpha Particles + FDC-P1 100 cGy	5.1	14.8	30.4	499.2	3/10	9/10
FDC-P1 (+ X-rays) 5 cGy	<0.1	<0.1	<0.1	0.4	-	-
FDC-P1 (+ X-rays) 50 cGy	<0.1	0.3	0.4	2.1	-	0/10
FDC-P1 (+ X-rays) 100 cGy	3.1	5.1	0.5	9.7	-	1/10
DBA/SC-3 (+ X-rays + FDC-P1 5 cGy	<0.1	<0.1	<0.1	0.2	-	-
DBA/SC-3 (+ X-rays + FDC-P1 50 cGy	<0.1	0.3	0.3	1.3	-	0/10
DBA/SC-3 (+ X-rays + FDC-P1 100 cGy	1.1	5.1	0.9	2.5	-	0/10

Relevance of These Results: These results demonstrate several key points important to low-dose radiation. First, they show that cells that are not traversed can be transformed by radiation to nearby cells. These results also demonstrate that there are radiation quality differences in the development of malignant cells in non-targeted cells between low- and high-LET radiations. The findings confirm that high-LET radiations have a more significant effect on the population of cells that are non-targeted than the targeted ones further implicating a role for the bystander effect in adverse effects of low-dose radiations.

2.3.3.3.2 *Effect of Targeted or Non-Targeted Radiation Exposure on Global Methylation in FDC-P1 Clonal Lines*

Rationale: Epigenetics including DNA methylation could be a missing link in understanding non-targeted radiation effects. The study was designed to determine if non-targeted radiation to FDC-P1 cells induces epigenetic alterations, i.e., DNA methylation that are LET-dependent. A second goal was to determine if early and late phase transformed clonal lines had similar epigenetic responses to radiation.

Experimental Design: Bone marrow stromal cells (DBA/2-SC3) and hematopoietic progenitor cells (FDC-P1) were used and radiation exposed as described above. Global methylation was evaluated by Methylation-Sensitive PCR (MS-PCR) as described [96]. From the above transformation study, FDC-P1 clones (at 10 and 42 days) post-radiation/co-culture were selected and expanded in culture. The clonal lines were tested for global DNA methylation.

Results: Clonal lines expanded from clones selected at 10 or 42 days post-radiation (5, 50, and 100 cGy X-ray and alpha particle) were examined. For all clonal lines, methylation at the internal cytosine (HpaII) and external cytosine (MspI) was evaluated. Transformed clonal lines are grouped into early phase (10 days post-radiation; Figure 2-30 A and B) and late phase (42 days post radiation; Figure 2-30 C and D).

Relevance: The data indicate that in targeted cell population X-rays and alpha particles did not have a significant effect on methylation status in early phase clones. Dose-rate has little effect on methylation in early-phase transformed clones following X-ray exposure to targeted population. In contrast, in both non-targeted X-ray and alpha particle populations, methylation was significantly higher at lower dose rates. In general methylation was greater in non-targeted populations in the early phase clones following either X-ray or alpha particles. Global methylation may not be an appropriate biomarker for early neoplastic changes following low-dose radiation. Additional epigenetic markers are being pursued.

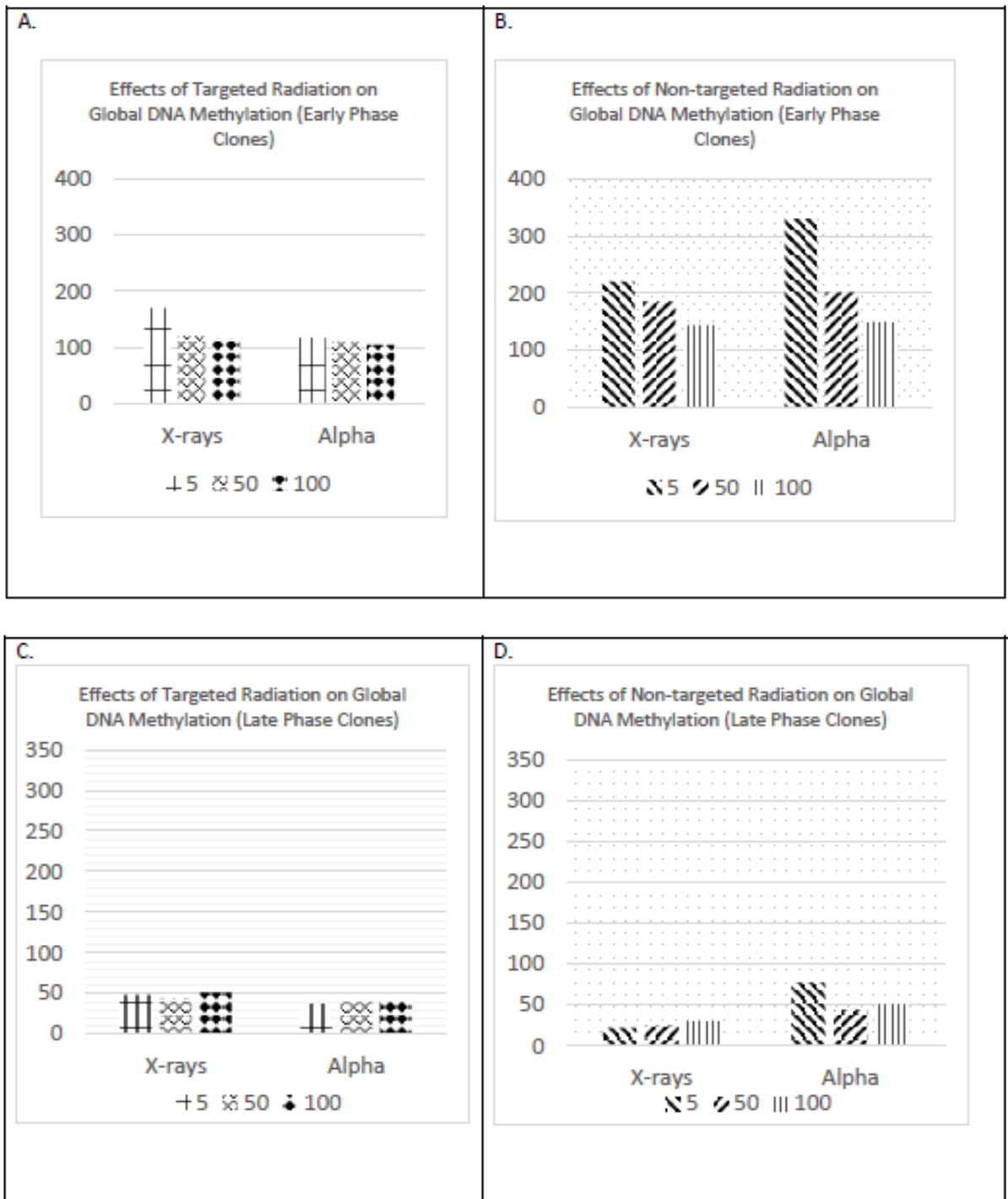


Figure 2-30: Global DNA Methylation: Early and Late Phase Transformed Clonal Cells.

2.3.3.3.3 Repeated Exposure to Low-Dose/High Dose Rate Radiation (Low LET vs. High LET)

Rationale: To determine whether repeated exposure to high dose rate alpha particles or X-rays can result in transformation in un-irradiated bystander cells. Currently risk standards do not include a contribution from non-targeted bystander cells. Studies with bystander cell models are critical to determining if repeated radiation exposure at low-dose/high-dose rates is underestimated as a radiation risk.

Results: An evaluation of multiple/protracted low-dose alpha particle exposures on neoplastic transformation in a non-targeted population was assessed (Figure 2-31). DBA/2-SC3 cells were exposed to alpha radiation (single dose of 5, 10, or 50 cGy or multiple doses of alpha radiation equaling 50 cGy; that is 5 cGy (10×), 10 cGy (5×) or 25 cGy (2×). The irradiated cells were then co-cultured immediately with FDC-P1 cells and the transformation frequency in FDC-P1 cells was measured. The results indicate that if 1 hour lapsed between each of the protracted radiations there was a significant increase in transformation frequency with multiple alpha particle radiations in the non-targeted cells (Figure 2-32). The dose response of single alpha particle doses of 5, 10, and 25 cGy to NTE populations shows an increase in neoplastic transformation of FDC-P1 cells. A single dose of 25 cGy resulted in a transformation frequency of 148×10^{-3} (+/- 15.2) in contrast to multiple doses of 5 cGy totaling 25 cGy which resulted in a transformation frequency of 201×10^{-3} (+/- 18.2.) These results suggest that protracted high-LET radiation like alpha particles can foster a neoplastically transforming environment to non-targeted cells.

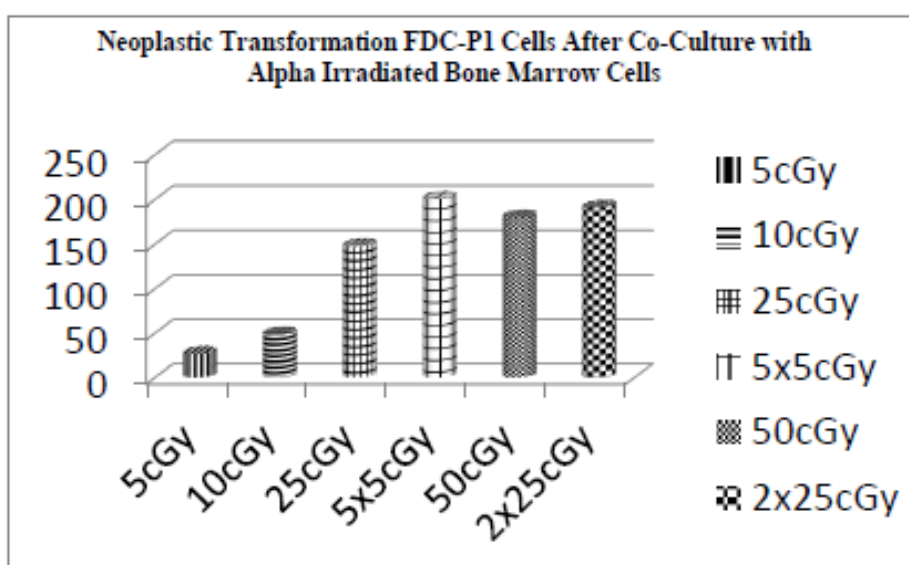


Figure 2-31: Neoplastic Transformation After Protracted Alpha Particle Exposure.

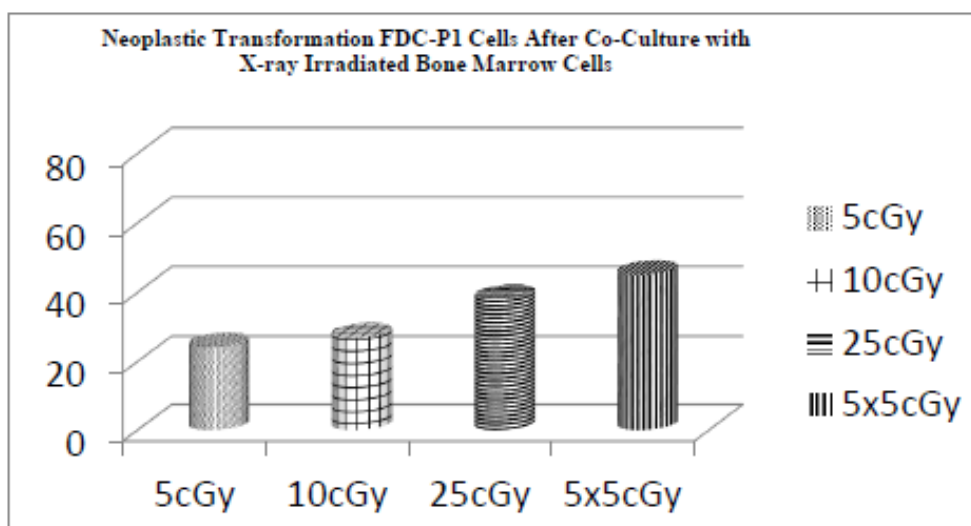


Figure 2-32: Neoplastic Transformation After Protracted X-Ray Exposure.

Multiple low-dose X-ray exposures and the effect on neoplastic transformation in a non-targeted population was also assessed. DBA/2-SC3 cells were exposed to X-ray radiation (single dose of 5, 10, or 25 cGy or multiple doses of X-rays equaling 25 cGy - 5 cGy (5×). The irradiated cells were then co-cultured with FDC-P1 cells for 1 hr and the transformation frequency in FDC-P1 cells was measured. A single dose of X-rays 25 cGy or protracted dose of X-rays 5 cGy × 5 yielded similar levels of transformation frequency in non-targeted cells ($38.3 \times 10^{-3} \pm 3.9$ and $45.1 \times 10^{-3} \pm 4.1$, respectively). These preliminary results suggest that protracted low-LET radiation like X-rays does not foster a neoplastically transforming environment to non-targeted cells.

Relevance: These studies suggest that protracted low-dose radiation is more transforming than a single-total low-dose exposure for both high-LET and low-LET radiations. These results imply that repeated exposure to low doses via medical and diagnostic tests may be more damaging than originally thought since non-targeted cells are not considered in estimating radiation risk.

2.3.3.4 Summary and Conclusions

2.3.3.4.1 Medical Benefits

These findings have significant implications for the military personnel and the development of radiation late effects. This work involves a low-dose radiation leukemia model and an attempt to understand the mechanisms involved in this process. This information can be useful in several ways. First an understanding of the genetic and epigenetic changes that occur during radiation-induced disease development can assist with the design of prognostic biomarkers and radiation risk stratification. The low-dose radiation field is searching for new ways to define increased cancer/leukemia risk and the information collected in this project will assist in that endeavour. Secondly, knowledge of the genetic and epigenetic mechanisms during radiation- or DU- leukemia development can facilitate the development of new classes of targeted drugs to leukemia. The combination of this information on molecular biomarkers during leukemogenesis and risk assessment could substantially increase our ability to develop non-toxic pre-treatments or chemoprevention agents that could reduce the development of cancer following radiation exposure in military personnel or their dependents. To better study the radiation late effects induced by the unique military radiation exposures this multi-parametric approach has been used in our laboratory at AFRRRI. Implementation of cell- and animal-based multi-parametric assays can provide predictive information and be a guide as to whether human studies should be pursued. This strategic research approach involving the progression from cellular studies to animal model has been applied to radiation and heavy metal studies in our laboratory and has provided a rapid and effective research approach to evaluating radiation risks for NATO and military personnel.

2.3.3.4.2 Military Health Benefits

Military concerns regarding radiation exposure have focused on high-dose radiation exposures from nuclear weapons or nuclear reactor accidents. The nuclear incident at Fukushima, Japan in 2011 increased the importance of low-dose radiation studies and whether that type of exposure can increase cancer risk for adults and children. Radiation research from NATO member laboratories has primarily focused on high-dose exposures, but low-dose radiation research can provide high-value scientific data for input in determining health risks from low levels of radiation. Performing measurements at low doses is critically relevant because radiation exposures associated with military actions, dirty bombs, and medical exposures are most likely at low doses of radiation or at different dose rates. A strong scientific underpinning for our risk regulation is critical to adequately and appropriately protecting military personnel.

2.4 REFERENCES

- [1] Abend, M., Azizova, T., Müller, K., Dörr, H., Doucha-Senf, S., Kreppel, H., Rusinova, G., Glazkova, I., Vyazovskaya, N., Unger, K., Braselmann, H. and Meineke, V. Association of radiation-induced genes with noncancer chronic diseases in Mayak workers occupationally exposed to prolonged radiation. *Radiat Res.* 2015 Mar;183(3):249-61.
- [2] Abend, M., Azizova, T., Müller, K., Dörr, H., Senf, S., Kreppel, H. *et al.* Gene expression analysis in Mayak workers with occupational prolonged radiation exposure. *Health Physics*, 2014a Jun;106(6): 664-76.
- [3] Abend, M., Azizova, T., Müller, K., Dörr, H., Senf, S., Kreppel, H., Rusinova, G., Glazkova, I., Vyazovskaya, N., Unger, K. and Meineke, V. Independent validation of candidate genes identified after a whole genome screening on Mayak workers exposed to prolonged occupational radiation. *Radiat Res.* 2014b Sep;182(3):299-309.
- [4] Abend, M., Pfeiffer, R.M., Ruf, C., Hatch, M., Bogdanova, T.I., Tronko, M.D. *et al.* Iodine-131 dose dependent gene expression in thyroid cancers and corresponding normal tissues following the Chernobyl accident. *PLoS One.* 2012;7(7):e39103.
- [5] Abend, M., Pfeiffer, R.M., Ruf, C., Hatch, M., Bogdanova, T.I., Tronko, M.D. *et al.* Iodine-131 dose dependent gene expression: alterations in both normal and tumor thyroid tissues of post- Chernobyl thyroid cancers. *Br J Cancer* 2013;574:1-9.
- [6] Al-Sarireh, B. and Eremin, O. (2000). Tumour-associated macrophages (TAMS): disordered function, immune suppression and progressive tumour growth. *J R Coll Surg Edinb* 45, 1-16.
- [7] Anon. (2001). Mixed messages about depleted uranium (editorial). *Lancet. Oncol.*; 2, 65.
- [8] Azizova, T.V., Muirhead, C.R., Druzhinina, M.B., Grigoryeva, E.S., Vlasenko, E.V., Sumina, M.V. *et al.* Cerebrovascular diseases in the cohort of workers first employed at Mayak PA in 1948-1958. *Radiat Res* 2010;174(6):851-64.
- [9] Azizova, T.V., Muirhead, C.R., Moseeva, M.B., Grigoryeva, E.S., Vlasenko, E.V., Hunter, N. *et al.* Ischemic heart disease in nuclear workers first employed at the Mayak PA in 1948-1972. *Health Phys* 2012;103(1):3-14.
- [10] Backer, L.C., Grindem, C.B., Corbett, W.T., Cullins, L. and Hunter, J.L. Pet dogs as sentinels for environmental contamination. *Sci Total Environ*, 2001;274:161-169.
- [11] Balkwill, F., Charles, K.A. and Mantovani, A. Smoldering and polarized inflammation in the initiation and promotion of malignant disease. *Cancer Cell.* 2005 Mar;7 (3):211-7.
- [12] Barao, I. and Ascensao, J.L. (1998). Human natural killer cells. *Arch Immunol Ther Exp* 46, 213-229.
- [13] Barcellos-Hoff, M.H. and Nguyen, D.H. Radiation carcinogenesis in context: how do irradiated tissues become tumors? *Health Phys.* 2009 Nov;97(5):446-57. doi: 10.1097/HP.0b013e3181b08a10.
- [14] Barcellos-Hoff, M.H., Park, C. and Wright, E.G. Radiation and the microenvironment - tumorigenesis and therapy. *Nat Rev Cancer.* 2005 Nov;5 (11):867-75.
- [15] Barcellos-Hoff, M.H. Cancer as an emergent phenomenon in systems radiation biology. *Radiat Environ Biophys.* 2008 Feb;47 (1):33-8. Epub 2007 Nov 20.

- [16] Barquinero, J.F., Knehr, S., Brasselmann, H., Figel, M. and Bauchinger, M. (1998). DNA-proportional distribution of radiation induced chromosome aberrations analysed by fluorescence in situ hybridization painting of all chromosomes of a human female karyotype. *Int. J. Radiat. Biol.* 74, 315-323.
- [17] Boffetta, P., van der Hel, O., Norppa, H., Fabianova, E., Fucic, A., Gundy, S., Lazutka, J., Cebulska-Wasilewska, A., Puskaierova, D., Znaor, A., Kelecsenyi, Z., Kurtinaitis, J., Rachtan, J., Forni, A., Vermeulen, R. and Bonassi, S. (2007). Chromosomal aberrations and cancer risk: results of a cohort study from Central Europe. *Am. J. Epidemiol.* 165, 36-43.
- [18] Bolognesi, C., Balia, C., Roggieri, P., Cardinale, F., Bruzzi, P., Sorcinelli, F., Lista, F., D'Amelio, R. and Righi, E. Micronucleus test for radiation biodosimetry in mass casualty events: visual and automated Radiation Measurements: 2011;46:169-175.
- [19] Bolognesi, C., Migliore, L., Lista, F., Caroli, S., Patriarca, M., De Angelis, R., Capocaccia, R., Amadori, S., Pulliero, A., Balia, C., Colognato, R., La Gioia, V., Bonassi, S. and Izzotti, A. Biological monitoring of Italian soldiers deployed in Iraq. Results of the SIGNUM project. *Int J Hyg Environ Health.* 2016;219(1):24-32.
- [20] Bonassi, S., Ugolini, D., Kirsch-Volders, M., Stromberg, U., Vermeulen, R. and Tucker, J.D. (2005). Human population studies with cytogenetic biomarkers: review of the literature and future perspectives. *Environ. Mol. Mutagen.* 45, 258-270.
- [21] Brasselmann, H., Kulka, U., Baumgartner, A., Eder, C., Mueller, I., Figel, M. and Zitseldberger, H. (2005). SKY and FISH analysis of radiation-induced chromosome aberrations: a comparison of whole and partial genome analysis. *Mutat. Res.* 578, 124-133.
- [22] Cai, L. (1999). Research of the adaptive response induced by low-dose radiation: Where have we been and where should we go? *Hum Exp Toxicol* 18, 419-425.
- [23] Caratero, A., Courtade, M., Bonnet, L., Planel, H. and Caratero, C. (1998). Effect of a continuous gamma irradiation at a very low dose on the life span of mice. *Gerontology* 44, 272-276.
- [24] Catena, C., Conti, D., Villani, P., Nastasi, R., Archilei, R. and Righi, E. Micronuclei and 3AB index in human and canine lymphocytes after in vitro X-irradiation. *Mutat Res* , 1994;312:1-8.
- [25] Cheda, A., Nowosielska, E.M., Wrembel-Wargocka, J. and Janiak, M.K. (2008). Production of cytokines by peritoneal macrophages and splenocytes after exposures of mice to low doses of X-rays. *Radiat Environ Biophys* 47, 275-283.
- [26] Cheda, A., Nowosielska, E.M., Wrembel-Wargocka, J. and Janiak, M.K. (2009). Single or fractionated irradiations of mice with low doses of X-rays stimulate innate immune mechanisms. *Int J Low Radiation* 6, 325-342.
- [27] Cheda, A., Wrembel-Wargocka, J., Lisiak, E., Marciniak, M., Nowosielska, E.M. and Janiak, M.K. (2004a). Inhibition of the development of pulmonary tumour nodules and stimulation of the activity of NK cells and macrophages in mice by single low doses of low-LET radiation. *Int J Low Radiation* 1, 171-179.
- [28] Cheda, A., Wrembel-Wargocka, J., Lisiak, E., Nowosielska, E.M., Marciniak, M. and Janiak, M.K. (2004b). Single Low Doses of X-Rays Inhibit the Development of Experimental Tumor Metastases and Trigger the Activities of NK Cells in Mice. *Radiat Res* 161, 335-340.

- [29] Cheda, A., Wrembel-Wargocka, J., Nowosielska, E.M. and Janiak, M.K. (2005). Stimulatory effect of a single low-level irradiation with X-rays on functions of murine peritoneal macrophages. *Nukleonika* 50(Suppl. 2), S13-S16.
- [30] Cheda, A., Wrembel-Wargocka, J., Nowosielska, E.M. and Janiak, M.K. (2006). Immune mechanism of the retarded growth of tumor nodules in mice exposed to single low-level irradiations with X-rays. *Centr Eur J Immunol* 31, 44-50.
- [31] Coates, P.J., Rundle, J.K., Lorimore, S.A. and Wright, E.G. (2008). Indirect macrophage responses to ionizing radiation: implications for genotype-dependent bystander signaling. *Cancer Res* 68, 450-456.
- [32] COMARE 2004, 9th Report of Committee on Medical Aspects of Radiation in the Environment.
- [33] Cooper, M.A., Fehniger, T.A., Turner, S.C., Chen, K.S., Ghaheri, B.A., Ghayur, T., Carson, W.E. and Caligiuri, M.A. Human natural killer cells: a unique innate immunoregulatory role for the CD56(bright) subset. *Blood*. 2001 May 15;97(10):3146-51.
- [34] Craig, J.M. and Wong, N.C. *Epigenetics. A reference manual*. Caister Academic Press, Norfolk, UK, 2011.
- [35] Cui, S., Reichner, J.S., Mateo, R.B. and Albina, J.E. (1994). Activated murine macrophages induce apoptosis in tumor cells through nitric oxide-dependent or -independent mechanisms. *Cancer Res* 54, 2462-2467.
- [36] Cuturi, M.C., Anegón, I., Sherman, F., Loudon, R., Clark, S.C., Perussia, B. and Trinchieri, G. Production of hematopoietic colony-stimulating factors by human natural killer cells. *J Exp Med*. 1989 Feb 1;169(2):569-83.
- [37] Dalbeth, N., Gundle, R., Davies, R.J., Lee, Y.C., McMichael, A.J. and Callan, M.F. CD56bright NK cells are enriched at inflammatory sites and can engage with monocytes in a reciprocal program of activation. *J Immunol*. 2004 Nov 15;173(10):6418-26.
- [38] De Sanctis, S., De Amicis, A., Di Cristofaro, S., Franchini, V., Regalbuto, E., Mammana, G. and Lista, F. Cytokinesis-block micronucleus assay by manual and automated scoring: calibration curves and dose prediction. *Health Phys.*, 2014;106(6):745-9.
- [39] Degli-Esposti, M.A. and Smyth, M.J. Close encounters of different kinds: dendritic cells and NK cells take centre stage. *Nat Rev Immunol*. 2005 Feb;5(2):112-24.
- [40] Demaria, S., Pikarsky, E., Karin, M., Coussens, L.M., Chen, Y.C., El-Omar, E.M., Trinchieri, G., Dubinett, S.M., Mao, J.T., Szabo, E., Krieg, A., Weiner, G.J., Fox, B.A., Coukos, G., Wang, E., Abraham, R.T., Carbone, M. and Lotze, M.T. Cancer and inflammation: promise for biologic therapy. *J Immunother*. 2010 May;33(4):335-51. doi: 10.1097/CJI.0b013e3181d32e74.
- [41] DeVisser, K.E., Eichten, A. and Coussens, L.M. Paradoxical roles of the immune system during cancer development. *Nat Rev Cancer*. 2006 Jan;6(1):24-37.
- [42] Donmez-Altuntas, H., Hamurecu, Z., Liman, N., Demirtas, H. and Imamoglu, N. Increased micronucleus frequency after oral administration of cadmium in dogs *Biol Trace Elem Res*, 2006;112:241-246.
- [43] Dorr, R.T. Radioprotectants: Pharmacology and Clinical applications of amifostine. *Semin Radiat Oncol*, 1998 Oct;8 (4 Suppl 1):10-13.

- [44] Duhrsen, U. and Metcalf, D. (1988). A model system for leukemic transformation of immortalized hemopoietic cells in irradiated recipient mice. *Leukemia*, 2, 329-333.
- [45] Duhrsen, U. and Metcalf, D. (1990). Effects of irradiation of recipient mice on the behavior and leukemogenic potential of factor-dependent hematopoietic cell lines. *Blood*, 75(1), 190-197.
- [46] Duhrsen, U. and Metcalf, D. Factors influencing the time and site of leukemic transformation of factor-dependent cells after injection into irradiated recipient mice. *International Journal of Cancer*, 1988;44:1074-1081.
- [47] Dutch Ministry of Defence. (2011). Cancer incidence and cause-specific mortality following Balkan deployment.
- [48] Edwards, A.A., Lindholm, C., Darroudi, F., Stephan, G., Romm, H., Barquinero, J., Barrios, L., Caballin, M.R., Roy, L., Whitehouse, C.A., Tawan, E.J., Moquet, J., Lloyd, D.C. and Voisin, R. (2005). Review of translocations detected by FISH for retrospective biological dosimetry applications. *Radiat. Prot. Dosimet.* 113, 396-402.
- [49] Empson, V.G., McQueen, F.M. and Dalbeth, N. The natural killer cell: a further innate mediator of gouty inflammation? *Immunol Cell Biol.* 2010 Jan;88(1):24-31. doi: 10.1038/icb.2009.91. Epub 2009 Nov 24.
- [50] Farias-Eisner, R., Sherman, M.P., Aeberhard, E. and Chaudhuri, G. (1994). Nitric oxide is an important mediator for tumoricidal activity in vivo. *Proc Natl Acad Sci USA* 91, 9407-9411.
- [51] Gebhart, E., Neubauer, S., Schmitt, G., Birkenhake, S. and Dunst, J. (1996). Use of three-color chromosome in situ suppression technique for the detection of past radiation exposure. *Radiat. Res.* 145, 47-52.
- [52] Glickman, L.T., Domanski, L.M., Maguire, T.G., Dubielzig, R.R. and Churg, A. Mesothelioma in pet dogs associated with exposure of their owners to asbestos. *Environ Res*, 1983;32:305-313.
- [53] Grant, L.R., Yao, Z.J., Hedrich, C.M., Wang, F., Moorthy, A., Wilson, K., Ranatunga, D. and Bream, J.H. Stat4-dependent, T-bet-independent regulation of IL-10 in NK cells. *Genes Immun.* 2008 Jun;9(4):316-27. doi: 10.1038/gene.2008.20. Epub 2008 Apr 10.
- [54] Grdina, D.J., Murley, J.S. and Kataoka, Y. Radioprotectants: Current Status and New Directions. *Oncology*, 2002;63 Suppl 2:2-10.
- [55] Greenberger, J. *et al.* Hematopoietic Stem Cell-and Marrow Stromal Cell-specific requirements for Irradiation Leukemogenesis in vitro. *Exp. Hematol.* 1990;18:408-415.
- [56] Gustavsson, P., Talback, M., Lundin, A., Lagercrantz, B., Gyllestad, P.E. and Fornell, L. (2004). Incidence of cancer among Swedish military and civil personnel involved in UN missions in the Balkans 1989-99. *Occup. Environ. Med.* 61, 171-3.
- [57] Hagmar, L., Bonassi, S., Strömberg, U., Brøgger, A., Knudsen, L.E., Norppa, H. and Reuterwall, C. (1998). European Study Group on Cytogenetic Biomarkers and Health. Chromosomal aberrations in lymphocytes predict human cancer: A report from the European study group on cytogenetic biomarkers and health (ESCH). *Cancer Research* 58, 411-4121.
- [58] Hamerman, J.A., Ogasawara, K. and Lanier, L.L. NK cells in innate immunity. *Curr Opin Immunol.* 2005 Feb;17(1):29-35.

- [59] Hande, M.P., Boei, J.J., Granath, F. and Natarajan, A.T. (1996). Induction and persistence of cytogenetic damage in mouse splenocytes following whole-body X-irradiation analysed by fluorescence in situ hybridization. I. Dicentrics and translocations. *Int. J. Radiat. Biol.* 69, 437-446.
- [60] Hande, M.P. and Natarajan, A.T. (1998). Induction and persistence of cytogenetic damage in mouse splenocytes following whole-body X-irradiation analysed by fluorescence in situ hybridization. IV. Dose response. *Int. J. Radiat. Biol.* 74, 441-448.
- [61] Hashimoto, S., Shirato, H., Hosokawa, M., Nishioka, T., Kuramitsu, Y., Matushita, K., Kobayashi, M. and Miyasaka, K. (1999). The suppression of metastases and the change in host immune response after low-dose total-body irradiation in tumor-bearing rats. *Radiat Res* 151, 717-724.
- [62] Hayes, H.M., Hoover, R. and Tarone, R.E. Bladder cancer in pet dogs: a sentinel for environmental cancer? *Am J Epidemiol*, 1981;114:229-233.
- [63] Hoar, S.K., Blair, A., Holmes, F.F., Boysen, C.D., Robel, R.J., Hoover, R. and Fraumeni, J.F. Jr. Agricultural herbicide use and risk of lymphoma and soft-tissue sarcoma. *J Am Med Assoc*, 1986;256:1141-1147.
- [64] Hosoi, Y. and Sakamoto, K. (1993). Suppressive effect of low dose total body irradiation on lung metastasis: dose dependency and effective period. *Radiother Oncol* 26, 177-179.
- [65] Ibuki, Y. and Goto, R. Ionizing radiation-induced macrophage activation: augmentation of nitric oxide production and its significance. *Cell Mol Biol (Noisy-le-grand)*. 2004;50 Online Pub:OL617-26.
- [66] Ina, Y., Tanooka, H., Yamada, T. and Sakai, K. (2005). Suppression of thymic lymphoma induction by life-long low-dose-rate irradiation accompanied by immune activation in C57BL/6 mice. *Radiat Res* 163, 153-158.
- [67] Ishii, K., Hosoi, Y., Yamada, S., Ono, T. and Sakamoto, K. (1996). Decreased incidence of thymic lymphoma in AKR mice as a result of chronic, fractionated low-dose total-body X irradiation. *Radiat Res* 146, 582-585.
- [68] Janiak, M.K., Wrembel-Wargocka, J., Cheda, A., Nowosielska, E.M., Lisiak, E. and Bilski, M. (2006). Modulation of the antitumour functions of murine NK cells and macrophages after single low-level exposures to X-rays. *Int J Low Radiation* 3, 178-191.
- [69] Jenkins, D.C., Charles, I.G., Thomsen, L.L., Moss, D.W., Holmes, L.S., Baylis, S.A., Rhodes, P., Westmore, K., Emson, P.C. and Moncada, S. (1995). Role of nitric oxide in tumor growth. *Proc Natl Acad Sci USA* 92, 4392-4396.
- [70] Ju, G.Z., Liu, S.Z., Li, X.Y., Liu, W.H. and Fu, H.Q. (1995). Effect of high versus low dose radiation on the immune system. In: Hagen, U., Harder, D., Jung, H., Streffer, C. (eds) *Radiat Res* 1895-1995. Proc of the Tenth Int Congress of Radiation Research, pp. 709-714. Würzburg, Germany.
- [71] Kataoka, T., Mizuguchi, Y., Notohara, K., Taguchi, T. and Yamaoka, K. (2006). Histological changes in spleens of radio-sensitive and radio-resistant mice exposed to low-dose X-ray irradiation. *Physiol Chem Phys & Med NMR* 38, 21-29.
- [72] Lanier, L.L. Up on the tightrope: natural killer cell activation and inhibition. *Nat Immunol*. 2008 May;9(5):495-502. doi: 10.1038/ni1581.

- [73] Lewis, C.E. and Pollard, J.W. Distinct role of macrophages in different tumor microenvironments. *Cancer Res.* 2006 Jan 15;66(2):605-12.
- [74] Li, M., Jendrossek, V. and Belka, C. The role of PDGF in radiation oncology. *Rad Oncol* 2007;2:1-9.
- [75] Lindholm, C., Romm, H., Stephan, G., Schmid, E., Moquet, J. and Edwards, A. (2002). Intercomparison of translocation and dicentric frequencies between laboratories in a follow-up of the radiological accident in Estonia. *Int. J. Radiat. Biol.* 78, 883-890.
- [76] Liu, S.Z. (2007). Cancer Control Related to Stimulation of Immunity by Low-Dose Radiation. *Dose Response* 5, 39-47.
- [77] Liu, S.Z., Han, Z.B. and Liu, W.H. (1994). Changes in lymphocyte reactivity to modulatory factors following low dose ionizing radiation. *Biomed Environ Sci* 7, 130-135.
- [78] High-mobility group box 1 protein (HMGB1): nuclear weapon in the immune arsenal. *Nat Rev Immunol.* 2005 Apr;5(4):331-42.
- [79] Lucas, J.N., Awa, A., Straume, T., Poggensee, M., Kodama, Y., Nakano, M., Ohtaki, K., Weier, H.U., Pinkel, D., Gray, J. and Littlefield, G. (1992). Rapid translocation frequency analysis in humans decades after exposure to ionizing radiation. *Int. J. Radiat. Biol.* 62, 53-63.
- [80] Lucas, J.N., Deng, W., Moore, D., Hill, F., Wade, M., Lewis, A., Sailes, F., Kramer, C. and Hsied, A., Galvan, N. (1999). Background Ionizing radiation plays a minor role in the production of chromosome translocations in a control population. *Int. J. Radiat. Biol.* 75, 819-827.
- [81] Lucas, J.N., Poggensee, M. and Straume, T. (1992). The persistence of chromosome translocations in a radiation worker accidentally exposed to tritium. *Cytogenet. Cell. Genet.* 60, 255-256.
- [82] Lucas, J.N., Tenjin, T., Straume, T., Pinkel, D., Moore II, D.H., Litt, M. and Gray, J.W. (1989). Rapid human chromosome aberration analysis using fluorescence in situ hybridization. *Int. J. Radiat. Biol.* 56, 35-44.
- [83] Madani, I., De Neve, W. and Mareel, M. Does ionizing radiation stimulate cancer invasion and metastasis? *Bull Cancer.* 2008 Mar;95(3):292-300. doi: 10.1684/bdc.2008.0598.
- [84] Mahaney, F.X. Military working dogs may be a sentinel for human cancer. *J. Natl Cancer Inst,* 1990;82:1002-3.
- [85] Mandelli, F., Biagini, C., Grandolfo, M., Mele, A., Onufrio, G. and Tricarico, A. Second Report of the Defense Ministry Commission on the Incidence of Malignant Neoplasms among Military Personnel in Bosnia and Kosovo. Ministry of Defense, Italy, 2002.
- [86] Mantovani, A., Allavena, P., Sica, A. and Balkwill, F. Cancer-related inflammation. *Nature.* 2008 Jul 24;454(7203):436-44. doi: 10.1038/nature07205.
- [87] McDiarmid, M.A., Keogh, J.P., Hooper, F.J., McPhaul, K., Squibb, K., Kane, R., DiPino, R., Kabat, M., Kaup, B., Anderson, L., Hoover, D., Brown, L., Hamilton, M., Jacobson-Kram, D., Burrows, B. and Walsh, M. Health effects of depleted uranium on exposed Gulf War veterans. *Environ. Res.* 2000;82:168-180.
- [88] Miller, A.C. *et al.* A review of depleted uranium biological effects in vitro and in vivo. *Reviews in Environ Health* 2007;22(1):75-89.

- [89] Miller, A.C. Leukemic transformation of hematopoietic cells in mice internally exposed to depleted uranium. *Molecular Cellular Biochemistry* 2005 Nov; 279(1-2):97-104.
- [90] Mills, C.D., Kincaid, K., Alt, J.M., Heilman, M.J. and Hill, A.M. (2000). M-1/M-2 Macrophages and the Th1/Th2 Paradigm. *J Immunol* 164, 6166-6173.
- [91] Ministero della Difesa. (2002). Relazione Finale della Commissione istituita dal Ministro della Difesa sull'incidenza di neoplasie maligne tra i militari impiegati in Bosnia e Kosovo.
- [92] Mitchel, R.E., Jackson, J.S., McCann, R.A. and Boreham, D.R. (1999). The adaptive response modifies latency for radiation-induced myeloid leukemia in CBAH mice. *Radiat Res* 152, 273-279.
- [93] Mitchel, R.E., Jackson, J.S., Morrison, D.P. and Carlisle, S.M. (2003). Low doses of radiation increase the latency of spontaneous lymphomas and spinal osteosarcomas in cancer-prone, radiation-sensitive Trp53 heterozygous mice. *Radiat Res* 159, 320-327.
- [94] Moretta, L., Ciccone, E., Poggi, A., Mingari, M.C. and Moretta, A. (1994). Origin and functions of human natural killer cells. *Int J Clin Lab Res* 24, 181-186.
- [95] Nakano, N., Nakashima, E., Pawel, D.J., Kodama, Y. and Awa, A. (1993). Frequency of reciprocal translocation and dicentrics induced in human blood lymphocytes by X-irradiation as determined by fluorescence in situ hybridization. *Int. J. Radiat. Biol.* 54, 565-569.
- [96] Naparstek, E. *et al.* Induction of Growth Alterations in Factor-Dependent Hematopoietic progenitor cell lines by co-cultivation with irradiated bone marrow stromal cells. *Blood* 1986;67:1395-1403.
- [97] Natarajan, A.T., Vyas, R.C., Darroudi, F. and Vermeulen, S. (1992). Frequencies of X-ray-induced chromosome translocations in human peripheral lymphocytes as detected by in situ hybridization using chromosome-specific DNA libraries. *Int. J. Radiat. Biol.* 61, 199-203.
- [98] Nathan, C. (1991). Mechanisms and modulation of macrophage activation. *Behrings Inst Mitt* 88, 200-207.
- [99] Neubauer, S., Gebhart, E., Schmitt, G., Birkenhake, S. and Dunst, J. (1996). Is chromosome in situ suppression (CISS) hybridization suited as a predictive test for intrinsic radiosensitivity in cancer patients? *Int. J. Oncol.* 8, 707-712.
- [100] Nowosielska, E.M., Cheda, A., Wrembel-Wargocka, J. and Janiak, M.K. (2011). Anti-neoplastic and immunostimulatory effects of low-dose X-ray fractions in mice. *Int J Radiat Biol* 87, 202-212.
- [101] Nowosielska, E.M., Cheda, A., Wrembel-Wargocka, J. and Janiak, M.K. (2008). Modulation of the growth of pulmonary tumour colonies in mice after single or fractionated low-level irradiations with X-rays. *Nukleonika* 53(Suppl. 1), S9-S15.
- [102] Nowosielska, E.M., Cheda, A., Wrembel-Wargocka, J. and Janiak, M.K. (2010). Immunological mechanism of the low-dose radiation-induced suppression of cancer metastases in a mouse model. *Dose-Response* 8, 209-226.
- [103] Nowosielska, E.M., Cheda, A., Wrembel-Wargocka, J. and Janiak, M.K. (2011). Stimulation of the natural anti-tumor cells by single and fractionated irradiations of mice with low doses of X-rays. *Health Physics* 100, 283-285.

- [104] Nowosielska, E.M., Cheda, A., Wrembel-Wargocka, J. and Janiak, M.K. (2012). Effect of low doses of low-let radiation on the innate anti-tumor reactions in radioresistant and radiosensitive mice. *Dose-Response* 10, 500-515.
- [105] Nowosielska, E.M., Wrembel-Wargocka, J., Cheda, A. and Janiak, M.K. (2006). A single low-dose irradiation with X-rays stimulates NK cells and macrophages to release factors related to the cytotoxic functions of these cells. *Centr Eur J Immunol* 31, 51-57.
- [106] Nowosielska, E.M., Wrembel-Wargocka, J., Cheda, A., Lisiak, E. and Janiak, M.K. (2005). Low-level exposures to ionising radiation modulate the anti-tumour activity of murine NK cells. *Nukleonika* 50 (Suppl. 2), S21-S24.
- [107] Nowosielska, E.M., Wrembel-Wargocka, J., Cheda, A., Lisiak, E. and Janiak, M.K. (2006). Enhanced cytotoxic activity of macrophages and suppressed tumor metastases in mice irradiated with low doses of X-rays. *J Radiat Res* 47, 229-236.
- [108] Okayasu, R., Suatomi, K., Yu, Y., Silver, A., Bedford, J.S., Cox, R. and Ullrich, R.L. (2000). A deficiency in DNA repair and DNA-PKcs expression in the radiosensitive BALB/c mouse. *Cancer Res* 60, 4342-4345.
- [109] Peragallo, M.S., Lista, F., Sarnicola, G., Marmo, F. and Vecchione, A. (2010). Cancer surveillance in Italian army peacekeeping troops deployed in Bosnia and Kosovo, 1996-2007: preliminary results. *Cancer Epidemiol.* 34, 47-54.
- [110] Ponnaiya, B., Cornforth, M.N. and Ullrich, R.L. (1997). Radiation-Induced Chromosomal Instability in BALB/c and C57BL/6 Mice: The Difference is as Clear as Black and White. *Radiat Res* 147, 121-125.
- [111] Potential radiation exposure in military operations. Protecting the soldier before, during and after (1999), Thaul, S., O'Maonaigh, H. (Eds) Institute of Medicine, National Academy Press Washington, DC, USA.
- [112] Pressl, S. and Stephan, G. (1998). Chromosome translocations detected by fluorescence in situ hybridization (FISH) – a useful tool in population monitoring. *Toxicol. Lett.* 96/97, 189-194.
- [113] Priest, N.D. (2001). Toxicity of depleted uranium. *Lancet* 357, 244-6.
- [114] Ramsey, M.J., Moore II, D.H., Briner, J.F., Lee, D.A., Olsen, L.A. and Senft, J.R. (1995). The effects of age and lifestyle factors on the accumulation of cytogenetic damage as measured by chromosome painting. *Mutat. Res.* 338, 95-106.
- [115] Rossner, P., Boffetta, P., Ceppi, M., Bonassi, S., Smerhovsky, Z., Landa, K., Juzova, D. and Sram, R.J. (2005). Chromosomal aberrations in lymphocytes of healthy subjects and risk of cancer. *Environ. Health Perspect.* 113, 517-520.
- [116] Rubartelli, A. and Lotze, M.T. Inside, outside, upside down: damage-associated molecular-pattern molecules (DAMPs) and redox. *Trends Immunol.* 2007 Oct;28(10):429-36. Epub 2007 Sep 12.
- [117] Safwat, A. (2000). The immunology of low-dose total-body irradiation: more questions than answers. *Radiat Res* 153, 599-604.
- [118] Samet, J.M. Epidemiologic studies of ionizing radiation and cancer: past successes and future challenges. *Environ Health Perspect* 1997;105:883-889.

- [119] Savage, J.R.K. and Simpson, P. (1994). On the scoring of FISH-“painted” chromosome-type exchange aberrations. *Mutation Res.* 307, 345-353.
- [120] Schmid, E., Zitzelsberg, H., Braselmann, H., Gray, J.W. and Bauchinger, M. (1992). Radiation-induced chromosome aberrations analysed by fluorescence in situ hybridization with a triple combination of composite whole chromosome-specific DNA probes. *Int. J. Radiat. Biol.* 628, 673-678.
- [121] Schröder, H., Heimers, A., Frentzel-Beyme, R., Schott, A. and Hoffmann, W. Chromosome aberration analysis in peripheral lymphocytes of Gulf war and Balkans war veterans. *Rad. Prot. Dos.* 103, 211-219, 2003.
- [122] Seed, T.M. *et al.* New Strategies for the Prevention of Radiation Injury. *J. Radiat. Res.*, 43: Suppl., S239-S244, 2002.
- [123] Seed, T.M. Radiation Protectants: Current Status and Future Prospects. *Health Physics*, 2005;89(5):531-545.
- [124] Sigurdson, A.J., Mina, H., Hauptmann, M., Bhatti, P., Sram, R.J., Beskid, O., Tawn, E.J., Whitehouse, C.A., Lindholm, C., Nakano, M., Kodama, Y., Nakamura, N., Vorobtsova, I., Oestreicher, U., Stephan, G., Yong, L.C., Bauchinger, M., Schmid, E., Chung, H.W., Darroudi, F., Roy, L., Voisin, P., Barquinero, J.F., Livingston, L.M., Blakey, D., Hayata, I., Zhang, W., Wang, C., Bennett, L.M., Littlefield, L.G., Edwards, A.A., Kleinerman, R.A. and Tucker, J.D. (2008). International study factors affecting human chromosome translocations. *Mutat. Res.* 652, 112-121.
- [125] Sorokine-Durm, I., Whitehouse, C. and Edwards, A. (2000). The variability of translocation yields amongst control populations. *Radiation Protection Dosimetry* 88, 93-99.
- [126] Storer, J.B., Mitchell, T.J. and Fry, R.J. (1988). Extrapolation of the relative risk of radiogenic neoplasms across mouse strains and to man. *Radiat Res* 114, 331-53.
- [127] Storm, H.H., Jorgensen, H.O., Kejs, A.M. and Engholm, G. (2006). Depleted uranium and cancer in Danish Balkan veterans deployed 1992-2001. *Eur. J. Cancer* 42, 2355-8.
- [128] Thompson, S.L. and Compton, D.A. (2011). Chromosomes and cancer cells. *Chromosome Res.* 19 433-444.
- [129] Tucker, J.D. (2001). Fish cytogenetics and the future of radiation biodosimetry. *Radiat. Prot. Dosim.* 97, 55-60.
- [130] Tucker, J.D., Lee, D.A., Ramsay, M.J., Briner, J., Olsen, L. and Moore II, DH. (1994). On the frequency of chromosome exchanges in a control population measured by chromosome painting. *Mutat. Res.* 313, 193-202.
- [131] Tucker, J.D., Morgan, W.F., Awa, A.A., Bauchinger, M., Blakey, D., Cornforth, M.N., Littlefield, L.G., Natarajan, A.T. and Shasserre, C. (1995). A proposed system for scoring structural aberrations detected by chromosome painting. *Cytogenet. Cell. Genet.* 68, 211-221.
- [132] Ullrich, R.L., Bowles, N.D., Satterfield, L.C. and Davis, C.M. (1996). Strain-dependent susceptibility to radiation-induced mammary cancer is a result of differences in epithelial cell sensitivity to transformation. *Radiat Res* 146, 353-5.

- [133] Ullrich, R.L. and Ponnaiya, B. (1998). Radiation-induced instability and its relation to radiation carcinogenesis. *Int J Radiat Biol* 74, 747-754.
- [134] UNSCEAR 2008 Report. United Nations, New York, 2010.
- [135] UNSCEAR 57th session documents 2010 (unpublished).
- [136] Verma, M., Lam, T.K., Hebert, E. and Divi, R.L. Extracellular vesicles: potential applications in cancer diagnosis, prognosis, and epidemiology. *BMC Clin Pathol*. 2015 Apr 15;15:6.
- [137] Vorobtsova, I.E., Tucker, J.D., Timofeeva, N.M., Bogomazova, A.N., Semenov, A.V. and Pleshanov, P.G. (2000). Effects of age and radiation exposure on the frequency of translocations and dicentrics detected by FISH method in human lymphocytes. *Radiat. Biol. Radioecol.* 40, 142-148.
- [138] Wells, C.A., Ravasi, T., Faulkner, G.J., Carninci, P., Okazaki, Y., Hayashizaki, Y., Sweet, M., Brandon, J., Wainwright, B.J. and Hume, D.A. (2003). Genetic control of the innate immune response. *BMC Immunol* 4, 5.
- [139] Xie, K. and Fidler, I.J. (1998). Therapy of cancer metastasis by activation of the inducible nitric oxide synthase. *Cancer Met Rev* 17, 55-75.
- [140] Young, H.A. and Ortaldo, J. (2006). Cytokines as critical co-stimulatory molecules in modulating the immune response of natural killer cells. *Cell Res* 16, 20-24.
- [141] Zeh, H.J. and Lotze, M.T. Addicted to death: invasive cancer and the immune response to unscheduled cell death. *J Immunother.* 2005 Jan-Feb;28(1):1-9.



Chapter 3 – MEDICAL RADIATION PREPAREDNESS

3.1 GENERAL INTRODUCTION

Following the 2011 inter-laboratory comparison, an exercise was set up to validate the METREPOL severity scoring strategy using SEARCH data base and METREPOL created cases [1]. Interestingly, highly irradiated victims (score H3 and H4 METREPOL) could be separated from worried wells and less irradiated cases underlying the usefulness of clinical dosimetry when completed with blood cell counts. Thus, a day2 – day3 secondary triage could be efficiently achieved.

3.2 DIAGNOSING ACUTE RADIATION SYNDROME AND MEDICAL MANAGEMENT BASED ON CLINICAL SIGNS AND SYMPTOMS NATO HFM-222 EXERCISE 2015 – PRELIMINARY RESULTS

Abstract

We examined the significance of early occurring (<5 days) clinical signs and symptoms after irradiation and the association with the late developing (>30 days) Hematological Acute Radiation Syndrome (HARS). Altogether 191 cases were collected using descriptions originating from real case scenarios stored in the database SEARCH (system for evaluation and archiving of radiation accidents based on case histories). The METREPOL (MEDical TREatment ProtocOLs for Radiation Accident Victims) approach was used in order to generate further cases. Participating eight teams from 5 Nations were asked predicting the severity (RC0 – 4), the late occurrence of a HARS and the requirement for hospitalization. Our preliminary analysis showed that teams categorized the 191 cases within 3 h or later. In particular the correct classification of very severe HARS (RC4) could be successfully performed by all teams. However, the discrimination of unexposed (RC0) versus low-exposed individuals (RC1) appeared challenging. In future analysis we will in particular focus on the following aspects:

- 1) The use of different tools by the teams, e.g., the H-module or the BAT biodosimetry software;*
- 2) Recommendations of the teams for future exercises;*
- 3) Limitations of METREPOL in terms of not comprising RC0;*
- 4) Reported diagnostic certainty of the teams and how reliable these parameters are;*
- 5) Comparing dose estimates based on clinical signs and symptoms with the dicentric chromosome analysis available for 21 of our SEARCH cases; and finally*
- 6) Reporting about the limitation of this study (e.g., excluding psychological aspects relevant for clinical signs and symptoms).*

The completed analysis will be published in a major radiation biology journal.

3.2.1 Introduction

Malevolent use of radiation sources or radioactive material has to be taken into account in the planning of military mission scenarios. The uses of Radiological Dispersion Device (RDD) and Radiation Exposure Device (RED) are considered serious threats. Therefore this exercise was performed within the frame of the NATO Human Factors and Medicine Panel 222 Research Task Group (Ionizing Radiation Bioeffects and Countermeasures).

Malevolent use of radiation sources or radioactive material can involve a few up to several hundreds or thousands of persons, depending on the type of the scenario and the amount of released material and doses involved.

In terms of clinical treatment decisions, it is crucial to rapidly obtain an estimate of individual radiation injury (or dose) to predict the expected severity of potential radiation-induced acute radiation syndrome or sickness and to develop strategies to manage medical treatment.

After significant acute whole body or partial body radiation exposure, these patients require immediate, intensive and interdisciplinary medical treatment approaches [1], [2]. In this context, the assessment of the patient's prognosis based on clinical signs and symptoms will be of utmost importance.

In the METREPOL system (Medical Treatment Protocols for Radiation Accident Victims), the estimation of radiation effects and the patients' prognosis will be based on clinical signs and symptoms and the clinical status will be categorized by using organ-specific checklists for the four most important organ systems:

- The Neurovascular (N) system;
- The Hematopoietic (H) system;
- The Cutaneous (C) system; and
- The Gastrointestinal (G) system [3].

Verification of clinical dosimetry systems like METREPOL on the basis of real clinical data from case histories of accidentally exposed patients has to our knowledge not been performed.

3.2.1.1 Concept of the Exercise

The objective of the exercise was training to triage a high number of potentially radiation exposed individuals regarding the later occurring Acute Radiation Syndrome (ARS).

Goals of the exercise were the comparison of existing and established systems for triage of ARS, evaluation of different data formats for data transfer and documentation, as well as proper information transfer in an accident situation, scoring of the correct diagnosis of the real case histories from the SEARCH database (System for Evaluation and Archiving of Radiation Accidents based on Case Histories [4]) and measurement of the response time for diagnosing all case histories.

The exercise set-up contained real cases from the SEARCH database of radiation accident victims as well as simulated cases on the basis of METREPOL. As this exercise was based on historical cases issued from different accidental situations (SEARCH database), only the respective times of casualties' clinical examination and clinical and biological analyses after the event were provided. Exposure conditions were limited to external radiation exposure without combined injuries due to the data available from the SEARCH database. The only indicators for the radiation exposure itself were clinical signs and symptoms of the affected persons.

3.2.1.2 Exercise Scenario

The Exercise was based on a scenario of a Radiological Exposure Devices (RED / "orphan source") mounted in a long-distance train. The scenario served as a basis for the exercise regarding the time of exposure and the number of potentially radiation exposed persons, but no detailed information about the nature of the radiation source was given to the participants. Other possible topics like detecting the radiation source, intelligence information and dealing with other topics regarding malicious acts have not been part of this exercise.

The radiation exposure took place on day 0 during a one hour train ride.

3.2.2 Material and Methods

3.2.2.1 The SEARCH Database and METREPOL

The development of the database system SEARCH started with the “Moscow-Ulm Radiation Accident Database (MURAD)”, which contained case histories of radiation accident victims of the Chernobyl accident. After that, an “International Computer Database for Radiation Exposure Case Histories” was created to include all available clinical data from radiation accident victims. Clinical data from radiation accidents from all over the world were then incorporated into the database system, from the beginning of nuclear technology until now. Today, the SEARCH database contains 824 clinical cases from 81 radiation accidents in 19 countries [4]. This exceptional collection of clinical data from accidentally radiation-exposed persons allows not only detailed analysis of the time course, prognostic factors, and multi-organ interactions of the ARS but also analysis of the efficacy of different therapeutic strategies. SEARCH was used to develop the METREPOL system (Medical Treatment Protocols for Radiation Accident Victims), which was an entirely new approach to managing radiation accident victims on the basis of indicators of effect and repair, taking into consideration multi-organ involvement and potential treatment options [4].

3.2.2.2 Exercise Cases

The data set contained 191 case histories with clinical signs and symptoms for day 0 – 3 and day 0 – 5 respectively, including the following groups:

- 24 real-case histories from the database SEARCH;
- 78 case histories created on the basis of METREPOL; and
- 89 case histories of non-exposed cases (“worried well”).

Cases from the database SEARCH that had excellent documentation of the clinical course in the first 5 days were selected. The datasets were pseudonymized, so that the real-case histories could not be discriminated from the created-case histories. Additional case histories were created on the basis of the METREPOL checklists for different Response Categories (RC’s). Clinical data created on the basis of normal values for the relevant clinical signs and symptoms were used as unexposed persons (“worried well”).

3.2.2.3 Input Data Format

Participants received information on a daily base regarding:

- Begin, end and degree of nausea, vomiting, anorexia, abdominal cramps/pain, diarrhea, fatigue syndrome, headache, neurological deficits (specified per case where applicable), cognitive deficits (specified per case where applicable).
- Rise in body temperature.
- Blood pressure (systolic and diastolic).
- Heart rate.
- Skin symptoms of the body surface (kind of symptoms, e.g., erythema, location, percent of body surface involved).
- Mucositis (location, degree).
- Peripheral blood cell counts (erythrocytes, lymphocytes, granulocytes, thrombocytes, hemoglobin).
- Laboratory parameter, e.g., CRP, gammaGT, LDH, AP, CK, S-Amylase.

3.2.2.4 Output Data Format

The participants were asked to return their results after finishing their analysis on the first dataset to receive the second dataset and then to send their results based on the second dataset containing the following details:

- Certainty of their diagnosis.
- Predicting the development of a late occurring ARS (categorical, yes, no, uncertain).
- Estimate the radiation damage of different organ systems according to the METREPOL severity grading scale.
- Decide in favor of a certain response category (RC0-4).
- Estimate the radiation dose (Gy).
- Predict the requirement for hospitalization (categorical, yes, no, uncertain).
- Add further information on the recommended therapeutic intervention (optional). However, this information was not considered for statistical analysis.

3.2.2.5 Participants

Eight (8) expert teams from 7 different institutions from five countries participated in the exercise:

- Bundeswehr Institute of Radiobiology affiliated to the University Ulm, Munich, Germany.
- Armed Forces Radiobiology Research Institute (AFRRI), Uniformed Services, University of the Health Sciences (USUHS), Bethesda, United States.
- Applied Research Associates Inc. (ARA), on behalf of (U.S.) Defense Threat Reduction Agency (DTRA), Arlington, United States.
- Army Medical and Veterinary Research Center, Roma, Italy.
- French Defence Radiation Protection Service (SPRA), Clamart, France.
- Institut de Recherche Biomédicale des Armées, Bretigny-sur-Orge, France.
- Department of Radiobiology, Faculty of Military Health Sciences, University of Defence, Hradec Králové, Czech Republic.

3.2.3 Results

3.2.3.1 Report Time

First responses were received after 3 hours (median 5 h). The preliminary mean response time was 9.15 hours for diagnosing 191 cases on the basis of input data file 1 (day 0 – 3). The response time for diagnosing the exercise cases based on the second input data file (day 0 – 5) was shorter than for the first data file.

Since this exercise was not carried out in real-time, the participating expert groups were able to set the time to start the exercise individually. Therefore analyses are based on the self-reported working time of all groups.

3.2.3.2 Recommendation for Hospitalization

The rating, if hospitalization of the patients would be necessary or not, was analyzed on the basis of input data file 1 (day 0 – 3). Possible Answers were “Yes”, “No” and “Uncertain”. All cases with grading H3 and H4 (SEARCH cases and created case histories on the basis of METREPOL) were rated with “YES” for

hospitalization except one H3 case with two ratings “UNCERTAIN” on the basis of clinical data for day 0-3. There have been no “false negative” results in the H3 / H4 group.

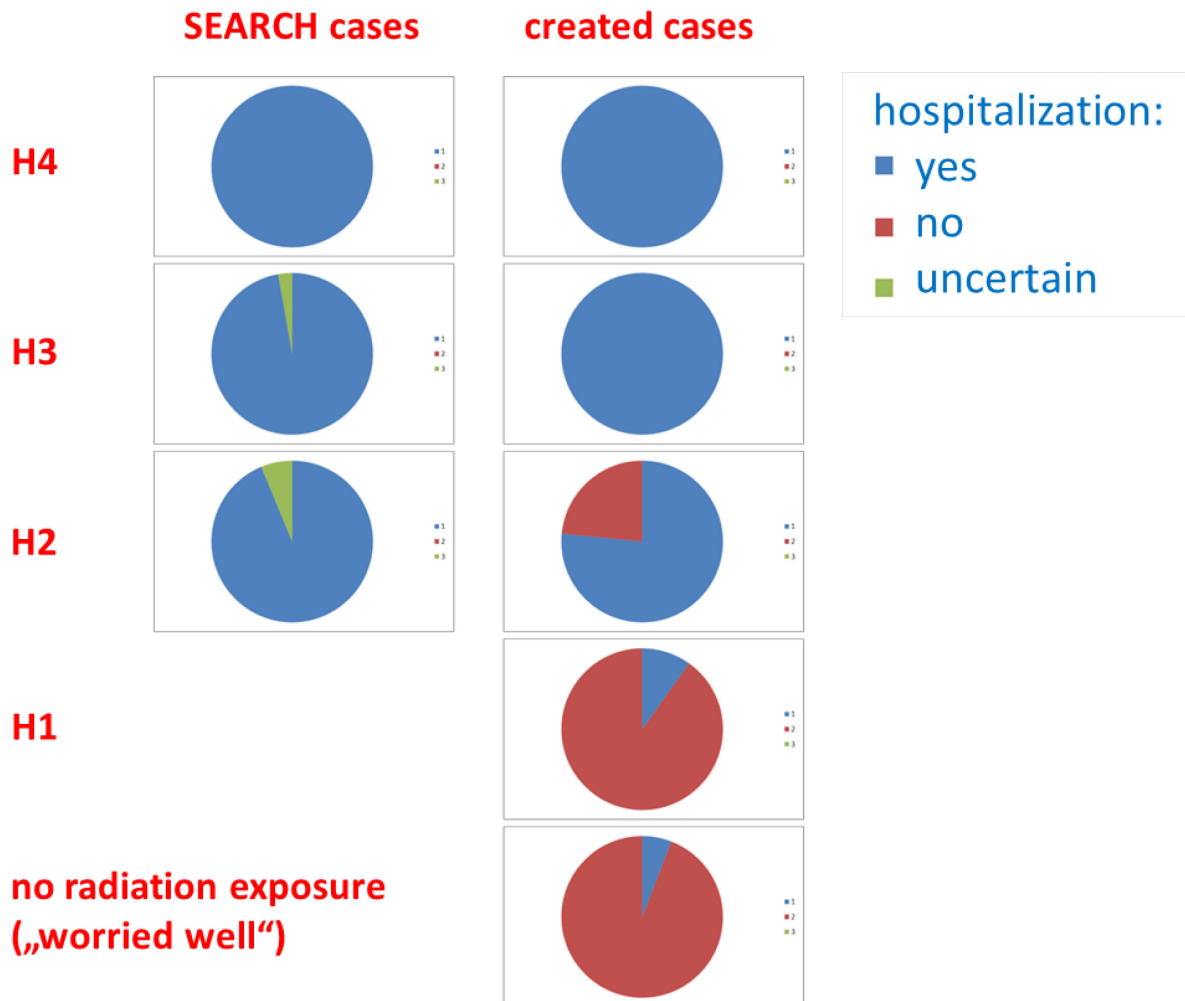


Figure 3-1: Analysis of the Results Regarding the Recommendation for Hospitalization of the Exercise Cases.

3.2.3.3 Estimation of the Response Category (RC)

Reported RC4 matched with true RC4 in almost all cases in all groups irrespective of the origin of the generated case data (METREPOL or SEARCH).

Systematically overestimation of RC2 and RC3 exercise cases could be seen, since most teams reported RC2 and RC3 for true RC2 and likewise RC3 and RC4 for true RC3 cases (irrespective of the data origin).

True RC2 appeared in particular problematic since they were partly reported as unexposed (RC0) and as RC2.

Unexposed individuals (RC0) were mainly reported as being RC0 or RC1.

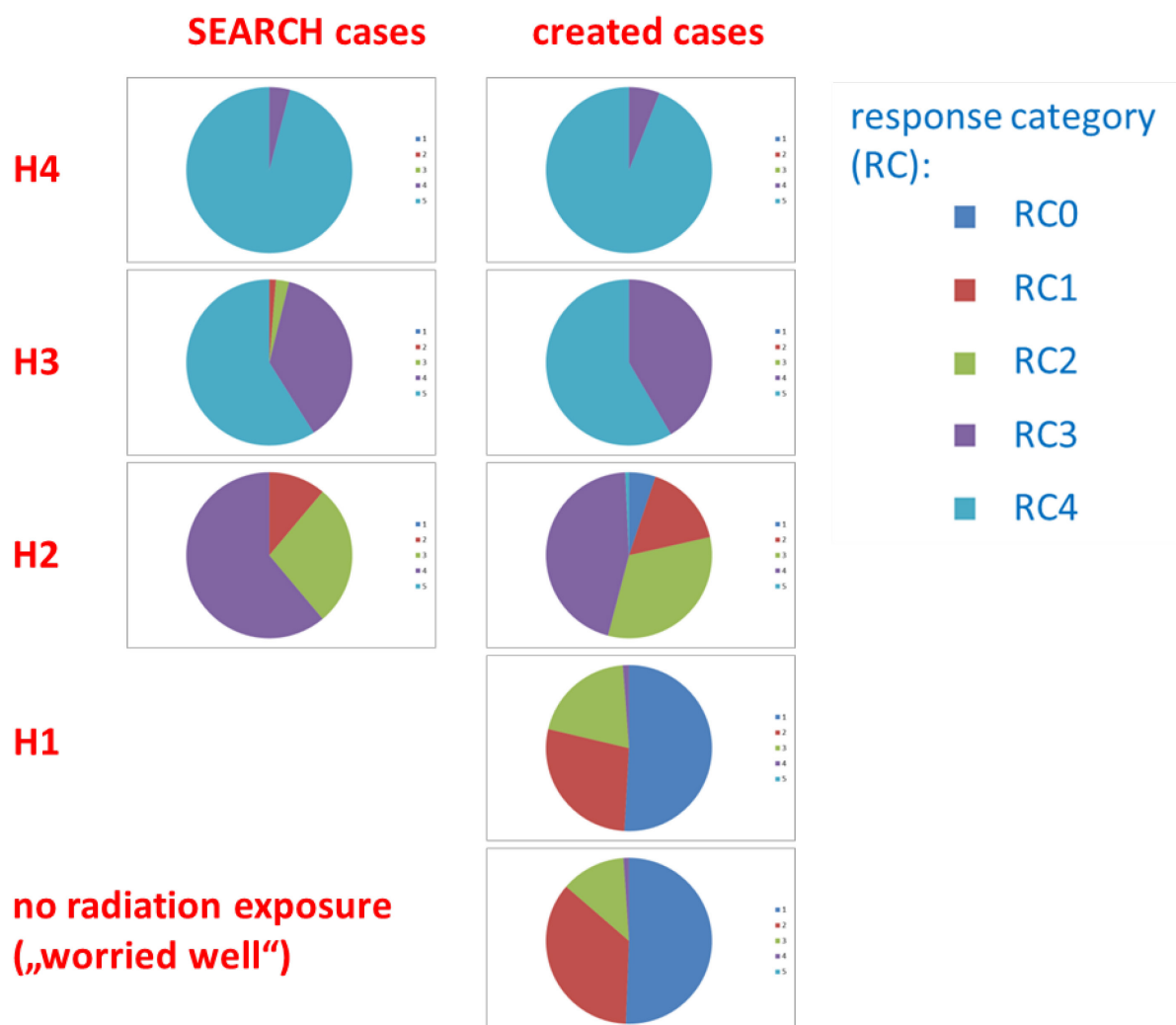


Figure 3-2: Analysis of the Results Regarding the Diagnosed Response Category (RC).

3.2.4 Discussion

For the medical management of individuals exposed to ionizing radiation, it is necessary to decide about hospitalization and treatment as early as possible.

Our preliminary results on the use of radiation-induced clinical signs and symptoms occurring within the first three and five days after irradiation showed that 191 cases could be classified within 3 hours or later. That is the main finding of our preliminary examinations. All 8 expert teams classified RC 4 ARS correctly, but discrimination among RC0 and RC1 appeared more challenging. It is our first interpretation of this preliminary analysis that detection of RC4 represents a strength of the clinical approach performed by the teams, while the discrimination among RC0 and RC1 seems to represent a challenge.

It also seemed that the teams experienced the same difficulties in categorization of, e.g., RC1 irrespective of whether they were generated using SEARCH or METREPOL. Therefore, in future analysis we plan to merge results of both approaches in order to increase the statistical power of our analysis.

In future analysis we will also focus on other issues, such as:

- 1) The use of different tools by the teams, e.g., the H-module or the BAT biodosimetry software.

- 2) Recommendations of the teams for future exercises.
- 3) Limitations of METREPOL in terms of not comprising RC0.
- 4) Reported diagnostic certainty of the teams and how reliable these parameters are.
- 5) Comparing dose estimates based on clinical signs and symptoms with the dicentric chromosome analysis available for 21 of our SEARCH cases.
- 6) Reporting about the limitation of this study (e.g., excluding psychological aspects relevant for clinical signs and symptoms).

The completed analysis will be published in a major radiation biology journal.

3.3 ACKNOWLEDGEMENTS

The opinions or assertions contained herein are the private views of the authors and are not necessarily those of the Armed Forces Radiobiology Research Institute, the Uniformed Services University of the Health Sciences, the Department of Defense, and/or the U.S. Government. This work was supported by the German Ministry of Defence. In addition, William F. Blakely and David L. Bolduc's efforts were partially supported under AFRRRI Protocol# RBB43523. We thank Mr. Andreas Hübsch from the Bundeswehr Institute of Radiobiology for his assistance in preparing the exercise case histories.

3.4 REFERENCES

- [1] Dörr, H.D. and Meineke, V. Appropriate radiation accident medical management: necessity of extensive preparatory planning. *Radiation and environmental biophysics*, 2006;45:237-44.
- [2] Dainiak, N., Waselenko, J.K., Armitage, J.O., MacVittie, T.J. and Farese, A.M. The hematologist and radiation casualties. *Hematology Am Soc Hematol Educ Program*, 2003:473-96.
- [3] Fliedner, T.M., Friesecke, I. and Beyrer, K. (Eds): *Medical Management of Radiation Accidents—Manual on the Acute Radiation Syndrome*. London: British Institute of Radiology, 2001.
- [4] Friesecke, I., Beyrer, K., Greiner, C., Wedel, R. and Fliedner, T.M. SEARCH: a system for evaluation and archiving of radiation accidents based on case histories. *Radiation and environmental biophysics*, 2000;39:213-217.



Chapter 4 – NATO HFM-222 RTG ROLE 4 BIODOSIMETRY ASSAYS SURVEY AND BIODOSIMETRY ASSAYS TECHNOLOGY READINESS LEVEL UPDATE

4.1 GENERAL INTRODUCTION

In order to better coordinate NATO structures, the inventory of their technical capacities was established including their respective technology readiness levels [6], but today no definite alternative Gold Standard to DIC can be recommended.

4.2 NATO ROLE 4 BIODOSIMETRY ASSAYS SURVEY

Abstract

The North Atlantic Treaty Organization (NATO) Human Factors and Medicine Panel (HFM) HFM-222 Research Task Group (RTG) – Ionizing Radiation Bioeffects and Countermeasures performed a survey to assess current biodosimetry capabilities in NATO Nations’ reach-back and associated (i.e., partner) laboratories.

4.2.1 Introduction

Recently members of the HFM-222 radiobiology RTG earlier reported on a laboratory inter-comparison of established and emerging biodosimetry assays [1] based on laboratory inter-comparison of the dicentric chromosome analysis assay [2], cytokinesis-blocked micronuclei assay [3], γ -H2AX foci assay [4], and gene expression assays [5].

As a follow-up to these laboratory inter-comparisons, a biodosimetry survey questionnaire was developed, modelled after a similar cytogenetic biodosimetry survey performed by the World Health Organization (WHO) BioDoseNet in 2009, to assess present capacity, capabilities, and needs of NATO Nations [6]; [7]. The survey was modified to reflect expanded dose and injury assessment capabilities beyond the use of cytogenetic biodosimetry assays by NATO Nations (Table 4-1).

Table 4-1: Radiation Dose and Injury Assessment Modalities.

Radiation Dose and Injury Assessment Modalities	Assays
Cytogenetic	Dicentric Chromosome Aberration (DCA) assay, Cytokinesis-Blocked Micronuclei (CBMN) assay, Premature Chromosome Condensation (PCC) assay, Fluorescence <i>In Situ</i> Hybridization (FISH) Translocation assay, γ -H2AX foci assay
Gene Expression Bioassays	mRNA and miRNA assays
Blood Chemistry (Proteomic) Bioassays	C-reactive protein, amylase activity, Flt-3 ligand, and multiple proteomic biomarker panel
Electron Paramagnetic Resonance (EPR)	Dose assessment using nail clippings, teeth, and bone by EPR dosimetry
Radioactivity Counting	Whole-body counting, radionuclide detection, radioactivity assessment of biofluids (i.e., urine, feces, blood, saliva), committed dose calculations
Other Assays	Physical dosimetry

Five NATO Nations participated in this survey questionnaire to reflect the biodosimetry capability within its reference (reach-back) laboratory(s) as well as capabilities of its partner or associated laboratories.

4.2.2 Biodosimetry Survey Questionnaire Responses

4.2.2.1 Contact Information

Contact information and additional details for the laboratories participating in this survey are described in Table 4-2.

Table 4-2: Contact Information.

Nation	USA	DEU	ITA	GBR	FRA
Laboratory	Armed Forces Radiobiology Research Institute (AFRRI)	Bundeswehr Institute of Radiobiology	Immunology and Toxicology Section, II Department, Army Medical and Veterinary Research Center	Public Health England Cytogenetics Group	Radiation BioEffects Department (DEBR – Département des effets biologiques des rayonnements)
Laboratory Head	Col Lester A. Huff	Col. Dr. Matthias Port	Col. Dr. Florigio Lista	Dr. Liz Ainsbury	Dr. Francis Hérodin
Contact Person(s)	Dr. W.F. Blakely	Col Dr. Michael Abend	Dr. Andrea De Amicis, Dr. Stefania De Sanctis, Col. Dr. Florigio Lista	Drs. Liz Ainsbury, Jayne Moquet, Stephen Barnard, Mingzhu Sun, David Lloyd	Dr. Marco Valente
Address	AFRRI, 8901 Wisconsin Avenue, Bethesda, MD 20889-5603	Neuherbergstr. 11 80937 Munich Germany	Via Santo Stefano Rotondo, 4 00184 Rome ITALY	Public Health England Centre for Radiation, Chemical and Environmental Hazards (PHE CRCE), Room C1.32, Chilton, Didcot, Oxon OX11 0RQ, UK	Institut de Recherche Biomédicale des Armées (IRBA), 1 Place du Général Valérie André (BP 73), 91223 Brétigny-sur-Orge, FRANCE
Email	william.blakely@usuhs.edu	michaelabend@bundeswehr.org	Andre.deamicis@gmail.com ; stefania.desanctis@gmail.com ; romano.lista@gmail.com	liz.ainsbury@phe.gov.uk / body.monitoring@phe.gov.uk	marco.valente@irba.fr
Secretary	301.295.1210	+49 89 992 692 2250		44 1235 825399 / +44 1235 831600 – ask to be transferred to a contact person	+ 33 1 78 65 14 14

Nation	USA	DEU	ITA	GBR	FRA
Tel	301.295.0530	+49 89 992 692 2280	+390677703916 0/135/344	+44 1235 825105	+ 33 1 78 65 14 20
Fax	301.295.1863	+49 89 992 692 2255	+390677703934 7	+44 1235 833891	
Website	www.usuhs.edu/afri/militarymedicaloperations	www.radiation-medicine.de		www.gov.uk/radiation-products-and-services (currently being updated)	
Associate Partner	Naval Dosimetry Center			RENEB	
Associate Partner Head	CAPT. Anthony Williams, sel			Ulrike Kulka	
Associate Partner Contact	Dr. Alexander Romanyukha			Ulrike Kulka	
Address	U.S. Naval Dosimetry Center, National Naval Medical Center, 8950 Brown Drive, Bldg. 4, Room 4200, Bethesda, MD 20889-5614			www.reneb.eu	
Email	Alexander.a.romanyukha.civ@mail.mil			RENEB@Bfs.de / ukulka@bfs.de	
Tel	301.319.4920				
Fax	301.295.5981				
Website	NA			www.reneb.eu	

4.2.2.2 General Information – Staffing of Laboratory

Information about the staffing relative to the various assays of the biodosimetry laboratories is described in Table 4-3.

Table 4-3: Information about the Staffing Relative to the Various Assays of the Biodosimetry Laboratories.

Nation	USA	DEU	ITA	GBR	FRA
Laboratory	AFRRI	Bundeswehr Institute of Radiobiology	Immunology and Toxicology Section, II Department, Army Medical and Veterinary Research Center	Public Health England Cytogenetics Group	Radiation BioEffects Department (DEBR – Département des effets biologiques des rayonnements)
Cytogenetic Assays					
Culturing	5	5	5	6	7
Preparation Samples	5	5	5	6	7
Scoring Dicentric	3	4	5	6	7
Scoring CBMN	–	3	5	6	7
Translocation	–	2	5	6	7
PCC	5		5	6	7
γ H2AX	–	1	5	6	7
Dose Estimation	2	1	5	3	2
Gene Expression					
Blood Cultures	–	3	5	3	0
RNA Extraction	–	3	3	3	0
Gene Expression Assay	–	3	1	3	0
Dose Estimation	–	1	2	2	0
Blood Chemistry Assay					
Blood Cultures	–	1	5	0	7
ELISA	–	1	5	0	2
Dose Estimation	–	1	5	0	1
EPR Dosimetry					
Sample	1	0	0	0	0
Assay	1	0	0	0	0
Dose Estimation	1	0	0	0	0
Radioactivity Counting and Bioassays					
Sample	0	6	0	3	0
Data Collection	3	6	0	5	0
Dose Estimation	1	1	0	3	0

Nation	USA	DEU	ITA	GBR	FRA
Informed Consent Protocol					
Approved	Yes	Yes	Yes	Yes	No
Voice Consenting	No	–	–	No	Yes

4.2.2.3 Biodosimetry Capability – From Blood Sample to Dose Estimation

The collection of samples (i.e., blood, nail clippings) for biological dosimetry and transport from the field to the laboratory varies in each country's laboratory.

At AFRRRI requests are funnelled for review and approval via AFRRRI's MMO Chief to AFRRRI's DIR. Upon approval, AFRRRI Technical Laboratory Director (TLD) coordinates sending appropriate materials (i.e., informed consent form, protocol for collection and shipping of blood) to AFRRRI, typically using a commercial carrier.

In Germany, a mobile task force can be forwarded to the place where the exposed individuals are. They take biological samples, analyse them in part immediately, and others will be stored and sent under defined conditions to the Role 4 labs in Germany.

In Italy collection and stabilization of the processed samples are done in the field, then sent to the Nation's reference laboratory to be spread and analysed.

In the UK blood and personal dosimeters are collected by medical personal supporting first responders – most likely (for blood), military medics, nuclear operator medical staff, civilian ambulance staff, A&E staff, or others depending on the exposure scenario.

In France sampling is done by the military radiation protection service.

Additional details concerning the specific assays and the laboratory's capability are described in Table 4-4.

Table 4-4: Laboratory Capabilities.

Nation	USA	DEU	ITA	GBR	FRA
Laboratory	AFRRRI	Bundeswehr Institute of Radiobiology	Immunology and Toxicology Section, II Department, Army Medical and Veterinary Research Center	Public Health England Cytogenetics Group	Radiation BioEffects Department (DEBR – Département des effets biologiques des rayonnements)
Arrangements with Medical Doctors	Yes	Yes	Yes	Yes	Yes
Aware of Shipping and Customs Requirements	Yes	N/A	Yes	Yes	Yes
Consumable Available	Yes	N/A	Yes	Yes	Yes

Nation	USA	DEU	ITA	GBR	FRA
DCA Triage Mode in 1 week	100	75 – 100	100	400	40
DCA Triage in 1 month	400	N/A	400	1200	150
CBMN 1 week	–	15/40	100	400	–
CBMN in 1 month	–	150	400	1200	–
PCC in 1 week	300	N/A	–	–	–
PCC in 1 month	1,200	N/A	–	–	–
FISH Translocations in 1 wk week	–	10 – 15	30	30	6
FISH Translocations in 1 month	–	40 – 60	120	120	30
γ -H2AX in 1 week	–	20	100	350	–
γ -H2AX in 1 month	–	80	400	1400	–
Gene Expression in 1 week	–	480	140	–	–
Gene Expression in 1 month	–	1920	560	–	–
Blood Chemistry in 1 week	–	160	1000	N/A	–
Blood Chemistry in 1 month	–	640	4000	N/A	–
EPR Dosimetry in 1 week	50 – 100	N/A	–	–	–
EPR in 1 month	200 – 400	N/A	–	–	–
WBC in 1 week	80	1 pt per 10 min	–	42	–
WBC in 1 month	320	N/A	–	100	–
Calibration Curves	DCA: X-rays 1 Gy/min; 60CO at 1 Gy/min, 0.6 Gy/min; PCC: 137Cs (0.6 Gy/min); WBC: multiple sources	DCA: X-ray and gamma rays; FISH: X-rays	DCA: X-rays, CBMN: X-rays	Dicentric assay: Cm242_alpha, 239Pu_alpha, He3_beta, 252Cf_fission_neutrons_2.1MeV, fission_neutrons_0.7MeV, fission_neutrons_0.9MeV, Co60_gamma (2 curves), He3ions_23.5MeV, 7.6MeV_neutrons,	DCA and FISH: Gamma rays from 60CO and X-rays. In both cases for human lymphocytes irradiated <i>in vitro</i> .

Nation	USA	DEU	ITA	GBR	FRA
Calibration Curves (cont'd)				14.9MeV_neutrons, 7.6MeV_neutrons, 14.9MeV_neutrons, 24keV_neutrons, protons_8.7MeV, 250kVp_Xrays FISH translocation, MN and gamma-H2AX assays: Co-60/X-ray curves – for H2AX at 4 and 24 hours post-irradiation (though we also always include a positive control).	
Statistical Methods	CABAS (cytogenetic assays); EPR: least squares fit; WBC: manufactures Geni 2000	FISH/DIC: Dose Estimate software; CBMN: curve fitting with Sigma Plot, dose estimate with Excel; Gene expression: curve fitting with Sigma Plot, dose estimate with Excel/SAS	Cytogenetic assays: Dose Estimate software	Dose Estimate [8], CytoBayesJ [9], [10], R radir and hermite [11], [12] and other bespoke R routines.	Cytogenetic assays: CABAS [16]

N/A = Not Available.

4.2.2.4 Laboratory Equipment, Experience, and Network Participation

Information about each laboratory's equipment, biodosimetry experience, and participation in networks and exercises are described in Table 4-5.

Table 4-5: Laboratory's Equipment, Biodosimetry Experience, and Participation in Networks and Exercises.

Nation	USA	DEU	ITA	GBR	FRA
Laboratory	AFRRI	Bundeswehr Institute of Radiobiology	Immunology and Toxicology Section, II Department, Army Medical and Veterinary Research Center	Public Health England Cytogenetics Group	Radiation BioEffects Department (DEBR – Département des effets biologiques des rayonnements)
Automation					
Automated Metaphase Finder	Yes (1)	Yes (2)	Yes (1)	Yes (1)	Yes (2)
Automated Harvester	Yes (2)	Yes (1)	–	Yes (1)	Yes (1)
Automated Spreader	Yes (1)	Yes (1)	–	–	–
Automated Gene Expression	–	Yes (4)	–	–	–
Automated Blood Chemistry	–	–	–	–	–
QA/QC	In progress	Yes (ISO 9001/2008)	No	Yes	Yes
Laboratory Accreditation	No	Yes	No	No	No
Exercise Participation	Yes	Yes	Yes	Yes	Yes
<i>In vivo</i> Biodosimetry Experience	No	Yes	No	Yes	Yes
Dose Assessment Experience	Yes (45 cases)	Yes (multiple)	Yes	Yes	Yes
Biodosimetry Network Participation	Yes	Yes	Yes	Yes	Yes

4.2.2.5 Experience with Collaboration and Networking

Participation in biodosimetry networks (i.e., WHO-REMPAN, WHO-Biodose, IAEA RANET, RENE, North American Network (Canada) is an important activity for laboratories involved in dose assessment.

In the United States, AFRRI's Cytogenetic Biodosimetry Laboratory participates in an informal U.S. Cytogenetic Biodosimetry Network via close interaction with the Radiation Emergency Assistance Center / Training Site (REAC/TS). Dr. Blakely is a Senior Faculty and speaker in REAC/TS Advanced Radiation Medicine course. AFRRI staff (Dr. W.F. Blakely) was a co-author contributor to the IAEA manual of use of cytogenetics for dose assessment and an active member of the relevant ISO working group (i.e., 18), who have developed the standards for use of cytogenetics for dose assessment. The technical director of the U.S. laboratory, Dr. W.F. Blakely, is an elected member of the National Council of Radiation Protection and Measurements and services on PAC-6 – Dosimetry Sub-Committee. He is also a member of the Radiation Advisory Council for the New York City Department of Public Health and Hygiene.

Germany's laboratory is a component of ZUB (cooperation with police, Zentrale Unterstützungsstelle des Bundes), WHO-REMPAN, WHO-Biodose, IAEA RANET, and RENE. They are also involved in Task Force exercises, exercising in contaminated areas in a military facility in Canada, MultiBiodose 2010 – 2013, and RENE 2012 – 2015.

Italy's laboratory participates with LABGenMil that involves the laboratory and Environmental Carcinogenesis Unit, National Institute of Cancer Research, Genoa; International NATO biodosimetry network inside the NATO Research Task Group (RTG-033 "Radiation Bioeffects and Countermeasures"), and is a candidate member in the RENE network.

The United Kingdom (UK)'s laboratory is a part of WHO-REMPAN (Biodosenet), IAEA RANET, RENE and maintains links to / collaborations with many others (i.e., IAEA-CRP, EU DoREMi, MELODI, OPERRA, CONCERT).

France's laboratory participates in an IAEA-CRP and is part of both Biodosenet a RENE networks.

4.2.2.6 Prospects and Expectations from Participation in a NATO Biodosimetry Network (NBN)

AFRRI (USA): We expect that participation in the NBN will provide enhancement of capabilities when surge requests exceed our laboratory capabilities. Use of partner laboratories that are distributed world-wide can also provide useful resources to provide rapid responses. Interactions with participating laboratories can also enhance our laboratory's knowledge and skills by sharing of new concepts and ideas. AFRRI's Cytogenetic Biodosimetry Laboratory welcomes participating and contributing in a NATO Biodosimetry Network by engaging in research interactions, participating in laboratory inter-comparisons, and networking. One key requirement is the need to have participating laboratories become "clinically certified" by their Nations qualified entity.

DEU: Ring trials to validate and maintain skills are expected. Also, exercises are needed for maintaining a potential future accreditation.

ITA: Following large-scale radiological incidents, a fast medical and radiological triage of patients according to the radiation exposure will be required. Besides individuals who were actually exposed to high doses of ionising radiation, there will be a large number of distressed people who have not received radiation doses (worried-well). Since, in large-scale scenarios, the number of people that may need to be screened could easily exceed the capacity of a single laboratory, NATO biodosimetry network could be recognised as a feasible and important emergency response strategy. Considering this we expect to facilitate sharing common protocols, criteria for quality assurance, guidance on certification, and common operational plans in order to participate in inter-comparison studies, training and exercises. These activities could prepare each participating Nation laboratory to be ready in case of a large-scale radiological or nuclear scenario.

GBR: Networking, particularly links with appropriate military authorities. Perhaps validation and standardisation of techniques.

FRA: A homogenisation of scoring methods, a valuable opportunity to share scientific results and ideas. The network also increases and strengthens the scientific collaborations in biodosimetry, which allows for the discovery and validation of dosimetry biomarkers of exposure. France is eager to increase their experience and scientific interactions to promote a well-coordinated NATO response in case of a NR crisis.

DEU: Participation primarily as satellite lab. It would be also possible to organize exercises.

ITA: We would have opportunities to share and to be able to provide reliable biodosimetry services in the future and be able to assist in the international network environment. This opportunity could be a chance to harmonize and standardize the national capabilities in order to improve a national reference laboratory that will coordinate the national network, along with all Italian biodosimetry labs.

GBR: We are happy to contribute in any way deemed helpful. We have a lot of experience so perhaps training newer members, if needed?

FRA: We have a relatively young lab, inside an institute with much experience in ionizing radiation exposure. We are eager to increase our experience and scientific interactions to promote a well-coordinated NATO response in case of a NR crisis.

4.2.2.7 The Value of the Establishment of a NATO Biodosimetry Network can be Useful for the Biodosimetry Laboratories

AFRRI (USA): The value of a NATO Biodosimetry Network is to provide enhanced readiness and capability to provide rapid and accurate dose assessment.

DEU: NBN comprises an intercontinental network. Other than WHO-Biodose it would be not focused on DIC only, but including other methods as well including:

- a) A military network could be faster and respond earlier in an emergency;
- b) A military network might have easier access to military logistics and could order them more easily; and
- c) Fewer problems with customs regarding intercontinental shipment due to military transport?

ITA: To create an operational basis on coordination of existing reliable and proven techniques in biological dosimetry. To ensure that the network remains up-to-date by providing implementation of appropriate new biological methods and by expanding through new partners. To assure high-quality standards for reliable dose assessment by education and training activities, inter-comparisons and quality assessment and management procedures.

GBR: Increased visibility and availability of biodosimetry for emergency response.

4.2.2.8 What are the Most Pressing Needs for your Laboratory?

AFRRI (USA): Completion of the preparations to request DoD laboratory certification inspection.

DEU: Experienced scientists are rare.

GBR: Funding for research into biomarker development and testing.

4.2.2.9 Other Comments

GBR: It might be useful to focus more closely on uncertainty assessment techniques, as this is something that has not been considered in detail for emergency triage biodosimetry.

There are several active networks for biodosimetry now – GBR would not want to see needless repetition of activities so the organizers should take care to ensure that there is a need for any specific networking activities planned under NATO going forward.

RTG Chairman: Establishment of a NATO Biodosimetry network, despite the presence of world-wide regional and international networks, facilitates support of NATO medical activities in cases of CBRN defensive operations.

4.2.3 Acknowledgements

The views expressed here are those of the authors; no endorsement by the U.S. Department of Defense has been given or inferred. AFRI supported this research under work unit RAB42674.

4.3 NATO ROLE 4 BIODOSIMETRY ASSAYS TECHNOLOGY READINESS LEVEL UPDATE

Abstract

The North Atlantic Treaty Organization (NATO) Human Factors and Medicine Panel (HFM) HFM-222 Research Task Group (RTG) – Ionizing Radiation Bioeffects and Countermeasures updated the Technology Readiness Levels (TRLs) assessment of current role 4 or reference laboratory biodosimetry capabilities used by NATO NATIONS’ reach-back and associated (i.e., partner) laboratories using a TRL assessment tool.

4.3.1 Introduction

In the prior NATO Radiobiology RTG (HFM-099) members of this RTG reported on a TRL assessment of various established and emerging biodosimetry assays using a novel tool that distinguished radiation biodosimetry assays based on multiple diagnostic criteria [13].

USA efforts recently performed a similar TRL assessment for existing and emerging diagnostic systems under the Next-Generation Diagnostic Systems (NGDS) – radiological program with a focus on roles 1 to 3 [14] and roles 4 [15].

NATO HFM-222 RTG performed an updated TRL assessment for Role 4 radiation biodosimetry assays as shown in Table 4-6.

Table 4-6: Radiation Dose and Injury Assessment Modalities.

Radiation Dose and Injury Assessment Modalities	Assays
Cytogenetic	Dicentric Chromosome Aberration (DCA) assay, Cytokinesis-Blocked Micronuclei (CBMN) assay, Premature Chromosome Condensation (PCC) assay, Fluorescence <i>In Situ</i> Hybridization (FISH) Translocation assay, γ -H2AX foci assay
Gene Expression Bioassays	mRNA and miRNA assays

Radiation Dose and Injury Assessment Modalities	Assays
Blood Chemistry (Proteomic) Bioassays	C-reactive protein, amylase activity, Flt-3 ligand, and multiple proteomic biomarker panel
Electron Paramagnetic Resonance (EPR)	Dose assessment using nail clippings, teeth, and bone by EPR dosimetry
Radioactivity Counting	Whole-body counting, radionuclide detection, radioactivity assessment of biofluids (i.e., urine, feces, blood, saliva), committed dose calculations

A component of NATO Nations participated in this Role 4 radiation biodosimetry assays TRL assessment, drawing upon appropriate subject-matter experts for various modalities.

4.3.2 Diagnostic Criteria

The various parameters for the diagnostic criteria that was used for this role 4 biodosimetry assay TRL assessment is based on those developed in the USA NGDS [14] and are distinguished for four uses:

- a) Triage for external exposures;
- b) Triage for internal exposures;
- c) Treatment triage; and
- d) Injury diagnostics (Table 4-7).

Table 4-7: Various Parameters for Diagnostic Criteria in Role 4 Biodosimetry Assays.

Parameter	Triage-External	Triage-Internal	Treatment Triage	Injury Diagnostics
Dose thresholds	0.5 Gy (exposed); 0.75 Gy (RTD*), 1.5 & 2 Gy (treatment), and ~10 Gy Uninjured (Expectant); ~1 Gy - Combined Injury (Combined injury)	1 CDG* (adults), 1/5 th CDG* (pregnant women, children)	0.5 to 10 Gy	1-4 RC
Dose accuracy	From ±0.25 Gy to ±0.5 Gy		Threshold: ±0.25 Gy Optimal: ±0.05 Gy	± 1/3 rd RC degree
Results obtained	Seconds to minutes per patient	Within 1 hour per patient	1 to < 24 hours (triage) Hours to Days (treatment)	< 1 to < 24 h
False positive	Moderate degree	Moderate degree	Moderate degree	Moderate degree
False negatives	Avoid	Avoid	Avoid	Avoid
Minimum detection level	0.5 Gy	1/5 th CDG	0.5 Gy	RC 0
Throughput	Optimal: 500 patients per hour Threshold: 30 Patients per hour	Threshold – 4 samples per hour Optimal 32 samples per hour	Threshold – 4 patients per hour Optimal 200 Patients/hour	Threshold – 4 patients per hour Optimal 200 Patients/h

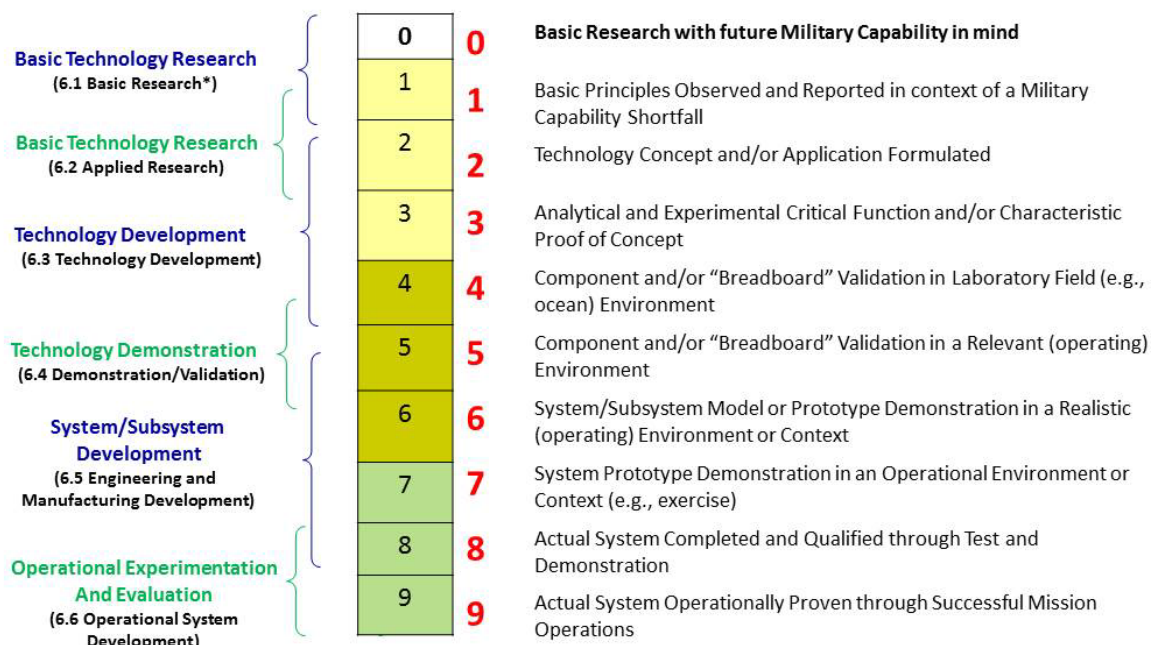
Parameter	Triage-External	Triage-Internal	Treatment Triage	Injury Diagnostics
Time period signal is present treatment triage	Signal is present and usable for at least 12 – 24 hours after the exposure	Signal is present and usable for at-least hours after the exposure	Signal is present and usable within hours and persists for days	Signal is present and usable within hours and persists for days
Time period signal is present treatment	Immediately to minutes after exposure	Immediately to minutes after exposure	Signal is present and usable within hours and persists for weeks	Signal is present and usable within hours and persists for weeks
Training	Minimal	Minimal	Advanced training is possible	Advanced training is possible
Required supplies	None to very limited	None to very limited	Similar to current hospitals	Similar to current hospitals

***RTD: Radiation Threshold Dose; CDG: Clinical Decision Guidance; RC: ARS response category**

4.3.3 NATO Technology Readiness Levels (TRLs)

The NATO scale for TRL assessment is shown in Figure 4-1. Definition of the maturity of the radiation biodosimetry assays using the U.S. TRL scale is also shown for comparison purposes.

NATO Technology Readiness Levels (TRLs)



*US Department of Defense Designation

**Figure 4-1: NATO Technology Readiness Levels (TRLs).
A comparison with the USA TRL is shown on the left.**

4.3.4 Biodosimetry Assays TRL Scoring Responses

Table 4-8 to Table 4-10 illustrate the templates used for NATO Nation SMEs to perform an updated TRL assessment for various biodosimetry assays. A TRL assessment rating for each diagnostic assay was performed based on the specific diagnostic criteria parameters.

Table 4-8: TRL Assessment for Cytogenetic Assays.

Assays	DCA	CBMN	PCC	Translocations (FISH)	γ-H2AX Foci	Other
Diagnostic criteria parameters	TRL rating for diagnostic assays based on specific diagnostic criteria parameters					
Dose threshold	9,9,9,8,9	6.5,9,9,8,-	-, -, -, 8,-	7,7,7,7,7	-,9,9,8,-	
Dose accuracy	9,9,9,8,8	6.5,9,9,7,-	6.5,-, -, 6,-	7,7,7,6,6	3.5,9,9,5,-	
Results obtained	-,9,9,6,8	-,9,9,5,-	-, -, -, 6,-	-,7,7,6,7	4,9,7,8,-	
False positives	8,9,9,8,8	6.5,9,9,7,-	6.5,-, -, 7,-	6.5,7,7,7,6	4,9,6,7,-	
False negatives	8,9,9,8,8	6.5,9,9,7,-	6.5,-, -, 7,-	6.5,7,7,7,7	4,9,6,7,-	
Minimum detection level	9,9,9,8,8	7,9,9,8,-	-, -, -, 8,-	7,7,7,8,7	-,9,9,8,-	
Throughput	-,9,9,6,8	-,9,9,6,-	-, -, -, 5,-	-,7,7,4,8	-,9,9,6,-	
Time period signal is present treatment triage	9,9,9,8,8	6.5,9,-,8,-	7,-, -, 8,-	8.5,7,7,8,7	4,9,9,8,-	
Time period signal is present treatment	9,9,9,8,9	6.5,9,9,8,-	7,-, -, 8,-	8.5,7,7,8,7	4,9,6,4,-	
Training	7,9,9,5,9	7,9,9,5,-	7,-, -, 5,-	7,7,7,5,7	7,9,9,8,-	
Required supplies	9,9,9,5,9	8,9,9,5,-	8,-, -, 5,-	8,7,7,4,8	8,9,9,5,-	
Mean TRL	8.4	8	6.8	6.9	7.4	

NATO Nation: DEU, FRA, GBR, ITA, USA

Table 4-9: TRL Assessment for Gene Expression and Biochemistry Assays.

	mRNA	miRNA	CRP	Amylase Activity	FLT-3L	Panel Proteomic Biomarkers
Diagnostic criteria parameters	TRL rating for diagnostic assays based on specific diagnostic criteria parameters					
Dose threshold	6,7,7,8,-	6,-,-,3,-	-,-,-,-,-	-,-,-,-,-	-,3,-,-,-	-,-,-,-,-
Dose accuracy	6.5,7,7,5,-	6.5,-,-,3,-	-,-,-,-,-	7,-,-,-,-	-,3,-,-,2	-,-,-,-,-
Results obtained	5.5,7,7,8,-	5.5,-,-,3,-	5.5,-,-,-,5	7,-,-,-,-	-,3,-,-,3	-,-,-,-,-
False positives	5.5,7,7,7,-	5.5,-,-,7,-	6,-,-,-,-	7,-,-,-,-	7,3,-,-,7	-,-,-,-,-
False negatives	5.5,7,7,7,-	5.5,-,-,7,-	6,-,-,-,-	7,-,-,-,-	7,3,-,-,7	-,-,-,-,-
Minimum detection level	4.5,7,7,8,-	4.5,-,-,3,-	-,-,-,-,-	-,-,-,-,-	-,3,-,-,3	-,-,-,-,-
Throughput	-,7,7,8,-	-,-,-,8,-	5.5,-,-,5	7.5,-,-,-	4,3,-,-,5	-,-,-,-,-
Time period signal is present treatment triage	5.5,7,7,5,-	5.5,-,-,3,-	5.5,-,-,4	7,-,-,-,-	6.5,3,-,-,6	-,-,-,-,-
Time period signal is present treatment	-,7,7,8,-	-,-,-,6,-	5.5,-,-,4	7,-,-,-,-	8,3,-,-,5	-,-,-,-,-
Training	7,7,7,4,-	7,-,-,4,4	8,-,-,-,-	8,-,-,-,-	8,3,-,-,4	-,-,-,-,-
Required supplies	8,7,7,5,-	6,-,-,5,4	8,-,-,-,-	9,-,-,-,-	7.5,3,-,-,4	-,-,-,-,-
Mean TRL	6.7	5.3	6	7.3	7.9	NA

NATO Nation: DEU, FRA, GBR, ITA, USA

Table 4-10: TRL Assessment for Physical Dosimetry and Radionuclide Counting Assays.

	Nail Clippings EPR	<i>In Vivo</i> Teeth EPR	<i>Ex Vivo</i> Teeth or Bone EPR	Biosample Radioactivity Counting	Whole Body Counting	Physical Dosimetry
Diagnostic criteria parameters	TRL rating for diagnostic assays based on specific diagnostic criteria parameters					
Dose threshold	3,3,3,3	3,3,3,3	3,3,3,3	*3,3,3,3	*3,3,3,3	9,9,3,3
Dose accuracy	3,3,3,3	3,3,3,3	3,3,3,3	*3,3,3,3	*3,3,3,3	9,9,3,3
Results obtained	6,3,3,3	6,3,3,3	6,3,3,3	9,3,3,3	9,3,3,3	9,9,3,3
False positives	4.5,3,3,3	4.5,3,3,3	4.5,3,3,3	9,3,3,3	9,3,3,3	9,9,3,3
False negatives	4.5,3,3,3	4.5,3,3,3	4.5,3,3,3	9,3,3,3	9,3,3,3	9,9,3,3
Minimum detection level	3,3,3,3	3,3,3,3	3,3,3,3	3,3,3,3	3,3,3,3	9,9,3,3
Throughput	4,3,3,3	4,3,3,3	4,3,3,3	9,3,3,3	9,3,3,3	9,9,3,3
Time period signal is present treatment triage	6,3,3,3	6,3,3,3	6,3,3,3	*3,3,3,3	*3,3,3,3	9,9,3,3
Time period signal is present treatment	6,3,3,3	6,3,3,3	6,3,3,3	*3,3,3,3	*3,3,3,3	9,9,3,3
Training	7,3,3,3	7,3,3,3	7,3,3,3	9,3,3,3	9,3,3,3	9,9,3,3
Required supplies	3,3,3,3	3,3,3,3	3,3,3,3	9,3,3,3	9,3,3,3	9,9,3,3
Mean TRL	5.4	5.4	5.4	9	9	9

NATO Nation: DEU, FRA, GBR, ITA, USA

4.3.5 Discussion and Summary

In general there was harmonization on the scoring of the diagnostic criteria used to perform a TRL assessment for the various biodosimetry assays. In selected cases, Nations did not indicate a diagnostic criteria scoring, which was interpreted either as limited data available to perform the score or the Nation did not have sufficient experience to enter an expert score.

The gold standard, cytogenetic – Dicentric Chromosome Aberration (DCA) assay, retained a high-TRL rating in this updated assessment. CBMN, FISH translocation, PCC, and γ -H2AX FOCI represent emerging cytogenetic assays that are rising in their maturation and use for dose assessment (Table 4-8).

Among the molecular assays used for dose assessment there is general consensus that the gene expression bioassay is the dominant candidate for acceptance. While not as mature of as the DCA assay, it has clearly shown significant improvement from the last time the biodosimetry assays are assessed. The proteomic assays acceptance appears to be varied among the NATO Nations.

The TRL rating of physical dosimetry and radionuclide counting assays was limited. Two Nations submitted use of conventional physical dosimetry as an optional assay and it was included in the survey even though it was not limited as a choice when the survey was initially distributed. The varied scoring of the EPR dosimetry assays is likely due to the limited use and operational experience of this diagnostic technology for dose assessment.

4.4 ACKNOWLEDGEMENTS

The views expressed here are those of the authors; no endorsement by the U.S. Department of Defense has been given or inferred. AFRI supported this research under work unit RAB42674. We thank Mr. Anthony Moton II from AFRI for his assistance in analysis of the results.

4.5 REFERENCES

- [1] Rothkamm, K., Beinke, C., Romm, H., Badie, C., Balagurunathan, Y., Barnard, S., Bernard, N., Boulay-Greene, H., Brengues, M., De Amicis, A., De Sanctis, S., Greither, R., Herodin, F., Jones, A., Kabacik, S., Knie, T., Kulka, U., Lista, F., Martigne, P., Missel, A., Moquet, J., Oestreicher, U., Peinnequin, A., Poyot, T., Roessler, U., Scherthan, H., Terbrueggen, B., Thierens, H., Valente, M., Vral, A., Zenhausem, F., Meineke, V., Braselmann, H. and Abend, M. Comparison of established and emerging biodosimetry assays. *Radiat Res.* 2013;180(2):111-9. doi: 10.1667/RR3231.1. Epub 2013 July 17.
- [2] Beinke, C., Barnard, S., Boulay-Greene, H., De Amicis, A., De Sanctis, S., Herodin, F., Jones, A., Kulka, U., Lista, F., Lloyd, D., Martigne, P., Moquet, J., Oestreicher, U., Romm, H., Rothkamm, K., Valente, M., Meineke, V., Braselmann, H. and Abend, M. Laboratory intercomparison of the dicentric chromosome analysis assay. *Radiat Res.* 2013;180(2):129-37. doi: 10.1667/RR3235.1. Epub 2013 July 17.
- [3] Romm, H., Barnard, S., Boulay-Greene, H., De Amicis, A., De Sanctis, S., Franco, M., Herodin, F., Jones, A., Kulka, U., Lista, F., Martigne, P., Moquet, J., Oestreicher, U., Rothkamm, K., Thierens, H., Valente, M., Vandersickel, V., Vral, A., Braselmann, H., Meineke, V., Abend, M. and Beinke, C. Laboratory intercomparison of the cytokinesis-block micronucleus assay. *Radiat Res.* 2013;180(2):120-8. doi: 10.1667/RR3234.1. Epub 2013 July 17.
- [4] Rothkamm, K., Horn, S., Scherthan, H., Rössler, U., De Amicis, A., Barnard, S., Kulka, U., Lista, F., Meineke, V., Braselmann, H., Beinke, C. and Abend, M. Laboratory intercomparison on the γ -H2AX foci assay. *Radiat Res.* 2013;180(2):149-55. doi: 10.1667/RR3238.1. Epub 2013 July 24.
- [5] Badie, C., Kabacik, S., Balagurunathan, Y., Bernard, N., Brengues, M., Faggioni, G., Greither, R., Lista, F., Peinnequin, A., Poyot, T., Herodin, F., Missel, A., Terbrueggen, B., Zenhausem, F., Rothkamm, K., Meineke, V., Braselmann, H., Beinke, C. and Abend, M. Laboratory intercomparison of gene expression assays. *Radiat Res.* 2013;180(2):138-48. doi: 10.1667/RR3236.1. Epub 2013 July 25.
- [6] Blakely, W.F., Carr, Z., Chu, M.C., Dayal-Drager, R., Fujimoto, K., Hopmeir, M., Kulka, U., Lillis-Hearne, P., Livingston, G.K., Lloyd, D.C., Maznyk, N., Perez Mdel, R., Romm, H., Takashima, Y., Voisin, P., Wilkins, R.C. and Yoshida, M.A. WHO 1st consultation on the development

- of a global biodosimetry laboratories network for radiation emergencies (BioDoseNet). *Radiat Res.* 2009;171(1):127-39. doi: 10.1667/RR1549.1.
- [7] Maznyk, N.A., Wilkins, R.C., Carr, Z. and Lloyd, D.C. The capacity, capabilities and needs of the WHO BioDoseNet member laboratories. *Radiat Prot Dosimetry.* 2012;151(4):611-20. Epub 2012 August 19.
- [8] Ainsbury, E.A. and Lloyd, D.C. Dose estimation for radiation biodosimetry. *Health Physics* 2010;174(4): 403-14.
- [9] Ainsbury, E.A., Vinnikov, V., Puig, P., Maznyk, N., Rothkamm, K. and Lloyd, D.C. CytoBayesJ: software tools for Bayesian analysis of cytogenetic radiation dosimetry data. 2013;756(1-2):184-91. doi: 10.1016/j.mrgentox.2013.06.005. Epub 2013 June 19.
- [10] Ainsbury, E.A., Vinnikov, V.A., Puig, P., Higuera, M., Maznyk, N.A., Lloyd, D.C. and Rothkamm K. Review of Bayesian statistical analysis methods for cytogenetic radiation biodosimetry, with a practical example. *Radiat Prot Dosimetry.* 2014;162(3):185-96. doi: 10.1093/rpd/nct301. Epub 2013.
- [11] Higuera, M., Puig, P., Ainsbury, E.A. and Rothkamm, K. A new inverse regression model applied to radiation biodosimetry. *Proc Math Phys Eng Sci.* 2015;471(2174):20140588.
- [12] Moríña, D., Higuera, M., Puig, P., Ainsbury, E.A. and Rothkamm, K. radir package: an R implementation for cytogenetic biodosimetry dose estimation. *J Radiol Prot.* 2015;35(3):557-69. doi: 10.1088/0952-4746/35/3/557. Epub 2015 July 10.
- [13] Wilkinson, D., Waller, E., Abend, M., Riecke, A., Ruf, C., Jaworska, A., Stricklin, D.L., Holt, D.C.B., Rothkamm, K., Blakely, W.F., Buddemeier, B.R., Curling, C.A., Disraelly, D.S., Homann, S., Levine, I.H., Millage, K., Nasstrum, J.S., Nemhauser, J.B., Ross, J.A., Sandgren, D.J. and Sugiyama, G. (2011) Biodosimetry and Biomarkers for Radiological Emergency Response. In “Radiation Bioeffects and Countermeasures” (Chapter 6, pp: 6-1 to 6-22), Blakely, W.F., Janiak, M.K., Edwards, K., Duffy, F. (Eds.), Technical Report, North Atlantic Treaty Organization, Research and Technology Organisation, Human Factors and Medicine RTO-TR-HFM-099, AC/323(HFM-099)TP/356, Neuilly-sur-Seine, France: RTO, 2011.
- [14] Daxon, E., Milner, E.E., Blakely, W.F., Nesler, J., Miller, R.L. and Anastasio, M.A. Technology Readiness Assessment of Diagnostic Technologies for the Next Generation Diagnostic System (NGDS). CBRNIAC Task Number CB-12-0352, 2012.
- [15] Milner, E.E., Daxon, E.G., Anastasio, M.T., Nesler, J.T., Miller, R.L. and Blakely, W.F. Concepts of Operations (CONOPS) for Biodosimetry Tools Employed in Operational Environments. *Health Phys.* 2016;110(4):370-9. doi: 10.1097/HP.0000000000000470.
- [16] Deperas, J., Szluinska, M., Deperas-Kaminska, M., Edwards, A., Lloyd, D., Lindholm, C., Romm, H., Roy, .L, Moss, R., Morand, J. and Wojcik, A. CABAS: a freely available PC program for fitting calibration curves in chromosome aberration dosimetry. *Radiat Prot Dosimetry.* 2007;124(2):115-23.

Chapter 5 – REFERENCES OF ARTICLES PUBLISHED BY HFM-222 MEMBERS DEALING WITH THE RTG’s ACTIVITIES (2012 – 2016)

5.1 IONIZING RADIATION BIOEFFECTS AND MECHANISMS

- [1] Cary, L.H., Noutai, D., Salber, R.E., Williams, M.S., Ngudiankama, B.F. and **Whitnall, M.H.** Interactions between endothelial cells and T cells modulate responses to mixed neutron/gamma radiation. *Radiat Res.* 2014;181:592-604.
- [2] Weissmann, R., Kacprowski, T., Peper, M., Esche, J., Jensen, L.R., van Diepen, L., **Port, M.**, Kuss, A.W. and Scherthan, H. Transcriptome Alterations in X-Irradiated Human Gingiva Fibroblasts. *Health Phys.* 2016;111:75-84.
- [3] Scherthan, H., Sotnik, N., Peper, M., Schrock, G., Azizova, T. and **Abend, M.** Telomere Length in Aged Mayak PA Nuclear Workers Chronically Exposed to Internal Alpha and External Gamma Radiation. *Radiat Res.* 2016;185:658-67.

5.2 DNA DAMAGE

- [4] Lamkowski, A., Forcheron, F., Agay, D., Ahmed, E.A., **Drouet, M.**, **Meineke, V.** and Scherthan, H. DNA damage focus analysis in blood samples of minipigs reveals acute partial body irradiation. *PLoS One.* 2014 Feb 3;9(2):e87458.
- [5] Pang, D., Nico, J.S., Karam, L., Timofeeva, O., **Blakely, W.F.**, Dritschilo, A., Dizdaroglu, M. and Jaruga, P. Significant disparity in base and sugar damage in DNA resulting from neutron and electron irradiation. *J Radiat Res.* 2014;55:1081-8.
- [6] Zárbynická, L., Vávrová, J., Havelek, R., Tichý, A., **Pejchal, J.** and Sinkorová, Z. Lymphocyte subsets and their H2AX phosphorylation in response to in vivo irradiation in rats. *Int J Radiat Biol.* 2013;89:110-7.

5.3 BIODOSIMETRY (CYTOGENETICS)

- [7] Beinke, C., **Port, M.**, Lamkowski, A. and **Abend, M.** Comparing sven mitogens with PHA-M for improved lymphocyte stimulation in dicentric chromosome analysis for biodosimetry. *Radiat Prot Dosimetry.* 2015 May 9. pii: ncv286. [Epub ahead of print].
- [8] Beinke, C., **Port, M.** and **Abend, M.** Automatic versus manual lymphocyte fixation: impact on dose estimation using the cytokinesis-block micronucleus assay. *Radiat Environ Biophys.* 2015;54:81-90.
- [9] Miura, T., Nakata, A., Kasai, K., Nakano, M., Abe, Y., Tsushima, E., Ossetrova, N.I., Yoshida, M.A. and **Blakely, W.F.** A novel parameter, cell-cycle progression index, for radiation dose absorbed estimation in the premature chromosome condensation assay. *Radiat Prot Dosimetry.* 2014;159:52-60.
- [10] **Port, M.** A Case Report: Cytogenetic Dosimetry after Accidental Radiation Exposure during (192) Ir Industrial Radiography Testing. *Radiat Res.* 2015;184:66-72.

- [11] **Rothkamm, K.**, Horn, S., Scherthan, H., Rössler, U., **De Amicis, A.**, Barnard, S., Kulka, U., **Lista, F.**, **Meineke, V.**, Braselmann, H., Beinke, C. and **Abend, M.** Laboratory intercomparison on the γ -H2AX foci assay. *Radiat Res.* 2013;180:149-55.
- [12] Romm, H., Barnard, S., Boulay-Greene, H., **De Amicis, A.**, **De Sanctis, S.**, Franco, M., **Herodin, F.**, Jones, A., Kulka, U., **Lista, F.**, Martigne, P., Moquet, J., Oestreicher, U., **Rothkamm, K.**, Thierens, H., Valente, M., Vandersickel, V., Vral, A., Braselmann, H., **Meineke, V.**, **Abend, M.** and Beinke, C. Laboratory intercomparison of the cytokinesis-block micronucleus assay. *Radiat Res.* 2013;180:120-8.
- [13] Beinke, C., Barnard, S., Boulay-Greene, H., **De Amicis, A.**, **De Sanctis, S.**, **Herodin, F.**, Jones, A., Kulka, U., **Lista, F.**, Lloyd, D., Martigne, P., Moquet, J., Oestreicher, U., Romm, H., **Rothkamm, K.**, Valente, M., **Meineke, V.**, Braselmann, H. and **Abend, M.** Laboratory intercomparison of the dicentric chromosome analysis assay. *Radiat Res.* 2013;180:129-37.
- [14] **Rothkamm, K.**, Beinke, C., Romm, H., Badie, C., Balagurunathan, Y., Barnard, S., Bernard, N., Boulay-Greene, H., Brengues, M., **De Amicis, A.**, **De Sanctis, S.**, Greither, R., **Herodin, F.**, Jones, A., Kabacik, S., Knie, T., Kulka, U., **Lista, F.**, Martigne, P., Missel, A., Moquet, J., Oestreicher, U., Peinnequin, A., Poyot, T., Roessler, U., Scherthan, H., Terbrueggen, B., Thierens, H., Valente, M., Vral, A., Zenhausern, F., **Meineke, V.**, Braselmann, H. and **Abend, M.** Comparison of established and emerging biodosimetry assays. *Radiat Res.* 2013;180:111-9.
- [15] **De Amicis, A.**, **De Sanctis, S.**, Di Cristofaro, S., Franchini, V., Regalbuto, E., Mammana, G. and **Lista, F.** Dose estimation using dicentric chromosome assay and cytokinesis block micronucleus assay: comparison between manual and automated scoring in triage mode. *Health Phys.* 2014;106:787-97.
- [16] **De Sanctis, S.**, **De Amicis, A.**, Di Cristofaro, S., Franchini, V., Regalbuto, E., Mammana, G. and **List, F.** Cytokinesis-block micronucleus assay by manual and automated scoring: calibration curves and dose prediction. *Health Phys.* 2014;106:745-9.
- [17] Moroni, M., Maeda, D., **Whitnall, M.H.**, Bonner, W.M. and Redon, C.E. Evaluation of the gamma-H2AX assay for radiation biodosimetry in a swine model. *Int J Mol Sci.* 2013;14:14119-35.
- [18] Ainsbury, E., Badie, C., Barnard, S., Manning, G., Moquet, J., **Abend, M.**, Bassinet, C., Bortolin, E., Bossin, L., Bricknell, C., Brzoska, K., Čemusová, Z., Christiansson, M., Cosler, G., Della Monaca, S., Desangles, F., Discher, M., Doucha-Senf, S., Eakins, J., Fattibene, P., Gregoire, E., Guogyte, K., Kriehuber, R., Lee, J., Lloyd, D., Lyng, F., Macaeva, E., Majewski, M., McKeever, S.W., Meade, A., M'kacher, R., Medipally, D., Oestreicher, U., Oskamp, D., Pateux, J., **Port, M.**, Quattrini, M.C., Quintens, R., Ricoul, M., Roy, L., Sabatier, L., Sholom, S., Strunz, S., Trompier, F., Valente, M., Van Hoey, O., Veronese, I., Wojcik, A. and Woda, C. Integration of new biological and physical retrospective dosimetry methods into EU emergency response plans - joint RENEB and EURADOS inter-laboratory comparisons. *Int J Radiat Biol.* 2016;20:1-10.
- [19] Beinke, C., **Port, M.**, Riecke, A., Ruf, C.G. and **Abend, M.** Adaption of the Cytokinesis-Block Micronucleus Cytome Assay for Improved Triage Biodosimetry. *Radiat Res.* 2016;185:461-72.

5.4 BIODOSIMETRY (PROTEOMICS)

- [20] **Hérodin, F.**, Richard, S., Grenier, N., Arvers, P., Gérome, P., Baugé, S., Denis, J., Chaussard, H., Gouard, S., Mayol, J.F., Agay, D. and **Drouet, M.** Assessment of total- and partial-body irradiation in a baboon model: preliminary results of a kinetic study including clinical, physical, and biological parameters. *Health Phys.* 2012;103:143-9.

- [21] **Hérodin, F.**, Valente, M. and **Abend, M.** Useful radiation dose biomarkers for early identification of partial-body exposures. *Health Phys.* 2014;106:750-4.
- [22] Ossetrova, N.I., Sandgren, D.J. and **Blakely, W.F.** Protein biomarkers for enhancement of radiation dose and injury assessment in nonhuman primate total-body irradiation model. *Radiat Prot Dosimetry.* 2014;159:61-76.
- [23] **Blakely, W.F.**, Sandgren, D.J., Nagy, V., Kim, S.Y., Sigal, G.B. and Ossetrova, N.I. Further biodosimetry investigations using murine partial-body irradiation model. *Radiat Prot Dosimetry.* 2014;159:46-51.
- [24] Valente, M., Denis, J., Grenier, N., Arvers, P., Foucher, B., Desangles, F., Martigne, P., Chaussard, H., **Drouet, M.**, **Abend, M.** and **Hérodin, F.** Revisiting Biomarkers of Total-Body and Partial-Body Exposure in a Baboon Model of Irradiation. *PLoS One.* 2015 Jul 15;10(7):e0132194.
- [25] Kim, D., Marchetti, F., Chen, Z., Zaric, S., Wilson, R.J., Hall, D.A., Gaster, R.S., Lee, J.R., Wang, J., Osterfeld, S.J., Yu, H., White, R.M., **Blakely, W.F.**, Peterson, L.E., Bhatnagar, S., Mannion, B., Tseng, S., Roth, K., Coleman, M., Snijders, A.M., Wyrobek, A.J. and Wang, S.X. Nanosensor dosimetry of mouse blood proteins after exposure to ionizing radiation. *Sci Rep.* 2013;3:2234.
- [26] Rybkina, V.L., Azizova, T.V., Scherthan, H., **Meineke, V.**, **Doerr, H.**, Adamova, G.V., Tepyakova, O.V., Osovets, S.V., Bannikova, M.V. and Zurochka, A.V. Expression of blood serum proteins and lymphocyte differentiation clusters after chronic occupational exposure to ionizing radiation. *Radiat Environ Biophys.* 2014;53:659-70.

5.5 BIODOSIMETRY (GENOMICS)

- [27] **Port, M.**, Seidl, C., Ruf, C.G., Riecke, A., **Meineke, V.** and **Abend, M.** Reliable and sample saving gene expression analysis approach for diagnostic tool development. *Health Phys.* 2012;103:159-68.
- [28] Riecke, A., Ruf, C.G., Cordes, M., Hartmann, J., **Meineke, V.** and **Abend, M.** Gene expression comparisons performed for biodosimetry purposes on in vitro peripheral blood cellular subsets and irradiated individuals. *Radiat Res.* 2012;178:234-43.
- [29] Badie, C., Kabacik, S., Balagurunathan, Y., Bernard, N., Brengues, M., Faggioni, G., Greither, R., **Lista, F.**, Peinnequin, A., Poyot, T., **Herodin, F.**, Missel, A., Terbrueggen, B., Zenhausem, F., **Rothkamm, K.**, **Meineke, V.**, Braselmann, H., Beinke, C. and **Abend, M.** Laboratory intercomparison of gene expression assays. *Radiat Res.* 2013;180:138-48.
- [30] **Abend, M.**, Badie, C., Quintens, R., Kriehuber, R., Manning, G., Macaeva, E., Njima, M., Oskamp, D., Strunz, S., Moertl, S., Doucha-Senf, S., Dahlke, S., Menzel, J. and **Port, M.** Examining Radiation-Induced In Vivo and In Vitro Gene Expression Changes of the Peripheral Blood in Different Laboratories for Biodosimetry Purposes: First RENEb Gene Expression Study. *Radiat Res.* 2016;185:109-23.
- [31] **Port, M.**, **Herodin, F.**, Valente, M., **Drouet, M.**, Lamkowski, A., Majewski, M. and **Abend, M.** First generation gene expression signature for early prediction of late occurring haematological acute radiation syndrome in baboons. *Radiat Res.* 2016;186:39-54.

5.6 RADIATION BIOMARKERS

- [32] Selmansberger, M., Kaiser, J.C., Hess, J., G thlin, D., Likhtarev, I., Shpak, V., Tronko, M., Brenner, A., **Abend, M.**, Blettner, M., Unger, K., Jacob, P. and Zitzelsberger, H. Dose-dependent expression of CLIP2 in post-Chernobyl papillary thyroid carcinomas. *Carcinogenesis*. 2015;36:748-56.
- [33] **Abend, M.**, Azizova, T., M ller, K., **D rr, H.**, Doucha-Senf, S., Kreppel, H., Rusinova, G., Glazkova, I., Vyazovskaya, N., Unger, K., Braselmann, H. and **Meineke, V.** Association of radiation-induced genes with noncancer chronic diseases in Mayak workers occupationally exposed to prolonged radiation. *Radiat Res*. 2015;183:249-61.
- [34] **Herodin, F.**, Voir, D., Vilgrain, I., Cour on, M., **Drouet, M.** and Boittin, F-X. Soluble vascular endothelial cadherin as a new biomarker of irradiation in highly irradiated baboons with bone marrow protection. *Health Phys*. 2016;110:598-605.
- [35] Selmansberger, M., Feuchtinger, A., Zurnadzhy, L., Michna, A., Kaiser, J.C., **Abend, M.**, Brenner, A., Bogdanova, T., Walch, A., Unger, K., Zitzelsberger, H. and Hess, J. CLIP2 as radiation biomarker in papillary thyroid carcinoma. *Oncogene*. 2015;34:3917-25.
- [36] **Abend, M.**, Azizova, T., M ller, K., D rr, H., Senf, S., Kreppel, H., Rusinova, G., Glazkova, I., Vyazovskaya, N., Unger, K. and **Meineke, V.** Independent validation of candidate genes identified after a whole genome screening on Mayak workers exposed to prolonged occupational radiation. *Radiat Res*. 2014;182:299-309.
- [37] Moroni, M., **Port, M.**, Koch, A., Gulani, J., **Meineke, V.** and **Abend, M.** Significance of bioindicators to predict survival in irradiated minipigs. *Health Phys*. 2014;106:727-33.
- [38] **Abend, M.**, Azizova, T., M ller, K., **D rr, H.**, Senf, S., Kreppel, H., Rusinova, G., Glazkova, I., Vyazovskaya, N., Schmidl, D., Unger, K. and **Meineke, V.** Gene expression analysis in Mayak workers with prolonged occupational radiation exposure. *Health Phys*. 2014;106:664-76.
- [39] **Abend, M.**, Pfeiffer, R.M., Ruf, C., Hatch, M., Bogdanova, T.I., Tronko, M.D., Hartmann, J., **Meineke, V.**, Mabuchi, K. and Brenner, A.V. Iodine-131 dose-dependent gene expression: alterations in both normal and tumour thyroid tissues of post-Chernobyl thyroid cancers. *Br J Cancer*. 2013;109:2286-94.
- [40] **Abend, M.**, Pfeiffer, R.M., Ruf, C., Hatch, M., Bogdanova, T.I., Tronko, M.D., Riecke, A., Hartmann, J., **Meineke, V.**, Boukheris, H., Sigurdson, A.J., Mabuchi, K. and Brenner, A.V. Iodine-131 dose dependent gene expression in thyroid cancers and corresponding normal tissues following the Chernobyl accident. *PLoS One*. 2012;7(7):e39103.
- [41] Hu, S., **Blakely, W.F.** and Cucinotta, F.A. HEMODOSE: A Biodosimetry Tool Based on Multi-type Blood Cell Counts. *Health Phys*. 2015;109:54-68.
- [42] Bolduc, D.L., Villa, V., Sandgren, D.J., Ledney, G.D., **Blakely, W.F.** and B nger, R. Application of multivariate modeling for radiation injury assessment: a proof of concept. *Comput Math Methods Med*. 2014;2014:685286.
- [43] Budworth, H., Snijders, A.M., Marchetti, F., Mannion, B., Bhatnagar, S., Kwoh, E., Tan, Y., Wang, S.X., **Blakely, W.F.**, Coleman, M., Peterson, L. and Wyrobek, A.J. DNA repair and cell cycle biomarkers of radiation exposure and inflammation stress in human blood. *PLoS One*. 2012;7(11):e48619.

- [44] Johnson, C.H., Patterson, A.D., Krausz, K.W., Kalinich, J.F., Tyburski, J.B., Kang, D.W., Luecke, H., Gonzalez, F.J., **Blakely, W.F.** and Idle, J.R. Radiation metabolomics. 5. Identification of urinary biomarkers of ionizing radiation exposure in nonhuman primates by mass spectrometry-based metabolomics. *Radiat Res.* 2012;178:328-40.
- [45] Prodosmo, A., **De Amicis, A.**, Nisticò, C., Gabriele, M., Di Rocco, G., Monteonofrio, L., Piane, M., Cundari, E., Chessa, L. and Soddu, S. p53 centrosomal localization diagnoses ataxia-telangiectasia homozygotes and heterozygotes. *J Clin Invest.* 2013;123:1335-42.
- [46] **Pejchal, J.**, Novotný, J., Mařák, V., Osterreicher, J., Tichý, A., Vávrová, J., Sinkorová, Z., Zárbybnická, L., Novotná, E., Chládek, J., Babicová, A., Kubelková, K. and Kuča, K. Activation of p38 MAPK and expression of TGF- β 1 in rat colon enterocytes after whole body γ -irradiation. *Int J Radiat Biol.* 2012;88:348-58.
- [47] Moroni, M., **Port, M.**, Gulani, J., Chappell, M. and **Abend, M.** Significance of Bioindicators for Early Predictions on Diagnosis and Therapy of Irradiated Minipigs. *Health Phys.* 2016 Aug;111(2):160-8.
- [48] Bolduc, D.L., Bünger, R., Moroni, M. and **Blakely, W.F.** Modeling H-ARS using hematological parameters: a comparison between the non-human primate and minipig. *Radiat Prot Dosimetry.* 2016 Jul 27. [Epub ahead of print].

5.7 RADIO-PROTECTANTS

- [49] Babicová, A., Havlínová, Z., Hroch, M., Rezáčová, M., **Pejchal, J.**, Vávrová, J. and Chládek, J. In vivo study of radioprotective effect of NO-synthase inhibitors and acetyl-L-carnitine. *Physiol Res.* 2013;62:701-10.
- [50] Li, X.H., Ghosh, S.P., Ha, C.T., Fu, D., Elliott, T.B., Bolduc, D.L., Villa, V., **Whitnall, M.H.**, Landauer, M.R. and Xiao, M. Delta-tocotrienol protects mice from radiation-induced gastrointestinal injury. *Radiat Res.* 2013;180:649-57.

5.8 ANIMAL MODELS FOR THE STUDY OF G-ARS AND RI-MODS

- [51] Elliott, T.B., Deutz, N.E., Gulani, J., Koch, A., Olsen, C.H., Christensen, C., Chappell, M., **Whitnall, M.H.** and Moroni, M. Gastrointestinal acute radiation syndrome in Göttingen minipigs (*Sus scrofa domestica*). *Comp Med.* 2014;64:456-63.
- [52] Moroni, M., Elliott, T.B., Deutz, N.E., Olsen, C.H., Owens, R., Christensen, C., Lombardini, E.D. and **Whitnall, M.H.** Accelerated hematopoietic syndrome after radiation doses bridging hematopoietic (H-ARS) and gastrointestinal (GI-ARS) acute radiation syndrome: early hematological changes and systemic inflammatory response syndrome in minipig. *Int J Radiat Biol.* 2014;90:363-72.
- [53] Boittin, F.X., Martigne, P., Mayol, J.F., Denis, J., Raffin, F., Coulon, D., Grenier, N., **Drouet, M.** and **Hérodin, F.** Experimental Quantification of Delayed Radiation-Induced Organ Damage in Highly Irradiated Rats With Bone Marrow Protection: Effect of Radiation Dose and Organ Sensitivity. *Health Phys.* 2015;109:134-44.
- [54] Boittin, F.X., Denis, J., Mayol, J.F., Martigne, P., Raffin, F., Coulon, D., Grenier, N., **Drouet, M.** and **Hérodin, F.** The extent of irradiation-induced long-term visceral organ damage depends on cranial/brain exposure. *PLoS One.* 2015 Apr 2;10(4):e0122900.

- [55] Ossetrova, N.I., **Blakely, W.F.**, Nagy, V., McGann, C., Ney, P.H., Christensen, C.L., Koch, A.L., Gulani, J., Sigal, G.B., Glezer, E.N. and Hieber, K.P. Non-human Primate Total-body Irradiation Model with Limited and Full Medical Supportive Care Including Filgrastim for Biodosimetry and Injury Assessment. *Radiat Prot Dosimetry*. 2016 Jul 29. [Epub ahead of print].

5.9 POST-IRRADIATION TREATMENTS AGAINST IONIZING RADIATION INJURY (H-ARS AND CRS)

- [56] Riccobono, D., Forcheron, F., Agay, D., Scherthan, H., **Meineke, V.** and **Drouet, M.** Transient gene therapy to treat cutaneous radiation syndrome: development in a minipig model. *Health Phys*. 2014;106:713-9.
- [57] **Drouet, M.** and **Hérodin, F.** Mitigating radiation-induced toxicity: an overview of new approaches developed at the French Military Biomedical Research Institute. *Health Phys*. 2014;106:682-8.
- [58] **Drouet, M.** Determining rational target for in vivo hedgehog gene therapy. *Exp Hematol*. 2014;42:159-60.
- [59] **Drouet, M.**, Garrigou, P., Peinnequin, A. and **Hérodin, F.** Short-term sonic-hedgehog gene therapy to mitigate myelosuppression in highly irradiated monkeys: hype or reality? *Bone Marrow Transplant*. 2014;49:304-9.
- [60] **Drouet, M.**, Agay, D., Garrigou, P., Peinnequin, A. and **Hérodin, F.** Gene therapy to mitigate radiation-induced bone marrow aplasia: preliminary study in highly irradiated monkeys. *Health Phys*. 2012;103:138-42.
- [61] Riccobono, D., Agay, D., Scherthan, H., Forcheron, F., Vivier, M., Ballester, B., **Meineke, V.** and **Drouet, M.** Application of adipocyte-derived stem cells in treatment of cutaneous radiation syndrome. *Health Phys*. 2012;103:120-6.
- [62] **Drouet, M.**, Grenier, N. and **Hérodin, F.** Revisiting emergency anti-apoptotic cytokinotherapy: erythropoietin synergizes with stem cell factor, FLT-3 ligand, trombopoietin and interleukin-3 to rescue lethally-irradiated mice. *Eur Cytokine Netw*. 2012;23:56-63.
- [63] Forcheron, F., Agay, D., Scherthan, H., Riccobono, D., **Herodin, F.**, **Meineke, V.** and **Drouet, M.** Autologous adipocyte derived stem cells favour healing in a minipig model of cutaneous radiation syndrome. *PLoS One*. 2012;7(2):e31694.
- [64] **Pejchal, J.**, Šinkorová, Z., Tichý, A., Kmochová, A., Ďurišová, K., Kubelková, K., Pohanka, M., Bureš, J., Tachecí, I., Kuča, K. and Vávrová, J. Attenuation of radiation-induced gastrointestinal damage by epidermal growth factor and bone marrow transplantation in mice. *Int J Radiat Biol*. 2015;3:1-12.
- [65] Moroni, M., Ngudiankama, B.F., Christensen, C., Olsen, C.H., Owens, R., Lombardini, E.D., Holt, R.K. and **Whitnall, M.H.** The Gottingen minipig is a model of the hematopoietic acute radiation syndrome: G-colony stimulating factor stimulates hematopoiesis and enhances survival from lethal total-body γ -irradiation. *Int J Radiat Oncol Biol Phys*. 2013;86:986-92.
- [66] Grace, M.B., Singh, V.K., Rhee, J.G., Jackson, W.E. 3rd, Kao, T.C. and **Whitnall, M.H.** 5-AED enhances survival of irradiated mice in a G-CSF-dependent manner, stimulates innate immune cell function, reduces radiation-induced DNA damage and induces genes that modulate cell cycle progression and apoptosis. *J Radiat Res*. 2012;53:840-53.

- [67] Krivokrysenko, V.I., Shakhov, A.N., Singh, V.K., Bone, F., Kononov, Y., Shyshynova, I., Cheney, A., Maitra, R.K., Purmal, A., **Whitnall, M.H.**, Gudkov, A.V. and Feinstein, E. Identification of granulocyte colony-stimulating factor and interleukin-6 as candidate biomarkers of CBLB502 efficacy as a medical radiation countermeasure. *J Pharmacol Exp Ther.* 2012;343:497-508.
- [68] Singh, V.K., Fatanmi, O.O., Singh, P.K. and **Whitnall, M.H.** Role of radiation-induced granulocyte colony-stimulating factor in recovery from whole body gamma-irradiation. *Cytokine.* 2012;58:406-14.
- [69] Riccobono, D., Agay, D., François, S., Scherthan, H., **Drouet, M.** and Forcheron, F. Contribution of intramuscular autologous adipose tissue-derived stem cell injections to treat cutaneous radiation syndrome: Preliminary results. *Health Phys.* 2016;111:117-26.
- [70] **Abend, M.** and **Port, M.** Combining Radiation Epidemiology With Molecular Biology-Changing From Health Risk Estimates to Therapeutic Intervention. *Health Phys.* 2016;111:183-5.

5.10 RADIOLOGICAL DECONTAMINATION

- [71] Rump, A., **Stricklin, D.**, Lamkowski, A., Eder, S., **Abend, M.** and **Port, M.** Reconsidering Current Decorporation Strategies after Incorporation of Radionuclides. *Health Phys.* 2016;111:204-11.

5.11 LOW-LEVEL RADIATION BIOEFFECTS

- [72] **Janiak, M.K.** Epidemiological evidence of childhood leukaemia around nuclear power plants. *Dose Response.* 2014;12:349-64.
- [73] Socol, Y., Dobrzyński, L., Doss, M., Feinendegen, L.E., **Janiak, M.K.**, Miller, M.L., Sanders, C.L., Scott, B.R., Ulsh, B. and Vaiserman, A. Commentary: ethical issues of current health-protection policies on low-dose ionizing radiation. *Dose Response.* 2013;12:342-8.
- [74] **Nowosielska, E.M.**, Cheda, A., Wrembel-Wargocka, J. and **Janiak, M.K.** Effect of low doses of low-let radiation on the innate anti-tumor reactions in radioresistant and radiosensitive mice. *Dose Response.* 2012;10:500-15.

5.12 MODELING AND MEDICAL GUIDANCE

- [75] **Stricklin, D.** and Millage, K. Evaluation of demographic factors that influence acute radiation response. *Health Phys.* 2012;103:210-6.
- [76] Went, J.M., Vainstein, V., Oldson, D., Gluzman-Poltorak, Z., Basile, L.A. and **Stricklin, D.** Mathematical Model of Radiation Effects on Thrombopoiesis in Rhesus Macaques and Humans. *J Theor Biol.* 2015 Jul 29. pii: S0022-5193(15)00349-5.
- [77] Sugarman, S.L., Livingston, G.K., **Stricklin, D.L.**, Abbott, M.G., Wilkins, R.C., Romm, H., Oestreicher, U., Yoshida, M.A., Miura, T., Moquet, J.E., Di Giorgio, M., Ferrarotto, C., Gross, G.A., Christiansen, M.E., Hart, C.L. and Christensen, D.M. The Internet's role in a biodosimetric response to a radiation mass casualty event. *Health Phys.* 2014;106:S65-70.
- [78] Cary, L.H., Ngudiankama, B.F., Salber, R.E., Ledney, G.D. and **Whitnall, M.H.** Efficacy of radiation countermeasures depends on radiation quality. *Radiat Res.* 2012;177:663-75.

- [79] Milner, E.E., Daxon, E.G., Anastasio, M.T., Nesler, J.T., Miller, R.L. and **Blakely, W.F.** Concepts of Operations (CONOPS) for Biodosimetry Tools Employed in Operational Environments. Health Phys. 2016;110:370-9.
- [80] **Port, M.** and Beinke, C. ConRad-Global Conference on Radiation Topics-Preparedness, Response, Protection and Research, Munich, 4-7 May 2015. Health Phys. 2016;111:73-4.

Annex A – ANNUAL MEETING AGENDAS

A.1 NATO HFM-222 RTG MEETING: IONIZING RADIATION BIOEFFECTS AND COUNTERMEASURES, 14-15 MAY 2012, NEUILLY-SUR-SEINE, FRANCE

Sunday, 13 May

1500 – 1900 Social activity and informal welcome reception: Visit of Jacquemart-André Museum, Paris, and refreshments at a location TBD.

Monday, 14 May

0845 – 0900 Onsite registration at the NATO RTA, Neuilly-sur-Seine

0900 – 0915 “Welcome addresses”

- General Dr. Erik Zerath, HFM Rep France
- Pr. Marek Janiak, Panel Mentor

0915 – 0930 “Introduction”, Dr. Francis Hérodin, HFM-222 Chair, IRBA

0930 – 0945 Tour de table

0945 – 1000 “Administrative Remarks”, LtCol. Ron Verkerk, NATO RTA, Neuilly-sur-Seine

1000 – 1030 Coffee break

1030 – 1130 “NATO RTO”, LtCol. Ron Verkerk, NATO RTA

Session 1: From HFM-099 RTG to HFM-222 RTG

Chair: Col. Dr. L. Andrew Huff, Deputy Director AFRRRI

1130 – 1200 “NATO HFM-099/RTG-033 Radiation Bioeffects and Countermeasures – Final Report”, Col. Dr. Huff, AFFRI

1200 – 1315 Lunch

1315 – 1330 “Terms of Reference for NATO HFM-222 RTG”, Dr. Francis Hérodin, IRBA

Keynote Session

Chair: Dr. Kai Rothkamm, HPA

1330 – 1400 “NATO 2011 Biological Dosimetry Exercise”, Col. Pr. Dr. Michael Abend, Institute of Radiobiology, Bundeswehr (IRBW)

1400 – 1430 “ARMENIA’s Interest in NATO N/R Defence Activities”, Dr. Artak Barseghyan, Engineering Academy of Armenia

**General Session: National Status Reports (2008 – 2011) on
Ionizing Radiation Bioeffects and Countermeasures**

Chairs: Col. Pr. Dr. Viktor Meineke, IRBW and Col. Dr. Michel Drouet, IRBA

- 1430 – 1500 “CANADA National Status Report”, Dr. Slavica Vlahovich
1500 – 1530 Coffee break and HFM-222 RTG Members’ photography
1530 – 1600 “CZECH REPUBLIC National Status Report”, Maj. Dr. Jaroslav Pejchal
1600 – 1630 “FRANCE National Status Report”, Col. Dr. Michel Drouet
1630 – 1700 “GERMANY National Status Report”, Col. Pr. Dr. Viktor Meineke
1930 – 2200 Dinner at Restaurant “St Ferdinand”

Tuesday, 15 May**Continuation of General Session: National Status Reports (2008 – 2011)
on Ionizing Radiation Bioeffects and Countermeasures**

Chair: Capt. John Gilstad, AFRI

- 0900 – 0930 “ITALY National Status Report”, Col. Dr. Florigio Lista
1000 – 1030 “POLAND National Status Report”, Pr. Marek Janiak
1030 – 1100 Coffee break

Chair: Pr. Marek Janiak, MIHE

- 1100 – 1130 “UNITED KINGDOM National Status Report”, Dr. Kai Rothkamm
1130 – 1200 “UNITED STATES National Status Report”, Capt. John Gilstad
1200 – 1315 Lunch
1315 – 1400 Extra time for General Session

Prospective Session

Chair: Dr. Francis Hérodin, IRBA

- 1400 – 1500 Agreement on HFM-222 working sub-groups and establish Program of Work (PoW)
1500 – 1530 Coffee break
1530 – 1630 Agreement on HFM-222 working sub-groups and establish Program of Work (PoW) (2)
1630 – 1700 General discussion
1700 – 1730 Extra time for discussion

Adjournment, 14-15 May 2012, HFM-222 Meeting

A.2 NATO HFM-222 RTG MEETING: IONIZING RADIATION BIOEFFECTS AND COUNTERMEASURES, 5-7 JUNE 2013, ROME, ITALY**Wednesday, 5 June**

- 1400 – 1415** Onsite registration at the Army Medical and Veterinary Research Centre, Rome
- 1415 – 1435** “Welcome addresses”
- Col. Dr. Florigio Lista, HFM-222 Host, IAMVRC
 - Pr. Marek Janiak, Panel Mentor
- 1435 – 1450** “Introduction”, Dr. Francis Hérodin, HFM-222 Chair, IRBA
- 1450 – 1505** Tour de table
- 1505 – 1520** “Administrative Remarks”, Col. Dr. Florigio Lista
- 1520 – 1550** “Terms of Reference for NATO HFM-222 RTG”, Dr. Francis Hérodin, IRBA

Scientific Presentations of Italian Guests

Chair: Pr. Michael Abend

- 1550 – 1610** “Cerium Oxide Nanoparticles as Radio-Protective Agents: Underlying Mechanisms and Potential Applications”, Dr. Anna Giovanetti, ENEA
- 1610 – 1630** Coffee break
- 1630 – 1650** “Physical Methods of Retrospective Dosimetry in Radiological Emergencies”, Dr. Paola Fattibene, ISS
- 1650 – 1710** “ENEA Activities in the Field of Radiobiology and Biodosimetry”, Dr. Antonella Testa, ENEA
- 1710 – 1740** “Report on NSA CBRN Med Working Group Activities”, Dr. Francis Hérodin

Thursday, 6 June**General Session: National Status Reports (2012) on Ionizing Radiation Bioeffects and Countermeasures**

Chairs: Dr. Romano Lista and Dr. Michel Drouet

- 0900 – 0930** “GERMANY National Status Report” and “News and Views from CONRAD 2013”, LtCol. Dr. Harrald Doerr, Bundeswehr Institute of Radiobiology (IRBW)
- 0930 – 0950** “N/R Defence Activities in ARMENIA”, Dr. Francis Hérodin for Dr. Artak Barseghyan, Engineering Academy of Armenia
- 0950 – 1010** “CZECH REPUBLIC National Status Report”, Maj. Dr. Jaroslav Pejchal
- 1010 – 1030** “FRANCE National Status Report”, Col. Dr. Michel Drouet, IRBA

- 1030 – 1050** Coffee break and HFM-222 RTG Members' photography
- 1050 – 1110** “ITALY National Status Report”, Col. Dr. Florigio Lista, IAMVRC
Chair: Dr. Harrald Doerr
- 1110 – 1130** “POLAND National Status Report”, Pr. Marek Janiak
- 1130 – 1150** “UNITED KINGDOM National Status Report”, Dr. Francis Hérodin for Dr. Kai Rothkamm
- 1150 – 1210** “UNITED STATES National Status Report”, Dr. Alexandra Miller, AFRRRI
- 1210 – 1310** Lunch

Session on Low-Level Radiation

Chair: Dr. Jaroslav Pejchal

- 1310 – 1340** “Low Dose Radiation Research at AFRRRI”, Dr. Alexandra Miller
- 1340 – 1410** “Effects of Low-Level Internal Contamination with HTO on the Activities of NK Cells and Cytotoxic Macrophages in Radio-Resistant and Radio-Sensitive Mice”, Pr. Marek Janiak

Session on High-Level Radiation

Chairs: Dr. Alexandra Miller and Dr. Stefania de Sanctis

- 1410 – 1435** “Acute Radiation Syndrome Management: Towards New Strategies to Mitigate Hematopoietic Syndrome”, Dr. Michel Drouet
- 1435 – 1500** “Effects of Nicotinic Acid Derivatives on Haematopoietic System in Mice Exposed to Sub-Lethal and Lethal Doses of Gamma Rays”, Pr. Marek Janiak
- 1500 – 1530** “AFRRRI’s Biodosimetry Research Program Overview”, Dr. William Blakely, via video conference
- 1530 – 2200** **Social afternoon and dinner guided by the Italian Hosts**

Friday, 7 June

Session on High Level Radiation (continuation):

Chairs: Pr. Marek Janiak and Dr. Daniella Stricklin

- 0900 – 0930** “AFRRRI Radiation Countermeasures Program”, Presented by Dr. Alexandra Miller, for Dr. Mark Whitnall
- 0930 – 0950** “Project on Chernobyl Workers”, Pr. Michael Abend
- 0950 – 1010** “Project on Oszerk Workers”, Pr. Michael Abend

- 1010 – 1040** “The Effect of Epidermal Growth Factor and Bone Marrow Transplantation on Gastrointestinal Damage”, Dr. Jaroslav Pejchal
- 1040 – 1100** Coffee break
- 1100 – 1130** “First Data on the Genomic Baboon Project”, Pr. Michael Abend
- 1130 – 1150** “A New Rat Model of RI-MODS/MOF”, Dr. Francis Hérodin
- 1150 – 1220** “Medical Countermeasure Models for Internalized Radionuclides”, Dr. Daniela Stricklin, ARA
- 1220 – 1320** Lunch
- 1320 – 1350** “Progress on Radiation and Burn Combined Injury Modeling”, Dr. Daniela Stricklin, ARA

Prospective Session

Chair: Dr. Francis Hérodin, IRBA

- 1350 – 1430** Revision of HFM-222 Program of Work (PoW)
- 1430 – 1530** Discussion on prospective joint activities
- 1530 – 1600** General discussion and conclusion

Adjournment, 5-7 June 2013, HFM-222 Meeting

A.3 NATO HFM-222 RTG MEETING: IONIZING RADIATION BIOEFFECTS AND COUNTERMEASURES, 16-18 JUNE 2014, BETHESDA, MD, USA

Sunday, 15 June

- 1900 – 2030** Dinner

Monday, 16 June

- 0845 – 0915** Onsite registration at the Armed Forces Radiobiology Research Institute, Bethesda, MD
- 0915 – 1000** “Welcome addresses”
- Dr. Charles Rice, Uniformed Services University Health Sciences, President
 - Col. Dr. Andrew L. Huff, AFRRRI Director, HFM-222 Host
 - Dr. Alexandra Miller, HFM-222 Meeting Manager, AFRRRI
- 1000 – 1015** “Introduction”, Dr. Francis Hérodin, HFM-222 Chair, IRBA and on behalf of Pr. Marek Janiak, Panel Mentor
- 1015 – 1030** Tour de table

ANNEX A – ANNUAL MEETING AGENDAS

- 1030 – 1045 “Administrative Remarks”, Lt. Dr. Joshua Swift, AFRRRI
1045 – 1110 “Terms of Reference for NATO HFM-222 RTG”, Dr. Francis Hérodin, IRBA
1110 – 1130 Coffee break

Keynote Session

Chair: Col. L. Andrew Huff

- 1130 – 1215 “Two Years After Fukushima / Follow Up of Tomadachi Operation”,
Dr. Michael Mittelman, RADM (Ret.)
1215 – 1300 **AFRRRI Tour**
1300 – 1400 Lunch

Future NATO HFM-222 RTG Exercise

- 1400 – 1500 “Presentation of the Exercise”, Dr. Harald Doerr, Bundeswehr Institute of Radiobiology
(IRBW)
1500 – 1630 “Workshop on the Exercise”
1500 – 1630 Coffee/tea/sodas available during workshop
1630 – 1700 “Report on NSA CBRN Med Working Group Activities”, Dr. Francis Hérodin
1900- 2100 **Dinner at Restaurant for HFM-222 members**

Tuesday, 17 June

General Session: National Status Reports (2013) on Ionizing Radiation Bioeffects and Countermeasures

Chairs: Dr. Kuipers and Dr. Whitnall

- 0900 – 0920 “GERMANY National Status Report”, Col. Pr. Michael Abend, IRBW
0920 – 0940 “CZECH REPUBLIC National Status Report”, Maj. Dr. Jaroslav Pejchal
0940 – 1000 “FRANCE National Status Report”, Col. Dr. Michel Drouet, IRBA
1000 – 1020 “ITALY National Status Report”, Col. Dr. Florigio Lista, IAMVRC
1020 – 1050 Coffee break and HFM-222 RTG Members’ photography

Chairs: Col. Drouet and Dr. Port

- 1050 – 1110 “NETHERLANDS National Status Report”, Dr. Tjerk Kuipers
1110 – 1130 “POLAND National Status Report”, Chair on behalf of Dr. Ewa Nowosielska

- 1130 – 1150** “UNITED KINGDOM National Status Report”, Dr. Kai Rothkamm, Public Health England, via video conference
- 1150 – 1210** “UNITED STATES National Status Report”, Col. Dr. Andrew L. Huff, AFRRRI
- 1210 – 1320** Lunch

Session on Low-Level Radiation

Chairs: Dr. Blakely and Dr. DeAmicis

- 1320 – 1400** “Low Dose Keynote”, Dr. John Boice President U.S. National Council Radiation Protection (NCRP)
- 1400 - 1430** “Low Dose Radiation Studies: Approaches to Study Late Effects”, Dr. Alexandra Miller, USA
- 1430 – 1500** Coffee break
- 1500 – 1645** Inventory of manuscripts for the Intermediate HFM-222 report
- 1900 –** **Dinner for HFM members and open to other AFRRRI scientists**

Wednesday, 18 June

Session on High-Level Radiation

Chairs: Dr. Stricklin and Dr. Lista

- 0900 – 0930** “Predicting Hematological ARS Using Gene Expression Changes Examined in the Peripheral Blood of Irradiated Baboons - A French-German Collaboration”, Dr. Matthias Port
- 0930 – 0100** “Association of Radiation-Induced Genes with Chronic Non-Cancer Diseases in Mayak Workers Occupationally Exposed to Prolonged Radiation”, Col. Pr. Michael Abend
- 1000 – 1020** “New Approaches to the Treatment of H-ARS”, Col. Dr. Michel Drouet
- 1020 – 1040** Coffee break

Chairs: Dr. Abend and Dr. Doerr

- 1040 – 1100** “Mechanisms Involved in Radiation-Induced Late Damage to Visceral Organs”, Dr. Francis Hérodin
- 1100 – 1120** “Long Term Effects of EGF and Bone Marrow Transplantation in Irradiated Mice”, Maj. Dr. Jaroslav Pejchal
- 1120 – 1150** “AFRRRI Radiation Countermeasures Program”, Dr. Mark Whitnall
- 1150 – 1220** “Progress on Modeling of Radiation and Burn Combined Injury”, Dr. Daniela Stricklin, Applied Research Associates
- 1220 – 1320** Lunch

Chairs: Dr. Pejchal and Dr. De Sanctis

- 1320 – 1350 “Italian Biodosimetry Report”, Col. Dr. Florigio Lista
- 1350 – 1420 “Proposed Consensus HFM-222 RTG Biological Dosimetry Report”, Dr. William Blakely, AFRRI

Prospective Session

Chair: Dr. Francis Hérodin, IRBA

- 1420 - 1440 Revision of HFM-222 Program of Work (PoW)
- 1440 – 1540 Discussion on prospective joint activities
- 1440 – 1540 Coffee/tea/sodas available
- 1540 – 1600 General discussion and conclusion

Adjournment, 16-18 June 2014, HFM-222 Meeting

A.4 NATO HFM-222 RTG MEETING: IONIZING RADIATION BIOEFFECTS AND COUNTERMEASURES, 7-9 MAY 2015, MUNICH, GERMANY

Thursday, 7 May

- 1330 – 1345 Onsite registration at the German Army Institute of Radiobiology – Institute of Pharmacology and Toxicology, Munich
- 1345 – 1400 “Welcome addresses”
- Col. Pr. Matthias Port, IRBW Director, HFM-222 Host
 - Col. Pr. Michael Abend, HFM-222 meeting manager, IRBW
- “Administrative Remarks”
- 1400 – 1415 “Introduction”, Dr. Francis Hérodin, HFM-222 Chair, IRBA and on behalf of Pr. Marek Janiak, Panel Mentor
- 1415 – 1430 Tour de table
- 1430 – 1445 “Report on NSA CBRN Med Working Group Activities”, Dr. Francis Hérodin

General Session: National Status Reports (2014 – 2015) on Ionizing Radiation Bioeffects and Countermeasures

Chairs: Dr. Kuipers and Dr. Whitnall

- 1445 – 1505 “GERMANY National Status Report”, Col. Pr. Matthias Port, IRBW
- 1505 – 1525 “CZECH REPUBLIC National Status Report” Maj. Dr. Jaroslav Pejchal

- 1525 – 1545** “FRANCE National Status Report”, Col. Dr. Michel Drouet, IRBA
- 1545 – 1605** Coffee break and HFM-222 RTG Members’ photography
- 1605 – 1625** “ITALY National Status Report”, Col. Dr. Florigio Lista, IAMVRC
- Chairs: Col. Port and Col. Drouet
- 1625 – 1645** “NETHERLANDS National Status Report”, Dr. Tjerk Kuipers
- 1645 – 1705** “POLAND National Status Report”, Dr. Ewa Nowosielska
- 1705 – 1725** “UNITED STATES National Status Report”, Dr. Alexandra Miller, AFRI

Friday, 8 May**Session on 2015 NATO HFM-222 RTG Exercise Planning**

Chair: Col. Lista

- 0900 – 0910** Administrative remarks Col. Abend
- 0910 – 1010** “Presentation of the Exercise”, LtCol. Dr. Harald Doerr, IRBW
- 1010 – 1050** “Comments, Amendments, Approval of Final Draft – Part 1”
- 1050 – 1110** Coffee Break
- 1110 – 1230** “Comments, Amendments, Approval of Final Draft – Part 2”
- 1230 – 1330** Lunch
- 1330 – 1430** **IRBW Tour**

Scientific Sessions

Chair: Maj. Pejchal and Col. Abend

- 1430 – 1450** “The Netherlands CBRN National Training Centre”, Dr. Tjerk Kuipers
- 1450 – 1510** “Introducing the New IRBA”, Dr. Francis Hérodin
- 1510 – 1520** “Recent Modeling Studies at ARA”, Dr. Daniela Stricklin
- 1520 – 1540** Coffee break
- 1540 – 1625** “Proposed Consensus HFM-222 RTG Biological Dosimetry Report”, Dr. William Blakely, AFRI
- 1625 – 1715** Inventory of manuscripts for the intermediate HFM-222 report
- 1715 – 1745** Discussion on prospective joint activities (Third NATO Exercise)

Saturday, 9 May**Conclusive and Prospective Session**

Chair: Dr. Francis Hérodin, IRBA

- 0900 – 0930** Strengths and Weaknesses of HFM-222 RTG
- 0930 – 1000** Recommendations for a next RTG on Ionizing Radiation Bioeffects and Countermeasures
- 1000 – 1050** Identification of ToRs and TAPs for a next RTG
- 1030 – 1100** General discussion and conclusion

Adjournment, 7-9 May 2015, HFM-222 Meeting**A.5 NATO HFM-222 RTG MEETING: IONIZING RADIATION BIOEFFECTS AND COUNTERMEASURES, 9-10 MAY 2016, NEUILLY-SUR-SEINE, FRANCE****Monday, 9 May**

- 0900 – 0930** Onsite registration at the STO Building, Neuilly-sur-Seine
- 0930 – 0940** “Welcome Address and Introduction”, Dr. Francis Hérodin, HFM-222 Chair, IRBA and on behalf of Pr. Marek Janiak, Panel Mentor
- 0940 – 0950** Tour de table
- 0950 – 1005** Recommendations of the CSO Publication Manager
- 1005 – 1020** “Report on NSO CBRN Med Working Group Activities”, Dr. Francis Hérodin

General Session I: Highlights of National Activities (2015 – 2016) on Ionizing Radiation Bioeffects and Countermeasures (*Activities of Interest for a Next HFM RTG*)

Chairs: Col. Abend and Dr. Whitnall

- 1020 – 1035** “NR Med Activities in GERMANY”, Col. Pr. Matthias Port, IRBW
- 1035 – 1050** “NR Med Activities in CZECH REPUBLIC”, Maj. Dr. Jaroslav Pejchal
- 1050 – 1110** Coffee break and HFM-222 RTG Members’ photography
- 1110 – 1125** “NR Med Activities in FRANCE”, Col. Dr. Michel Drouet, IRBA
- 1125 – 1140** “NR Med Activities in ITALY”, Dr. Andrea DeAmicis, IAMVRC

Chairs: Dr. Blakely and Col. Drouet

- 1140 – 1155** “NR Med Activities in NETHERLANDS”, Dr. Tjerk Kuipers
- 1155 – 1210** “NR Med Activities in POLAND”, Dr. Ewa Nowosielska

1210 – 1225 “NR Med Activities in the UNITED STATES”, Dr. Alexandra Miller, AFRI

1225 – 1340 Lunch

Session on the 2015 NATO HFM-222 RTG Exercise

Chair: Dr. Miller and Maj. Pejchal

1340 – 1530 “Results of the 2015 NATO Exercise”, LtCol. Dr. Harald Doerr, IRBW

1530 – 1550 Coffee Break

1550 – 1605 “Radiological MASCAL Worksheet”, LTC. Matthew Hofer, AFRI

1605 – 1700 Discussion on the manuscript “Using Clinical Signs and Symptoms for Medical Management and Prediction of Late Occurring HARS, NATO Exercise 2015”, The German Team

1700 – 1730 “Proposals for a Third NATO HFM Exercise”

Tuesday, 10 May

General Session II: Content of the HFM-222 Technical Report, Translation of HFM-222 into Standardization, Prospective Work

Chair: Dr. Francis Hérodin, IRBA

0915 – 1000 “HFM-222 Biological Dosimetry Report”, Dr. William Blakely, AFRI

1000 – 1100 Medical recommendations to be included in Annex 35C “Significant Radiological Medical Countermeasures” of AMedP-7.1 for triage optimization of radiation casualties (external irradiation)

1100 – 1120 Coffee break

1120 – 1220 Inventory of manuscripts for the HFM-222 Technical Report

1220 – 1330 Lunch

1330 – 1430 “Identification of ToRs and TAPs for a next HFM RTG”, Col. Michael Abend

1430 – 1500 General discussion and conclusion

Adjournment, 9-10 May 2016, Last HFM-222 Meeting



REPORT DOCUMENTATION PAGE			
1. Recipient's Reference	2. Originator's References	3. Further Reference	4. Security Classification of Document
	STO-TR-HFM-222 AC/323(HFM-222)TP/731	ISBN 978-92-837-2055-3	PUBLIC RELEASE
5. Originator Science and Technology Organization North Atlantic Treaty Organization BP 25, F-92201 Neuilly-sur-Seine Cedex, France			
6. Title Biological Effects of Ionising Radiation and Countermeasures			
7. Presented at/Sponsored by Final Report of Research Task Group HFM-222.			
8. Author(s)/Editor(s) Edited by Francis Hérodin, PharmD, PhD, FRA			9. Date January 2018
10. Author's/Editor's Address Institut de Recherche Biomédicale des Armées BP 73 - 91223 Brétigny-sur-Orge, France			11. Pages 244
12. Distribution Statement There are no restrictions on the distribution of this document. Information about the availability of this and other STO unclassified publications is given on the back cover.			
13. Keywords/Descriptors			
Acute radiation syndrome	Early and late effects	Medical management	
Biological and clinical dosimetry	External/internal contamination	Mitigator	
Biomarkers	High-level radiation	Radio-protectant	
Combined injury	Ionizing radiation bioeffects	Therapeutics	
Cutaneous radiation syndrome	Low-level radiation	Triage and diagnosis	
14. Abstract			
<p>The HFM-222 RTG (active 2012 – 2016) addressed the medical challenges of NATO military defensive operations that could be conducted in a nuclear/radiological (NR) environment. The HFM-222 Technical Report deals with high level and low level radiation issues through the following cross-cutting themes: i) biomarkers of exposure and effects; ii) early and late effects; iii) medical countermeasures; iv) modelling; v) guidance. Several deliverables taking into account military medical relevant research and operational needs were accomplished such as seventy peer-reviewed publications and one exercise dealing with radiological triage/diagnosis based on clinical dosimetry following a first biological dosimetry exercise implemented in 2011. The RTG produced different mature and deployable software tools dealing with the assessment triage (i.e., Mobile-FRAT, which is an Android and IOS based application) or the evaluation of Radiation Induced Performance Decrement (RIPD) and Health Effects from Nuclear and Radiological Environments (HENRE) which integrate complex exposure scenarios. Biomarkers of effect and damage were developed in order to diagnose and predict the clinical outcome of irradiated victims. Regarding treatment strategies, the RTG contributed to the FDA approval of granulocyte colony-stimulating factor (filgrastim) to mitigate radiation-induced neutropenia in NR accident victims. For high dose localized exposures adipose tissue-derived stem cells represent a promising cell drug to mitigate cutaneous radiation syndrome. Moreover, as low dose NR events may disrupt military operations, relevant models were developed to address related medical issues and retrospective epidemiological studies were conducted.</p>			





BP 25
F-92201 NEUILLY-SUR-SEINE CEDEX • FRANCE
Télécopie 0(1)55.61.22.99 • E-mail mailbox@cs0.nato.int



DIFFUSION DES PUBLICATIONS
STO NON CLASSIFIEES

Les publications de l'AGARD, de la RTO et de la STO peuvent parfois être obtenues auprès des centres nationaux de distribution indiqués ci-dessous. Si vous souhaitez recevoir toutes les publications de la STO, ou simplement celles qui concernent certains Panels, vous pouvez demander d'être inclus soit à titre personnel, soit au nom de votre organisation, sur la liste d'envoi.

Les publications de la STO, de la RTO et de l'AGARD sont également en vente auprès des agences de vente indiquées ci-dessous.

Les demandes de documents STO, RTO ou AGARD doivent comporter la dénomination « STO », « RTO » ou « AGARD » selon le cas, suivi du numéro de série. Des informations analogues, telles que le titre et la date de publication sont souhaitables.

Si vous souhaitez recevoir une notification électronique de la disponibilité des rapports de la STO au fur et à mesure de leur publication, vous pouvez consulter notre site Web (<http://www.sto.nato.int/>) et vous abonner à ce service.

CENTRES DE DIFFUSION NATIONAUX

ALLEMAGNE

Streitkräfteamt / Abteilung III
Fachinformationszentrum der Bundeswehr (FIZBw)
Gorch-Fock-Straße 7, D-53229 Bonn

BELGIQUE

Royal High Institute for Defence – KHID/IRSD/RHID
Management of Scientific & Technological Research
for Defence, National STO Coordinator
Royal Military Academy – Campus Renaissance
Renaissancelaan 30, 1000 Bruxelles

BULGARIE

Ministry of Defence
Defence Institute "Prof. Tsvetan Lazarov"
"Tsvetan Lazarov" bul no.2
1592 Sofia

CANADA

DGSIST
Recherche et développement pour la défense Canada
101 Colonel By Drive, 6 CBS
Ottawa, Ontario K1A 0K2

DANEMARK

Danish Acquisition and Logistics Organization
(DALO)
Lautrupbjerg 1-5
2750 Ballerup

ESPAGNE

Área de Cooperación Internacional en I+D
SDGPLATIN (DGAM)
C/ Arturo Soria 289
28033 Madrid

ESTONIE

Estonian National Defence College
Centre for Applied Research
Riia str 12
Tartu 51013

ETATS-UNIS

Defense Technical Information Center
8725 John J. Kingman Road
Fort Belvoir, VA 22060-6218

FRANCE

O.N.E.R.A. (ISP)
29, Avenue de la Division Leclerc
BP 72
92322 Châtillon Cedex

GRECE (Correspondant)

Defence Industry & Research General
Directorate, Research Directorate
Fakinos Base Camp, S.T.G. 1020
Holargos, Athens

HONGRIE

Hungarian Ministry of Defence
Development and Logistics Agency
P.O.B. 25
H-1885 Budapest

ITALIE

Centro Gestione Conoscenza
Secretariat General of Defence
National Armaments Directorate
Via XX Settembre 123/A
00187 Roma

LUXEMBOURG

Voir Belgique

NORVEGE

Norwegian Defence Research
Establishment
Attn: Biblioteket
P.O. Box 25
NO-2007 Kjeller

PAYS-BAS

Royal Netherlands Military
Academy Library
P.O. Box 90.002
4800 PA Breda

POLOGNE

Centralna Biblioteka Wojskowa
ul. Ostrobramska 109
04-041 Warszawa

PORTUGAL

Estado Maior da Força Aérea
SDFA – Centro de Documentação
Alfragide
P-2720 Amadora

REPUBLIQUE TCHEQUE

Vojenský technický ústav s.p.
CZ Distribution Information Centre
Mladoboleslavská 944
PO Box 18
197 06 Praha 9

ROUMANIE

Romanian National Distribution
Centre
Armaments Department
9-11, Drumul Taberei Street
Sector 6
061353 Bucharest

ROYAUME-UNI

Dstl Records Centre
Rm G02, ISAT F, Building 5
Dstl Porton Down
Salisbury SP4 0JQ

SLOVAQUIE

Akadémia ozbrojených síl gen.
M.R. Štefánika, Distribučné a
informačné stredisko STO
Demänová 393
031 06 Liptovský Mikuláš 6

SLOVENIE

Ministry of Defence
Central Registry for EU & NATO
Vojkova 55
1000 Ljubljana

TURQUIE

Milli Savunma Bakanlığı (MSB)
ARGE ve Teknoloji Dairesi
Başkanlığı
06650 Bakanlıklar – Ankara

AGENCES DE VENTE

**The British Library Document
Supply Centre**
Boston Spa, Wetherby
West Yorkshire LS23 7BQ
ROYAUME-UNI

**Canada Institute for Scientific and
Technical Information (CISTI)**
National Research Council Acquisitions
Montreal Road, Building M-55
Ottawa, Ontario K1A 0S2
CANADA

Les demandes de documents STO, RTO ou AGARD doivent comporter la dénomination « STO », « RTO » ou « AGARD » selon le cas, suivie du numéro de série (par exemple AGARD-AG-315). Des informations analogues, telles que le titre et la date de publication sont souhaitables. Des références bibliographiques complètes ainsi que des résumés des publications STO, RTO et AGARD figurent dans le « NTIS Publications Database » (<http://www.ntis.gov>).



BP 25
F-92201 NEUILLY-SUR-SEINE CEDEX • FRANCE
Télécopie 0(1)55.61.22.99 • E-mail mailbox@cs.o.nato.int



**DISTRIBUTION OF UNCLASSIFIED
STO PUBLICATIONS**

AGARD, RTO & STO publications are sometimes available from the National Distribution Centres listed below. If you wish to receive all STO reports, or just those relating to one or more specific STO Panels, they may be willing to include you (or your Organisation) in their distribution.

STO, RTO and AGARD reports may also be purchased from the Sales Agencies listed below.

Requests for STO, RTO or AGARD documents should include the word 'STO', 'RTO' or 'AGARD', as appropriate, followed by the serial number. Collateral information such as title and publication date is desirable.

If you wish to receive electronic notification of STO reports as they are published, please visit our website (<http://www.sto.nato.int/>) from where you can register for this service.

NATIONAL DISTRIBUTION CENTRES

BELGIUM

Royal High Institute for Defence – KHID/IRSD/
RHID
Management of Scientific & Technological
Research for Defence, National STO Coordinator
Royal Military Academy – Campus Renaissance
Renaissancelaan 30
1000 Brussels

BULGARIA

Ministry of Defence
Defence Institute "Prof. Tsvetan Lazarov"
"Tsvetan Lazarov" bul no.2
1592 Sofia

CANADA

DSTKIM
Defence Research and Development Canada
101 Colonel By Drive, 6 CBS
Ottawa, Ontario K1A 0K2

CZECH REPUBLIC

Vojenský technický ústav s.p.
CZ Distribution Information Centre
Mladoboleslavská 944
PO Box 18
197 06 Praha 9

DENMARK

Danish Acquisition and Logistics Organization
(DALO)
Lautrupbjerg 1-5
2750 Ballerup

ESTONIA

Estonian National Defence College
Centre for Applied Research
Riaa str 12
Tartu 51013

FRANCE

O.N.E.R.A. (ISP)
29, Avenue de la Division Leclerc – BP 72
92322 Châtillon Cedex

GERMANY

Streitkräfteamt / Abteilung III
Fachinformationszentrum der
Bundeswehr (FIZBw)
Gorch-Fock-Straße 7
D-53229 Bonn

GREECE (Point of Contact)

Defence Industry & Research General
Directorate, Research Directorate
Fakinos Base Camp, S.T.G. 1020
Holargos, Athens

HUNGARY

Hungarian Ministry of Defence
Development and Logistics Agency
P.O.B. 25
H-1885 Budapest

ITALY

Centro Gestione Conoscenza
Secretariat General of Defence
National Armaments Directorate
Via XX Settembre 123/A
00187 Roma

LUXEMBOURG

See Belgium

NETHERLANDS

Royal Netherlands Military
Academy Library
P.O. Box 90.002
4800 PA Breda

NORWAY

Norwegian Defence Research
Establishment, Attn: Biblioteket
P.O. Box 25
NO-2007 Kjeller

POLAND

Centralna Biblioteka Wojskowa
ul. Ostrobramska 109
04-041 Warszawa

PORTUGAL

Estado Maior da Força Aérea
SDFA – Centro de Documentação
Alfragide
P-2720 Amadora

ROMANIA

Romanian National Distribution Centre
Armaments Department
9-11, Drumul Taberei Street
Sector 6
061353 Bucharest

SLOVAKIA

Akadémia ozbrojených síl gen
M.R. Štefánika, Distribučné a
informačné stredisko STO
Demänová 393
031 06 Liptovský Mikuláš 6

SLOVENIA

Ministry of Defence
Central Registry for EU & NATO
Vojkova 55
1000 Ljubljana

SPAIN

Área de Cooperación Internacional en I+D
SDGPLATIN (DGAM)
C/ Arturo Soria 289
28033 Madrid

TURKEY

Milli Savunma Bakanlığı (MSB)
ARGE ve Teknoloji Dairesi Başkanlığı
06650 Bakanlıklar – Ankara

UNITED KINGDOM

Dstl Records Centre
Rm G02, ISAT F, Building 5
Dstl Porton Down, Salisbury SP4 0JQ

UNITED STATES

Defense Technical Information Center
8725 John J. Kingman Road
Fort Belvoir, VA 22060-6218

SALES AGENCIES

**The British Library Document
Supply Centre**
Boston Spa, Wetherby
West Yorkshire LS23 7BQ
UNITED KINGDOM

**Canada Institute for Scientific and
Technical Information (CISTI)**
National Research Council Acquisitions
Montreal Road, Building M-55
Ottawa, Ontario K1A 0S2
CANADA

Requests for STO, RTO or AGARD documents should include the word 'STO', 'RTO' or 'AGARD', as appropriate, followed by the serial number (for example AGARD-AG-315). Collateral information such as title and publication date is desirable. Full bibliographical references and abstracts of STO, RTO and AGARD publications are given in "NTIS Publications Database" (<http://www.ntis.gov>).